NASA Contractor Report 4295

The Biogeochemistry of Metal Cycling

CONTRACT NASW-4324

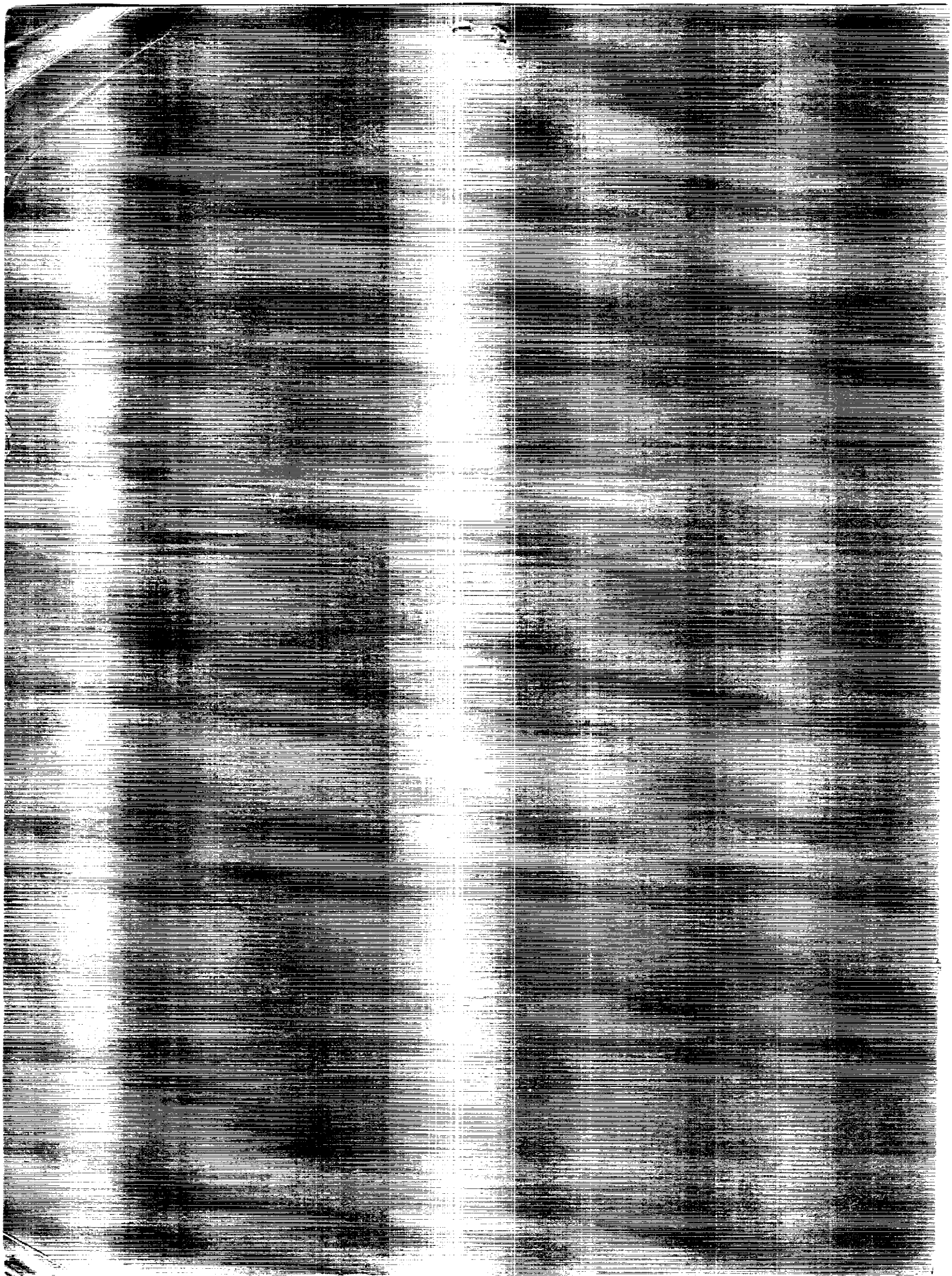

NASA Contractor Report 4295

The Biogeochemistry of Metal Cycling

Edited by
Kenneth H. Nealson and Molly Nealson
University of Wisconsin at Milwaukee
Milwaukee, Wisconsin

F. Ronald Dutcher
The George Washington University
Washington, D.C.

Prepared for
NASA Office of Space Science and Applications
under Contract NASW-4324

NASA
National Aeronautics and
Space Administration
Office of Management
Scientific and Technical
Information Division

1990

Table of Contents

Introduction

In the summer of 1987, the NASA Planetary Biology and Microbial Ecology (PBME) program was conducted at Oneida Lake, New York, utilizing the facilities of the Cornell University field station. This was the fourth in a series of PBME programs, and was the first one to be conducted at a site remote from NASA Ames Research Center.

The goals of this intensive summer program were twofold: (1) to examine, via lectures and laboratory work, several aspects of the biogeochemistry of metal cycling; and (2) to examine the ways in which remote sensing and the study of biogeochemistry interface, and to accomplish the exchange of information between microbial ecologists and scientists actively involved in remote sensing work.

The lectures covered areas of limnology, metal chemistry, metal geochemistry, and microbial ecology and interactions with metals. They were presented by a series of distinguished visitors during the summer program. Abstracts and bibliographies of the individual talks are presented in this document. The laboratory projects were supervised by the co-directors of the course, Dr. K.H. Nealson and Dr. T.M. Schmidt. Both of these workers have had extensive experience in the area of metal biogeochemistry. Descriptions of the various projects and the data obtained are contained in this report. Through this approach we attempted to bring the participants to the "state-of-the-art" in knowledge and techniques.

To accomplish the second goal, we used a twofold approach. First we had a series of lectures by Robert Wrigley of NASA Ames, a recognized expert in remote sensing and image analysis. Dr. Wrigley is not only an expert in the general area of remote sensing, but was currently involved in a project using remote sensing to study the biogeochemical cycling of metals in Oneida Lake. His lectures thus included images of Oneida Lake itself, and it was possible to discuss in some detail the philosophy of ground truth data as it related to our own study site. It was then possible for the students to be involved with the planning strategy and gathering of ground truth data for use in satellite analyses.

Previous NASA PBME courses have used similar formats to the one used for the 1987 course, and they are described in NASA Technical Memoranda #86043 and #87570. The format for the 1987 course was similar to that used throughout the PBME program with the exceptions noted above. As with the previous courses, it proved exceptionally valuable for transferring information and techniques between microbial ecologists, geochemists, and NASA personnel.

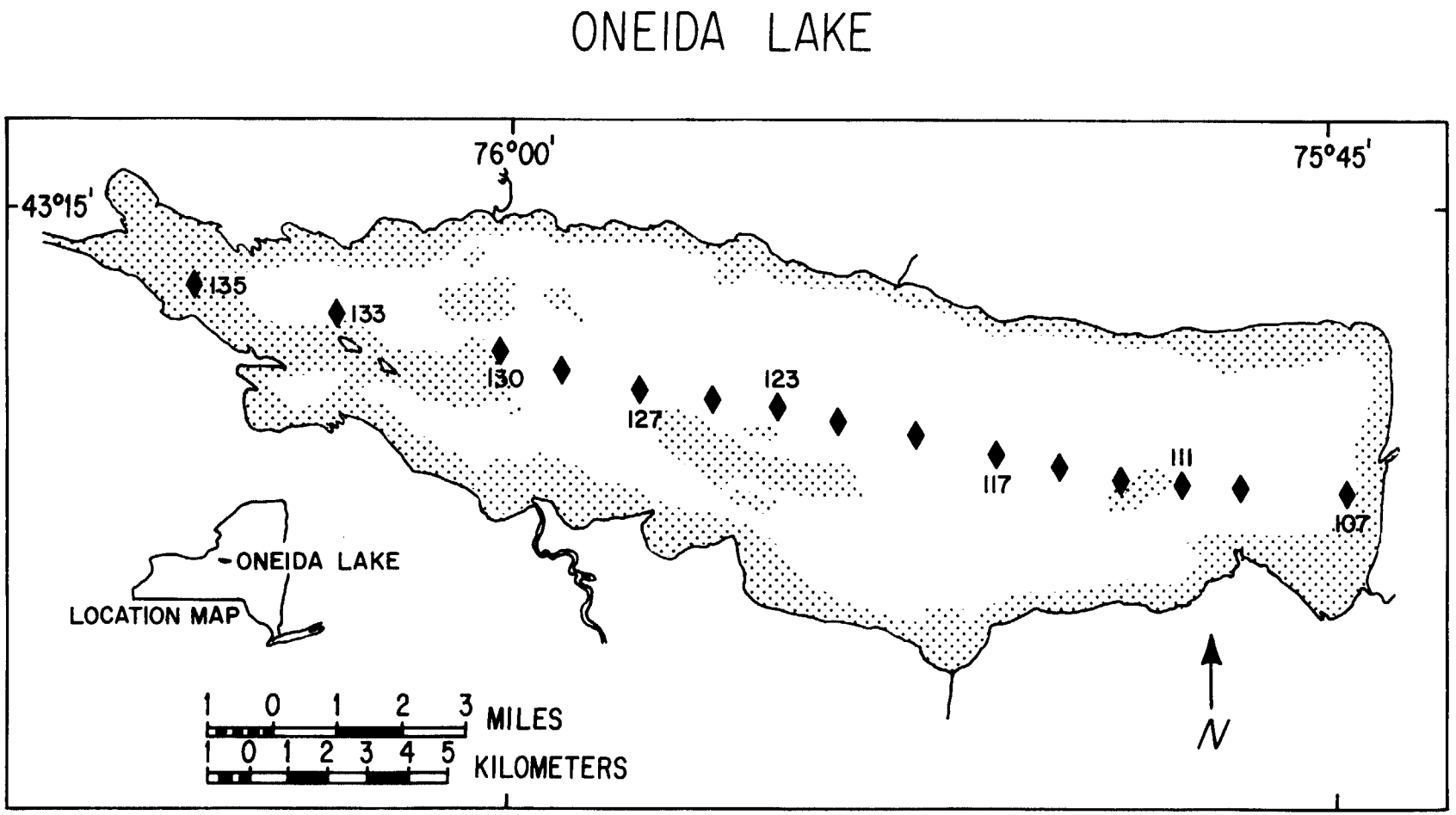

Map of Oneida Lake, New York

Numbered symbols (black diamonds) indicate location of permanent buoys which are part of the New York Barge Canal System and were used as sampling sites during the course.

PBME Summer Schedule 1987

Date		Lecturer	Title
6/22	am	J. Forney	Introduction to Oneida Lake
		E. Mills	Oneida Lake food chains
	pm	K. Nealson	Introduction to Mn biogeochemistry
		T. Schmidt	Mn oxidation & reduction projects
	ni	KN/TS	Laboratory introduction to microbiology
6/23	am	A. Brooks	General limnology of large temperate lakes
		F. Azam	Microbial food web dynamics
	pm	A. Brooks	Primary productivity measurements
	ni	KN/TS	Isolation of Mn-active bacteria
6/24	am	F. Azam	Bacterial growth and productivity
		A. Brooks	Growth and productivity of phytoplankton
	pm	F. Azam	Methods for determination of bacterial productivity
6/25	am	R. Wrigley	Remote sensing: theoretical considerations
		R. Wrigley	Remote sensing: results of lake studies
6/26	am	A. Brooks	Water, water everywhere (& ice & steam!)
	pm		Laboratory work
6/27	ni	J. Lawless	Remote sensing & global biology at NASA
6/29	am	L. Richardson	Mn oxidation by algae, a mechanism
6/30	am	L. Richardson	Field studies on algal Mn oxidation (phytoplankton and attached algae)
			Laboratory demonstration of Mn uptake by phytoplankton
7/1			Laboratory work all day
7/2			Laboratory work all day
7/3	am	P. Kepkay	Construction and use of microelectrodes
			Laboratory demonstration of microelectrodes
7/6		Jim Morgan	Aqueous solution, precipitation and absorption equilibrium of Mn
		Bob Howarth	Trace metal studies of aquatic environments
7/7		Alan Stone	Reduction of Mn(IV) oxides (part 1)
		Jim Morgan	Rates of Mn(II) oxidation in aquatic systems

7/8		Billy Moore	Radionuclides as tools for the study of aquatic systems
		Alan Stone	Manganese reduction (part II)
7/9		Billy Moore	Studies of Mn nodules and sediments in Oneida Lake
		Bill Ghiorse	Survey of iron and Mn depositing microbe
7/10		Jim Murray	Properties of Mn and iron oxides
		Bill Ghiorse	Leptothrix discophora: Mn oxidizing activity in the lab and field
7/11		Jim Murray	Trace metals in marine aquatic systems
		Liesbeth de Vrind Dept. of Bio-chemistry, U. of Leiden, Holland	Biomineralization (calcification) by Coccolithophores (abstract not included)
7/13	am	P. Kepkay	Modified dialysis chambers for the study of sediment biogeochemistry Mn biogeochemistry of natural sediments
7/14	am	C. Sandgren	Phytoplankton mineralization & mineral metabol. I. Silicon mineralization II. Carbonate and metal mineralization
7/15	am	R. Rosson B. Tebo	Poison controls and the study of Mn oxidation Methods for evaluation of microbial Mn oxidation in nature
7/16	am	B. Tebo R. Slepecky Syracuse U.	Mn cycling at redox interfaces Manganese involvement in formation and heat resistance of spores in Bacillus (abstract not included)
7/17	am	B. Tebo W. Sunda	Bacterial Mn oxidation in the light and dark Mn redox cycling in the photic zone
7/18	ni	R. Rosson	RNA hybridization probes for the study of natural populations of microbes
7/20	am	J. Buyer	Microbial iron metabolism: chemistry and biochem.
		W. Sunda	Trace metal interactions with microbes

7/21	am	S. Silver	A bug's eye view of the periodic table: microbial mineral metabolism
		J. Stolz	Biological magnetite formation
7/22	am	S. Silver	Bacterial resistance to toxic heavy metals: molecular genetics of survival in the real world
		J. Buyer	Microbial iron metabolism: ecology
	ni	J. Titus	Interactions of mercury and cadmium with bacterial populations
7/23	am	J. Stolz	Magnetotactic bacteria in sediments
		K. Nealson	Mn reduction by bacteria
7/24	ni	K. Nealson	Bioluminescence: Emission of light by living organisms
7/27 - 8/8			No scheduled lectures

Faculty and Lecturers of the PBME 1987 Course

NAME AND ADDRESS	PHONE
Azam, Farooq Scripps Institution of Oceanography Food Chain Research Group A-018 La Jolla, CA 92093	619-534-3196 (3194)
Brooks, Art Center for Great Lakes Studies 600 E. Greenfield Ave. Milwaukee, WI 53204	414-649-3004
Buyer, Jeff SMSL, ARS, USDA Building 318 BARC-East Beltsville, MD 20705	301-344-3436
Forney, John Director, Cornell Field Station RR #1 Bridgeport, NY 13030	315-633-9243
Ghiorse, Bill Dept. of Microbiology Cornell University Ithaca, NY 14850	607-256-3086
Howarth, Bob Ecology & Systematics Corson Hall Cornell University Ithaca, NY 14850	607-255-4703
Kepkay, Paul Biological Oceanography Bedford Institute P.O. Box 1006 Dartmouth, Nova Scotia Canada B2Y 4A2	902-426-7256 477-9621
Mills, Ed Cornell Biology Field Station RR #1 Bridgeport, NY 13030	315-633-9243
Moore, Bill Dept. Geology University of South Carolina Columbia, SC 29208	803-777-2262

Morgan, Jim Environmental Engineering Cal Tech 138-78 Pasadena, CA 91125	818-356-4394
Murray, Jim Dept. of Oceanography University of Washington Seattle, WA 98195	206-543-4730
Nealson, Ken Center for Great Lakes Studies 600 E. Greenfield Ave. Milwaukee, WI 53204	414-649-3006
Richardson, Laurie NASA Ames Research Center Moffett Field, CA 94035	415-694-5900
Rosson, Reinhardt Center for Great Lakes Studies 600 E. Greenfield Ave. Milwaukee, WI 53204	414-649-3017
Sandgren, Craig Dept. Biological Sciences Univ. Wisconsin-Milwaukee Lapham Hall Milwaukee, WI 53201	414-963-4279
Schmidt, Tom Dept. of Biology Jordan Hall 138 Bloomington, IN 47405	812-335-6159
Silver, Simon Dept. Microbiology Univ. Illinois-Chicago Chicago, IL 60880	312-996-9608
Stolz, John Dept. Biochemistry Univ. Massachusetts-Amherst Amherst, MA 01003	413-545-0353
Stone, Alan Dept. Geography & Environ. Engineering Johns Hopkins University Baltimore, MD 21218	301-338-8476

Sunda, Bill
N.M.F.S., Southeast Fisheries Center
Beaufort Laboratory
Beaufort, NC 28516
919-728-8754

Tebo, Brad
Scripps Institution of Oceanography
Marine Biology A-002
La Jolla, CA 92093
619-534-5470

Wrigley, Bob
Ecosystems Science and Technology Branch
Mail Stop 242-4
NASA Ames Research Center
Moffett Field, CA 94035
415-694-6060

Students of the PBME 1987 Course

Bolgrien, David W.
Center for Great Lakes Studies
600 E. Greenfield Ave.
Milwaukee, WI 53204
414-649-3000

de Vrind, Liesbeth
Dept. Biochemistry
University of Leiden
Wassenaarseweg 64
2333 AL Leiden
The Netherlands

de Vrind, J.P.M.
Dept. Biochemistry
University of Leiden
Wassenaarseweg 64
2333 AL Leiden
The Netherlands

Enzien, Michael V.
Dept. Biology
Boston Univ.
2 Cummington St.
Boston, MA 02215
617-353-2443

Haberstroh, Sara
Tyler House
Smith College
Northhampton, MA 01063

Hinkle, Gregory J.
Dept. Biology
Boston Univ.
2 Cummington St.
Boston, MA 02215
617-353-2443

Mandernack, Kevin W.
Scripps Inst. Oceanography A-008
U.C.S.D.
La Jolla, CA 92093
619-587-1561 (h)
534-0638 (w)

Riege, Heike
Geomicrobiology Division
University of Oldenburg
PF 2503
D-2900, Oldenburg
West Germany

Robbins, Eleanora I.
US Geological Survey
National Center MS 956
Reston, VA 22092
703-648-6527

Rose, Susan
Dept. Biology
Univ. Wisconsin-Milwaukee
Lapham Hall
Milwaukee, WI 53201

Wickham, Stephen Anthony
Dept. of Biological Sciences
Dartmouth College
Hanover, NH 03755
603-646-3367

Lecturers' Abstracts and References

Farooq Azam
Scripps Institute of Oceanography

"Microbial Food Web Dynamics"

In recent years there has been a dramatic change in our view of the role of heterotrophic bacteria in the matter and energy flow in pelagic aquatic ecosystems. The use of new methods for measuring bacterial biomass and growth rates has shown that 1/3-1/2 of the primary production is required to support the measured rates of bacterial production. Somehow 50% of the primary production becomes dissolved (DOM) and bacteria are able to virtually monopolize the DOM flux. The resulting bacterial production presumably serves as the energetic base for a microbial part of the food web involving predation of protozoa on bacteria.

Farooq Azam
Scripps Institute of Oceanography

"Mechanisms in Bacteria-Organic Matter Interactions
in Aquatic Environments"

The finding that bacteria represent a major pathway for organic matter flux in pelagic ecosystems has raised questions about the coupling mechanisms which allow bacteria to compete so well for the organic matter. I will develop the argument that a tight metabolic coupling exists between DOM production in the environment and the uptake of DOM by bacteria. It is argued that bacteria respond to the presence of DOM production microzones with effective physiological and behavioral strategies to optimize uptake and maintain the utilizable DOM components in the bulk phase at exceedingly low concentrations. The available information on this matter is used to develop conceptual models of bacteria-algae and bacteria-DOM interactions in an ecosystem context.

References (Azam)

Azam, F. and B.C. Cho (1987) Bacterial utilization of organic matter in the sea. In: Ecology of Microbial Communities, M. Fletcher, T.R.G. Gray and J.G. Jones (Eds.) Cambridge University Press.

Azam, F., T. Fenchel, J.G. Field, J.S. Gray, L.A. Meyer-Reil and F. Thingstad (1983) The ecological role of water column microbes in the sea. Marine Ecology Progress Series 10:257-263.

Riemann, B. and M. Sondergaard (1986) Carbon dynamics in eutrophic temperature lakes. Elsevier, Amsterdam and New York.

Williams, P.J. LeB. (1981) The incorporation of microheterotrophic processes in the classical paradigm of the planktonic food web. 115th European Symposium on Marine Biology, Kiel, FRG. Kieler Meeresforsch., Sonderh. 5:1-28.

Jeffrey S. Buyer
United States Department of Agriculture

"Microbial Iron Transport: Chemistry and Biochemistry"

Low molecular weight iron-chelating agents, collectively referred to as siderophores, are produced by virtually all bacteria and fungi under iron-limiting conditions. These chelators, typically hexadentate, utilize catechol functionalities, hydroxamic acids, and alpha-hydroxy carboxylic acids to chelate iron, and have iron-binding constants in the range of 10^{30}. One such siderophore, aerobactin, has been intensively studied in E. coli. An operon containing five genes, responsible for aerobactin biosynthesis and production of the outer membrane receptor protein, is regulated by ferrous iron-binding protein. In higher plants, the response to iron stress includes either reduction of Fe(III) to Fe(II) or production of phytosiderophores. A new method for detection of siderophores (Schwyn and Neilands) utilizes the ferric dye complex Chrome Azurol S.

Preparation of Chrome Azurol S Plates

Dissolve 60.5 mg Chrome Azurol S (CAS) in 50 ml H_2O

Dissolve 72.9 mg Hexadecyltrimethyl ammonium bromide (HDTMA) in 40 ml H_2O

Combine these two with vigorous stirring

Add dropwise 10 ml 10^{-3} M $FeCl_3$ in 10^{-2} M HCl while stirring rapidly

Autoclave. Concentration = 10^{-3} M CAS, 10^{-4} M Fe^{3+}, 2 x 10^{-3} M HDTMA

This is a 10x stock-use 100 ml for 1 L of media

Autoclave the appropriate media and let cool to 45-50°C. Add the CAS mixture slowly while swirling the molten agar rapidly. Swirl some more and pour plates.

The media should be buffered at pH 6.8-7.5 with 0.1M PIPES or HEPES. Total PO_4 should be less than 0.8 g/L, organic acids less than 0.4 g/L. Yeast extract, tryptone, and other complex media all interfere at above 0.1 g/L.

All glassware should be acid-washed!

References (Buyer - lecture 1)

Bagg, A. and J.B. Neilands (1987) Molecular mechanism of regulation of siderophore-mediated iron assimilation. Microbiol. Rev. 51:509-518.

de Lorenzo, V. and J.B. Neilands (1986) Characterization of iuc A and iuc C genes of the aerobactin system of plasmid ColV-K30 in Escherichia coli. J. Bacteriol. 167:350-355.

de Lorenzo, V., S. Wee, M. Herrero and J.B. Neilands (1987) Operator sequences of the aerobactin operon of plasmid ColV-K30 binding the ferric uptake regulation (fur) repressor. J. Bacteriol. 169:2624-2630.

Neilands, J.B. (Ed.) (1984) Siderophores from microorganisms and plants. In: Structure and Bonding 58, Springer-Verlag, New York.

Neilands, J.B. (1981) Microbial iron compounds. Ann. Rev. Biochem. 50:715-731.

Schwyn, B. and J.B. Neilands (1987) A universal method for the detection of siderophores. Anal. Biochem. 160:47-56.

Jeffrey S. Buyer
United States Department of Agriculture

"Microbial Iron Transport: Ecology"

E. coli has several systems for iron uptake. The aerobactin system is associated with virulence in clinical isolates. In addition, E. coli utilizes a number of fungal siderophores for iron transport, presumably to enable the bacteria to compete with fungi for iron while living outside a host. Certain pseudomonads promote plant growth by depriving deleterious organisms of iron, thus providing a better environment for root growth. This competition for iron is mediated by the ability of some organisms to use other organisms' siderophores for iron transport. The structure of one pseudomonad's siderophore, pseudobactin A214, was determined by two-dimensional NMR and partial acid hydrolysis. Iron is believed to be a limiting nutrient in marine systems, yet very little is known about iron uptake mechanisms in phytoplankton. Both siderophores and reduction may play a role. A moderately halophilic Vibrio species was isolated from a cyanobacteria culture and shown to produce aerobactin, a siderophore previously found only among enteric bacteria.

References (Buyer - lecture 2)

Anderson, M. and F.M. Morel (1980) Uptake of Fe(II) by a diatom in oxic culture medium. Mar. Biol. Lett. 1:263-268.

Buyer, J.S. and J. Leong (1986) Iron transport-mediated antagonism between plant growth-promoting and plant-deleterious Pseudomonas. J. Biol. Chem. 261:791-794.

Buyer, J.S., J. Wright and J. Leong (1986) Structure of pseudobactin A214, a siderophore from a bean-deleterious Pseudomonas. Biochemistry 25:5492-5499.

Carbonetti, N., S. Boonchai, S. Parry, V. Vaisanen-Rhen, T. Korhonen and P. Williams (1986) Aerobactin-mediated iron uptake by Escherichia coli isolates from human extraintestinal infections. Infect. Immun. 51:966-968.

Hong, H. and D. Kester (1986) Redox state of iron in the offshore waters of Peru. Limnol. Oceanogr. 31:512-524.

Trick, C.G., R.J. Anderson, A. Gillam and P.J. Harrison (1983) Procentrin: An extracellular siderophore produced by the marine dinoflagellate Procentrum minimum. Science 219:306-308.

Arthur S. Brooks
Center for Great Lakes Studies
University of Wisconsin -- Milwaukee

"General Limnology and Primary Productivity"

To understand the biogeochemistry of aquatic systems one must first have a working knowledge of the basic physics, chemistry and biology of these systems. Water, the essence of such systems, has some unique properties which must be kept in mind in studying lakes. These properties include: 1) the solid phase is lighter than the liquid, 2) the temperature of maximum density is 3.98°C and 3) the temperature-density relationship is not linear; density changes more rapidly per degree at higher temperatures than low. Hence, ice floats, lakes do not freeze solid and warm water overlies cold during periods of stratification. Water also has a very high specific heat, which moderates temperature changes in aquatic systems and influences the overall heat budgets of lakes. The high heat of fusion (80 cal/cc) and vaporization (580 cal/cc) are also important factors to consider in examining the heat flux in lakes. The unique properties listed above are all related to the fact that water molecules form hydrogen bonds with adjacent molecules of water, imparting a structural arrangement that requires energy to break apart.

Light, the source of energy driving most biological processes in the aquatic environment, enters directly from the sun or as scattered, diffuse light from the sky. At the surface of a lake, some light is reflected and some penetrates through the surface. The light which enters the lake water is selectively absorbed by the water molecules themselves as well as by particulate material and dissolved substances. Blue light (460 nm) penetrates the deepest in pure water, while red and infrared are rapidly absorbed near the surface where the most heat is absorbed. Most relatively clear lakes have maximum penetration in the blue-green region of the spectrum due to dissolved substances and particles therein. Dissolved organics in a lake may shift the color of maximum penetration toward the red end of the spectrum.

Lakes in temperate regions are generally well mixed from top-to-bottom in the spring, but become stratified in summer as the surface waters warm and their density decreases relative to that in the deeper layers. Such conditions, where the bottom waters are isolated from atmospheric contact, create an environment which may be quite different from conditions at the surface and may be of geochemical significance, as oxygen and pH may decrease, while CO_2 rises. In the fall of the year as surface temperatures cool and the density difference between the upper (epilimnion) and the lower (hypolimnion) decrease, the energy of the wind and convective mixing combine forces to "turn over" the lake and restore homothermal and uniform chemical conditions once again. The forces of the wind blowing over the surface of a lake, in addition to forming surface waves and inducing mixing, may also set up surface seiches and internal waves which slosh water about in the basin and transport dissolved materials horizontally as well as vertically.

Algae and cyanobacteria living in a lake are the primary producers which fix the energy of the sun and utilize CO_2 to form the organic material which drives the food chain. A cell suspended in the water is moved about through a changing light environment as it is mixed in the water column. The rate of productivity is, therefore, largely determined by the availability of key nutrients, the depth to which light penetrates in the water and the rapidity with which a photosynthesizing cell is moved along the light gradient. The rates at which

mineral nutrients are absorbed and recycled by these cells are to a large degree determined by the basic limnological processes briefly characterized above.

References (Brooks)

American Public Health Assoc. et al. (1985) Standard Methods for the Analysis of Water and Wastewater, 16th ed. APHA Washington.

Fogg, G.E. (1975) Algal Cultures and Phytoplankton Ecology, 2nd ed. Univ. of Wisconsin Press.

Harris, Graham P. (1986) Phytoplankton Ecology: Structure, Function and Fluctuation, Chapman Hall.

Munawar, M. and I.F. Munawar (1986) The seasonality of phytoplankton in the North American Great Lakes, a comparative synthesis. Hydrobiologia 138:85-115.

Parsons, T.R., M. Takahashi and B. Hargrave (1984) Biological Oceanographic Processes, 3rd ed. Pergamon Press.

Parsons, T.R., Y. Maita and C.M. Lalli (1984) A Manual of Chemical and Biological Methods for Seawater Analysis, Pergamon Press.

Platt, T.R. (Ed.) (1981) The physiological basis of phytoplankton ecology. Can. Bull. Fish. Aq. Sci. 210.

Reynolds, C.S. (1984) The Ecology of Freshwater Phytoplankton, Cambridge Univ. Press.

Shearer, J.A., E.R. DeBruyn, D.R. DeClercq, D.W. Schindler and E.J. Fee (1975) Manual of Phytoplankton Primary Production Methodology. Can. Tech. Rept. Fish. and Aquatic Sci. no. 1341.

Sommer, U., X.M. Gilwicz, W. Lampert and A. Dunca (1986) The PEG [Plankton Ecology Group] - model of seasonal succession of planktonic events in fresh waters. Arch. Hydrobiol. 106:433-471.

Wetzel, R.G. and G.E. Likens (1979) Limnological Methods, W.B. Saunders Co.

Wollenweider, R.A. (Ed.) (1974) A Manual on Methods for Measuring Primary Productivity in Aquatic Environments, IBP Handbook No. 12., 2nd ed. Blackwell.

William C. Ghiorse
Cornell University

"Survey of Fe/Mn-depositing (Oxidizing) Microorganisms"

"Iron bacteria" traditionally have been described by the structure of their encrusted extracellular parts (e.g., Gallionella stalks, Leptothrix sheaths, Siderocapsa capsules, and Metallogenium particles). Such description has led to considerable confusion over the identity of the microorganisms producing the structures. Some of the confusion and misconceptions still exist.

Enrichment and isolation of ferromanganese-depositing organisms from natural samples is readily achieved. Usually heterotrophic metal depositors (bacteria and fungi) are obtained when low nutrient selective conditions are employed. Enrichment and isolation of manganese mixotrophs and autotrophs is possible, but has not been achieved reproducibly.

Isolation and study of ferromanganese-depositing budding bacteria led to the hypothesis that at neutral pH, biological Mn oxidation commonly occurs extracellularly in association with acid exopolymers. Iron may be oxidized abiologically, but also accumulates in association with exopolymers. Many bacteria and fungi deposit ferromanganese oxides in this way, possibly employing extracellular oxidizing factors.

References (Ghiorse - lecture 1)

Cowen, J.P. and K.W. Bruland (1985) Deep Sea Res. 32:253.

Dubinina, G.A. (1984) Curr. Microbiol. 11:349-356.

Ehrlich, H.L. (1984) In: Microbial Chemoautotrophy, W.R. Strohl and O.H. Tuovinen (Eds.) Ohio State University Press, Columbus, Ohio, pp.47-56.

Ehrlich, H.L. (1978) Inorganic energy sources for chemolithotrophic and mixotrophic bacteria. Geomicrobiol. J. 1:65-83.

Emerson, S., et al. (1982) Geochim. Cosmochim. Acta 46:1073.

Ghiorse, W.C. (1984) Biology of iron- and manganese-depositing bacteria. Ann. Rev. Microbiol. 38:515-550.

Ghiorse, W.C. and P. Hirsch (1982) Appl. Environ. Microbiol. 43:1464-1472.

Ghiorse, W.C. (1980) In: Biogeochemistry of Ancient and Modern Environments, P.A. Trudinger, M.R. Walter, and B.J. Ralph (Eds.) Springer Verlag, New York, pp.345-354.

Lundgren, D.G. and W. Dean (1979) In: Biogeochemical Cycling of Mineral-Forming Elements, P.A. Trudinger and D.J. Swain (Eds.) Elsevier, N.Y., pp.211-251.

Marshall, K.C. (1979) In: Biogeochemical Cycling of Mineral-Forming Elements, P.A. Trudinger and D.J. Swain (Eds.) Elsevier, N.Y., pp.253-292.

Nealson, K.H. (1983) In: Biomineralization and Biological Metal Accumulation, P. Westbroek and E.W. de Jong (Eds.) D. Reidel, Boston, p.459.

Nealson, K.H. (1983) In: Microbial Geochemistry, W.E. Krumbein (Ed.) Blackwell Scientific Publ., Boston, pp.159-222.

Tebo, B.M. and S. Emerson (1985) Appl. Environ. Microbiol. 50:1268-1273.

William C. Ghiorse
Cornell University

"Leptothrix discophora: Mn Oxidation in Field and Laboratory"

Leptothrix spp. dominate the surface film on Sapsucker Woods swamp and appear to regulate the concentration of Mn and Fe at the air-water interface during the growth season (April-November). Association of L. discophora with Lemna sp. root surfaces also appears to influence the cycle of Fe and Mn in the swamp water.

L. discophora strain SS-1 was isolated from the surface film and has been studied extensively in the laboratory as a model Mn-oxidizing bacterium, even though it has lost the ability to form a sheath. Mn-oxidation occurs extracellularly and does not appear to provide physiologically useful energy to support growth. Mn oxidation may be useful to protect cells from environmental hazards by sequestering toxic metals outside cells, by destroying H_2O_2 or other toxic oxygen species produced by photochemical reactions, or by preventing predation. The extracellular Mn-oxidizing activity of SS-1 has been partly characterized. The activity is associated with a complex of protein-polysaccharide-lipid heteropolymers excreted by the cells. It is inhibited by agents that may alter enzyme proteins (e.g., heat, heavy metals, detergents, pronase) and by some heme protein inhibitors (e.g., azide, cyanide, o-phenanthroline). An SDS-stable 100-110 kDa Mn-oxidizing protein has been identified, but other Mn-oxidizing factors may also be present. The product of the oxidation by concentrated extracellular material was an amorphous Mn (III,IV) oxide under laboratory conditions. Extrapolation of these data to natural systems will require experimental conditions closer to those of natural waters.

References (Ghiorse - lecture 2)

Adams, L.F. and W.C. Ghiorse (1985) Appl. Environ. Microbiol. 49:556-562.

Adams, L.F. and W.C. Ghiorse (1986) Arch. Microbiol. 145:126-135.

Adams, L.F. and W.C. Ghiorse (1987) J. Bacteriol. 169:1279-1285.

Boogerd, F.C. and J.P.M. de Vrind (1987) J. Bacteriol. 169:489-494.

deVrind, J.P.M., et al. (1986) Appl. Environ. Microbiol. 52:1096-1100.

Dubinina, G.A. (1979) Microbiology (USSR) 47:471-478.

Ghiorse, W.C. (1984) In: Current Perspectives in Microbial Ecology, C.A. Reddy and M.J. Klug (Eds.) Am. Soc. Microbiol., Washington, D.C., p.615.

Hastings, D. and S. Emerson (1986) Geochim. Cosmochim. Acta 50:1819-1824.

Robert W. Howarth
Cornell University

"Nutrient Limitation in Aquatic Ecosystems: Regulation by Trace Metals"

Primary production in most lakes is limited by phosphorus availability, while in many estuaries and coastal seas, production is nitrogen limited. A variety of factors contribute to this difference, but the most important difference is in the response of nitrogen fixation. Most lakes will not remain nitrogen limited even if they receive inputs with low N:P ratios and even if they have large nitrogen losses due to denitrification; nitrogen-fixing cyanobacteria will bloom and make up deficits in nitrogen relative to phosphorus, returning the lake to a phosphorus-limited state. However, when estuaries and coastal seas are driven toward nitrogen limitation due to inputs with low N:P ratios or due to denitrification, they tend to remain nitrogen limited; nitrogen fixation does not make up nitrogen deficits in these marine ecosystems as it usually does in lakes.

Why is nitrogen fixation different in lakes than in marine ecosystems? Nitrogen fixation requires iron and molybdenum, both essential components of nitrogenase. These trace metals appear to be much less available in seawater than in most freshwaters, and their low availability in seawater seems to be a major factor keeping rates of nitrogen fixation low in marine ecosystems. For iron, concentrations are much lower in seawater than in most freshwaters since iron typically precipitates from solution in estuaries as freshwater hits the salt wedge. For molybdenum, concentrations are actually higher in seawater than in freshwaters. However, molybdenum availability is nonetheless lower in seawater than in freshwaters because sulfate inhibits the assimilation of molybdenum in seawater. Sulfate concentrations are much higher in seawater than in freshwaters, making it difficult for planktonic organisms to assimilate molybdenum.

References (Howarth)

Cole, J.J., R.W. Howarth, S. Nolan and R. Marino (1986) Sulfate inhibition of molybdate assimilation by planktonic algae and bacteria: Some implications for the aquatic nitrogen cycle. Biogeochem. 2:179-196.

Howarth, R.W. and J.J. Cole (1985) Molybdenum availability, nitrogen limitation, and phytoplankton growth in natural waters. Science 229:653-655.

Howarth, R.W., R. Marino and J.J. Cole (1987) Nitrogen fixation in freshwater, estuarine and marine ecosystems: 2. Biogeochemical controls. Limnol. and Oceanog. (in press).

Howarth, R.W., R. Marino, J.Lane and J.J. Cole (1987) Nitrogen fixation in freshwater, estuarine and marine ecosystems: 1. Rates and importance. Limnol. and Oceanog. (in press).

Paul E. Kepkay
Bedford Institute, Nova Scotia

"Microelectrodes, Microgradients and Microbial Metabolism"

Oxygen and CO_2 microelectrodes are now commonplace. They allow gradients of dissolved oxygen and CO_2 to be determined on mm or sub-mm scales. However, the quantitative analysis of these gradients has lagged behind the sophistication of the measurements. This lack of analysis is particularly important in light of how useful microgradients can be in defining and quantifying changes in metabolism. A microgradient technique has recently been tested on surface-colonizing bacteria associated with manganese nodules in Lake Charlotte, Nova Scotia.

Short-term (65-h) bacterial colonization of 0.2 um (pore size) filters submerged in water from Lake Charlotte is characterized by a well-defined succession of cell types in which small cocci give way to larger, rod-shaped cells. This succession agrees with the concept of attachment as a strategy for survival, in which inactive cocci can attach to a surface and grow into larger, rod-shaped cells by using endogenous nutrients and/or the nutrients accumulated at the solid-liquid interface. The simultaneous measurement and the analysis of oxygen and CO_2 microgradients above colonized surfaces indicate that a peak of respiration accompanies the succession of rods from cocci. CO_2 fixation then becomes apparent as the rods bind manganese and iron to their surfaces. This means that survival by attachment may not be just the province of heterotrophs. It could also be a strategy adopted by metal-oxidizing chemoautotrophs. Long-term (34-day) colonization of similar filters indicates that, while a succession of attached cell types may indeed be a natural occurrence, other factors (such as the selective grazing of larger cells) will tend to obscure the development of this succession.

Further work on suspended aggregates and the benthic boundary layer has demonstrated the power of the microgradient technique when it is used to determine microbial metabolism.

References (Kepkay - lecture 1)

Crank, J. (1975) The Mathematics of Diffusion, 2nd ed. Oxford Univ. Press, Inc., New York.

Kepkay, P.E., P. Schwinghamer, T. Willar and A.J. Bowen (1986) Metabolism and metal binding by surface-colonizing bacteria: Results of microgradient measurements. Appl. Environ. Microbiol. 51:163-170.

Kjelleberg, S., B.A. Humphrey and K.C. Marshall (1982) The effects of interfaces on small, starved bacteria. Appl. Environ. Microbiol. 43:1166-1172.

Kjelleberg, S., B.A. Humphrey and K.C. Marshall (1983) Initial phases of starvation and activity of bacteria at surfaces. Appl. Environ. Microbiol. 46:978-984.

Reimers, C.E., S.K. Kalhorn, S.A. Emerson and K.H. Nealson (1984) Oxygen consumption rates in pelagic sediments from the Central Pacific: First estimates from microelectrode profiles. Geochim. Cosmochim. Acta 48:903-910.

Revsbech, N.P. (1983) In situ measurement of oxygen profiles of sediments by use of oxygen microelectrodes. In: Polarographic Oxygen Sensors, E. Gnaiger and H. Forstner (Eds.) Springer-Verlag, New York, pp.265-273.

Revsbech, N.P. and D.M. Ward (1983) Oxygen microelectrode that is insensitive to medium chemical composition: use in an acid microbial mat dominated by Cyanidium caldarium. Appl. Environ. Microbiol. 45:755-759.

Paul E. Kepkay
Bedford Institute, Nova Scotia

"In Situ Dialysis:
A Tool for Studying Biogeochemical Processes"

An in situ dialysis technique has been developed to examine chemical and bacterial rates of manganese binding as Mn^{2+} diffuses into sediments. With this method, the microbial and abiotic components of manganese binding have been delineated quantitatively in laboratory sediments spiked with manganese oxidizing bacteria. The abiotic removal of manganese by the same sediments has also been determined independently to define the relative importance of adsorbtion, ion exchange and autocatalytic oxidation in the removal of Mn^{2+} from solution. Independent measurements of both bacterial and abiotic manganese binding were in good agreement with the diffusion-controlled rate data, validating the use of this dialysis technique as a means of examining manganese oxidation in situ.

Application of the technique to natural environments has shown that the results can be expressed in two ways. Microbial manganese binding can be expressed as an apparent adsorbtion coefficient and directly compared to the effects of rapid, linear adsorbtion. The kinetics of microbial manganese binding can also be expressed from dialysis cell gradients by assuming the process follows Michaelis-Menten kinetics. To date, the technique has been applied to environments ranging from shallow, organic-rich lakes to deep-ocean, hemipelagic clays. Radionuclides such as ^{241}Am and ^{137}Cs (which are often used to represent the isotopes found in radioactive waste) appear to be inextricably associated with manganese binding and/or oxidation.

References (Kepkay -lecture 2)

Berner, R.A. (1980) Early Diagenesis, A Theoretical Approach. Princeton Univ. Press, Princeton, N.J.

Burdige, D.J. and P.E. Kepkay (1983) Determination of bacterial manganese oxidation rates in sediments using an in situ dialysis technique. I. Laboratory studies. Geochim. Cosmochim. Acta 47:1907-1916.

Crank, J. (1975) The Mathematics of Diffusion. Clarendon Press, Oxford.

Kepkay, P.E. (1985) Kinetics of microbial manganese oxidation and trace metal binding in sediments: Results from an in situ dialysis technique. Limnol. Oceanog. 30:713-726.

Kepkay, P.E., D.J. Burdige and K.H. Nealson (1984) Kinetics of bacterial manganese binding and oxidation in the chemostat. Geomicrob. J. 3:245-262.

Kepkay, P.E. (1986) Microbial binding of trace metals and radionuclides in sediments: Results from an in situ dialysis technique. J. Environ. Radioactivity 3:85-102.

Edward L. Mills
Cornell University

"Oneida Lake and its Food Chain"

Oneida Lake is a shallow eutrophic lake with a surface area of 20,700 ha located on the Ontario Lake Plain of central New York. Mean depth is 6.8 m and 26% of the area is less than 4.3 m. The lake is alkaline and water chemistry is strongly influenced by nutrient-rich streams that flow from the south over outcroppings of Onondaga limestone and through the fertile and highly populated Ontario Lake Plain (Mills et al. 1978).

The walleye (Stizostedion vitreum vitreum) is the dominant piscivorous fish and it shares the limnetic region with yellow perch (Perca flavescens) and smaller numbers of white perch (Morone americana) (Forney 1980). Age-0 yellow perch along with age-0 white perch and young-of-the-year of other species serve as the primary link in the transfer of energy from secondary to higher trophic levels. Development of the Oneida Lake food chain is an annual event and the pattern of maturation is governed by the abundance of age-0 yellow perch. Abundance of yellow perch cohorts by fall have varied 100-fold and it is these annual fluctuations that have lead to complex interactions that are transmitted through the food chain.

The key feature in the development of the walleye-yellow perch-zooplankton food chain is the consistent collapse of the Daphnia pulex population in years when biomass of age-0 yellow perch exceeds 20 kg/ha (Mills et al. 1987). A generalized model of annual biomass cycles of algae and Daphnia when biomass of young yellow perch is high is shown in Figure 1. As young yellow perch approach their maximum summer standing crop, predation suppresses stocks of D. pulex, smaller herbivorous zooplankton appear, and reduced grazing allows an increase in biomass of both nano- and net phytoplankton. Conversely, when yellow perch biomass is less than 10 to 15 kg/ha, large bodied daphnids dominate and stocks of nanophytoplankton are depressed as a consequence of intense grazing.

Seasonal patterns of species succession of the algal community is well defined. A spring algal bloom of diatoms and small flagellates occurs soon after ice-out. Subsequent decline in diatom populations results in a period of maximum water clarity in June when cryptomonads and small flagellates dominate. Cyanobacterial biomass begins to rise in late June through early July, culminating in one or more summer blooms. Daphnia pulex contributes to the regularity of observed phytoplankton and water clarity patterns. As Daphnia biomass increases in the spring, digestible diatom species are heavily grazed on, and by June diatoms give way to faster growing small flagellates. These flagellates are ideal food for Daphnia but fail to reach a high biomass. By July, cyanobacterial biomass peaks, leading to a marked decline in both consumable food resources and reproductive potential of Daphnia pulex. Such food limitation of Daphnia creates a bottleneck in the flow of energy in the pelagic food web of Oneida Lake despite the relatively high productivity of this eutrophic system.

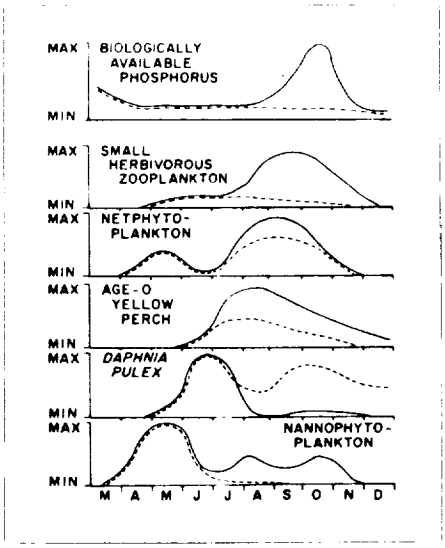

Figure 1. Generalized annual cycle of biologically available phosphorus, phytoplankton, and zooplankton in Oneida Lake when the July-August standing crop of young yellow perch is >20-40 kg/ha (-) and <10-15 kg/ha (--) (after Mills et al. 1987).

References (Mills)

Forney, J.L. (1980) Evolution of a management strategy for walleye in Oneida Lake, New York. New York Fish and Game J. 27:105-141.

Mills, E.L., J.L. Forney, M.D. Clady, and W.R. Schaffner (1978) Oneida Lake. In: Lakes of New York State, Vol. II, J.A. Bloomfield (Ed.) Academic Press, New York, pp.367-451.

Mills, E.L., J.L. Forney, and K.J. Wagner (1987) Fish predation and its cascading effect on the Oneida Lake food chain. In: Predation: Direct and Indirect Impacts on Aquatic Communities, Kerfoot, W.C. and A. Sih (Eds.) University Press of New England, Hanover, New Hampshire, USA, pp.118-131.

William S. Moore
University of South Carolina

"Isotopic Tracers of Scavenging and Sedimentation"

Radioactive isotopes produced by the decay of uranium and thorium provide powerful tracers in studies of scavenging and sedimentation in natural systems. By relating the proper parent-daughter pair, processes having time scales of days to hundreds of thousands of years may be quantified.

One of the most useful isotopes for lake studies is Pb-210, an isotope with a 22 year half life which is produced in the U-238 decay chain. But any use of this or any other isotope depends on the validity of assumptions about processes which control its distribution. In some cases these assumptions may be checked using other isotopes or other information about the system. In other cases the assumptions are accepted on faith. The distribution of Pb-210 with depth in recent (<100 years) sediments often fits a pattern that may be described as a mixing profile near the surface and a decay process further down. But to quantitatively interpret the mixing profiles, we must measure another isotope with a different half life such as Be-7 (half life = 53 days), Th-234 (half life = 24 days) or Th-228 (half life = 1.9 years). To translate the deeper decay profile to a sedimentation rate, we must assume that sedimentation has been constant (or that it has changed abruptly, not gradually), that the sediment always began with the same initial activity of Pb-210 (or that we can normalize Pb-210 to another parameter to correct for changes), that mixing only affects the upper part of the profile (the mixing curve), and that Pb-210 is immobile in the sediments. There are other features which may help constrain the Pb-210 data such as physical variables which have a known time relationship (varves) or other tracers (e.g. bomb-produced ^{137}Cs or Pu which had peak imputs in 1962-63). Without these additional constraints, the Pb-210 data may be modeled in many different ways.

The removal of particle-reactive isotopes provides critical information on the rate of scavenging in natural systems. Using the Th-234 / U-238 pair, scavenging residence times on the order of days may be determined. Using the Th-230 / U-234 pair, the time scale increases to potentially tens of thousands of years, but in fact, is rarely observed to be greater than a few hundred years.

Studies which incorporate isotopic tracers can provide a great deal of information; but, the results are always constrained by the model used to interpret the results. Careful planning and sampling, good lab techniques, and realistic data interpretation are all necessary for a successful study. Too often, studies are conducted which make the difficult isotopic measurements without making the easy measurements of sediment porosity, major components or physical characterictics.

References (Moore - lecture 1)

Benninger, L.K. and S. Krishnaswami (1981) Sedimentary processes in the inner New York Bight: evidence from excess ^{210}Pb and $^{239,240}Pu$. Earth Planet. Sci. Lett. 53:158-174.

Broecker, W.S. and T.-H. Peng (1982) Tracers in the Sea, Eldigio Press.

Cochran, J.K. and R.C. Allen (1979) Particle reworking in sediments of the New York Bight apex: evidence from $^{234}Th/^{238}I$ disequilibrium. Estuarine Coastal Mar. Sci. 9:739.

Robbins, J.A. and D.N. Edgington (1975) Determination of recent sedimentation rates in Lake Michigan using ^{210}Pb and ^{137}Cs. Geochim. Cosmochim. Acta 39:285-304.

Sharma, P., L.R. Gardner, W.S. Moore and M.S. Bollinger (1987) Sedimentation and bioturbation in a salt marsh as revealed by ^{210}Pb, ^{137}Cs and ^{7}Be studies. Limnol. Oceanog. 32:313-326.

William S. Moore
University of South Carolina

"Manganese Nodules from the Deep-Sea and Oneida Lake"

A significant fraction of the deep-sea floor contains nodules of mixed manganese-iron oxides. The processes which control the supply of Mn and Fe as well as the other nodule components, Si, Al, Ca, Co, Ni, Cu, etc. are not well understood. Nor have the processes that produce a dense, hard nodule rather than a diffuse oxide mixture been addressed in a quantitative fashion.

It is now well established from Th-230, Ra-231 and Be-10 dating studies that deep-sea Mn nodules grow very slowly, on the order of 1-5 mm per million years. Why they do not become buried by sediments that accumulate at rates of a few mm per thousand years has been an enigma for 25 years. The answer may be that deep sea organisms mix sediments underneath the nodules much more rapidly than the sediments accumulate. Thus the interface sediments slowly expand upward as new particles are incorporated into the mixed layer. Since the sediments have sufficient structural integrity to support the nodules, they rise with the interface.

The environment of Oneida Lake provides a dynamic regime to study nodule production and destruction. During the summer, the rate of Mn(II) oxidation is rapid. Coatings rich in Mn are observed on objects exposed to the lake bottom waters for only a few weeks to years. There is some evidence that the reduction of Mn(IV) in the nodules and the removal of Mn(II) is necessary to concentrate the iron oxides which appear to give the nodules structural integrity.

Cycling of Mn between the nodule-bearing shoals and the deeper parts of the lake which contain fine grained, organic-rich sediments seems to be regulated by nodule destruction which provides a continual rain of Mn oxides to the reducing sediments and by oxidation of Mn(II) in the lake water. The exact mechanism(s) of Mn oxidation and removal are not well understood.

References (Moore - lecture 2)

Dean, W.E., W.S. Moore and K.H. Nealson (1981) Manganese cycles and the origin of manganese nodules, Oneida Lake, New York, USA. Chem. Geol. 34:53-64.

Krishnaswami, S.A., A. Mangini, J.H. Thomas, P. Sharma, J.K. Cochran, K.K. Turekian and P.D. Parker (1982) ^{10}Be and Th isotopes in manganese nodules and adjacent sediments: nodule growth histories and nuclide behavior. Earth Planet. Sci. Lett. 59:217-234.

Moore, W.S. (1981) Iron-manganese bonding in Oneida Lake ferromanganese nodules. Nature 292:233-235.

Moore, W.S., W.E. Dean, S. Krishnaswami and D.V. Borole (1980) Growth rates of manganese nodules in Oneida Lake, New York. Earth Planet. Sci. Lett. 46:191-200.

Moore, W.S., T.-L. Ku, J.D. Macdougall, V.M. Burns, R. Burns, J. Dymond, M. Lyle and D.Z. Piper (1981) Fluxes of metals to a manganese nodule: radiochemical, chemical, structural and mineralogical studies. Earth Planet. Sci. Lett. 52:151-171.

James J. Morgan
California Institute of Technology

"Aqueous Solution, Precipitation and Redox Equilibria of Manganese in Water"

The stable species of Mn in aquatic systems are discussed. The equilibria and rates of Mn(II) are considered in detail, including solvent (water) exchange, hydrolysis, metal-ligand and complexes and precipitation. Models for seawater and freshwater Mn(II) speciation are reviewed. The general chemical properties of Mn(II) as a rather "hard" transition metal cation are discussed. The Mn(III) and Mn(IV) oxidation states exist, in almost all conditions of natural waters, as oxides or oxide hydroxides, i.e., Mn_3O_4, Mn_2O_3, MnOOH, and MnO_2. (Products of oxygenation of Mn(II) are frequently "non-stoichiometric", i.e., MnO_x, $1<x<2$). The redox energetics, i.e., reduction-oxidation potentials as a function of pH are reviewed for carbonate-free as well as carbonate-containing waters. While energetic treatment of manganese redox reactions, e.g.

$$Mn(II) \rightarrow MnOOH$$

$$Mn(II) \rightarrow MnO_2 \quad \text{, etc.}$$

is straightforward, kinetic experiments are required, together with suitable equilibrium considerations of the Mn(II) reactant species, in order to understand manganese chemistry in aquatic systems.

James J. Morgan
California Institute of Technology

"Rates of Mn(II) Oxidation in Aquatic Systems:
Abiotic Reactions and the Importance of Surface Catalysis"

Early kinetic studies revealed the "autocatalytic" nature of Mn(II) oxidation by O_2. A key step in the mechanism was found to be adsorption of Mn(II) onto the MnO_x reaction product. New experiments in the catalytic role of other surfaces in Mn(II) oxygenation are discussed, in particular the recent thesis results of Simon Davis [Caltech] for goethite, lepidocrocite, alumina and silica. The pH dependance, surface species modeling and activation energies of Mn(II) + O_2 -> MnO_x on the different surfaces are examined and a simplified surface coordination and electron transfer mechanism is proposed. Results of these kinetic experiments have been applied to create models for rates of Mn(II) oxygenation in fresh waters and seawater. The competition of other ions for surface sites in alpha - FeOOH (lepidocrocite) is a key feature of these models. Surface coordination of Mn(II), other cations and major anions is probably one of the dominant processes in mineral catalysis of Mn(II) oxygenation.

References (Morgan)

General Thermodynamics and Energetics

Stumm, W. and J.J. Morgan (1981) Aquatic Chemistry, 2nd ed., Wiley, New York.

Morel, F.M.M. (1983) Principles of Aquatic Chemistry, Wiley, New York.

Garrels and Christ (1965) Solutions, Minerals and Equilibria.

Lerman, A. (1979) Geochemical Processes, Water and Sediment Environments, Wiley-Interscience, New York.

Burgess, J. (1978) Metal Ions in Solution, Horwood, Chichester.

Kinetics

Burgess, J. (1978) Metal Ions in Solution, Horwood, Chichester.

Laidler, K.J. (1963) Reaction Kinetics, Vol. 2, Reactions in Solution, MacMillan, New York.

Basolo, F. and R.C. Pearson (1967) Mechanisms of Inorganic Reactions, 2nd ed., Wiley, New York.

Morgan, J.J. and A.T. Stone (1985) Ch.17. In: Chemical Processes in Lakes, W. Stumm (Ed.) Wiley, New York.

Pankow, J.F. and J.J. Morgan (Nov. 1981) Kinetics for the aquatic environment. Environ. Sci. Technol. 15:1155, 1306.

Fallab, S. (1967) Reactions with molecular O_2. Angew. Chem. 6:496.

Manganese(II) Oxygenation

Morgan, J.J. (1967) Principles and Applications of Water Chemistry, Faust and Hunter (Eds.) Wiley, New York, pp.561-624.

Diem, D. and W. Stumm (1984) Geochim. Cosmochim. Acta 48:1571-1573.

Emerson, S. et al. (1982) Geochim. Cosmochim. Acta 46:1073-1079.

Hastings, D. and S. Emerson, (1986) Oxidation of manganese by spores of a marine Bacillus: Kinetic and thermodynamic considerations. Geochim. Cosmochim. Acta 50:1819.

Davies, S.H.R. (1986) In: Geochemical Processes at Mineral Surfaces, Amer. Chem. Soc. Symp. Ser., No. 323.

Sung, W. and J.J. Morgan (1981) Mn(II) oxidations on the (alpha-FeOOH) lepidocrocite surface. Geochim. Cosmochim. Acta 45:2377-2383.

Davies, S.H.R. and J.J. Morgan (1987) Manganese(II) oxidation kinetics on metal oxide surfaces (manuscript, in preparation)

Davies, S.H.R. (1985) Ph.D. Thesis, Cal Tech.

James W. Murray
University of Washington

"Mechanisms Controlling the Distribution of
Trace Metals in Oceans and Lakes"

There have been few studies of the distribution of trace elements (with the exception being Fe and Mn which are not always trace elements in lakes) in lakes. In the oceans, such studies have been extremely valuable for understanding controlling processes. Such studies are easier in the ocean because steady state can probably be assumed. Unfortunately, the vertical distributions in lakes are much more complicated because they are driven by time-dependent processes of days to seasons. In addition, the sediment area to water volume ratios are much larger in lakes, resulting in a dominant role by sediment-boundary processes.

In the ocean, most data have been generated since 1975. The rules of "oceanographic consistency" have been the essential criteria for the acceptance of data. Accordingly, profiles should be smooth because of the effects of mixing, and elements controlled by the same process should show correlations. There are six main types of profiles in the ocean reflecting a slightly longer list of controlling mechanisms. They are:

1. conservative

2. surface enrichment
   - atmospheric input - natural
   - anthropogenic
   - photochemical production
   - biological excretion
   - river and shelf input

3. nutrient-like
   - hard parts - deep regeneration
   - soft parts - shallow regeneration

4. mid-water maximum
   - hydrothermal
   - isopycnal transport from sea surface
   - oxygen minimum

5. bottom water enrichment
   - sediment flux

6. deep ocean depletion
   - scavenging

The main processes expected to be important in lakes are those previously mentioned, with the exception of hydrothermal. Present data can be used to illustrate nutrient-like behavior, benthic fluxes, redox coupling and scavenging.

Data for Mn, Fe, Cu, Ni, and Cd from Lake Zurich and Lake Washington were used to illustrate these processes. For example, Cd-PO_4 correlations are seen in the ocean and the

ratio is 3.5×10^{-4}. Similar correlations have been seen in the summer in Lake Zurich ($Cd/PO_4 = 1.4 \times 10^{-5}$) and Lake Washington ($Cd/PO_4 = 7.0 \times 10^{-5}$). This suggests that Cd is involved in the nutrient regeneration cycle. During the winter, when lakes are well mixed and productivity is low, there is no increase of Cd and PO_4 with depth. As the lakes stratify, Cd and PO_4 increase with depth and these correlations can be seen. Later in the summer, the Mn and Fe cycles become more intense in the deep water and Cd is removed by scavenging . Thus, there is only a relatively narrow time window during which this nutrient-like behavior can be seen.

Sediment fluxes can be estimated by several independent approaches. Manganese was used as an example. The vertical profiles increase with depth progressively with time over the summer. Using the hypsometric curve for the lake, the rate of increase in depth layers can be calculated and compared to the area of sediment contact. Another approach is to measure the pore water gradient of the sediment-water interface and calculate the flux from Fick's law. A third approach is to measure the flux directly using a bottom lander or a bell jar device. In our study of Lake Washington these three approaches gave reasonably good agreement.

References (Murray - lecture 1)

Baccini, P. and T. Joller (1981) Transport processes of copper and zinc in a highly eutrophic and meromictic lake. Schweiz. Z. Hydrol. 43:186.

Baccini P. and U. Suter (1979) Melimex, an experimental heavy metal pollution study: chemical speciation and biological availability of copper in lake water. Schweiz Z. Hydrol. 41:291.

Boyle E.A. et al. (1981) Cu, Ni and Cd in the surface waters of the North Atlantic and North Pacific oceans. J. Geophys. Res. 86:8048.

Bruland, K.W. (1980) Oceanographic distributions of Cd, Zn, Ni and Cu in the North Pacific. Earth Planet. Sci. Lett. 47:176.

Davison, W., S.I. Heaney, J.F. Talling and E. Rigg (1981) Seasonal transportations and movements of iron in a productive English lake with deep-water anoxia. Schweiz Z. Hydrol. 42:196.

Davison W. and C. Woof (1984) A study of the cycling of manganese and other elements in a seasonally anoxic lake, Rostherne Mere, U.K. Water Research 18:727.

Finlay, B.J., N.B. Hetherington and W. Davison (1983) Active biological participation in lacustrine barium chemistry. Geochim. Cosmochim. Acta. 47:1325.

Hesslein, R.H. (1980) Whole lake model for the distribution of sediment-derived chemical species. Can. J. Fish. Aquat. Sci. 37:552.

Murray, J.W. (1987) Mechanisms controlling the distribution of trace elements in oceans and lakes. In: Sources and Fates of Aquatic Pollutants, Hites, R.A. and Eisenreich, S.J. (Eds.) ACS, Advances in Chemistry Series 216:153-184.

Sholkowitz, E.R. and D. Copland (1982) The chemistry of suspended matter in Esthwaite Water, a biologically productive lake with seasonally anoxic hypolimnion. Geochim. Cosmochim. Acta 46:393.

Articles in:
Stumm, E. (Ed.) (1985) Chemical Processes in Lakes, John Wiley.

a. Davison, W., Conceptual models for transport at a redox boundary, pp.31-54.

b. Morel, F.M.M. and R.J.M. Hudson, The geobiological cycle of trace elements in aquatic systems: Redfield revisited, pp.251-282.

c. Morgan, J.J. and A.T. Stone, Kinetics of chemical processes of importance in Lacustrine environments, pp.389-426.

d. Sholkowitz, E.R., Redox-related geochemistry in lakes: alkali metals, alkaline earth elements and ^{137}Cs, pp.119-142.

e. Sigg, L., Metal transfer mechanisms in lakes: the role of settling particles, pp.283-310.

James W. Murray
University of Washington

"Diagenesis in the Sediments of Lakes"

Organic matter is decomposed at the sediment-water interface and within the sediments of lakes. The products of this decomposition are important for the cycles of many elements in lakes. Alkalinity is generated by the diagenetic reactions and is a sensitive indicator of the extent of diagenesis. Its profile reflects the net effect of all of the individual diagenetic reactions. In addition, the alkalinity flux is important because it indicates the ability of a lake to neutralize acid deposition.

In order to illustrate the effects of organic matter diagenesis in lake sediments, a set of data from Lake Washington sediments was presented and discussed. The data included pore water profiles of alkalinity, total CO_2 methane, iron, manganese, sulfate, ammonia, phosphate, oxygen, calcium and magnesium. The rates of sulfate reduction and methane production from bicarbonate and acetate have been measured directly as well as the Michaelis-Menten kinetic parameters (K_m, V_{max}) for CH_4 oxidation by O_2.

In Lake Washington (a monomictic, mesotrophic lake) there appear to be three zones of diagenesis. At the sediment-water interface (0-7 mm) there is an aerobic zone where dissolved O_2 decreases from bottom water to zero. These profiles have been measured by microelectrodes. Slightly deeper is a sulfate reduction zone over which [SO_4] decreases from the bottom water value of about 100 uM to a "threshold" value of approximately 20 uM. The sulfate reduction zone extends to about 20 cm, but the measured sulfate reduction rates have a maximum at about 8 cm. In this zone acetate and hydrogen are low and constant at about 10 uM and 15 nM respectively. Methane production takes place below the sulfate reduction zone. The maximum methane production rates are in the depth range of 20-27 cm and 69 to 85% of the production comes from acetate fermentation rather than CO_2 reduction.

The alkalinity balance for the pore waters indicate that several processes contribute. Iron reduction, SO_4 reduction, Mn reduction, and Ca and Mg dissolution all contribute about 10-20 % each. Ammonia production from the reactions:

$$\text{Org N} \rightarrow NH_3$$
$$NH_3 + H_2O \rightarrow NH_4^+ + OH^-$$

contributes the largest amount of alkalinity (33-43%). Even after SO_4 reduction is completed, the alkalinity continues to increase. This, together with the fact that we could not account for all the increase in alkalinity by summing the individual diagenetic reactions, led us to search for another contribution. We discovered that adsorbed or exchangeable NH_4^+ on the sediments could account for the missing alkalinity. Direct measurements of exchangeable NH_4^+ confirmed our hypothesis.

The C/N ratio of the decomposing organic matter increased with depth from 3.9 at 7 cm to 14.7 at 53 cm. The primary production had a ratio of 6.8 and the carbon reaching the sediments had a value of 12.6. Thus, the first organic matter decomposed is nitrogen rich relative to the bulk organic matter.

From a balance for total CO_2 (done similarly to that for alkalinity) we calculated the excess total CO_2. When compared with the measured CH_4 we calculated the ratio of CO_2/CH_4 produced during methanogenesis. This ratio varied from 0.77 to 0.92 and suggests that the oxidation state of the organic matter being decomposed is $C_{1.0}H_{2.2}O_{0.9}$ rather than CH_2O.

From these data we have calculated the fluxes for the methane cycle in the surface layer of the sediments.

Process	flux umol/m
Diffusive flux of CH_4 from the anaerobic zone	560 ± 130
Flux of CH_4 to the overlying water as measured by the tripod.	240 to 290
CH_4 oxidation rate	
- by differences from the above fluxes	270 to 320
- calculated from the Michaelis-Menten kinetic parameters.	340 to 740

It appears that about 50% of the upward flux of CH_4 is oxidized to CO_2 by reaction with O_2 within the sediments. The rest of the CH_4 escapes to the overlying water (Figure 1).

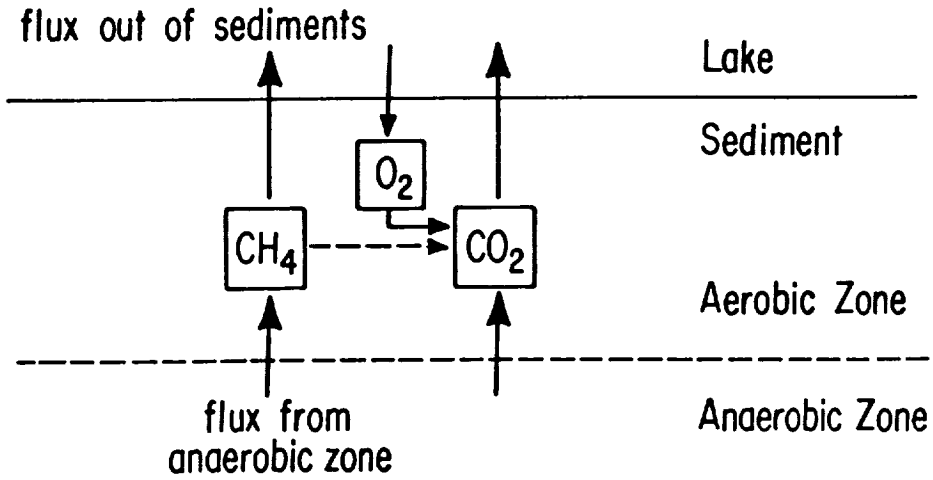

Figure 1. Diagram of carbon flux in lake sediments showing reactions at the oxic/anoxic boundary and at the sediment/water interface.

The breakdown for the carbon cycle is as follows:

Process	flux (μmol/m^2/d)	
primary production (avg. annual basis)	36,000	
carbon flux to sediments from traps	12,500	(30% of primary production)
permanent burial of organic C in sediments	9400	(80% of carbon flux to sediments)
regeneration of carbon from input minus burial	3100	(20% of flux)
Methane production		
a) Diffusive flux of CH_4 to 1 cm.	560	approx. 5% of carbon flux to sediments
b) Diffusive flux into and out of box from 15-35 cm.	240	
c) Integration of direct measurements. Sum of CO_2 and acetate pathways (69-85% from acetate).	401	

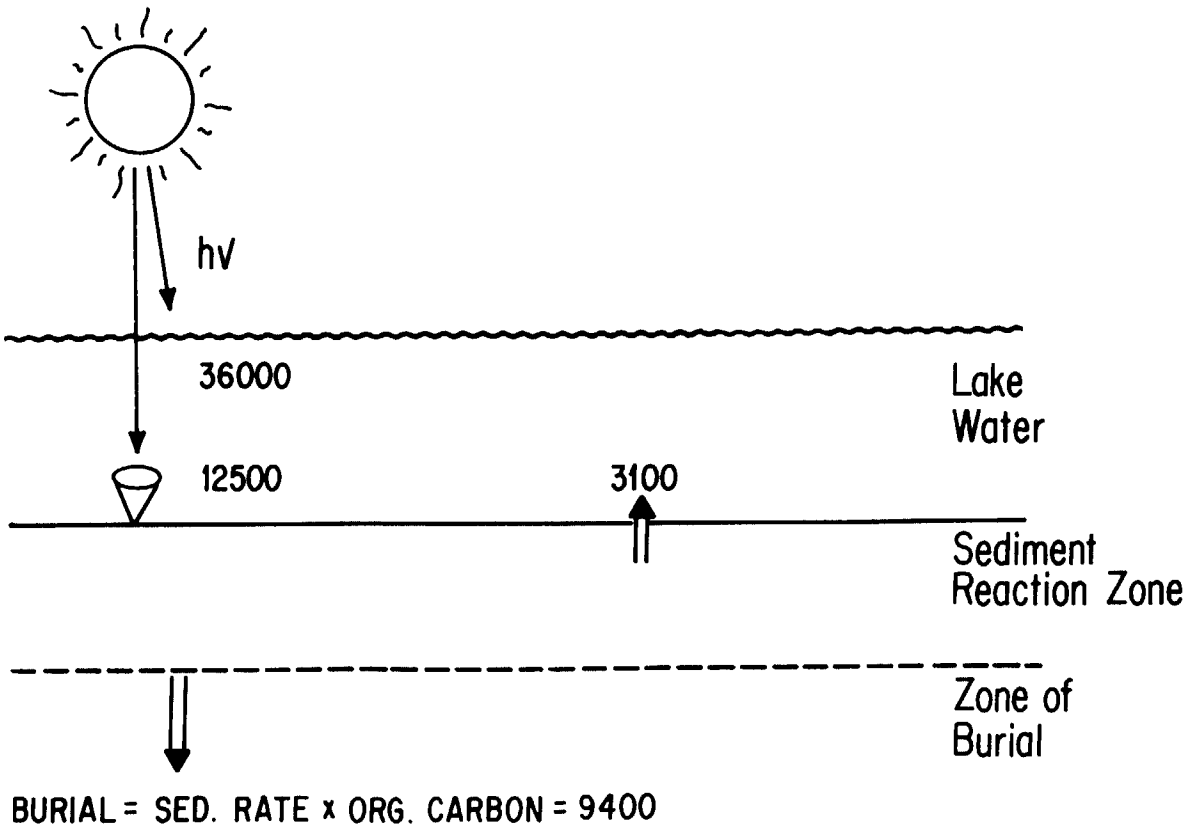

Figure 2. Diagram of carbon cycle in a freshwater lake, including carbon fixation by photosynthetic organisms (36,000), sedimentation of organic carbon (12,500), reoxidation of sedimented carbon (3,100), and carbon burial (9,400).

References (Murray - lecture 2)

Emerson, S. et al. (1980) Early diagenesis in sediments from the eastern equatorial Pacific. 1. Pore water nutrient and carbonate results. Earth Planet. Sci. Lett. 49:57-80.

Fallon, R.D., S. Harrits, R.S. Hanson, and T.D. Brock (1980) The role of methane in internal carbon cycling in Lake Mendota during summer stratification. Limnol. Oceanog. 25:357-360.

Jannasch, H.W. (1975) Methane oxidation in Lake Kivu (Central Africa). Limnol. Oceanog. 20:860-864.

Kuivila, K.M. and J.W. Murray (1984) Organic matter diagenesis in freshwater sediments: The alkalinity and total CO_2 balance and methane production. Limnol. Oceanog. 29:1218-1230.

Kuivila, K.M., J.W. Murray, A.N. Devol, M.E. Lidstrom and C.E. Reimers (1987) Methane cycling in the sediments of Lake Washington. Limnol. Oceanog. (in press).

Lidstrom, M.E. and L. Somers (1984) Seasonal study of methane oxidation in Lake Washington. Appl. Environ. Microbiol. 47:1255-1260.

Quay, P.D., S.E. Emerson, B.M. Quay and A.H. Devol (1986) The carbon cycle in Lake Washington-a stable isotope study. Limnol. Oceanog. 31:596-611.

Rudd, J.W., A. Furutani, R.J. Flett and R.D. Hamilton (1976) Factors controlling rates of methane oxidation and the distribution of methane oxidizers in a small stratified lake. Arch. Hydrobiol. 75:522-538.

Rudd, J.W. and R.D. Hamilton (1979) Methane cycling in Lake 227 in perspective with some components of carbon and oxygen cycles. Hydrobiol. Beih. 12:115-122.

Rudd, J.W. and R.D. Hamilton (1978) Methane cycling in a eutrophic shield lake and its effects on whole lake metabolism. Limnol. Oceanog. 23:337-348.

Rudd, J.W., R.D. Hamilton and N.E. Campbell (1974) Measurements of microbial oxidation of methane in Lake Water. Limnol. Oceanog. 19:519-524.

Rudd, J.W. and C.D. Taylor (1980) Methane cycling in aquatic environments. Adv. Aquat. Microbiol. 2:77-150.

Winfrey, M.S. and Zeikus, J.G. (1977) Effect of sulfate on carbon and electron flow during microbial methanogenesis in freshwater sediments. Appl. Environ. Microbiol. 33:275-281.

Kenneth H. Nealson
Center for Great Lakes Studies
University of Wisconsin -- Milwaukee

"Microbial Manganese Reduction"

Dissolution of insoluble manganese oxides occurs as a result of the reduction of manganese from the oxidized Mn(III) or Mn(IV) states to the reduced manganous Mn(II) state, where it is a soluble cation. Reductive dissolution occurs under conditions of low pH and Eh, and the rates of dissolution can be markedly enhanced by photic processes (as discussed by Sunda), by inorganic ions (sulfide, ferrous iron) and organic compounds such as catechols, organic thiols or organic acids (as discussed by Stone). Bacterial involvement in dissolution is not well understood, but can conceivably occur at several levels and by several mechanisms (Ehrlich, 1981, 1987; Ghiorse, 1988; Nealson, 1983). First, the organisms alter environmental Eh and pH conditions to favor the dissolution of the metal oxides. Second, the organisms can excrete inorganic reductants such as sulfide. Third, the organisms can excrete organic reductants such as pyruvate. Finally, and least well understood, the organisms might use Mn oxides as a terminal electron acceptor for respiration. While this is an attractive hypothesis, no convincing evidence has been presented to support it (Ehrlich, 1987).

Burdige (1983, 1986) reported studies of the kinetics of Mn(IV) reduction by sulfide and sulfate reducing bacteria. In these studies it was shown that sulfide produced by marine sulfate reducing bacteria rapidly catalyzed the following reaction:

$$MnO_2 + H_2S \text{ -------> } Mn^{2+} + S^o + 2\,OH^-$$

The rate limiting step was shown to be the production of sulfide during growth, and the rate of Mn reduction was closely related to the growth rate of the bacteria. Addition of molybdate totally inhibited the reduction of Mn, and stopped growth. Under all conditions tested, when growth was inhibited, sulfate reduction was also inhibited, as was Mn reduction.

Based on these results, Burdige and Nealson (1986) proposed that in environments where Mn is high, the oxidation and reduction of this metal could act as a connecting metabolic link between the sulfur and carbon cycles as shown in the diagram below.

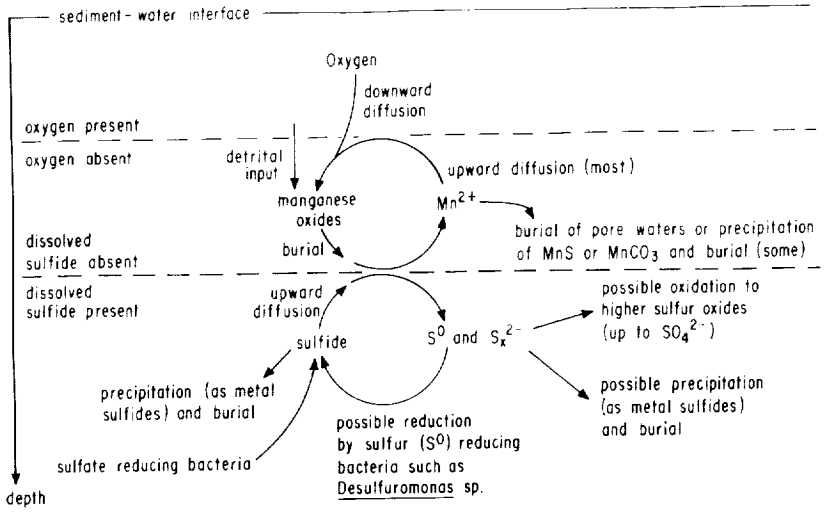

When cultures were enriched on sulfate-free seawater other types of organisms were isolated which were also active in Mn reduction. These enrichments were not inhibited by addition of molybdate or nitrate, but were strongly inhibited by oxygen or azide, suggesting that some part of the activities in the enrichment cultures was due to anaerobic respiration.

One organism (SK13 sp) was isolated from one of the sulfate-free seawater enrichment cultures (Strand, 1985). This organism was a marine Bacillus and was very active in Mn reduction. Reduction was indirect in the sense that no contact was required between the SK13sp cells and the Mn oxides. The cells can produce potent reductants either anaerobically or aerobically, and irrespective of whether Mn oxides are included in the growth medium. Mn reduction was rapid under anaerobic conditions, where the pH was lowered to about 4 during growth. Aerobically, the pH was not lowered, and Mn reduction occurred to a smaller extent. Under anaerobic conditions, the growth yield was enhanced by the addition of Mn oxides.

Studies of the used growth medium (e.g. with cells removed) indicated that a pH sensitive reductant was produced that quantitatively accounted for the Mn that was reduced. Mn was rapidly reduced by used medium when the pH was adjusted to 5 or below. Preliminary analyses of the medium indicated that the reductant was pyruvate. The enhancement of growth yield was apparently due to a buffering of the pH during Mn reduction. These studies are consistent with the hypothesis that the mechanism of Mn reduction by this organism is the production and excretion of organic acid and the alteration of environmental conditions (Stone, 1983, 1987; Stone and Morgan, 1984 a,b).

References (Nealson)

Burdige, D. (1983) The biochemistry of manganese redox reactions: Rates and mechanisms. PhD Thesis, University of California, San Diego.

Burdige, D. and K.H. Nealson (1985) Microbial Mn reduction by enrichment cultures from coastal marine sediments. Appl. Environ. Microbiol. 50:491-497.

Burdige, D. and K.H. Nealson (1986) Chemical and microbiological studies of sulfide-mediated manganese reduction. Geomicrobiol. J. 4:361-387.

Ehrlich, H.P. (1981) Geomicrobiology, Marcel Dekker, Inc., New York.

Ehrlich, H. (1987) Manganese oxide reduction as a form of anaerobic metabolism. Geomicrobiol. J. 5:423-431.

Ghiorse, W.C. (1988) Microbial reduction of manganese and iron. In: Biology of Anaerobic Microoganisms, A.J.B. Zehnder (Ed.) John Wiley & Sons, N.Y.

Nealson, K.H. (1983) The microbial manganese cycle. In: Microbial Geochemistry, W.E. Krumbein (Ed.) Blackwell Sci. Pub. Ltd., Oxford, U.K., pp. 191-222.

Stone, A. (1983) The reduction and dissolution of Mn(III) and Mn(IV) oxides by organics. PhD Thesis, Cal. Inst. Technol.

Stone, A.T. (1987) Microbial metabolites and the reductive dissolution of Mn oxides: oxalate and pyruvate. Geochim. Cosmochim. Acta 51:919-925.

Stone, A.T. and J.J. Morgan (1984) Reduction and dissolution of Mn(III) and Mn(IV) oxides by organics: 1. Reaction with hydroquinone. Env. Sci. Tech. 18:450-456.

Stone, A.T. and J.J. Morgan (1984) Reduction and dissolution of Mn(III) and Mn(IV) oxides by organics: 2. Survey of the reactivity of organics. Env. Sci. Tech. 18:617-624.

Strand, D. (1985) Microbial manganese(III,IV) reduction: Isolation of a marine manganese reducing bacterium and subsequent reduction studies. M.S. Thesis, University of California, San Diego.

Sunda, W. (see abstract in this volume).

Laurie Richardson
NASA Ames Research Center

"Manganese Oxidation and Microbial Activity in Sediments"

The influence of microbial activity is an important consideration when studying the biogeochemical cycling of manganese. Microorganisms have been shown to both oxidize and reduce manganese, thus can directly mediate transformations between soluble (reduced) and particulate (oxidized) forms (for a review, see Nealson et al., 1988). These redox transformations can occur by both direct and indirect mechanisms.

Redox reactions are of particular importance in manganese cycling in sediments, where diffusion is the major physical means of transport of chemical species. Microorganisms are an important component in the reduction, and subsequent remobilization, of manganese below the oxic/anoxic interface (Froelich et al., 1979). The remobilized manganese then diffuses towards the sediment surface, where, under oxic conditions, it is reprecipitated to the solid form. The vertical distributions of both soluble and solid phase manganese in sediments can afford much information about the flux of this element (Graybeal and Heath, 1984).

Reprecipitation of manganese occurs both chemically and biologically. In an effort to separate the two effects, three cores were analyzed from several (z = 900 to 1336 ft) depositional basins of oligotrophic Lake Superior (Richardson and Nealson, 1987). The three cores represented a range of organic carbon content. Vertical profiles of dissolved oxygen, soluble and solid-phase Mn and Fe, % organic carbon, and % nitrogen were measured, along with numbers of viable aerobic and facultatively aerobic heterotrophic bacteria and manganese-oxidizing bacteria. Apparently, environments which contain high (3-5%) organic carbon and a source of soluble manganese favor the growth and metabolism of manganese-oxidizing bacteria.

References (Richardson - lecture 1)

Froelich, P.N., et al. (1979) Early oxidation of organic matter in pelagic sediments of the eastern equatorial Atlantic: suboxic diagenesis. Geochim. Cosmochim. Acta 43:1075-1090.

Graybeal, A.L. and G.R. Heath (1984) Remobilization of transition metals in surficial pelagic sediments from the eastern Pacific. Geochim. Cosmochim. Acta 48:965-975.

Nealson, K.H., B.M. Tebo and R.R. Rosson (1988) Occurrence and mechanisms of microbial oxidation of manganese. Adv. Appl. Microbiol. 33:279-319.

Richardson, L.R. and K.H. Nealson (1987) Distributions of manganese, iron and manganese-oxidizing bacteria in Lake Superior sediments of different organic carbon content. J. Great Lakes Res. (in press).

Laurie Richardson
NASA Ames Research Center

"Phytoplankton and the Manganese Cycle"

Manganese is a required micronutrient. It is of particular importance for phytoplankton and other photosynthetic organisms because it is a co-factor in the water-splitting enzyme of photosystem II (Sauer, 1980). Phytoplankton actively take up and accumulate Mn(II), the reduced biologically available form, to differing degrees (Sunda and Huntsman, 1985; Larch, 1977). In some cases, manganese has been implicated as a limiting micronutrient in aquatic environments (Paerl, 1982).

It has recently been demonstrated, in both the laboratory and the field, that some species of phytoplankton actively oxidize Mn(II) to particulate MnO_x (Richardson, et al., 1988). The oxidation reaction is indirect, and occurs in microenvironments produced by photosynthesizing aggregates of cells. Laboratory experiments, using pH buffers, the photosystem II inhibitor DCMU, and light vs. dark culture conditions, demonstrated that manganese oxidation by phytoplankton is due to a pH effect. A rapid oxidation reaction occurs when pH values rise to 9.5 or above. These results are in agreement with the kinetics of chemical manganese oxidation (Stumm and Morgan, 1981). Phytoplankton which have been shown to oxidize manganese by this mechanism include diatoms, green algae and cyanobacteria (unpublished data).

Investigations using mini-electrodes demonstrated that naturally occurring pelagic aggregates of Microcystis generate microgradients of pH and oxygen which, under calm conditions, can extend 2 mm into the surrounding aquatic environment, as shown in the figure below, from Richardson et al., 1987. The interior of some aggregates have pH values up to 10.75. Large amounts of particulate manganic oxides were found to be physically associated with these aggregates. The oxides were detected by colorimetric reaction with leucoberbelin blue (Krumbein and Altmann, 1973).

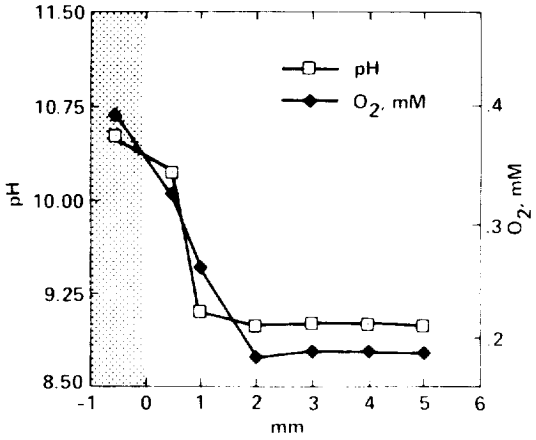

The algal-mediated manganese oxidation mechanism is analagous to $CaCO_3$ precipitation by aquatic macrophytes (Borowitzka, 1984), but is not ubiquitous for all species of aggregate-forming phytoplankton examined. Non-oxidizing forms, such as Gloeotrichia, may have microaerobic as opposed to high pH and oxygen-saturated microenvironments. Aphanizomenon flos-aquae, a non-oxidizing species, does, in fact,

have microaerobic conditions in the interior of "flakes" (Hans Paerl, personal communication).

Oxidation and precipitation of manganese by phytoplankton appears to be important in the seasonal cycling of manganese in Oneida Lake (Richardson, Aguilar, and Nealson, 1987).

References (Richardson - lecture 2)

Borowitzka, M.A. (1984) Calcification in aquatic plants. Plant Cell Env. 7:457-466.

Krumbein, W.E. and H.J. Altmann (1973) A new method for the detection and enumeration of manganese oxidizing and reducing microorganisms. Helgolander Wiss. Meeresunters 25:347-356.

Lorch, D.W. (1977) The action of toxic metals on the green alga Microthamnion Kuetzingianum Chaetophoraceae. 1. Accumulation of manganese, mercury and lead and their influence on growth and development of the alga. Mitt. Inst. Algae Bot. Hamb. 15:5-14.

Paerl, H.W. (1982) Factors limiting productivity of freshwater ecosystems. In: Advances in Microbial Ecology, Vol. VI, K. Marshall (Ed.) Plenum Press, N.Y.

Richardson, L.L., C. Aguilar and K.H. Nealson (1987) Manganese oxidation in pH and oxygen microenvironments produced by phytoplankton. Limnol. Oceanog. (in press).

Sauer, K. (1980) A role for manganese in oxygen evolution in photosynthesis. Acct. Chem. Res. 13:249-256.

Stumm, W. and J.J. Morgan (1981) Aquatic Chemistry, John Wiley and Sons, N.Y.

Sunda, W.G. and S.A. Huntsman (1985) Regulation of cellular manganese and manganese transport rates in the unicellular alga Chlamydomonas. Limnol. Oceanogr. 30:71-80.

Reinhardt Rosson
Center for Great Lakes Studies
University of Wisconsin -- Milwaukee

"RNA Hybridization Probes for the Study of Natural Populations of Microbes"

Bacterial metabolism and growth have a significant impact on the biology and chemistry of aquatic environments. Bacteria have long been recognized as the primary agents responsible for biogeochemical cycling of elements such as carbon, nitrogen and sulfur (Fenchel and Blackburn, 1979). Bacteria are also considered to be important members of a secondary food chain. It has been estimated that the bacterial secondary production level may be as much as 50% of primary production (Azam et al., 1983; Azam and Ammerman, 1984) and that bacteria are actively preyed upon by heterotrophic and omnivorous microflagellates (Fenchel, 1982; Azam et al., 1983; Goldman and Caron, 1985). Unfortunately, the study of bacterial distribution, diversity and community structure is limited by the techniques currently available. While it is often important for the microbial ecologist to identify the members of a given natural community, it remains at best difficult, and at times impossible, to enumerate, identify and quantify specific groups of bacteria in natural environments.

Standard methods for enumeration and estimation of microbial distribution and diversity include: 1) standard plate count methods for estimation of culturable microorganisms; 2) direct counts on stained materials using transmitted light (eucaryotic algae), epifluorescence techniques (bacteria) or scanning electron microscopy for determination of total numbers; 3) ATP measurements, quantification of specific cell wall components, or electron microscopy (used to determine total microbial biomass in a natural sample); and 4) methods that quantify "chemical signatures" of specific groups of bacteria to determine numbers and kinds of organisms present (these techniques have, to date, been primarily applied to sedimentary environments where fermentation and anaerobic respiration predominate). While all microbial ecologists realize that each of these approaches have advantages as well as limitations, these techniques are routinely the best alternatives available.

The microbial ecologist would benefit, in almost every instance, from knowledge of the microbial composition of the natural samples being studied. It is apparent that application of nucleic acid hybridization techniques, in which whole cells, DNA, or RNA extracted from environmental samples is probed or analyzed for specific genetic information, offers several advantages over traditional approaches; these molecular techniques are sensitive, potentially extremely specific, and are relatively rapid and easy to employ.

The recognition that certain oligonucleotide sequences are unique and characteristic of specific functional genes or of groups, genera, or even species of bacteria, has led to the development of DNA and RNA "probe" technology. Radioactive deoxyribo-oligonucleotide probes, applied in hybridization assays of extracted nucleic acids or for direct detection of specfic sequences in whole cells from natural populations, can be used to detect oligonucleotide sequences present in either chromosomal DNA for ribosomal RNA genes (rDNA) or ribosomal RNA (rRNA) within ribosomes. The specificity of hybridization reactions, and the degree of homology necessary for hybridization between the probe and its target nucleic acid sequences to occur, can be controlled by the use of various stringency conditions in the hybridization mixture, which include temperature, salt concentration and formamide content.

Our approach (K.H. Nealson and R.A. Rosson) to application of hybridization probes to studies of natural populations of microbes is primarily based on work by Dr. N. Pace and his colleagues (Pace et al., 1986). Dr. Pace's group has developed a phylogenetic technique in which rRNA nucleotide sequence homologies are used to relate, in a straightforward way, one organism to another (Olsen et al., 1986). The distribution of sequence changes in homologous stretches of the 16S rRNA's (from procaryotes, or 18S from eucaryotes) from different organisms is not random; some segments are nearly perfectly conserved while others are not. In general, several hundred 16S rRNA nucleotides of sequences homologous to reference sequences are sufficient for phylogenetic placement; as the number of homologous sequences compared increases, the more precise becomes phylogenetic placement. This approach is dependent upon isolation of rRNA from specific organisms of interest.

However, when studying natural populations, it is not always possible to directly isolate rRNA in sufficient quantity. Even if sufficient rRNA from a mixed population is available, it is usually impossible to separate all of the 16S rRNA's of the different microorganisms present for direct sequence analysis. Thus, Pace's group is currently developing techniques to extract DNA from natural samples, "shotgun clone" the DNA, and sequence ribosomal DNA (rDNA) containing clones, to identify the various groups of microorganisms present in the original natural population (Stahl et al., 1984; Olsen et al., 1985; Stahl et al., 1985). This is an exciting technique which is still in the early stages of development.

A second approach is to prepare hybridization probes, targeted at either chromosomal DNA or at rRNA. It is possible to identify specific rRNA sequences (obtained from the cloning approach or by direct isolation of rRNA) which are characteristic and representative of all known (or even nonculturable) members of a given genus or species. Preparation of appropriate oligonucleotides, and hybridization of these oligonucleotide probes to bulk DNA or rRNA within whole cells from a natural population provides an estimate of the abundance of that gene in the natural population, respectively. A similar oligonucleotide probe complementary to all known 16S genes (rDNA) would provide a measure of total rDNA present (or similarly, for rRNA, of total ribosomal targets). The specific/total rDNA (or rRNA) ratio yields an approximate estimate of relative cell numbers (Pace et al., 1986). Alternatively, one can combine direct cell counting with autoradiographic detection of specific probes targeted to rRNA (single cell hybridization technique) to visualize, identify, and enumerate specific individuals within a natural population.

There have recently been at least two reports of rRNA probes developed by groups other than Pace and his colleagues. A rRNA probe specific for mycoplasma-like organisms, many of which are difficult to culture or are not culturable (Nur et al., 1986) and a Pseudomonas fluorescens group-specific 23S rRNA probe (Festl et al., 1986) have been described. These probes have been used in dot (naked DNA) and colony (whole cell) hybridizations to show the presence of a specific organism, even in mixed cultures.

Our laboratory (Nealson and Rosson) is developing two separate, but related, types of molecular probes to study the distribution and community structure of both culturable and nonculturable bioluminescent bacteria. Taxa-specific rRNA probes, specifically targeted for ribosomal RNA, will be used to delineate the distribution of marine bacteria (specifically Vibrio and Photobacterium species) in a variety of habitats including planktonic, symbiotic and parasitic. In parallel experiments, function-specific (luciferase) gene probes will be used to distinguish those bacteria carrying the genes for bioluminescence (these probes, similar to the rRNA probes, will be targeted at chromosomal DNA). We feel this two-pronged approach is valuable, because it is known that both luminescent and nonluminescent members of these taxa exist (Reichelt and

Baumann, 1972; Nealson, 1978; Hastings and Nealson, 1981). In a more general sense, while identification of taxa gives information about the distribution of specific groups of organisms, information about metabolism cannot currently be inferred from such taxonomic data (for example, see reviews by Pace et al., 1985, 1986), and hence knowledge of the presence of a specific gene allows a more specific inference of metabolic potential within the identified group of bacteria. Our studies will begin with culturable bioluminescent bacteria, so we can evaluate hybridization probe sensitivity and specificity by comparison to standard methods. We will then proceed to the study of nonculturable bioluminescent bacterial symbionts.

It is clear that this area of research is ready for further study from a variety of approaches, especially those that will make these techniques more quantitative. We have no doubt that this kind of approach, one day, will be used routinely by all microbial ecologists.

References (Rosson - lecture 1)

Azam, F. and J.W. Ammerman (1984) Cycling of organic matter by bacterioplankton in pelagic marine ecosystems; microenvironmental considerations. In: Flows of Energy and Material in Marine Ecosystems: Theory and Practice, M.R.J. Fasham (Ed.) Plenum Press, New York, pp.345-360.

Azam, F., T. Fenchel, J.G. Field, J.S. Gray, L.A. Meyer-Reil and F. Thingstad (1983) The ecological role of water-column microbes in the sea. Mar. Ecol. Prog. Ser. 10:257-263.

Fenchel, T. (1982) Ecology of heterotrophic microflagellates. IV. Quantitative occurrence and importance as bacterial consumers. Mar. Ecol. Prog. Ser. 9:35-42.

Festl, H., W. Ludwig and K.H. Schleifer (1986) DNA hybridization probe for the Pseudomonas fluorescens group. Appl. Environ. Microb. 52:1190-1194.

Goldman, J.C. and D.A. Caron (1985) Experimental studies on an omnivorous microflagellate: implications for grazing and nutrient regeneration in the marine microbial food chain. Deep-Sea Res. 32:899-915.

Hastings, J.W. and K.H. Nealson (1981) The symbiotic luminous bacteria. In: The Prokaryotes, Vol. II, M.P. Starr, H. Stolp, H.G. Truper, A. Balows and H.G. Schlegel (Eds.) Springer-Verlag, Berlin, pp.1332-1346.

Nealson, K.H. (1978) Isolation, identification and manipulation of luminous bacteria. Methods in Enzymology 57:153-166.

Nur, I., J.M. Bove, C. Saillard, S. Rottem, R.M. Whitcomb and S. Razin (1986) DNA probes in detection of spiroplasmas and mycoplasma-like organisms in plants and insects. FEMS Microbiol. 35:157-162.

Olsen, G.J., D.J. Lane, S.J. Giovannoni and N.R. Pace (1986) Microbial ecology and evolution: a ribosomal RNA approach. Ann. Rev. Microbiol. 40:337-365.

Olsen, G.J., N.R. Pace, M. Nuell, B.P. Kaine, R. Gupta and C.R. Woese (1985) Sequence of the 16S rRNA gene from the thermoacidophilic archaebacterium Sulfolabus solfataricus and its evolutionary implications. J. Mol. Evol. 22:301-307.

Pace, N.R., D.A. Stahl, D.J. Lane and G.J. Olsen (1985) Analyzing natural microbial populations by rRNA sequences. ASM News 51:4-12.

Pace, N.R., D.A. Stahl, D.J. Lane and G.J. Olsen (1986) The analysis of natural microbial population by ribosomal RNA sequences. Advan. Microbial Ecol. 9:1-55.

Reichelt, J.L. and P. Baumann (1973) Taxonomy of the marine, luminous bacteria. Archiv fur Mikrobiol. 94:283-330.

Stahl, D.A., D.J. Lane, G.J. Olsen and N.R. Pace (1984) Analysis of hydrothermal vent-associated symbionts by ribosomal RNA sequences. Science 224:409-411.

Stahl, D.A., D.J. Lane, G.J. Olsen and N.R. Pace (1985) Characterization of a yellowstone hot spring microbial community by 5S rRNA sequences. Appl. Environ. Microbiol. 49:1379-1384.

Reinhardt Rosson
Center for Great Lakes Studies
University of Wisconsin -- Milwaukee

"Poison Controls and the Study of Mn Oxidation"

Only a few years ago, evidence for the importance of microbes in catalyzing the oxidation or reduction of manganese in nature was largely circumstantial; direct evidence was unavailable. In certain environments, the presence of high numbers of culturable Mn(II)-oxidizing bacteria, microscopic analysis by scanning and transmission electron microscopy of natural manganese oxide-containing precipitates showing bacteria encrusted and associated with these precipitates, and geochemical studies that suggested the mean residence time of manganese with respect to oxidation was orders of magnitude faster than could be predicted by chemical methods alone, all suggested that biological catalysis of manganese oxidation can be important in many natural environments.

Because of such results and observations, efforts were begun to distinguish biological from chemical Mn(II) oxidation. Using ^{54}Mn as an added tracer, it was possible to easily measure uptake of Mn(II) from solution or removal of Mn(II) from solution by either bacteria, by adsorption to particulates, by oxidation or by a combination of these processes. The problem is to distinguish biological from chemical Mn oxidation. One approach was to measure uptake and removal of Mn(II) from solution in the presence and absence of poisons which specifically inhibit biological activity such as metabolic inhibitors, antibiotics or fixatives (Brock, 1978). By difference, one can determine abiotic (poisoned) and biological (untreated - poisoned) catalysis rates.

In order for the poison approach to be useful, the poisons should not interfere in the solution chemistry of manganese (Rosson et al., 1984). An effective poison will minimally meet the following criteria: 1) the poison should not catalyze Mn(II) oxidation; 2) the poison should not reduce MnO_x; 3) the poison should not displace Mn(II) adsorbed into MnO_x; and 4) the poison should not interfere in adsorbtion of Mn^{2+} onto MnO_x. In addition, when working with sediments, the poison should not interact with dissolved chemical species or with sediment particles, which may make the poison unavailable to inhibit bacterial activity.

After an exhaustive study, several poisons were selected that met these criteria, including sodium azide, well-buffered formaldehyde, and mercuric chloride (Rosson et al., 1984). Virtually all other poisons tested failed to meet one or more of the above criteria.

When the poison control approach is applied to Mn oxidation studies, it should be recognized that the technique measures Mn(II) removal rates from solution, and hence can be used to determine rates of Mn(II) uptake, binding to particulates and removal from solution, but not oxidation rates per se.

Using the poison approach, a variety of studies of Mn(II) binding and oxidation rates have now been completed in a number of different environments. In all of these environments, it was concluded that biological catalysis was important: Saanich Inlet, B.C., Canada (Emerson et al., 1982; Rosson et al., 1984; Tebo and Emerson, 1985); Framvaren Fjord, Norway (Tebo et al., 1984); Oneida Lake, N.Y. (Chapnik et al., 1982); Lake Washington, WA (Maki et al., 1987); Scheldt Estuary, Germany (Wollast et al., 1979); River Tamar Estuary, Southwest England (Vojak et al., 1984); Juan de Fuca Ridge,

Northwest Pacific hydrothermal vent plumes (Cowen et al., 1986); and in Lake Charlotte, Nova Scotia sediments (Kepkay, 1985).

References (Rosson - lecture 2)

Brock, T.D. (1978) The poisoned control in biogeochemical investigations. In: Environmental Biogeochemistry and Geomicrobiology, Vol. 3, W.E. Krumbein (Ed.) Ann Arbor: Ann Arbor Science Publishers, pp.717-725.

Chapnick, S.D., W.S. Moore and K.H. Nealson (1982) Microbially mediated manganese oxidation in a freshwater lake. Limnol. Oceanog. 27:1004-1014.

Cowen, J.P., G.J. Mossoth and E.T. Baker (1986) Bacterial scavenging of Mn and Fe in a mid- to far-field hydrothermal particle plume. Nature 322:169-171.

Emerson, S., S. Kalhorn, L. Jacobs, B.M. Tebo, K.H. Nealson and R.A. Rosson (1982) Environmental oxidation rate of manganese(II): bacterial catalysis. Geochim. Cosmochim. Acta 46:1073-1079.

Rosson, R.A., B.M. Tebo and K.H. Nealson (1984) Use of poisons in determination of microbial manganese binding rates in seawater. Appl. Environ. Microbiol. 47:740-745.

Tebo, B.M., K.H. Nealson, S. Emerson and L. Jacobs (1984) Microbial mediation of Mn(II) and Co(II) precipitation at the O_2/H_2S interfaces in two anoxic fjords. Limnol. Oceanog. 29:1247-1258.

Tebo, B.M. and S. Emerson (1985) Effect of oxygen tension, Mn(II) concentration and temperature on the microbially catalyzed Mn(II) oxidation rate in a marine fjord. Appl. Environ. Microbiol. 50:1268-1273.

Wollast, R., G. Billen and J.C. Duinker (1979) Behavior of manganese in the Rhine and Scheldt estuaries. Estuarine Coast. Mar. Sci. 9:161-169.

Craig Sandgren
University of Wisconsin -- Milwaukee

"Phytoplankton Biomineralization and Nutrition"

An introduction to biological utilization of silicon by freshwater planktonic algae was presented. The geochemical cycling of silicon in lakes was discussed with regard to mineral sources, cycling and solubility in a variety of lake types (Reynolds 1986). Both abiotic and biogenic components of cycling were emphasized. The groups of planktonic microorganisms that biomineralize silicon were listed (Table 1) and the silicification process was compared among these groups (Leadbeater and Ryding 1986). Important processes inherent to silicon biomineralization were dicussed generally and then presented in some detail for two important groups of freshwater phytoplankton: diatoms and chrysophyte flagellates. The processes discussed included silicon uptake, silicon deposition vesicle formation, actual silicon deposition, vesicle exocytosis and super assembly of silicified structures on the cell surface. Primary references for these processes in diatoms include: Werner 1977, Schmidt 1979 & 84, Volcani and Sullivan 1981. Primary references for chrysophyte flagellates include: Sandgren 1980, Leadbeater 1984 & 86, Cronberg 1986 and Preisig 1986, as well as recent and unpublished data of the lecturer.

Table 1. Protistant groups that biomineralize silica.

Group	Structure*	Site	Process
1. diatoms	frustule, cysts (some)	intracellular	biologically controlled
2.a) chrysophytes	cysts, scales (some)	"	"
b) silicoflagellates	skeleton (Dictyocha)	"	"
3. zanthophytes	cysts (rare)	?	?
4. amoebae			
a) testate amoebae	"test" or lorica (some)	extracellular	accretion
b) actinopods (heliozoans)	scales, scaly cyst	intracellular	biologically controlled
c) radiolarians	skeleton	"	"
5. choano-(collar) flagellates	lorica/basket strips	"	"
6. dinoflagellates	internal skeletons rare (Ebria)	"	"

*also a metabolic requirement for Si(pico M) - enzyme cofactor; DNA polymerase

References (Sandgren - lecture 1)

DeHaan, H., T. DeBoer and H.L. Hoogveld (1981) Metal binding capacity in relation to hydrology and algal periodicity in Tjeukemeer, The Netherlands. Arch. Hydrol. 92:11-23.

DeHaan, H., T. DeBoer, J. Voerman, H.A. Kramer and J.R. Moed (1984) Size classes of "dissolved" nutrients in shallow, alkaline, humic and eutrophic Tjeukemeer, The Netherlands, as fractionated by ultrafiltration. Verh. Internat. Verein. Limnol. 22:876-881.

DeHaan, H., M.J.W. Veldhuis and J.R. Moed (1985) Availability of dissolved iron from Tjeukemeer, The Netherlands, for iron-limited growing Scenedesmus quadricauda. Water Res. 19:235-239.

Lehman, J.T. and C.D. Sandgren (1985) Species-specific rates of growth and grazing loss among freshwater algae. Limnol. Oceanogr. 30:34-46.

Craig Sandgren
University of Wisconsin -- Milwaukee

"Algal Biomineralization"

The second lecture included a continuation of the above silicification discussion, and then concluded with information regarding calcification in microscopic algae and a brief overview of algal mineralization of other elements (Tables 2,3). Model systems presented for the study of calcification include: extracellular calcification of the green filamentous alga

Table 2. $CaCl_3$ biomineralization in Protista.

Group	Structure	Site	Process
1. coccolithophorids	coccoliths (scales)	intracellular	biologically controlled
2. green algae:	calcareous "covering"	extracellular	"
a) coenocytic forms	(amorphous)		
b) filaments			
c) charophytes			
3. chrysophytes	impregnation of lorica (Kephyrim)	"	"
4. cyanobacteria	crystalline coverings	"	"
5. brown algae (rare)	" (Padina)	"	"
6. foraminiferans	chambered "test"	either	either
7. red algal corals	ordered cellular encrustation	in wall	biologically controlled?

Table 3. Other types of microalgal mineralization - a survey.

Group	Mineral	Site	Structure
Englenoids (Trachelommas)	Fe & Mn oxides	extracellular	lorica impregnation
chrysophytes (Chrysococcus)	"	"	"
green flagellate (Chlamydomonas)	Mn oxides	"	amorphous precipitation
(Haematococcus)	Fe oxides	"	lorica impregnation
Cyanobacteria (planktonic colonies)	Mn oxides	"	amorphous precipitation
green algae (desmids)	$CaSO_4$ (gypsum)	intracellular (vesicles)	waste accumulation
green algal filaments Spirogyra Chara	$BaSO_4$	intracellular (cytoplasmic)	statoliths

Chara, filamentous cyanobacteria and "coralline" red algae, as well as intercellular formation of coccoliths by prymnesiophyte flagellates (Borowitzka). The importance of chemiosmotic hydrogen ion pumps and of nucleation sites on biological molecules (polysaccharides, cellulose fibrils) in these mechanisms was stressed. Other mineralization processes were summarized from chapters in Leadbeater and Ryding (1986).

References (Sandgren - lecture 2)

Aston, S.R. (1983) Silicon Geochemistry and Biogeochemistry. Academic Press, 248 p.

Barnes, L.S.D., P.L. Walne and J.R. Dunlap (1986) Cytological and taxonomic studies of the Euglenales. I. Ultrastructural and envelope elemental composition in Trachelomonas. Br. Phycol. J. 21:387-97.

Borman, A.H., E.W. DeJong, R. Thierry, P. Westbroek, L. Bosch, M. Gruter and J.P. Kamerling (1987) Coccolith-associated polysaccharides from cells of Emiliana huxleyi (Haptophyceae). J. Phycol. 23:118-23.

Borowitzka, M.A. (1982) Mechanisms in algal calcification. In: Progress in Phycological Research, Vol. 1, F.E. Round and D.J. Chapman (Eds.) Elsevier Biomedical Press, pp.137-177.

Borowitzka, M.A. (1984) Calcification in aquatic plants. Plant Cell Env. 7:457-466.

Darley, W.M. (1973) Silicification and calcification. In: Algal Physiology and Biochemistry, W.D.P. Stewart (Ed.) Univ. California Press, Berkeley, pp.655-675.

Dunlop, J.R. and P.L. Walne (1985) Fine structure and biomineralization of the mucilage in envelopes of Trachelomonas lefevrei. J. Protozool. 32:437-41.

Dunlop, J.R., P.L. Walne and P.A. Kivic (1986) Cytological and taxonomic studies of the Euglenales. II. Comparative microarchitecture and cytochemistry of envelope of Strombomonas and Trachelomonas. Br. Phycol. J. 21:399-405.

Herth, W. and P. Zugenmaier (1979) The lorica of Dinobryon. J. Ultra. Res. 69:262-72.

Leadbeater, B.S.C. (1984) Silicification of "cell walls" of certain protistan flagellates. Phil. Trans. R. Soc. Lond. B. 304:529-536.

Leadbeater, B.S.C. (1986) Scale case construction in Synura petersenii Korsch. (Chrysophyceae). In: Chrysophytes - Aspects and Problems, J. Kristiansen and R.A. Andersen (Eds.) Cambridge Univ. Press, pp.121-131.

Leadbeater, B.S.C. and R. Riding (1986) Biomineralization in Lower Plants and Animals. Oxford Univ. Press, Oxford, 401 p.

Preisig, H.R. and D.J. Hibberd (1983) Ultrastructure and taxonomy of Paraphysomonas (Chrysophyceae) and related genera. 3. Nord. J. Bot. 3:695-723.

Pringsheim, E.G. (1946) On iron flagellates. Phil. Trans. R. Soc. Lond. B. 232:311-342.

Sandgren, C.D. (1980) An ultrastructural investigation of resting cyst formation in Dinobryon cylindricum Imhof (Chrysophyceae). Protistologica 16:259-276.

Schmid, A-M. M. (1979) The development of structure in the shells of diatoms. Nova Hedwigia Beiheft 64:219-231.

Schmid, A-M. M. (1985) Organization and function of cell structures in diatoms and their morphogenesis. In: Proceedings of the Eighth Diatom Symposium, Paris, 1984, M. Ricard (Ed.) pp.271-292.

Simpson, T.L. and B.E. Volcani (1981) Silicon and Siliceous Structures in Biochemical Systems. Springer-Verlag.

Sullivan, C.W. (1976) Diatom mineralization of silicic acid. I. $Si(OH)_4$ transport characteristics in Navicula pelliculosa. J. Phycol. 12:390-396.

Van Emburg, P.R., E.W. DeJong and W.Th. Daems (1986) Immunochemical localization of a polysaccharide from biomineral structures (coccoliths) of Emiliana huxleyi. J. Ultra. Mol. Struct. Res. 94:246-259.

Thomas M. Schmidt
Indiana University

"The Filamentous Sulfur Bacteria: Life at the Interface"

The finding of Thioploca - a filamentous sulfur bacterium - in the sediments of Oneida Lake prompted this lecture. The presence of Thioploca indicates that sulfide is present in the lake sediments, because like the other filamentous sulfur bacteria Beggiatoa and Thiothrix, Thioploca exists at anoxic/oxic interfaces created by hydrogen sulfide and oxygen. The occurrence of sulfides is important to the study of metal cycling in the lake because sulfide reacts quickly with metals (see Nealson abstact this volume).

The filamentous sulfur bacteria are characterized by the presence of periplasmic sulfur inclusions, which result from the aerobic oxidation of sulfide to elemental sulfur. Under oxic conditions, the sulfur in these inclusions is further oxidized to sulfate in some strains. The oxidation of sulfur compounds can be the sole energy source for chemolitho-autotrophic growth of these bacteria. Under anoxic conditions, the elemental sulfur is reduced back to sulfide, serving as a terminal electron acceptor. In additon to these transformations of sulfur, which occur in some strains of each genus, the sheaths of Thioploca may accumulate iron and manganese oxides. The interactions between the cycling of metals and sulfur then might be best studied in an environment like Oneida Lake.

References (Schmidt)

Larkin, J.M. and W.R. Strohl (1983) Beggiatoa, Thiothrix and Thioploca. Ann. Rev. Microbiol. 37:341-367.

Maier, S. and W.C. Preissner (1979) Occurence of Thioploca in Lake Constance and Lower Saxony, Germany. Microbial Ecol. 5:117-119.

Nelson, D.C., N.P. Revsbech, and B.B. Jorgensen (1986) Microoxic-anoxic niche of Beggiatoa spp.: Microelectrode survey of marine and freshwater strains. Appl. Environ. Microbiol. 52:161-168.

Nelson, D.C., B.B. Jorgensen, and N.P. Revsbech (1986) Growth pattern and yield of a chemoautotrophic Beggiatoa sp. in oxygen-sulfide microgradients. Appl. Environ. Microbiol. 52:225-233.

Schmidt, T.M., B. Arieli, Y. Cohen, E. Padan, and W.R. Strohl (1987) Sulfur metabolism in Beggiatoa alba. J. Bacteriol. 169:5466-5472.

Simon Silver
University of Illinois, Chicago

"A Bug's Eye View of the Periodic Table"

Bacterial cells interact with the cations and anions formed from the elements of the Periodic Table. For essentially every cation and anion there are different systems that are genetically determined. Basically, the Periodic Table divides into three classes: (a) good ions that are needed for nutrition of all living cells, (b) abundant but unessential ions that can be used for specific tasks, and (c) bad toxic ions without cellular function. For the good ions (for example K^+, Mg^{2+}, Fe^{2+}, SO_4^{2-} and PO_4^{3-}) there are chromosomal genes that determine membrane transport systems that accumulate these nutrients highly specifically and under careful control. As a generalization there are separate transport systems for every specifically required ion; frequently there is more than a single system (2 each for K^+, Mg^{2+}, and PO_4^{3-}; as many as 5 systems for Fe^{3+} in E. coli). For generally unessential ions such as Ca^{2+}, Cl^- and Na^+ there are also chromosomal genes that code for membrane transport systems. These systems may be oriented inwardly or outwardly as the intracellular concentrations are carefully regulated. Sometimes inward transport serves a specific role (such as Ca^{2+} in bacterial sporulation) and sometimes concentration gradients are used to drive uphill transport of needed nutrients (as in Na^+-amino acid co-transport). For the toxic ions, there are many resistance systems generally coded for by genes found on plasmids and transposons. Hg-resistance is the best understood with three diverse examples having been cloned and sequenced. Mercurial resistance results from two detoxification enzymes, an organomercurial lyase (that breaks the Hg-C bond in phenylmercury, methlmercury and other substrates releasing inorganic Hg^{2+}) and a mercuric reductase, which reduces soluble Hg^{2+} (highly toxic) to volatile Hg^0 (not toxic to bacterial cells). For cadmium and arsenic resistances, the mechanisms of plasmid-determined resistances are not enzymatic detoxification, but rather highly specific outwardly oriented membrane transport systems that excrete the toxic ions as rapidly as they enter the cells. The best-known of the cadmium resistance systems is a $Cd^{2+}/2\ H^+$ electroneutral exchange system. Both AsO_3^{2-} and AsO_4^{3-} are exported by highly specific ATPase systems, for which the responsible DNA has recently been sequenced. Other resistance systems exist for a wide range of toxic cations and anions.

References (Silver - lecture 1)

Laddaga, R.A., R. Bessen and S. Silver (1985) Cadmium-resistant mutant of Bacillus subtilis 168 with reduced cadmium uptake. J. Bacteriol. 162:1106-1110.

Rosen, B.P. and S. Silver (Eds.) (1987) Ion Transport in Prokaryotes, Academic Press, N.Y. (in press).

Silver, S. (1978) Transport of cations and anions. In: Bacterial Transport, B.P. Rosen (Ed.) Marcel Dekker Publ., pp.221-324.

Silver, S. and R.D. Perry (1982) Bacterial inorganic cation and anion transport systems: a bug's eye view of the periodic table. In: Membranes and Transport, Vol. 2, A.N. Martonosi (Ed.) Plenum Press, New York, pp.115-121.

Silver, S. and J. Lusk (1987) Magnesium, manganese and zinc transport. In: Ion Transport in Prokaryotes, B.P. Rosen and S. Silver (Eds.) (in press, manuscript available).

Simon Silver
University of Illinois, Chicago

"What DNA Sequence Analysis Tells Us About Bacterial Toxic Heavy Metal Resistances"

DNA-determined resistances to toxic heavy metals including Hg, As, Cd, Cr, Cu, Bi, Sb, Te, Pb and Zn have been found in a wide range of bacteria. The physiological and biochemical mechanisms of Hg, As, Cd and Cr resistances have been studied. For Hg and As resistances, DNA sequence analysis has clarified the mechanisms involved. The mercurial resistance determinants of gram-negative bacteria consist of regulatory gene (merR), followed by its site of regulation (operator/promoter) followed by up to 6 structural genes (merTPCABD). merT and merP determine a membrane protein and periplasmic binding protein, respectively, required for transporting Hg^{2+} into the cell where it is detoxified (Hg^{2+}--> Hg^{O}) by the mercuric reductase enzyme, product of the merA gene. Mercuric reductase is closely homolgous to other FAD-containing NAD(P)H-requiring enzymes glutathione reductase and lipoamide dehydrogenase. The merB gene (when present) determines organomercurial lyase, the enzyme which cleaves the Hg-C bond in organomercurials such as phenylmercury, yielding less toxic benzene and Hg^{2+}. The mercuric reductase and organomercurial lyase of gram positive bacteria are about 40% identical (at the amino acid level) to those from gram negatives. The roles of the merC (when present) and of the merD gene are not clear. The arsenic resistance operon of both gram-positives and -negatives consists of a regulatory gene plus 3 structural genes: the arsA product appears to be an ATPase, which couples with the arsB product (an inner membrane channel-forming protein) and the smaller arsC gene product (which confers specificity) to form an arsenate and arsenite efflux "pump". There are perhaps five different cadmium-resistance mechanisms governed by genes in different plasmids. The best understood of these is the cadA system of Staphylococcus aureus. Cd^{2+} enters the cell via the Mn^{2+} transport system, for which it is an alternative substrate. It is then transported out from the cell by an electroneutral $Cd^{2+}/2H^{+}$ exchange system that is plasmid encoded and constitutively sythesized. Chromosomal mutations altering the specificity of the Mn^{2+} transport system leads to Cd^{2+} resistance in Bacillus subtilis. Intracellular thiol-rich Cd^{2+} binding proteins sequester Cd^{2+} in Pseudomonas putida. S. aureus has two additional mechanisms of Cd^{2+} resistance: the cadB system confers Cd^{2+} and Zn^{2+} resistance (like cadA), but apparently without a transport basis; and a newly found Cd^{2+} resistance mechanism has an outward transport basis, but involves Cd^{2+}, but not Zn^{2+} and shows no detectable DNA sequence homology with the cadA genes. In summary, for each toxic heavy metal, there is one or more genetically determined resistance system that is highly specific and carefully regulated.

References (Silver - lecture 2)

Chen, C.-M., T.K. Misra, S. Silver and B.P. Rosen (1986) Nucleotide sequence of the structural genes for an anion pump. The plasmid-encoded arsenical resistance operon. J. Biol. Chem. 261:15030-15038.

Griffin, H., T.J. Foster, S. Silver and T.K. Misra (1987) Cloning and DNA sequence of the mercuric and organomercurial resistance determinants of plasmid pDU1358. Proc. Natl. Acad. Sci. USA 84:3112-3116.

Laddaga, R., L. Chu, T.K. Misra and S. Silver (1987) Nucleotide sequence and expression of the mercurial resistance operon from Staphylococcus aureus plasmid pI258. Proc. Natl. Acad. Sci. USA 84, (in press), August issue.

Misra, T.K., N.L. Brown, D.C. Fritzinger, R.D. Pridmore, W.M. Barnes, L. Haberstroh and S. Silver (1984) The mercuric ion resistance operons of plasmid R100 and transposon Tn501: the beginning of the operon including the regulatory region and the first two structural genes. Proc. Natl. Acad. Sci. USA 81:5975-5979.

Misra, T.K., N.L. Brown, L. Haberstroh, A. Schmidt, D. Goddette and S. Silver (1985) Mercuric reductase structural genes from plasmid R100 and transposon Tn501: functional domains of the enzyme. Gene 34:253-262.

Mobley, H.L.T., C.-M. Chen, S. Silver and B.P. Rosen (1983) Cloning and expression of R-factor mediated arsenate resistance in Escherichia coli. Molec. Gen. Genet. 191:421-426.

Ohtake, H., C. Cervantes and S. Silver (1987) Decreased chromate uptake in Pseudomonas fluorescens carrying a chromate resistant plasmid. J. Bacteriol. 169:3853-3856.

Perry, R.D. and S. Silver (1982) Cadmium and manganese transport in Staphylococcus aureus membrane vesicles. J. Bacteriol. 150:973-976.

Silver, S. (1982) Bacterial interactions with mineral cations and anions: good ions and bad. In: Biomineralization and Biological Metal Accumulation, P. Westbroek and E.W. deJong (Eds.) D. Reidel, Dordrecht, The Netherlands, pp.439-457.

Silver, S. and T.K. Misra (1984) Bacterial transformations of and resistances to heavy metals. In: Genetic Control of Environmental Pollutants, G.S. Omenn and A. Hollaender (Eds.) Plenum Press, N.Y., pp.23-46.

Silver, S. (1985) Bacterial transformations of and resistances to heavy metals. In: Environmental Inorganic Chemistry, K.J. Igrolic and A.E. Martell (Eds.) VCH Publishers, Deerfield Beach, Florida, pp.513-540.

Silver, S. (1986) Introduction. In: Biotechnology: Potentials and Limitations, Springer-Verlag, Berlin, pp.1-3.

Silver, S., B.P. Rosen and T.K. Misra (1987) DNA sequencing analysis of the mercuric and arsenic resistance determinants of plasmids of Gram negative and Gram positive bacteria. Proceedings of the Fifth International Symposium on the Genetics of Industrial Microorganisms.

Witte, W., L. Green, T.K. Misra and S. Silver (1986) Resistance to mercury and cadmium in chromosomally-resistant Staphylococcus aureus. Antimicrob. Agents Chemother. 29:663-669.

John Stolz
University of Massachusetts - Amherst

"Biogenic Magnetite in Marine Sediments and Stromatolites"

Magnetotactic bacteria are found in both marine and lacustrine stromatolitic environments. At Laguna Figueroa, Baja California, Mexico, they are abundant in salt marsh pools adjacent to the evaporite flat where laminated sediments are being deposited. The laminated sediments and the microbial community involved in their deposition have been suggested as an analog to communities found preserved in Pre-Cambrian rocks. Magnetotactic bacteria were also found associated with stromatolitic nodules forming in the carbonate oozes at Sugarloaf Key, Florida resulting in the proposal that bacterial magnetites are the primary remanence carrier in limestones. These bacteria can have a profound effect on the magnetic properties of sediments as well. In the Santa Barbara Basin it was discovered that bacterial magnetites increase the natural magnetic remanence of the surface sediments by two orders of magnitude. A survey of many different lacustrine and marine stromatolites by rock magnetic methods indicated many contained single domain magnetite. Bacterial magnetites were successfully extracted from material from Shark Bay, Australia; Palma Solo Pond, Bahamas; and Walker Lake, Nevada, U.S.A.

The occurrence of bacterial magnetite with stromatolites and laminated sediments suggests they should be found in analogous ancient formations. The biogenicity of the magnetofossils are determined by: 1) composition, 2) morphometrics (size, shape, crystal habit) and 3) environment of deposition. Fossil bacterial magnetites have been extracted from deep sea sediments as old as 50 Myr as well as many stromatolitic carbonates and cherts. The oldest definitive magnetofossil is from a 500 Myr old organic rich limestone from the Sinskian formation in China. Putative magnetofossils have been found in microfossiliferous cherts of the 2 Gyr old Gunflint Formation. These findings suggest the bacterial magnetites might be used as a trace fossil and the mechanism of magnetite biomineralization may be older than 2 billion years.

Magnetotactic Bacteria in Oneida Lake

Magnetotactic bacteria were found in all surface sediments examined. Several morphologies were observed including rods, coccoids and colonial coccoids. They numbered between 10^5 and 10^7 bacteria/cm^3, depending on where and how the sediments were collected. Sediments collected in bottles (where only the surface flocculent was

Locality	Magnetic bacteria/cm^3
Buoy 123 surface sediment, bottle (s.s.b.)	10^5
Buoy 127 s.s.b. (7/21/87) nodule area	10^7
Buoy 127 s.s.b. (7/23/87) "anoxic"	10^6
Buoy 127 s.s.b. (7/23/87) "oxic"	10^6
Buoy 127 core (7/23/87) "oxic" 0-1 cm	4×10^5
Buoy 127 core (7/23/87) "anoxic" 0-1 cm	10^5
Buoy 127 core (7/23/87) "anoxic" 1-2 cm	10^4
Buoy 127 core (7/23/87) "anoxic" 2-3 cm	$< 10^3$
Hitchcock stream	10^6

collected) yielded consistently higher numbers than those collected as cores (where the sediments were examined in 1 cm intervals). The highest numbers were found in the surface sediments directly associated with the manganese nodules at Buoy 127 ($> 10^7$). Electron microscopy and magnetometry of the sediments are in progress. These data suggest that magnetic bacteria may play a significant role in the microbial iron cycle of Oneida Lake.

John Stolz
University of Massachusetts - Amherst

"Formation of Biogenic Magnetite"

Magnetite (Fe_3O_4) is an iron oxide which contains both ferric and ferrous iron. This mineral is highly magnetic and when formed at high temperatures (>500°C) may contain a considerable amount of titanium (as much as 25%) as well as other cations (Mn, Al, Cr). The magnetic properties are dependent on composition and particle size. Crystals which are too small to be intrinsically magnetic (i.e. smaller than 40 nm) are called superparamagnetic. Crystals which are just large enough to be naturally magnetic (roughly between 40 nm and 120 nm) are said to be single domain and behave as a dipole (with a north and south pole). Larger multi-domain crystals (>120 nm) contain many magnetic domains, which tend to cancel each other resulting in a poorly magnetized mineral.

Biologically produced magnetites, especially those which are deposited within a specialized membrane bound structure, are usually very pure. They are typically single-domain and can be detected in both biological (e.g. bacteria, tissue) and geological (e.g. sediments, rocks) samples by rock magnetic techniques (e.g. SQUID magnetometry, coercivity spectra). To date, biogenic magnetite has been found in bacteria, algae (Anisonema sp.), monarch butterflies, honeybees, chitons, tuna, salmon, pigeons, and several cetaceans (Table 1). Three different types of magnetite biomineralization are summarized here (one eucaryotic and two procaryotic systems).

Table 1. Biogenic magnetite in nature.

Procaryotes
- Aquaspirillum magnetotacticum GS-15[5]

Protoctists
- Anisonema sp.

Animalae
- Monarch butterflies
- Honeybees (Apis mellifera)
- Chitons
- Tuna (Thunnus albacaes)
- Salmon (Oncorhynchus tshawytscha)
- Pigeons
- Cetaceans (e.g. dolphins, whales)

Chitons (Cryptochiton stelleri, Chiton tuberculatus, Acanthopleura echinatum)

Chitons are invertebrate animals (Polyplacophora) which typically feed on endolithic bacteria and algae. They graze the surface of rocks with hard mineralized teeth, digesting the organisms and discarding the rock. The teeth are found on a grinding organ, the radula, and contain magnetite as well as other minerals (lepidocrocite and francolite in C. tuberculatus; amorphous ferric phosphate in C. stelleri; lepidocrocite and dahlite in A.

echinatum). Magnetite is formed in the organic framework of the teeth in the radula (unmineralized teeth in rear, gradual mineralization to the anterior) by the sequence shown in Table 2.

Aquaspirillum magnetotacticum

A. magnetotacticum is a microaerophilic, heterotrophic (tartrate, succinate, fumarate), chemotactic (O_2 phobic), magnetotactic spirillum. It contains a chain of single domain magnetite crystals which are precipitated in a membrane bound organelle, the magnetosome. Free oxygen (1%) is necessary for growth and magnetite production, and although nitrate enhances magnetite formation, NO_3 alone does not support growth. The pathway shown in Table 2 has been determined, with ferric quinate located extracellularly, and all else occurring in the magnetosome, with Fe^{+2} "appearing as a transient between step 1 and 2."

GS-15

GS-15 is a non-motile, non-magnetotactic, strictly anaerobic, nitrate-reducing heterotroph (acetate, butyrate). When using ferric iron as the terminal electron acceptor to oxidize acetate, it converts ferric oxide to magnetite, extracellularly. Although little else is known of its physiology, it apparently forms the magnetite as shown in Table 2.

Table 2. Mechanisms of biomineralization.

Chitons (Cryptochiton stelleri, Chiton tuberculatus)

Invertebrate; aerobic magnetite formed in organic framework of teeth in radula (unmineralized teeth in rear, gradual mineralization anterior)

ferritin ---> ferrihydrite (5 $Fe_2O_3 \cdot H_2O$) ---(reduction)---> magnetite

associated minerals: lepidocrocite, francolite (C. tuberculatu)
amorphous ferric phosphate (C. stelleri)
dahlite (carbonate apatite)

Aquaspirillum magnetotacticum

Magnetotactic bacterium; microaerophile; nitrogen fixation (acetylene reduction); heterotrophic (tartarate, succinate, famarate); magnetite precipitated in membrane bounded organelle "magnetosome"; O_2 necessary (1%); nitrate enhances magnetite formation, but can't grow anaerobically with nitrate; chemotactic (O_2 phobic).

ferric quinate ---(Fe^{+2})---> low density hydrous ferric oxide--->

ferrihydrite ---(reduction)---> magnetite.

GS-15

Non-motile; non-magnetotactic; strict anaerobe; nitrate reducer; heterotrophic (acetate, butyrate); when using ferric iron as terminal electron acceptor to oxidize acetate, converts ferric oxide to magnetite, extracellularly

amorphous ferric oxide + acetate ---> $Fe_3O_4 + CO_2$

References (Stolz)

Balkwill, D.L., D. Maratea and R.P. Blakemore (1980) Ultrastructure of a magnetotactic spirillum. J. Bacteriol. 141:1399-1408.

Bazylinski, D.A. and R.P. Blakemore (1983) Nitrogen fixation (acetylene reduction) in Aquaspirillum magnetotacticum. Curr. Microbiol. 9:305-308.

Bazylinski, D.A. and R.P. Blakemore (1983) Denitrification and assimilatory nitrate reduction in Aquaspirillum magnetotacticum. Appl. Environ. Microbiol. 46:1118-1124.

Blakemore, R.P. (1975) Magnetotactic bacteria. Science 190:377-379.

Blakemore, R.P. (1982) Magnetotactic bacteria. Ann. Rev. Microbiol. 36:217-238.

Blakemore, R.P. and R.B. Frankel (1981) Magnetic navigation in bacteria. Sci. Amer. 245:58-65.

Blakemore, R.P., R.B. Frankel and A.J. Kalmijn (1980) South-seeking magnetotactic bacteria in the Southern Hemisphere. Nature 286:384-385.

Blakemore, R.P., D. Maratea and R.S. Wolfe (1979) Isolation and pure culture of a freshwater magnetic spirillum in chemically defined medium. J. Bacteriol. 140:720-729.

Chang, S.R. and J.L. Kirschvink (1984) Bacterial magnetofossils as probes of Precambrian ecological and biochemical evolutionary events. Abstracts of Ann. Meeting of Geol. Soc. Amer. 16:468.

Chang, S.R. and J.L. Kirschvink (1985) Possible origin of biogenic magnetite fossils from the Miocene marine clays of Crete. In: Magnetite Biomineralization and Magnetoreception in Organisms, J.L. Kirschvink, D.S. Jones and B.J. McFadden (Eds.) Plenum Press, N.Y., pp. 647-669.

Chang, S-B.R., J.F. Stolz and J.L. Kirschvink (1987) Biogenic magnetite as a primary remanence carrier in limestone deposits. Phys. Earth Plan. Phys. 46:289-303.

Esquivel, D.M.S. and H.G.P. Lins de Barros (1986) Motion of magnetotactic microorganisms. J. Exp. Biol. 121:153-163.

Frankel, R.B. (1984) Magnetic guidance of organisms. Ann. Rev. Biophys. Bioeng. 13:85-103.

Frankel, R.B. (1986) Magnetic skeletons in Davy Jones' locker. Nature 320:575.

Frankel, R.B., R.P. Blakemore, F.F. Torres de Araujo, D.M.S. Esquivel, and J. Danon (1981) Magnetic bacteria at the geomagnetic equator. Science 212:1269-1270.

Frankel, R.B., R.P. Blakemore and R.S. Wolfe (1978) Magnetite in freshwater magnetotactic bacteria. Science 203:1355-1356.

Frankel, R.B., G.C. Papaefthymiou, R.P. Blakemore and W.D. O'Brien (1983) Fe_3O_4 precipitation in magnetotactic bacteria. Biochim. Biophys. Acta 763:147-159.

Kirschvink, J.L. (1980) South-seeking magnetic bacteria. J. Exper. Biol. 86:345-347.

Kirschvink, J.L. (1980) Biogenic magnetite (Fe_3O_4): A ferromagnetic mineral in bacteria, animals and man. In: Ferrites: Proceedings of the International Conference, September-October, Japan, pp.135-138.

Kirschvink, J.L. (1982) Birds, bees and magnetism. Trends in Neurosci. 5: 160-167.

Kirschvink, J.L. (1982) Paleomagnetic evidence for fossil biogenic magnetite in western Crete. Earth Plan. Sci. Lett. 59:388-392.

Kirschvink, J.L. (1983) Biomagnetic geomagnetism. Ann. Rev. Geophys. Space Phys. 21:672-675.

Kirschvink, J.L. and S.R. Chang (1984) Ultrafine-grained magnetite in deep-sea sediments: Possible bacterial magnetofossils. Geology 12:559-562.

Kirschvink, J.L. and J.L. Gould (1981) Biogenic magnetite as a basis for magnetic field detection in animals. BioSystems 13:181-201.

Kirschvink, J.L. and H.A. Lowenstam (1979) Mineralization and magnetization of chiton teeth: Paleomagnetic, sedimentologic and biologic implications of organic magnetite. Earth Plan. Sci. Lett. 44:193-204.

Kirschvink, J.L., A.E. Dizon and J.A. Westphal (1986) Evidence from strandings for geomagnetic sensitivity in cetaceans. J. Exp. Biol. 120:1-24.

Kirschvink, J.L., D.S. Jones, and B.J. MacFadden (1985) Magnetite Biomineralization and Magnetoreception in Organisms: A New Biomagnetism. Plenum Publishing Co., New York.

Kirschvink, J.L., M.M. Walker, S-B. Chang, A.E. Dizon, and K.A. Peterson (1985) Chains of single-domain magnetite particles in chinook salmon. Oncorhynchus tshawytscha. J. Comp. Physiol. A 157:375-381.

Lovley, D.R., G.L. Nord Jr., E.J.P. Phillips and J.F. Stolz (in press) Anaerobic production of magnetite by a dissilatory iron reducing bacterium. Nature 336:252-254.

Lowenstam, H.A. (1962) Magnetite in denticle capping in recent chitons (Polyplacophora). Geol. Soc. Amer. Bull. 73:435-438.

Lowenstam, H.A. (1967) Lepidocrocite, an apatite mineral, and magnetite in teeth of chitons (Polyplacophora). Science 156:1373-1375.

Lowenstam, H.A. (1986) Mineralization processes in monerans and protoctists. In: Biomineralization of Lower Plants and Animals, B. Leadbeater and J. Riding (Eds.) Oxford University Press, pp.1-17.

Lowenstam, H.A. and S. Weiner (1985) Transformation of amorphous calcium phosphate to crystalline dahlite in the radular teeth of chitons. Science 227:51-53.

Mann, S., R.B. Frankel and R.P. Blakemore (1984) Structure, morphology and crystal growth of bacterial magnetite. Nature 310:405-407.

Matsuda, T., J. Endo, N. Osakabe and A. Tonomura (1983) Morphology and structure of biogenic magnetite particles. Nature 302:411-412.

Moench, T.T. and W.A. Konetzka (1978) A novel method for the isolation and study of a magnetotactic bacterium. Arch. Microbiol. 119:203-212.

Petersen, N., T. von Dobeneck and H. Vali (1986) Fossil bacterial magnetite in deep-sea sediments from the South Atlantic Ocean. Nature 320:611-615.

Rosenblatt, C., F.F. Torres de Araujo and R.B. Frankel (1982) Light scattering determination of magnetic moments of magnetotactic bacteria. J. Appl. Physiol. 53:2727-2729.

Rosenblatt, C., F.F. Torres de Araujo and B.B. Frankel (1982) Birefringence determination of magnetic moments of magnetotactic bacteria. Biophys. J. 40:83-85.

Spormann, A.M. (1987) Unusual swimming behavior of magnetotactic bacterium. FEMS Microbiol. Ecol. 45:37-45.

Spormann, A.M. and R.S. Wolfe (1984) Chemotactic, magnetotactic and tactile behaviour in a magnetic spirillum. FEMS Microbiol. Lett. 22:171-177.

Stolz, J.F., S-B.R. Chang and J.L. Kirschvink (1986) Magnetotactic bacteria and single-domain magnetite in hemipelagic sediments. Nature 321:849-851.

Stolz, J.F., S-B.R. Chang and J.L. Kirschvink (1987) The effect of magnetotactic bacteria on the magnetic properties of marine sediments. In: Proceedings of the Fifth International Symposium on Biomineralization, R.E. Crick (Ed.) Chicago University Press (in press).

Towe, K.M. and H.A. Lowenstam (1967) Ultrastructure and development of iron mineralization in the radular teeth of Cryptochiton stelleri (Mollusca). J. Ultrastruct. Res. 17:1-13.

Towe, K.M. and T.T. Moench (1981) Electron-optical charaterization of bacterial magnetite. Earth Plan. Sci. Lett. 52:213-220.

Torres de Araujo, F.F., M.A. Pires, R.B. Frankel and C.E.M. Bicudo (1986) Magnetite and magnetotaxis in algae. Biophys. J. 50:375-378.

Von Dobeneck, T., N. Petersen and H. Vali (1987) Bakterielle magnetofossilien. Geowissenschaften in unserer Zeit 5:27-35.

Walcott, C., J.L. Gould, and J.L. Kirschvink (1979) Pigeons have magnets. Science 205:1027-1029.

Walker, M.M. and M.E. Bitterman (1985) Conditioned responding to magnetic fields by honeybees. J. Comp. Physiol. A 157:67-71.

Walker, M.M., A.E. Dizon and J.L. Kirschvink (1982) Geomagnetic Field detection in Yellowfin Tuna. Oceans '82 Conference Record, IEEE Press, New York, p.755-758.

Walker, M.M., A.E. Dizon and J.L. Kirschvink (1985) Magnetoreception and biomineralization of magnetite in fish. In: Magnetite Biomineralization and Magnetoreception in Organisms, J.L. Kirschvink, D.S. Jones and J.J. McFadden (Eds.) Plenum Press, N.Y., pp.417-437.

Walker, M.M., J.L. Kirschvink, S-B.R. Chang and A.E. Dizon (1984) A candidate magnetic sense organ in the Yellowfin Tuna Thunnus albacares. Science 224:751-753.

Wolfe, R.S., R.K. Thauer and N. Pfennig (1987) A "capillary racetrack" method for isolation of magnetotactic bacteria. FEMS Microbiol. Ecol. 47:31-35.

Alan Stone
Johns Hopkins

"Influence of Metals and Metal Oxides on Transformations of Organic Compounds"

Metal ions and metal-bearing minerals influence the chemistry of organic compounds in natural waters because of their ability to (i) form dissolved complexes and surface complexes with organic ligands, (ii) participate in oxidation-reduction reactions involving organic compounds, and (iii) catalyze hydrolysis and nucleophilic substitution reactions of organic compounds. Susceptibilities of organic compounds towards reactions involving metal ions and mineral surfaces vary substantially. Chelation of metals can take place when organic compounds possess two or more donor atoms in the proper configuration. Chelation dramatically increases the capacity for metal coordination, often facilitating transformation reactions involving metals.

Adsorption of organic compounds at mineral surfaces arises from the combined effect of surface complex formation, electrostatic interaction with the charged surface and exclusion. Rates of organic compound oxidation or hydrolysis can be promoted by adsorption, since local chemical conditions and concentrations of reactive species are different from overlying solution. Thus, adsorption onto mineral surfaces can affect both the distribution of organic compounds and their ultimate fate in natural waters.

References (Stone - lecture 1)

Balistrieri, L.S. and J.W. Murray (1987) The influence of the major ions of seawater on adsorption of simple organic acids by goethite. Geochim. Cosmochim. Acta. 51:1151-1160.

Barcelona, M.J. and D.K. Atwood (1978) Gypsum-organic interactions in natural seawater: effect of organics on precipitation kinetics and crystal morphology. Mar. Chem. 6:99-115.

Buckingham, D.A. (1977) Metal-OH and its ability to hydrolyze (or hydrate) substrates of biological interest. In: Biological Aspects of Inorganic Chemistry, A.W. Addison, W.R. Cullen, D. Dolphin and B.R. James (Eds.) Wiley, N.Y.

Colliene, R.H. (1983) Photoreduction of iron in the epilimnion of acidic lakes. Limnol. Oceanogr. 28:83-100.

Gieskes, W.W.C. and G.W. Kraay (1982) Effect of enclosure in large plastic bags on diurnal change in oxygen concentration in tropical ocean water. Mar. Biol. 70:99-104.

Hoffmann, M.R. (1980) Trace Metal Catalysis in Aquatic Environments. Environ. Sci. Technol. 14:1061-1066.

Houghton, R.P. (1979) Metal Complexes in Organic Chemistry. Cambridge University Press, Cambridge.

Kummert, R. and W. Stumm (1980) The surface complexation of organic acids on hydrous gamma-Al_2O_3. J. Colloid Interface Sci. 75:373-385.

Larson, R.A. and J.M. Hufnal (1980) Oxidative polymerization of dissolved phenols by soluble and insoluble inorganic species. Limnol. Oceanogr. 25:505-512.

Loder, T.C. and P.S. Liss (1985) Control by organic coatings of the surface charge of estuarine suspended particles. Limnol. Oceanogr. 30:418-421.

Miles, C.J. and P.L. Brezonik (1981) Oxygen consumption in humic-colored waters by a photochemical ferrous-ferric catalytic cycle. Environ. Sci. Technol. 15:1089-1095.

Plastourgou, M. and M.R. Hoffman (1984) Transformation and fate of organic esters in layered-flow systems - the role of trace metal catalysis. Environ. Sci. Technol. 18:756-764.

Schindler, P.W. (1981) Surface complexes at oxide-water interfaces. In: Adsorption of Inorganics at Solid-Liquid Interfaces, M.A. Anderson and A.J. Rubin (Eds.) Ann Arbor, MI: Ann Arbor Science.

Schindler, P.W. and W. Strumm (1987) The surface chemistry of oxides, hydroxides, and oxide minerals. In: Aquatic Surface Chemistry, W. Strumm (Ed.) New York: Wiley-Interscience.

Sigg, L. and W. Stumm (1980) Interaction of anions and weak acids with the hydrous goethite (alpha-FeOOH) surface. Colloids and Surfaces 2:101-117.

Tanford, C. (1980) The Hydrophobic Effect. New York: Wiley.

Ulrich, H.J., B. Cosovic and W. Stumm (1987) Adsorption of aliphatic fatty acids on aquatic surfaces: comparison between two model surfaces; the mercury electrode and delta-Al_2O_3 colloids. Environ. Sci. Technol. (in press).

Wells, C.F. and G. Davies (1967) Kinetics of the reaction of aquamanganese(III) ions with isopropanol. Trans. Farad. Soc. 63:2737-2744.

Westall, J. and H. Hohl (1980) A comparison of electrostatic models for the oxide/solution interface. Adv. Colloid Interface Sci. 12:265-294.

Westall, J.C. (1987) Adsorption mechanisms in aquatic surface chemistry. In: Aquatic Surface Chemistry, W. Stumm (Ed.) New York: Wiley-Interscience.

Alan Stone
Johns Hopkins

"Reductive Dissolution of Iron and Manganese Oxides in Natural Waters"

Oxide/hydroxide minerals of manganese(III,IV) and iron(III) are thermodynamically stable in oxygenated solutions at neutral pH, but are reduced to divalent metal ions under anoxic conditions in the presence of reducing agents. Field investigations have shown that at the onset of reducing conditions, reductive dissolution of manganese oxides occurs earlier and more quickly than iron oxides. In order to understand these observations, the kinetics and mechanism of surface chemical reactions responsible for reductive dissolution have been studied in the laboratory.

Several classes of natural organic compounds found in natural waters are facile reductants of metal oxides, including hydroxy- and alkoxy- aromatics, unsaturated alcoholic and carbonyl compounds, amines, and thiols. Rates of reductive dissolution measured in the laboratory are a complex function of reductant structure, reductant concentration, pH, and medium concentration. A mechanism for the surface chemical reaction has been postulated to account for these effects, and involves (i) surface precursor complex formation, (ii) intramolecular electron transfer, (iii) release of oxidized organic product, and (iv) release of divalent metal ions.

References (Stone - lecture 2)

Balzer, W. (1982) On the distribution of iron and manganese at the sediment/water interface: thermodynamic versus kinetic control. Geochim. Cosmochim. Acta 46:1153-1161.

Burdige, D.J. and K.H. Nealson (1986) Chemical and microbiological studies of sulfide-mediated manganese reduction. Geomicrobiology 283:29-47.

Davies, G. and K.O. Watkins (1970) Inner-sphere mechanisms of oxidation. Stoichiometry and kinetics of the cobalt(III) oxidation of oxalic acid in acid perchlorate solution. Inorg. Chem. 9:2735-2739.

Drummond, A.Y. and W.A. Waters (1955) Stages in oxidations of organic compounds by potassium permanganate. Part VI. Oxidations of ketones and pyruvic acid. J. Chem. Soc. 497-504.

Froelich, P.N., G.P. Klinkhammer, M.L. Bender, N.A. Luedtke, G.R. Heath, D. Cullen, P. Dauphin, D. Hammond, B. Hartman and V. Maynard (1979) Early oxidation of organic matter in pelagic sediments of the eastern equatorial Atlantic: suboxic diagenesis. Geochim. Cosmochim. Acta 43:1075-1090.

Furrer, G. and W. Stumm (1983) The role of surface coordination in the dissolution of delta-Al_2O_3 in dilute acids. Chimia 37:338-341.

Giovanoli, R. (1976) Vom Hexaquo-Mangan zum Mangan-Sediment: Readtionssequenzen fienteiliger fester Manganoxidhydroxide. Chimia 30:102-103.

Murray, J.W., J.G. Dillard, R. Giovanoli, H. Moers and W. Stumm (1985) Oxidation of Mn(II): initial mineralogy, oxidation state, and aging. Geochim. Cosmochim. Acta 49:463-470.

Stone, A.T. (1986) Adsorption of organic reductants and subsequent electron transfer on metal oxide surfaces. In: Geochemical Processes at Mineral Surfaces, J.A. Davis and K.F. Hayes (Eds.) Washington, D.C.: American Chemical Society Symposium Series, 323.

Stone, A.T. and J.J. Morgan (1987) Reductive dissolution of metal oxides. In: Aquatic Surface Chemistry, W. Stumm (Ed.) New York: Wiley-Interscience.

Stone, A.T. and J.J. Morgan (1984) Reduction and dissolution of manganese(III) and manganese(IV) oxides by organics. 1. Reaction with hydroquinone. Environ. Sci. Technol. 18:450-456.

Stone, A.T. and J.J. Morgan (1984) Reduction and dissolution of manganese(III) and manganese(IV) oxides by organics. 2. Survey of the reactivity of organics. Environ. Sci. Technol. 18:617-624.

Stone, A.T. (1987) Reductive dissolution of manganese(III,IV) oxides by substituted phenols. Environ. Sci. Technol. 21:979-988.

Stone, A.T. (1987) Microbial metabolites and the reductive dissolution of manganese oxides: oxalate and pyruvate. Geochim. Cosmochim. Acta 51:919-925.

Stumm, W. and R. Giovanoli (1976) On the nature of particulate manganese in simulated lake waters. Chimia 30:423-425.

Sunda, W.G., S.A. Huntsman and G.R. Harvey (1983) Photoreduction of manganese oxides in seawater and its geochemical and biological implications. Nature 301:234-236.

Tipping, E., D.W. Thompson and W. Davison (1984) Oxidation products of Mn(II) in Lake Waters. Chem Geol. 44:359-383.

Waite, T.D. and F.M.M. Morel (1984) Photoreductive dissolution of colloidal iron oxide: effect of citrate. J. Colloid Interface Sci. 102:121-137.

Waite, T.D. and F.M.M. Morel (1984) Photoreductive dissolution of colloidal iron oxides in natural waters. Environ. Sci. Technol. 18:860-868.

Waite, T.D and J.D. Smith (1988) Dissolution of colloidal manganese oxides by hydrogen peroxide. Environ. Sci. Technol.

Waite, T.D., A. Torikov and J.D. Smith (1988) Photoenhanced dissolution of colloidal iron oxides by thiol-containing compounds. I. Dissolution of hematite. J. Colloid Interface Sci. 112:412-420.

Waite, T.D., A. Torikov and J.D. Smith (1986) Photoenhanced dissolution of colloidal iron oxides by thiol-containing compounds. II. Comparison of lepidocrocite and hematite dissolution. Submitted to J. Colloid Interface Sci.

William G. Sunda
N.M.F.S., Southeast Fisheries Center
Beaufort Laboratory

"Manganese Redox Cycles in Sunlit Marine Waters"

Manganese exists in natural waters as soluble Mn(II) and as insoluble Mn(III and IV) oxides (MnO_x). It is an important micronutrient for procaryotic and eukaryotic algae, and is available for uptake by these organisms as dissolved Mn(II), but not MnO_x. There is mounting evidence that sunlight plays an important role in maintaining manganese in the soluble reduced state, minimizing its loss from the water column via sinking of particulate MnO_x. The role of sunlight is twofold: 1) it markedly stimulates the reductive dissolution of MnO_x by organic reducing agents such as humic and fulvic acids, and 2) it inhibits the metabolism of bacteria that catalyze the oxidation of Mn(II) to MnO_x. Evidence for the photodissolution of MnO_x was obtained both with synthetic ^{54}Mn-labeled MnO_x produced in the laboratory from the oxidation of $^{54}MnCl_2$ by permanganate, and with natural radiolabeled MnO_x particles formed by microbial oxidation of $^{54}MnCl_2$ added to seawater samples. The reductive dissolution of the $^{54}MnO_2$ was strongly stimulated by sunlight and by the addition of humic compounds. Experiments showed that a major mechanism for this "photoreduction" was the production of hydrogen peroxide, an effective reducing agent for manganese oxides, which is released by reactions involving sunlight, dissolved organic compounds and molecular oxygen. It accumulates in sunlit marine water at concentrations of around 10^{-7} M, within the range for the reductive dissolution of the synthetic MnO_x particles. Experiments with radiolabeled natural MnO_x particles also showed a strong enhancement of MnO_x reductive dissolution by sunlight. The photodissolution of the natural $^{54}MnO_x$ particles, however, does not appear primarily to involve the accumulation of H_2O_2 in the bulk medium. Rather, it may involve the build up of localized high concentrations of H_2O_2 or superoxide radicals within aggregates containing MnO_x, microbial cells and extracellular organic matter. It may also be caused by photochemical charge transfer reactions between MnO_x particles and adsorbed extracellular organic matter.

Experiments and measurements were conducted in the southwestern Sargasso Sea to more closely examine the role of sunlight in manganese distributions and redox cycles. Concentrations of dissolved manganese, particulate manganese, and MnO_x (ascorbate reducible particulate Mn) were measured at various depths. Rates of particulate ^{54}Mn formation were determined from ^{54}Mn radiotracer additions, and these rates in conjunction with MnO_x concentrations were used to compute steady state first order dissolution rates for manganese oxides. There was a pronounced maximum in dissolved manganese of 4-5 nM in the surface Sargasso seawater and concentrations decreased to < 1 nM below a depth of 200 m. Such surface maxima are typical of manganese depth profiles in the ocean. Greater than 99% of the manganese in the surface mixed layer (0-40 m) was present as dissolved Mn(II) and there was no evidence for the presence of manganese oxides in this layer. Below the mixed layer, there was both a decrease in total manganese and an accompanying sharp increase in manganese oxide concentrations up to a value of 30% of the total manganese at a depth of 160 m. Radiotracer experiments indicated that the low concentration of manganese oxides near the surface was largely due to a sharp decrease in manganese oxidation rates, which was shown in subsequent experiments to be caused by photoinhibition of manganese oxidizing microorganisms. Low surface MnO_x concentrations also resulted from high rates of MnO_x dissolution, consistent with photodissolution of MnO_x.

In conclusion, both photoinhibition of manganese oxidizing microorganisms and photodissolution of MnO_x results in low concentrations of MnO_x in near surface seawater. The low concentrations of particulate MnO_x caused by sunlight-driven photoreduction greatly reduce the loss of manganese from surface seawater via sinking of MnO_x particles, insuring an adequate supply of manganese to meet the metabolic requirements of marine photosynthetic organisms.

References (Sunda - lecture 1)

Eaton, A. (1979) The impact of anoxia on Mn fluxes in the Chesapeake Bay. Geochim. Cosmochim. Acta 43:429-432.

Erlich, H.L. (1980) Different forms of microbial manganese oxidation and reduction and their environmental significance. In: Biogeochemistry of Ancient and Modern Environments, P.A. Trudinger et al. (Eds.) Australian Academy of Sciences, pp.327-332.

Emerson, S., S. Kalhorn, L. Jacobs, B.M. Tebo, K.H. Nealson and R.A. Rosson (1982) Environmental oxidation rate of manganese(II): bacterial catalysis. Geochim. Cosmochim. Acta 46:1073-1079.

Graham, W.F., M.L. Bender and G.P. Klinkhammer (1976) Manganese in Narragansett Bay. Limnol. Oceanog. 21:637-766.

Grill, E.V. (1982) Kinetic and thermodynamic factors controlling manganese concentrations in oceanic waters. Geochim. Cosmochim. Acta 46:2435-2446.

Klinkhammer, G.P. and M.L. Bender (1980) The distribution of manganese in the Pacific Ocean. Earth Planet. Sci. Lett. 46:361-384.

Landing, W.M. and K.W. Bruland (1980) Manganese in the North Pacific. Earth Planet. Sci. Lett. 49:45-56.

Martin, J.H. and G.A. Knauer (1980) Manganese cycling in Northeast Pacific waters. Earth Planet. Sci. Lett. 51:266-274.

Morris, A.W. and A.J. Bale (1979) Effect of rapid precipitation of dissolved Mn in river water on estuarine Mn distributions. Nature 279:318-319.

Nealson, K.H. (1978) Isolation and characterization of marine bacteria which catalize manganese oxidation. In: Environmental Biogeochemistry and Geomicrobiology, W.E. Krumbein (Ed.) Ann Arbor Science, pp.847-858.

Nealson, K.H. and B. Tebo (1980) Structural features of manganese precipitating bacteria. Origins Life 10:117-126.

Stone, A.T. (1983) The reduction and dissolution of Mn(III) and Mn(IV) oxides by organics. Ph.D. Thesis, California Institute of Technology.

Stumm, W. and J.J. Morgan (1981) Aquatic Chemistry: An Introduction Emphasizing Chemical Equilibria in Natural Waters, Wiley, New York.

Sunda, W.G., R.T. Barber and S.A. Huntsman (1981) Phytoplankton growth in nutrient rich seawater: Importance of copper-manganese cellular interactions. J. Mar. Res. 39:567-586.

Sunda, W.G. and S.A. Huntsman (1983) Effect of competitive interactions between manganese and copper on cellular manganese and growth in estuarine and oceanic species of the diatom Thalassiosira. Limnol. Oceanog. 28:924-934.

Sunda, W.G. and S.A. Huntsman (1987) Microbial oxidation of manganese in a North Carolina estuary. Limnol. Oceanog. 32:552-564.

Sunda, W.G., S.A. Huntsman and G.R. Harvey (1983) Photoreduction of manganese oxides in seawater and its geochemical and biological implications. Nature 301:234-236.

Tebo, B.M., K.H. Nealson, S. Emerson and L. Jacobs (1984) Microbial mediation of Mn(II) and Co(II) precipitation at the O_2/H_2S interfaces in two anoxic fjords. Limnol. Oceanog. 29:1247-1258.

Vojak, P.W.L., C. Edwards and M.V. Jones (1985) Evidence for microbial manganese oxidation in the River Tamar Estuary, South West England. Estuar. Coast. Shelf Sci. 20:661-671.

Wollast, R., G. Billen and J.C. Duinker (1979) Behavior of manganese in the Rhine and Scheldt estuaries. Estuar. Coast. Mar. Sci. 9:161-169.

Zafiriou, O.C. (1983) Natural water photochemistry. In: Chemical Oceanography, Vol. 8, J.P. Riley and R. Chester (Eds.) Academic Press, pp.339-379.

Zika, R.G., J.W. Moffett, R.G. Petasne, W.J. Cooper and E.S. Saltzman (1985) Spatial and temporal variations of hydrogen peroxide in Gulf of Mexico waters. Geochim. Cosmochim. Acta 49:1173-1184.

William G. Sunda
N.M.F.S., Southeast Fisheries Center
Beaufort Laboratory

"Interactions Between Phytoplankton and Trace Metals in the Marine Environment"

Trace metals are important to organisms, both as essential nutrients and as toxins at elevated concentrations. To understand the interactions between trace metals and marine algae, one must deal with several levels of complexity as represented schematically in Figure 1. The first is the chemistry of these metals in seawater, which controls their biological availability. Both total metal concentrations and chemical speciation are important, and both exhibit wide spatial and temporal variations for individual metals leading to large differences in trace metal availability. Most trace metals exist in oceanic seawater at far lower concentrations than they occur in coastal and estuarine waters.

Reactive trace metals such as copper are often highly complexed by natural organic ligands in seawater. There is mounting evidence that the biological availability of trace metals is controlled by their free ion concentrations rather than the concentration of total metal or that of individual complexes. The dependence of biological uptake on the free metal ion concentration has provided an important central concept, helping us to better assess the biological availability of these metals in natural waters and to quantify and control trace metal availability in experimental cultures through the use of trace metal ion buffer systems.

The second level of complexity is the chemical interaction of metals with various biomolecules on the surface and within the interior of the cell (Figure 1, circle 2). The outer lipid membrane of cells is impermeable to charged ions or to charged or polar complexes, and consequently, for metals to be taken up by cells, they generally must first bind to specialized transport proteins on this membrane. If the reactions leading to the binding of metal to these sites are sufficiently fast, then the metal bound to the sites will reach equilibrium with that in the medium. At equilibrium, the amount of bound metal ions, and therfore, the metal ion transport rate will be determined by the free metal ion concentration. Such an equilibration appears to provide the underlying mechanism for the observed widespread dependence of biological availability on free trace metal ion concentration.

Several trace metals (Fe, Mn, Zn, Co, Ni, Cu, Mo) are essential to algal metabolism due to their catalytic roles in enzymes. A number of these metals as well as other nonessential metals (Cd, Hg, Pb) are toxic at sufficiently high free ion concentrations, and can compete with specific nutrient metals for membrane transport sites and for active sites on enzymes. Because of this competition, trace metal nutrition and toxicity are often closely intertwined, and biological effects can be determined as much by ratios among nutrient and toxic metals as by the absolute concentrations of individual metals ions. For example, manganese growth rate limitation in marine diatoms and green algae is brought about by either low concentrations of free manganese ions or by high free ion concentrations of copper, zinc, or cadmium. The latter three metals contribute to manganese deficiency by inhibiting cellular manganese uptake.

The sum of the reactions of trace metals with various biomolecular sites determines their overall effect on cellular processes such as photosynthetic rate and growth rate (Figure 1, circle 3), and the sum of the effects on individual cells determines the overall effect on

populations and on the algal community as a whole (Figure 1, circle 4). The large spatial and temporal differences that exist in trace metal concentrations and chemical speciation appear to influence both the productivity and species composition of marine algal communities. Low manganese to cupric ion ratios appear to limit productivity and nitrogen fixation in oceanic seawater. Marine algae, however, have evolved striking differences in their abilities to grow at low nutrient metal ion concentrations or to resist trace metal toxicity, and consequently, the most important influence of trace metals in the sea may well be on species composition. In this regard, marked differences in the availability of trace metal nutrients between coastal and oceanic seawater appear to play an important role in delineating the neritic/oceanic boundary in phytoplankton speciation.

The interaction of trace metals and marine algae is reciprocal: trace metals not only influence marine algae, but the algal community as a whole affects trace metal concentrations and chemical speciation, providing a biological feedback on the bioavailability of these metals. Such feedback is often beneficial, reducing the availability of toxic metals such as copper via the production of extracellular chelators, and enhancing the availability of manganese and iron, via photoreductive reactions between manganese and iron oxides and extracellular organic compounds.

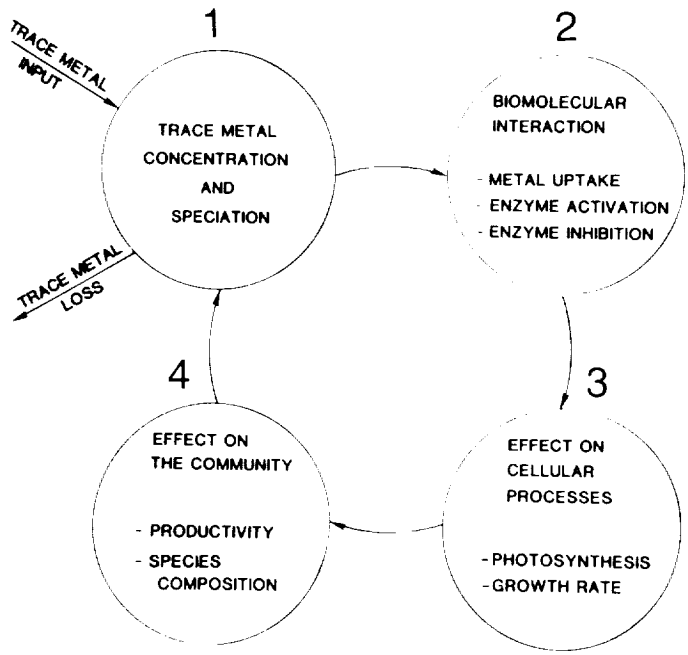

Figure 1. Schematic diagram of trace metal interactions in the marine environment.

References (Sunda - lecture 2)

Anderson, D.M. and F.M. Morel (1978) Copper sensitivity of Gonyaulax tamarensis. Limnol. Oceanog. 23:283-295.

Anderson, M.A. and F.M. Morel (1982) The influence of aqueous iron chemistry on the uptake of iron by coastal diatom Thalassiosira weissflogii. Limnol. Oceanog. 27:789-813.

Anderson, M.A. and F.M. Morel (1980) Uptake of Fe(II) by a diatom in oxic culture medium. Mar. Biol. Lett. 1:263-268.

Brand, L.E., W.G. Sunda and R.R.L. Guillard (1983) Limitation of marine phytoplankton reproduction rates by zinc, manganese and iron. Limnol. Oceanog. 28:1182-1198.

_____. (1986) Reduction of marine phytoplankton reproduction rates by copper and cadmium. J. Exper. Mar. Biol. Eco. 96:225-250.

Bruland, K.W. (1980) Oceanographic distributions of cadmium, zinc, nickel and copper in the North Pacific. Earth Planet. Sci. Lett. 47:176-198.

_____. (1983) Trace elements in seawater. In: Chemical Oceanography, J.P. Riley and R. Chester (Eds.) Academic Press, London, England, pp.157-220.

Bruland, K.W. and R.P. Franks (1983) Mn, Ni, Cu, Zn and Cd in the Western North Atlantic. In: Trace Metals in Seawater, C.S. Wong, E. Boyle, K.W. Bruland, J.D. Burton and E.D. Goldberg (Eds.) Plenum Press, New York, pp.395-414.

Entsch, B., R.G. Sim and B.G. Hatcher (1983) Indications from photosynthetic components that iron is a limiting nutrient in primary producers on coral reefs. Mar. Biol. 73:17-30.

Fitzwater, S.E., G.A. Knauer and J.H. Martin (1982) Metal contamination and its effect on primary production measurements. Limnol. Oceanog. 27:544-551.

Glover, H.E. (1978) Iron in Maine coastal waters: seasonal variation and its apparent correlation with a dinoflagellate bloom. Limnol. Oceanog. 23:534-537.

Gordon, E.M., J.H. Martin and G.A. Knauer (1982) Iron in northeast Pacific waters. Nature 299:611-612.

Hart, B.A., P.E. Bertram and B.D. Scaife (1979) Cadmium transport by Chlorella pyrenoidosa. Environ. Res. 18:327-335.

Harrison, G.I. and F.M. Morel (1983) Antagonism between cadmium and iron in the marine diatom Thalassiosira weissflogii. J. Phycol. 19:495-507.

Huntsman, S.A. and W.G. Sunda (1980) The role of trace metals in regulating phytoplankton growth. In: The Physiological Ecology of Phytoplankton, I. Morris (Ed.) Blackwell Scientific Pub., Oxford, pp.285-328.

Landing W.M. and K.W. Bruland (1980) Manganese in the north Pacific. Earth Planet. Sci. Lett. 49:45-56.

Morel, F.M. (1983) Principles of Aquatic Chemistry. John Wiley and Sons, New York.

Morel, F.M., J.G. Rueter, D.M. Anderson and R.R.L. Guillard (1979) Aquil, a chemically defined phytoplankton media for trace metal studies. J. Phycol. 15:135-141.

Rueter, J.G. Jr. and F.M. Morel (1981) The interaction between zinc deficiency and copper toxicity as it affects the silicic acid uptake mechanisms in Thalassiosira pseudonana. Limnol. Oceanog. 26:67-73.

Sunda, W.G., R.T. Barber and S.A. Huntsman (1981) Phytoplankton growth in nutrient rich seawater: Importance of copper-manganese cellular interactions. J. Mar. Res. 39:567-586.

Sunda, W.G. and P.A. Gillespie (1979) The response of a marine bacterium to cupric ion and its use to estimate cupric ion activity in seawater. J. Mar. Res. 37:761-777.

Sunda, W.G. and R.R.L. Guillard (1976) The relationship between cupric ion activity and the toxicity of copper to phytoplankton. J. Mar. Res. 34:511-529.

Sunda, W.G. and A.K. Hanson (1987) Measurement of free cupric ion concentration in seawater by a ligand competition technique involving copper sorption onto C_{18} SEP-PAK cartridges. Limnol. Oceanog. (in press).

Sunda, W.G. and S.A. Huntsman (1983) Effect of competitive interactions between manganese and copper on cellular manganese and growth in estuarine and oceanic species of the diatom Thalassiosira. Limnol. Oceanog. 28:924-934.

_____. (1985) Regulation of cellular manganese and manganese transport rates in the unicellular alga Chlamydomonas. Limnol. Oceanog. 30:71-80.

_____. (1986) Relationships among growth rate, cellular manganese concentrations and manganese transport kinetics in estuarine and oceanic species of the diatom Thalassiosira. J. Phycol. 22:259-270.

Sunda, W.G., S.A. Huntsman and G.R. Harvey (1983) Photoreduction of manganese oxides in seawater and its geochemical and biological implications. Nature 301:234-236.

Waite, T.D. and F.M. Morel (1984) Coulometric study of the redox dynamics of iron in seawater. Anal. Chem. 56:787-792.

Bradley M. Tebo
Scripps Institute of Oceanography

"Application of Rate Measurements to the Differentiation of Biological and Chemical Manganese(II) Oxidation"

Bacteria have long been known to catalyze manganese(II) oxidation, but their quantitative contribution in specific environments has not been known. In order to determine the bacterial component of manganese oxidation, the methodology employed must distinguish between chemical and biological oxidation, which are apt to co-occur in nature. In the past few years, sensitive methods have been developed using radioactive $^{54}Mn(II)$ as a tracer to measure either the rates of removal of dissolved Mn(II) or rates of formation of particulate Mn. The amount of the label that is oxidized as opposed to bound or adsorbed at a given time is discerned by incubation in the presence and absence of O_2, by dissolution of the particulate ^{54}Mn with mild (non-toxic) reducing agents or by measuring the change in oxidized equivalents during the course of the incubation. Thus, time course incubations conducted under environmental conditions of pH, O_2 tension and temperature can provide a good measure of <u>in situ</u> Mn(II) oxidation rates. To distinguish biological from non-biological activity, various treatments such as the addition of poisons that don't interfere in manganese chemistry, incubation at high temperatures, or sonication have been used. Application of these methods to a variety of environments such as anoxic fjords, estuaries, hydrothermal vent plumes and lakes have provided overwhelming evidence that manganese(II) oxidation is usually quite rapid and predominantly a biologically mediated process.

Bradley M. Tebo
Scripps Institute of Oceanography

"Rates and Kinetics of Manganese(II) Oxidation at the O_2/H_2S Interface in the Saanich Inlet, B.C., Canada"

In situ rates of Mn(II) oxidation above the O_2/H_2S interface in the Saanich Inlet, British Columbia, Canada were measured during five cruises during the summers of 1983 and 1984. The rates were determined by measuring the uptake of $^{54}Mn(II)$ in water samples under in situ conditions of pH and temperature and in the presence and absence of oxygen. Experiments in the absence of oxygen provide a measure of the exchange of the tracer between the dissolved and solid pools of Mn(II); the difference between experiments in the presence and absence of oxygen is interpreted as a measure of Mn(II) oxidation. Using this method, the effects of oxygen tension, Mn(II) concentration and temperature on the initial in situ Mn(II) oxidation rate (Vo) were examined. Mn(II) oxidation was almost twice as fast under conditions of 67% air saturation (Vo = 5.5 nM/h) as with the in situ concentration of 15 uM (5% air saturation; Vo = 3.1 nM/h). Additions of ca. 18 uM Mn(II) completely inhibited all Mn(II) oxidation at three different depths in the oxidizing zone, and there was a temperature optimum for Mn(II) oxidation of between 20-35°C. These results are consistent with biologically mediated Mn(II) oxidation.

A model based on the experimental results has been developed to describe the general mechanism of Mn(II) oxidation. Mn(II) oxidation is modeled as a two step process in which Mn(II) is first bound by a site on the bacterial surface and then oxidized. The model is analogous to the Langmuir isotherm model for surface catalyzed gas reactions or the Michaelis-Menten model for enzyme kinetics. Since in situ rates of oxidation were measured as a function of depth and therefore as a function of Mn(II) concentration, the model could be applied to natural gradients of these parameters in the water column. Calculated from the model are the apparent equilibrium binding constant (K_S = 0.18 uM), the apparent half saturation constant for biological Mn(II) oxidation (K_m = 0.22 to 0.89 uM/h), the maximum rate of Mn(II) oxidation (V_{max} = 3.5 to 12.1 nM/h), and the total microbial surface binding site concentration (E = 51 nM). V_{max} for Mn(II) oxidation agrees with the rates calculated from the value of the flux of Mn(II) to the oxidizing zone using the Mn(II) gradient and estimates of the eddy diffusion coefficient. This consistency verifies the methodology and indicates that the rate of Mn(II) oxidation is nearly equal to the V_{max} for the reaction. Therefore, in Saanich Inlet the Mn(II) oxidation rate is limited by the concentration of microbial binding sites. For this to be true, some nutrient other than Mn(II) must be limiting the growth of Mn(II) oxidizing bacteria or Mn(II) oxidation is not providing the energy necessary for the growth of the bacteria that catalyze the reaction.

References (Tebo)

Brewer, P.G. and D.W. Spencer (1971) Colorimetric determination of manganese in anoxic waters. Limnol. Oceanog. 16:107-110.

Chapnick, S.D., W.S. Moore and K.H. Nealson (1982) Microbially mediated manganese oxidation in a freshwater lake. Limnol. Oceanog. 27:1004-1014.

Cowens, J.P., G.J. Massoth and E.T. Baker (1986) Bacterial scavenging of Mn and Fe in a mid- to far-field hydrothermal particle plume. Nature 322:169-171.

Emerson, S., L. Jacobs, S. Kalhorn, B.M. Tebo, K.H. Nealson and R.A. Rosson (1982) Environmental oxidation rate of manganese(II): bacterial catalysis. Geochim. Cosmochim. Acta 46:1073-1079.

Emerson, S., R.E. Cranston and P.S. Liss (1979) Redox species in a reducing fjord; equilibrium and kinetic considerations. Deep-Sea Res. 26A:859-873.

Fitzwater, S.E., G. Knauer and J. Martin (1982) Metal contamination and its effect on primary production measurements. Limnol. Oceanog. 27:544-551.

Froehlich, P.N., G.P. Kinkhammer, M.L. Bender, N.A. Luedtke, G.R. Heath, D. Cullen, P. Dauphin, D. Hammond, B. Hartman and V. Maynard (1979) Early oxidation of organic matter in pelagic sediments of the eastern equatorial Atlantic: suboxic diagenesis. Geochim. Cosmochim. Acta 43:1075-1090.

Hastings, D. and S. Emerson (1986) Oxidation of manganese by spores of a marine Bacillus: Kinetic and thermodynamic considerations. Geochim. Cosmochim. Acta 50:1819-1824.

Hem, J.D. (1980) Redox coprecipitation mechanisms of manganese oxides: particulates in water. In: Advances in Chemistry Series No. 189, M.C. Kavanaugh and J.O. Leckie (Eds.) American Chemical Society, Washington D.C., pp.45-72.

Hem, J.D. and C.J. Lind (1983) Nonequilibrium models for predicting forms of precipitated manganese oxides. Geochim. Cosmochim. Acta 47:2037-2046.

Kalhorn, S. and S. Emerson (1984) The oxidation state of manganese in surface sediments of the Pacific Ocean. Geochim. Cosmochim. Acta 48:897-902.

Maki, J.S., B.M. Tebo, F.E. Palmer, K.H. Nealson and J.T. Staley (1987) The abundance and biological activity of manganese oxidizing bacteria and Metallogenium-like morphotypes in Lake Washington, USA. FEMS Microbiol. Ecol. 45:21-29.

Marshall, C.S. (1979) Biogeochemistry of manganese minerals. In: Biogeochemical Cycling of Mineral-forming Elements, P.A. Trudinger and D.J. Swaine (Eds.) Elsevier Scientific Publ. Co., New York, pp.253-292.

Murray, J.W., J.G. Dillard, R. Giovanoli, H. Moers and W. Stumm (1985) Oxidation of Mn(II): Initial mineralogy, oxidation state and aging. Geochim. Cosmochim. Acta 49:463-470.

Murray, J.W., L.S. Balistrieri and B. Paul (1984) The oxidation state of manganese in marine sediments and ferromanganese nodules. Geochim. Cosmochim. Acta 48:1237-1247.

Nealson, K.H. and B. Tebo (1980) Structural features of manganese precipitating bacteria. Origins of Life 10:117-126.

Piper, D.Z., J.R. Basler and J.L. Bischoff (1984) Oxidation state of marine manganese nodules. Geochim. Cosmochim. Acta 48:2347-2355.

Rosson, R.A., B.M. Tebo and K.H. Nealson (1984) The use of poisons in the determination of microbial manganese oxidation rates in seawater. Appl. Environ. Microbiol. 47:740-745.

Sunda, W.G. and S.A. Huntsman (1987) Microbial oxidation of manganese in a North Carolina estuary. Limnol. Oceanog. (in press).

Tebo, B.M. and S. Emerson (1985) The effect of oxygen tension, Mn(II) concentration and temperature on the microbially catalyzed Mn(II) oxidation rate in a marine fjord. Appl. Environ. Microbiol. 50:1268-73.

Tebo, B.M. and S. Emerson (1986) Microbial manganese(II) oxidation in the marine environment: a quantitative study. Biogeochemistry 2:149-161.

Tebo, B.M., C.D. Taylor, K.H. Nealson and S. Emerson (1985) In situ manganese(II) binding rates at the oxic/anoxic interface in Saanich Inlet, B.C., Canada. In: Planetary Ecology, D.E. Caldwell, J.A. Brierley and C.L. Brierley (Eds.) Van Nostrand Reinhold Co., New York, pp.210-221.

Tebo, B.M., K.H. Nealson, S. Emerson and L. Jacobs (1984) Microbial mediation of Mn(II) and Co(II) precipitation at the O_2/H_2S interfaces in two anoxic fjords. Limnol. Oceanog. 29:1247-1258.

Tipping, E. (1984) Temperature dependence of Mn(II) oxidation in lakewaters: a test of biological involvement. Geochim. Cosmochim. Acta 48:1353-1356.

Tipping, E., D.W. Thompson and W. Davison (1984) Oxidation products of Mn(II) in lakewaters. Chem. Geol. 44:359.

Jeffrey A. Titus
Bristol Meyers Inc., Syracuse, New York

"Interactions of Mercury and Cadmium with Bacterial Populations"

The contamination of environments with the heavy metals mercury and cadmium has been shown to be of great importance from a human health related perspective. These metals are also toxic to many microorganisms, although some bacterial strains have developed mechanisms of resistance to the metals. Bacteria and other microorganisms have been shown to be active in the movement of metals throughout the environment and into the food chain.

The work described here encompasses laboratory model systems with Hg and Cd, a metal contaminated environmental site, and pure culture studies on a cadmium resistant Bacillus subtilis. The work was done in the Department of Microbiology, The Ohio State University, Columbus, Ohio and represents the efforts of a number of people, including J.E. Parsons, R.M. Pfister, K. Surowitz and J.A. Titus.

Model aquatic systems were set up in 20 gallon aquarium tanks. The tanks had stratified bed sediments which included diversified macro- and microorganisms and goldfish (Carassius auratus). Water level was maintained by the addition of double distilled water with an automatic leveling device. A one-gram globule of metallic mercury was placed in the mud layer of the sediment.

The mercury traveled through the sediment at an increasing rate as it moved away from the site of the mercury globule. Mercury traversed the sediments before reaching detectable levels in the water column. The equilibrium levels of Hg were 0.1 ug/g in the sediment and 0.06 ug/ml in the water column. After 40 weeks the Hg level in the goldfish had reached 90 ug/g and had not reached equilibrium.

A second experiment was done to evaluate the bacterial population's response to the addition of mercury to the system. Increased Hg loads in the sediment caused an increase in the percentage of the bacterial population that was resistant to 6 ug Hg^{2+}/ml.

Studies of Hg resistant bacterial populations showed that volatilization of Hg from microbiological media could affect the amount of mercury remaining in agar plates at the time of use. The presence of complex organics such as yeast extract slowed the loss of Hg^{o}, and reducing sugars such as glucose accelerated the volatilization of Hg^{o}.

Cadmium-resistant bacterial populations were examined in sediments of the Ottawa River, near Lima, Ohio, at a site that had elevated levels of Cd, Cr, Cu, Fe, Ni and Zn. The metal contaminated site had a higher percentage of the bacterial population that was resistant to 15 ug Cd^{2+}/ml than at a less contaminated site downstream. The most abundant genus of the total river sediment population recovered was Bacillus and the most abundant Cd-resistant genus recovered was Pseudomonas. Types and distribution of bacterial populations in tanks similar to those described for Hg studies were examined over a ten week period during the continuous addition of 10 mg Cd^{2+} per day to the water column. The Cd level in the water column rose rapidly through the first two weeks and reached a maximum of 3 ug Cd/ml. Sediment Cd levels rose most rapidly after 5 weeks and reached a concentration of 270 ug/g after 10 weeks. The bacteria in the water column responded more quickly and to a greater degree than the bacteria in the sediment. The types of Cd-

resistant bacteria isolated in the model systems were similar to Cd-resistant bacteria isolated from sediments of the Ottawa River.

The effects of cadmium on the growth and respiration of two strains of Bacillus subtilis were compared. The accumulation of Cd by viable and cyanide-killed cells, protoplasts and cell fractions of the two strains were also examined. Growth and respiration of strain 1A1 were significantly inhibited at 10 ug Cd^{2+}/ml, while the growth and respiration of strain 1A1R, a selected mutant of 1A1, were only slightly affected. Strain 1A1R was capable of growth at Cd concentrations of up to 50 ug Cd^{2+}/ml. 1A1R protoplasts were more resistant to Cd than were 1A1 protoplasts. The differential resistance of the strains correlate with the accumulation of Cd by the two strains, with 1A1 accumulating 10 times more Cd after a 4-hour exposure to 1 ug Cd^{2+}/ml. The distributions of the Cd throughout the cells, however, were similar between the strains. Based on the accumulation of Cd by cyanide-killed protoplasts, uptake of Cd by 1A1 appeared to be an active process while for 1A1R, Cd accumulation was independent of protoplast viability.

References (Titus)

Laggaga, R.A., R. Bessen and S. Silver (1985) Cadmium-resistant mutant of Bacillus subtilus 168 with reduced cadmium uptake. J. Bacteriol. 162:1106-1110.

Mills, A.L. and R.R. Colwell (1977) Microbiological effects of metal ions in Chesapeake Bay water and sediment. Bull. Environ. Contam. Toxicol. 18:99-103.

Nelson, J.D. and R.R. Colwell (1975) The ecology of mercury-resistant bacteria in Chesapeake Bay. Microbial. Ecol. 1:191-218.

Surowitz, K.G., J.A. Titus and R.M. Pfister (1984) Effects of cadmium accumulation on growth and respiration of a cadmium-sensitive strain of Bacillus subtilis and a selected cadmium-resistant mutant. Arch. Microbiol. 140:107-112.

Timoney, J.F., J. Port, J. Giles and J. Spanier (1978) Heavy-metal and antibiotic resistance in the bacterial flora of New York Bight. Appl. Environ. Microbiol. 36:456-485.

Titus, J.A., J.E. Parsons and R.M. Pfister (1980) Translocation of mercury and microbial adaptation in a model aquatic system. Bull. Environ. Contam. Toxicol. 25:456-464.

Titus, J.A. and R.M. Pfister (1982) Effects of pH, temperature and Eh on the uptake of cadmium by bacteria and an artificial sediment. Bull. Environ. Contam. Toxicol. 28:697-704.

Titus, J.A. and R.M. Pfister (1984) Bacteria and cadmium interactions in natural and laboratory model systems. Arch. Environ. Contam. Toxicol. 13:271-277.

John R. Vande Castle
University of Wisconsin - Madison

"Large-Scale Remote Sensing of Water Quality Parameters Using Polar Orbiter Weather Satellite Data"

The primary function of the many sensors aboard the NOAA polar orbiting satellites is to provide weather forecast information in tandem with the geostationary (GOES) satellites. However, the use of data from the Advanced Very High Resolution Radiometer (AVHRR) on the polar orbiting satellites for vegetation monitoring is well documented (e.g. Roller and Colwell, 1986). These data are also capable of providing water quality information. Differences in turbidity due to phytoplankton concentration, dissolved organic materials and sediment loads alter the reflectivity or absorption of the visible (0.58-0.68 um) and near infrared (0.725-1.0 um) AVHRR bands. This information is useful for studying changes in turbidity due to sediment input and phytoplankton growth. The two (3.55-3.93 um, 10.5-11.5 um) or three (3.55-3.93 um, 10.5-11.3 um, 11.5-12.5 um) thermal infrared bands are capable of providing atmosphere-correlated measurements of surface water temperature with a relative accuracy better than 0.5 degrees centigrade (Maturi et al., 1986; Deschamps and Phulpin, 1980; Bernstein, 1982). The differences in water density caused by temperature gradients form a barrier to mixing and often define separate water masses. However these barriers can be a temporary phenomenon due to wind events which tend to mix the water masses. This information is very important in water quality evaluation.

Satellite sensor systems such as the Landsat Thematic Mapper (TM) or the High Resolution Visible (HRV) sensor of the SPOT satellite are useful water quality monitoring tools when limited geographic areas are of interest. However the data volume and scene dimensions of these high resolution systems present serious limitations for large area analysis. This becomes even more of a problem for temporal monitoring purposes where many scenes must be processed. The 16-day overpass frequency of Landsats-4 and 5 would seem sufficient for most monitoring purposes. In reality this is a serious limitation when weather and cloud cover is considered. The SPOT-1 satellite does not have a thermal channel and temperature measurement is often the most important parameter in water quality assessment.

The daily coverage provided by AVHRR data, in contrast, provides a powerful tool for monitoring environmental parameters requiring high temporal resolution in the visible, near infrared and thermal portion of the spectrum. The two NOAA series satellites in normal operation provide information at a resolution of 1 km from daytime passes near 7:30 and 14:30 local time. The night pass from each satellite 12 hours later is particularly useful for surface temperature measurements. This temporal resolution provides the opportunity to observe changes in water quality and thermal structure on a daily basis, limited only by cloud cover. Depending on satellite position, areas the size of the Great Lakes can be viewed in the 2400 km swath width of a single overpass.

Unlike Landsat or Spot data, there are no licensing fees for AVHRR data. Transmissions from the NOAA polar orbiting satellites can be received by anybody with the proper equipment. There are 110 known stations in the world which receive full resolution AVHRR data with 33 (mostly Department of Defense) stations in the United States. AVHRR data are also routinely archived by the Satellite Data Services Division of NOAA. These data can be ordered in a number of formats. The current cost for full resolution AVHRR imagery from the SDSD archive is less than $200 per full scene. Limited area orders such as the Great Lakes region cost less than $50 per scene. AVHRR

data are also available from other sources such as the University of Miami, University of Wisconsin and Scripps Institute of Oceanography to name just a few. The public domain nature of the data reduces their cost and makes them particularly attractive for monitoring purposes.

Close correlations (R^2 0.89 to 0.92) of AVHRR data have been observed with parameters such as chlorophyll a, suspended particulates, turbidity and surface temperature using preliminary data collected in Lake Michigan's Green Bay (Vande Castle and Lillesand, 1987). This level of correlation is close to the range observed for processed SPOT-HVR (Lillesand, 1987) and Landsat-TM (Lathrop and Lillesand, 1986) data. It is important to note that correlations in this range are difficult to obtain even from direct observations and measurements.

AVHRR data are able to depict temperature patterns, coastal upwelling and turbidity in large systems such as the Great Lakes. Seasonal AVHRR images show dramatic circulation patterns and provide instantaneous whole lake temperature measurements which are cost-prohibitive to obtain by conventional sampling procedures. These observations provide information needed to develop a fundamental understanding of the horizontal variability in surface water temperature and transparency on a temporal basis. The monitoring of upwelling events also aids in the prediction of nutrient availability and the subsequent potential increases in phytoplankton production.

References (Vande Castle)

Bernstein, R. (1982) SST from NOAA 6. J. Geophys. Res. 87:9455-9465.

Deschamps, P.Y. and T. Phulpin (1980) Atmospheric correction of infrared measurements of sea surface temperature using channels at 3.7, 11, and 12 um. Boundary Layer Meteorol. 18:131-143.

Lathrop, R.G. Jr. and T.M. Lillesand (1986) Use of Thematic Mapper data to assess water quality in southern Green Bay and Lake Michigan. Photogrammetric Engineering and Remote Sensing 52:671-680.

Lillesand, T.M. (1987) A multi-purpose first look at Spot-1 data. Proceeding: ASPRS/ ACSM Meeting, March, 1987 (in press).

Maturi, E., J. Pritchard and P. Clemente-Colon (1986) An experimental technique for producing moisture corrected imagery from 1 km Advanced Very High Resolution Radiometer (AVHRR) data. NOAA/NESDIS Tech. Memo. 15. Nat. Oceanic Atmos. Admin., Wash. D.C.

Roller, N.E.G. and J.E. Colwell (1986) Coarse-resolution satellite data for ecological surveys. BioScience 36:461-467.

Vande Castle, J.R. and T.M. Lillesand (1987) The utility of AVHRR data for monitoring large-scale temporal changes in Great Lakes water quality. Proceedings: Pecora XI Symposium, Sioux Falls, South Dakota (in press).

Robert C. Wrigley
NASA Ames, Moffett Field

"Remote Sensing of Aquatic Environments: Theoretical Considerations"

Three general areas were discussed: 1) some additional thoughts on Dr. Brooks' figures, 2) recent advances in remote sensing of oceanic environments, and 3) scattered results from some studies of lakes I conducted in the mid-1970s.

1) Additional Thoughts

Dr. Brooks discussed the solar spectrum in the 300-1600 nm region but concentrated on the PAR region (400-700 nm). I pointed out that remote sensing utilizes the near-infrared region (700-1100 nm) which has high reflectance for terrestrial vegetation as well as high concentrations of surface aquatic vegetation. In addition, thermal infrared radiation between 3,000 to 15,000 nm responds to temperature differences and has been used to monitor water masses; satellite sensors minimize water vapor absorption by limiting the spectral region to 10,500-12,500 nm. Dr. Brooks also discussed primary productivity as a function of depth. I pointed out that at the Secchi depth, where light is reduced to approximately 30% of surface levels, the integrated primary productivity to that depth accounts for the vast majority of the total primary productivity on his diagram. The implication is that remote sensing, which responds to light down to 1-2 Secchi depths, should be capable of determining effects due to a significant portion of the primary productivity.

2) Oceanic Environments

Recent advances in the remote sensing of oceanic environments were discussed to demonstrate the concepts involved, indicate the level of success that has been attained, and show where the methods have failed. In oceanic environments, waters low in chlorophyll pigments are very blue. As the chlorophyll concentration increases, the water gradually becomes greener due to absorption of blue light in photosynthesis (and other processes) as well as greater scattering at longer wavelenths. A family of spectra has been observed which has a hinge point at 520 nm such that the spectral radiance decreases below the hinge point and increases above it as the pigment concentration increases (Clarke et al., 1970; Gordon et al., 1980). Significant departures from this family of spectra occur at high pigment concentrations (>3-5 mg/m^3), high humic concentrations, and when suspended sediment particles are present. When water bodies can be represented by the regular behavior of the family of spectra, i.e. in oceanic waters, a reasonably quantitative regression equation can be determined between pigment concentration and various ratios of spectral radiances of light just below the water's surface. L(443)/L(550) and L(520)/L(550) have proven useful to cover a range of pigment concentrations. These regression equations are known as bio-optical algorithms.

Unfortunately, the sky is also blue and atmospheric effects cause major perturbations to oceanic optical spectra when observed from aircraft or satellites, contributing up to 90-95% of the total signal in some cases. Consequently, the quantitative removal of atmospheric effects has been a central effort in the processing of satellite oceanic data to derive quantitative estimates of oceanic pigment concentrations. A simple model of atmospheric

effects can be written as:

$$L_t = L_p + t * L_w$$

where L_t is the total radiance at the satellite, L_p is the path radiance or air-light scattered to the satellite from the atmosphere, t is the transmittance of the atmosphere, and L_w is the water-leaving radiance. The path radiance, L_p, can be divided into two parts: that due to Rayleigh scattering from gases (nitrogen, oxygen, etc.) which can be calculated and that due to paticulate or aerosol scattering which is highly variable and cannot be calculated a priori. Thus,

$$L_t = L_{pr} + L_{pa} + t * L_w.$$

If it is possible to find a spectral region where the water-leaving radiance, L_w, is zero, then

$$L_t = L_{pr} + L_{pa}.$$

Since L_t is measured and L_{pr} can be calculated, then L_{pa} is known at that wavelength. Various schemes have been used to propagate this known aerosol radiance to other spectral regions of interest. The best uses a nearby region of "clear water" and some a priori knowledge of the radiance of that water. Since a good approximation to the atmospheric transmittance can be calculated, the equation can be solved for L_w at the wavelengths of interest:

$$L_w = (L_t - L_{pr} - L_{pa}) / t.$$

At this point, the L_{ws} can be used in the above-mentioned bio-optical algorithms to calculate pigment concentrations.

The Coastal Zone Color Scanner, or CZCS, was launched in 1978 to measure the color of the ocean and attempt to derive estimates of pigment concentrations and, hopefully, biomass (Hovis et al., 1980). The CZCS had four 20-nm-wide spectral bands in the visible portion of the spectrum centered at 443, 520, 550 and 670 nm as well as a near-infrared band (700-800 nm) and a thermal infrared band (10,500-12,500 nm). The spatial resolution of 825 meters at nadir was designed for oceanic scales. The instrument scanned a swath width of 1600 km across the image. The orbit had a repeat cycle of 5.5 days and permitted viewing a given area 3 days out of 5. The near-infrared band was originally expected to be the band with zero water-leaving radiance for use in aerosol measurement, but its sensitivity was too low. The 670 nm band was substituted for aerosol measurement with the understanding that the assumption of zero water-leaving radiance might be violated on occasion.

The initial results from comparing ship chlorophyll data from continuous transects with estimates made using the CZCS data showed reasonable agreement within 0.5 on a logarithmic scale, i.e. within a factor of three (Gordon et al., 1980). More careful analysis of data from the early spring of 1979 showed much better agreement. The average rms difference between ship transects and CZCS estimates was just under 40% (Gordon et al., 1983). Smith and Baker (1982) developed an iterative scheme to alleviate the assumption that the 670 nm band had zero water-leaving radiance. Using their iterative approach in the Southern California Bight in March of 1979, they found agreement with ship data to be about 30-40%. On the other hand, Wrigley and Klooster (1983) reported that the agreement deteriorated severely when more productive waters off Monterey Bay, CA were

included (> 1-3 mg/m^3). They suggested that the assumption of zero radiance in the 670 nm band was at fault.

3) Lake Spectra

In 1974 we mounted a rapid scanning spectrometer in a light twin-engined aircraft and took spectra in conjunction with the EPA National Lake Eutrophication Survey (Wrigley and Klooster, 1977). Spectra of some forty lakes were obtained close to the time of the EPA data collection (within a few days). Each lake appeared to have a characteristic spectrum. After examining the EPA data, an attempt was made to organize these lake spectra into general categories to reduce their seeming individuality. One category consisted of lakes dominated by resuspended sediments; they had a broad spectral response not unlike that of soils but varied in overall intensity and had subtle differences in spectral shape. Although an attempt was made to correlate a measure of brightness to suspended solids as reported by the EPA, an obvious relationship was not apparent. Similarly, all the lakes with a strong green peak near 560 nm were grouped together; differences in spectral shape appeared to be minor. The intensity of the 560 nm peak was plotted against the EPA's measured chlorophyll concentrations and a loose correlation was observed. Lakes with low spectral responses were grouped together and some of them formed a sequence similar to the family of spectra observed in oceanic waters which are not affected by suspended sediments or other terrigenous materials. Their chlorophyll concentrations roughly followed the expected sequence. On the other hand, a number of these dark lakes were distinctly apart from the family of spectra. One of them, Iron Canyon Reservoir, was independently described a having high humic acid concentrations.

I believe the message from these very preliminary studies of lake spectra is that the concentrations of suspended sediments and phytoplankton are so high that the spectral characteristics are influenced by individual sediment characteristics and phytoplankton species. Only in the darkest or clearest lakes does the family of spectra observed in the oceanic environment occur and even there other factors can be important. Oceanic approaches, such as assuming zero water-leaving radiance in the 670 nm band, will be totally inappropriate; even the basic form of the bio-optical algorithms may have to change in order to estimate pigment concentrations in lakes.

A study of an hypereutrophic lake, Clear Lake, CA which is not unlike Oneida Lake, using the rapid scanning spectrometer from a small boat revealed an unexpected relationship between the surface chlorophyll concentrations and a reflectance peak above 700 nm (Wrigley et al., 1975). When chlorophyll concentrations of the cyanobacterium Aphanizomenon flos-aquae exceeded about 15 mg/m^3, the 700 nm peak emerged and continued to grow as the chlorophyll grew to 25, 50, 100, 200, 400, 1000 mg/m^3 and even up to 41,000 mg/m^3. When the area under the 700 nm peak was plotted against chlorophyll concentration on a semi-log scale, a linear relation was observed over some five orders of magnitude. This infrared response by cyanobacteria is similar to that of terrestrial vegetation, but is modified by the suspension of the phytoplankton in a medium that absorbs strongly with increasing wavelength. The current study of Oneida Lake utilizes this infrared response. Thus, the loss of the simplicity of the oceanic environment can lead to other opportunities as well as complications.

References (Wrigley)

Clarke, G.L., G.C. Ewing and C.J. Lorenzen (1970) Spectra of backscattered light from the sea obtained from aircraft as a measure of chlorophyll concentration. Science 167:1119-1121.

Gordon, H.R., D.K. Clark, J.L. Mueller and W.A. Hovis (1980) Phytoplankton pigments from the Nimbus-7 Coastal Zone Color Scanner: Comparisons with surface measurements. Science 210:63-66.

Gordon, H.R., D.K. Clark, O.B. Brown, R.H. Evans, and W.W. Broenkow (1983) Phytoplankton pigment concentrations in the Middle Atlantic Bight: comparison of ship determinations and CZCS estimates. Appl. Opt. 22:20-33.

Hovis, W.A., D.K. Clark, F. Anderson, R.W. Austin, W.H. Wilson, E.T. Baker, D. Ball, H.R. Gordon, J.L. Mueller, S.Z. El-Sayed, B. Sturm, R.C. Wrigley and C.S. Yentsch (1980) Nimbus-7 Coastal Zone Color Scanner: system description and initial imagery. Science 210:60-63.

Smith, R.C. and K. S. Baker (1982) Oceanic chlorophyll concentrations as determined by satellite (Nimbus-7 Coastal Zone Color Scanner). Mar. Biol. Res. 66:269-279.

Wrigley, R.C. and S.A. Klooster (1975) Airborne spectra of California-Nevada lakes (Abstract). 3rd Sectional Meeting of the American Society of Limnology and Oceanography, San Francisco, CA, Nov. 19-21.

Wrigley, R.C., S.A. Klooster, M.J. Leroy, H.A. Anderson and A.J. Horne (1975) Field measurement of algal biomass by infrared reflectance. NASA TM-X 73:107.

Wrigley, R.C. and S.A. Klooster (1983) Coastal Zone Color Scanner data in rich coastal waters. Digest of IEEE Int'l Geosci. and Remote Sensing Sympos., San Francisco, CA, Aug. 31-Sept. 2, Vol. II, FA-6, 2.1-2.5.

Robert C. Wrigley
NASA Ames, Moffett Field

"Remote Sensing of Aquatic Environments: Results of Lake Studies"

Three subjects were discussed: 1) the instruments available for remote sensing of aquatic environments, 2) a methodology for using simultaneous sampling to derive site and time specific relationships from remote sensing data and 3) the application of that methodology to determining the surface chlorophyll concentration in Oneida Lake from Thematic Mapper data.

1) Available Instruments

The Landsat series of satellites began in 1972 and at first only carried the Multispectral Scanner System (MSS) which had four spectral bands and 80 meter spatial resolution with a swath width of 185 km. The bands were somewhat arbitrary (500-600 nm, 600-700 nm, 700-800 nm and 800-1100 nm) and not well suited for the low reflectance of most water bodies. The Thematic Mapper (TM) was a second generation instrument with seven bands better suited for vegetation analysis (450-520, 520-600, 630-690, 760-900, 1550-1750, 2080-2350, and 10,500-12,500 nm). Although the TM had greater spatial resolution (30 meters), its radiometric sensitivity was not much better than the MSS. The CZCS was mentioned in the earlier lecture but it is no longer functioning. A follow-on instrument has been proposed many times, but has not yet been approved. The suggestions for improving the CZCS have been incorporated into an aircraft instrument called the Airborne Ocean Color Imager (AOCI) which flies aboard NASA's high altitude aircraft. The AOCI has six 20-nm bands in the visible region centered at 445, 490, 520, 565, 620, and 665 nm as well as three 60-nm near-infrared bands centered at 765, 865, and 1030 nm and a thermal band. The AOCI was designed to have a high radiometric sensitivity and a 50 meter spatial resolution with a swath width of 33 km. NASA's most recent aircraft instrument is the Airborne Visible-Infrared Imaging Spectrometer (AVIRIS) which has 224 contiguous spectral bands covering the 400-2400 nm range with a 20 meter spatial resolution and a swath width of 11 km. Its capabilities in aquatic environments are currently under investigation (e.g. at Oneida Lake).

2) Simultaneous Sampling

Khorram (1985) used a large number of nearly simultaneous samples in conjunction with a Landsat Multispectral Scanner overpass of the San Francisco Bay and Delta. He deployed several sampling boats over the 100 mile length of the Bay-Delta system and conducted the sampling such that 73 sites were acquired within one hour of the overpass time. He divided the sites into those used to develop regression models (50 sites) and those used to test the models (23 sites). The sites were sampled for chlorophyll, turbidity, salinity, and total suspended solids. The regression models ranged between simple linear combinations of two of the MSS bands (turbidity) to linear combinations of all MSS bands and their squares (chlorophyll). Since there is no physical reason MSS can determine salinity directly, it is most likely the MSS is responding to the higher suspended sediment load of the fresher waters. The R^2 values for the regression equations were 0.90, 0.91, 0.81, and 0.76 for turbidity, salinity, suspended solids and chlorophyll, respectively. When the test sites were used in the models, the R^2 values were 0.88, 0.64, 0.62, and 0.60, respectively. Although the area sampled by Khorram was an estuary with high suspended sediment loads, the principles apply to a number of situations. Most likely,

models developed for one date and location may not apply to another, but Khorram suggests that only a few sites may be required for another date at the same location (i.e. the Bay-Delta).

3) Surface Chlorophyll Concentrations at Oneida Lake

Chlorophyll pigment concentrations were determined at one instant in time for the entire surface of Oneida Lake during a cyanobacterial bloom by a combination of remote sensing and surface sampling techniques (Wrigley et al., 1987). The TM acquired spectral radiance data of the lake at the same time as a fluorometer measured chlorophyll pigment concentrations along continuous transects in the lake. After registration of the two data sets, the best correlation between them occurred using a combination of TM bands 2 (green) and 4 (near-infrared) corresponding to the green reflectance of the pigments and the high near-infrared reflectance of near-surface cyanobacteria. The regression equation (log chl = -1.74 + 0.131 * B2 - 0.068 * B4) was used to construct a map of chlorophyll pigment concentration over the entire lake. It is anticipated that the R^2 for the fit of the data to the equation (0.5) can be improved by more accurate navigation of the transects and other improved sampling techniques.

References (Wrigley - lecture 2)

Khorram, S. (1985) Development of water quality models applicable throughout the entire San Francisco Bay and Delta. Photogramm. Eng. and Remote Sensing 52:53-62.

Wrigley, R.C., L.L. Richardson, E.L. Mills, C. Aguilar and K.H. Nealson (1987) Surface chlorophyll concentrations in Oneida Lake (Abstract). Fiftieth Annual Meeting of the American Society of Limnology and Oceanography, Madison, WI, June 15-18.

Participants' Research Results

Carmen Aguilar
Hans de Vrind
Liesbeth de Vrind

"Mn Immobilization in Lake Water Samples: Binding, Oxidation and Reduction"

Introduction

In our experiments we attempted to develop methods for the measurement of rates of Mn cycling in the water column in Oneida Lake. We first measured the immobilization of Mn^{2+} (which may include binding, uptake and oxidation by the biota, and abiotic binding and oxidation) by adding the radioactive tracer ^{54}Mn to water samples and measuring the amount of radioactivity trapped on filters. By measuring the effect of $HgCl_2$ and DCMU we tried to discriminate between abiotic and biotic immobilization of Mn^{2+}. Because manganese oxides may be solubilized at high light intensities by photo-reduction, we also measured the release of manganese from preformed oxides in the light.

Methods

Mn immobilization in lake water: photosynthetron experiments.

Water samples were collected from different buoys at different depths as indicated in the text. A sample of 100 ml was spiked with 2.5 uCi of ^{54}Mn. A second 100 ml sample was supplemented with $HgCl_2$ (final concentration 0.01%) 15 minutes prior to ^{54}Mn spiking. Portions of 10 ml from both the unpoisoned and poisoned sample were then transferred to counting vials and incubated in the photosynthetron at about 750 uE/s^2/m. Portions of 1 ml were transferred to counting vials, supplemented with scintillation liquid (Optifluor, Packard) and counted for determination of the specific activity. Duplicate samples were removed from the photosynthetron after 1/2, 2 and 12 hours after the ^{54}Mn spike. Five ml portions of the samples were filtered immediately over 0.2 um Gelman filters, and washed twice with 2.5 ml of 0.2 um filtered lakewater. The filters and 0.5 ml from the filtrates were transferred to counting vials, supplemented with scintillation liquid and counted in the liquid scintillation counter.

Five ml hydroxylamine was then added (final concentration 0.1%) to reduce all oxidized manganese, and the samples filtered and further treated as described above. Some samples were incubated for 4 hours more, but in the dark, and then were treated as described above. The detection of ^{54}Mn by liquid scintillation counting is based on secondary activity: the radiation from the isotope releases electrons from the solvent molecules (Compton effect). The efficiency of counting ^{54}Mn by this method was estimated to be about 30%.

The other experiments were performed in essentially the same way, except that: a) non-radioactive Mn was added as well as radioactive Mn; and b) DCMU was added as a poison. Concentrations are given in the text and figure legends.

Determination of manganese binding and oxidation in lake water-aquarium experiments.

The determination of Mn immobilization in lake water samples by incubating them with radioactive Mn in the photosynthetron has some serious limitations. Only a limited number of samples can be tested and the incubation volumes are small. In particular the limitation on sample volume can cause significant errors: fast (unnatural) rises in pH due to photosynthesizing cyanobacteria, adsorption of Mn to the glass wall due to a relative large glass surface area as compared to sample volume, and fast predation of bacteria by zooplankton trapped in the samples. Therefore, we performed some preliminary experiments in which larger sample volumes were used. The samples were incubated in 1 or 2 L nalgene flasks in aquaria filled with tap water, and placed on stands under natural light/dark conditions. Samples of 400 ml were spiked with 5 uM $MnCl_2$ (final concentration) and 2 uCi of ^{54}Mn. Samples serving as dark controls were wrapped in aluminum foil. The flasks were incubated in plastic bags in the aquaria. At given times duplicate samples of 30 ml were taken from the flasks and filtered (0.2 uM Gelman filters). The filters were rinsed three times with 5 ml of 0.2 um filtered lake water and counted. Simultaneously lake water samples (400 ml) were spiked with 5 uM $MnCl_2$, and at the times given in the text, 20 or 10 ml samples (depending on the amount of Mn oxides) were filtered through 0.6 um nuclepore filters. The filters were then incubated in 2 ml of Leucoberbelin blue for the determination of the concentration of Mn oxides (Leucoberbelin blue assay, in text of de Vrind, de Vrind, and Robbins, this volume).

Measurement of photoreduction of preformed Mn oxides.

Lake water samples were spiked with ^{54}Mn (0.005 uCi/ml) and incubated in the dark at room temperature for 12 hours. Then $MnCl_2$ (final concentration 100 uM) was added and the incubation was continued for another hour to desorb any non-oxidized Mn(II) from the oxides. Then samples of 150-200 ml were filtered through 0.6 um Gelman filters. The filters were rinsed three times with 5 ml portions of 0.2 um filtered Lake water. The filters were then incubated in capped 50 ml test tubes in fresh 0.2 um filtered lake water (surface water, Buoy 127). Dark controls were wrapped in aluminum foil. The tubes were incubated in an aquarium filled with tap water under natural light conditions (sunlight). At times given in the figures, 2.5 ml samples were filtered through 0.6 um Gelman filters, and 2 ml of the filtrates were transferred to counting vials. Scintillation liquid (Optifluor) was added and radioactivity was determined in the liquid scintillation counter.

Results

Mn-immobilization in lake water samples: photosynthetron experiments.

Water samples collected at the lake surface at Buoy 123 were spiked with ^{54}Mn and incubated in the photosynthetron at about 750 uE/m^2/s. These samples immobilized more than 50% of the added radiotracer within 2 hours as shown in Figure 1 (open squares). The rate of Mn-immobilization then decreased in the following period of 10 hr. When the light was subsequently switched off, the rate of immobilization increased again (Figure 1). In the presence of 0.01% $HgCl_2$, almost no Mn-immobilization was measured (Figure 1, closed triangles). Samples which were treated with hydroxylamine to reduce Mn oxides prior to the determination of Mn-immobilization did not contain immobilized Mn at all (not shown). The fact that a decrease in Mn-immobilization rate was measured during a light period, followed by an increase during a subsequent dark period made us assume that photosynthesizing cyanobacteria played a minor role in Mn-immobilization. If so, the addition of DCMU should have little or no effect on Mn-immobilization rates. In Figures 2

FIGURE 1

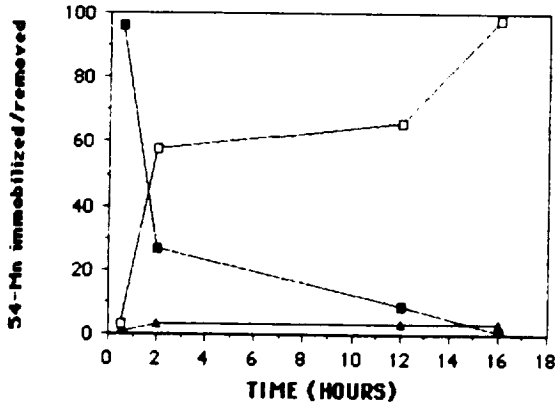

Figure 1 Immobilization of ^{54}Mn in lake water samples spiked with ^{54}Mn
Surface water was collected at Buoy 123. 5 ml of sample were spiked with 0 2 uCi ^{54}Mn and incubated in the photosynthetron at 750 uE/m^2/s. After 1/2. 2 and 12 hours the samples were filtered through 0.2 u Nuclepore filters and the radioactivity on the filters (open squares) and in the filtrate (closed squares) was counted. Closed triangles: lake water samples incubated with 0.2 uCi ^{54}Mn and 0 01% $HgCl_2$ and treated as described above After 12 hours the light was turned off and the remaining samples were incubated for another 4 hours in the dark, after which they were filtered and counted as described above

FIGURE 2

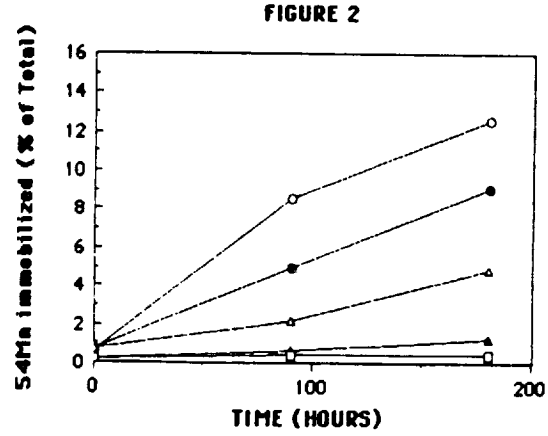

Figure 2 Mn immobilization in lake water samples spiked with 1 0 uM $MnCl_2$ and ^{54}Mn
Samples were collected from the surface water at Buoy 127 5 ml samples were spiked with 1 0 uM $MnCl_2$ and ^{54}Mn (0 03 uCi/ml), open circles: with 1 uM $MnCl_2$, ^{54}Mn and 100 uM DCMU (closed circles); with 1 uM $MnCl_2$, ^{54}Mn and $HgCl_2$, final concentration 0 005 % (open triangles) Closed triangles represent the filtrates of 0 2 u filtered samples, both spiked with 1 uM $MnCl_2$ and ^{54}Mn
The samples were incubated at 750 uE/m^2/s in the photosynthetron and filtered after 0. 90 and 120 minutes

and 3 the results are shown of two experiments where water samples were incubated with ^{54}Mn and 1 uM $MnCl_2$ (Figure 2) or 10 uM $MnCl_2$ (Figure 3) for a period of 3 hours. The open squares represent the Mn-immobilization by unpoisoned samples, and the open circles the rates of Mn-immobilization of samples containing 100 uM DCMU. Especially in the sample supplemented with 10 uM $MnCl_2$ the photosynthetic inhibitor did not appear to affect the immobilization rate. The samples poisoned with $HgCl_2$ (0.005% in this case, open triangles) showed decreased Mn-immobilization rates, although the degree of inhibition was less than shown in Figure 1. We also tested whether Mn-immobilization activity was preferentially associated with samples containing particles of a certain size. The filtrate of lake water filtered through 1.2 uM filters did not contain any activity (Figure 2, closed circles and triangles).

Discussion

Although the experiments described above have to be considered preliminary, they suggest that photosynthesizing cyanobacteria were not involved in Mn-immobilization in the samples under study. Since all the radioactivity was released by adding hydroxylamine, the ^{54}Mn was probably associated with pre-existing Mn oxides and a non-detectable portion was taken up by the cyanobacteria. Microscopic examination did not reveal any lysis of cyanobacteria by the hydroxylamine treatment. The inhibition of Mn-immobilization by $HgCl_2$ suggests that biota are involved in this process: $HgCl_2$ should not interfere with Mn-chemistry (Rosson, Tebo and Nealson, 1984). It may be possible, however, that $HgCl_2$ stimulates the photoreduction of Mn oxides, resulting in an underestimation of Mn-immobilization. Clearly, experimentation is needed to investigate this possibility. Since water samples containing particulates < 1 um did not contain any Mn-immobilization activity, free-living, small bacteria were not involved in the activity either.

We suggest that the Mn may have been immobilized by particulate oxides (presumably Mn oxides) and partly by bacteria attached to particles and cyanobacteria. The bacteria possibly stimulated oxidation of Mn to Mn oxides. Decreased rates of Mn immobilization may have resulted from photoinhibition of the Mn-immobilizing organisms or from photoreduction of the Mn oxides.

Mn-immobilization in lake water samples: aquarium experiments.

In a first attempt to discriminate between Mn-binding and Mn-oxidation in lake water, 400 ml samples were incubated with 5 uM nonradioactive $MnCl_2$, with or without a radioactive $MnCl_2$ spike. Lake water samples were taken from the surface or from 10 m depth at Buoy 127. They were incubated either under natural light conditions (the 10 m samples in a screened aquarium) or in the dark by wrapping the samp bottles in Al foil.

The rates of Mn-immobilization were measured over the first three hours after the spike with ^{54}Mn and 5 uM $MnCl_2$ (Figure 4). The 8 m sample incubated in the dark (Figure 3, open squares) had the same Mn uptake rate as the 8 m sample incubated at its ambient light intensity (not shown). The rate was significantly higher than those of the surface samples incubated in the light (Figure 3, open circles) or in the dark (Figure 3, open triangles). The uptake rates of the latter samples did not seem to differ significantly. The Mn-oxidation rates were determined with the Leucoberbelin blue assay. Because this assay is far less sensitive to measuring increases in Mn oxide concentrations than the use of radioisotopes, the rates were measured over a much longer period (Figure 5). The Mn-oxidation rates of

FIGURE 3

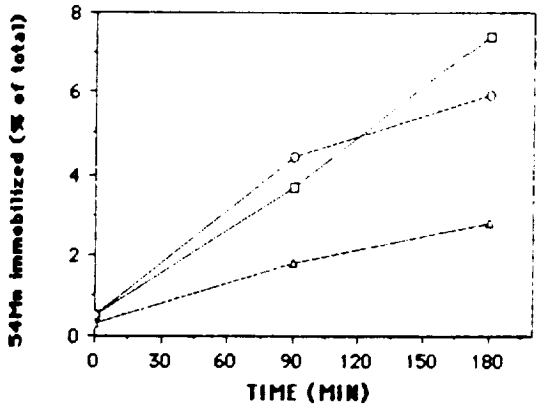

Figure 3 Mn immobilization in lake water samples spiked with 10 µM $MnCl_2$ and ^{54}Mn

5 ml surface samples from Buoy 127 were spiked with 10 µM $MnCl_2$ and ^{54}Mn (0.03 µCi/ml), open squares; or with 10 µM $MnCl_2$, ^{54}Mn and 100 µM DCMU (open circles), or with 10 µM $MnCl_2$, ^{54}Mn and 0.01 % $HgCl_2$ (open triangles) The samples were incubated in the photosynthetron at 750 uE/m^2/s, filtered after 0, 90 and 180 minutes and counted

FIGURE 4

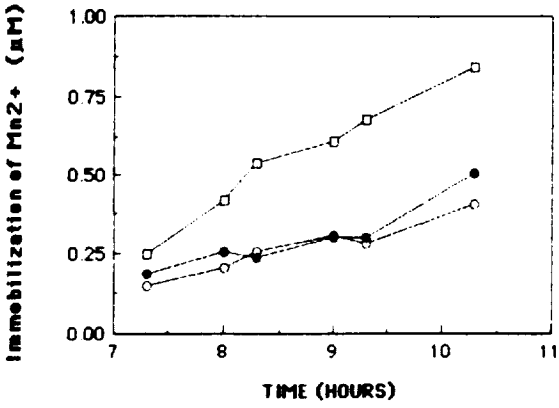

Figure 4 Manganese immobilization in lake water Samples collected July 30 at 0800 hours from the surface and 10 m were then spiked with 5 µM Mn^{2+} and ^{54}Mn as tracer. At times shown in the figure subsamples of 30 ml were filtered. Manganese immobilization was calculated from the radioactivity trapped on the filters (total free manganese assumed to be 5 µM).
Open circles: surface sample incubated in sunlight
Closed circles: surface sample incubated in the dark.
Open squares: sample from 10 m incubated in the dark

FIGURE 5

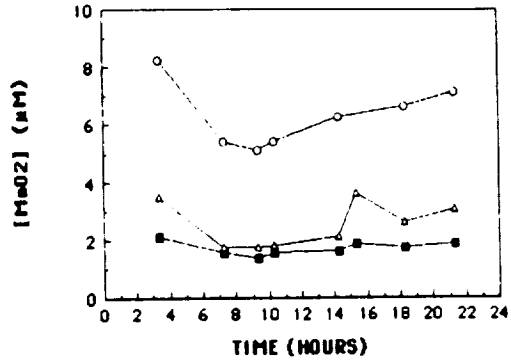

Figure 5. Manganese oxidation in lake water. Water samples similar to those described in Fig. 4, were spiked with 5 μM Mn^{2+}. At times given in the figure subsamples of 20 ml were filtered and manganese oxide concentration was calculated from the Leucoberbelin blue assay.
Closed squares: surface samples in sunlight
Open triangles: surface samples in the dark
Open circles: samples from 10 m incubated in the dark.

FIGURE 6

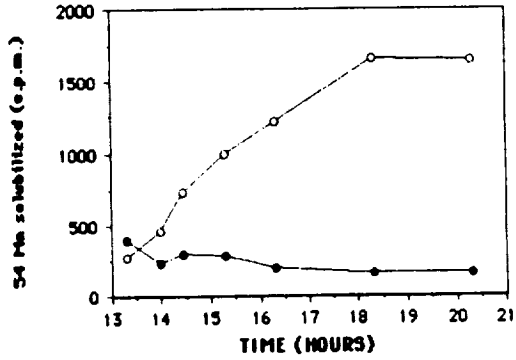

Figure 6. Dissolution of ^{54}Mn labeled MnOx in the light and in the dark. Particulate manganese was formed naturally from added $^{54}MnCl_2$ over three days in the dark in a 8 m lake water sample from Buoy 127. The radiolabeled particles were treated with non-radioactive $MnCl_2$ (100 μM) to desorb non-oxidized tracer,and the particles were filtered. The filters were rinsed and incubated in fresh 0.2μ filtered surface lake water. Release of soluble ^{54}Mn was measured through time.
Open circles:samples incubated in sunlight
Closed circles: samples incubated in the dark
Data represent mean values of duplicate experiments.

FIGURE 7

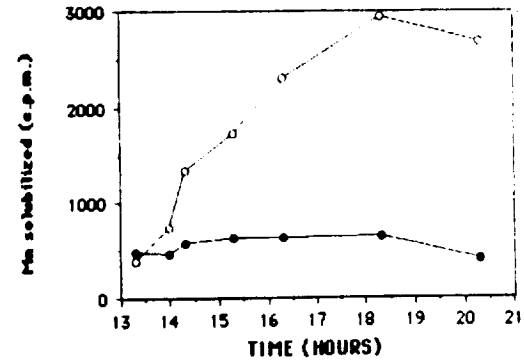

Figure 7. Dissolution of ^{54}Mn labeled MnOx in the light and in the dark. Particulate manganese was formed from $^{54}MnCl_2$ in an 8 m sample from Buoy 127 in the dark during a 24 hour period.

the 10 m samples, incubated in ambient light or dark, were very similar (dark rates are shown, Figure 5, open circles). The rates were significantly higher than those of the light and dark incubated surface samples (Figure 5, closed squares and open triangles, respectively). Also, the original amount (natural amount) of Mn oxides was about 3 times as high in the 10 m samples. The surface sample incubated in the light seemed to have a lower Mn-oxidation rate than the surface sample incubated in the dark. The calculated rates of Mn-immobilization and those of Mn-oxidation from the slopes of the straight parts of the curves are shown in Table 1. Except for the light incubated surface sample, the Mn-oxidation rates approximated the Mn-binding rates.

Table 1. Calculated Mn-immobilization and Mn-oxidation rates.

Sample	Mn-immobilization rate, uM, h^{-1}	Mn-oxidation rate uM, h^{-1}
8 m, dark	0.18	0.20
surf. dark	0.10	0.11
surf. light	0.04	0.09

Discussion

The results of this experiment suggest that the immobilized Mn as measured with the radioactive isotope ^{54}Mn was almost completely oxidized. This result predicts that the average oxidation state of the natural oxides should be very high (see below). The oxidation rates seem to be correlated with the number of oxide particles present in the samples at the onset of the experiments. Because we did not include experiments with poisoned controls, we cannot discriminate between biotic or abiotic oxidation in this experiment. The difference in light intensity may also have influenced the Mn-binding and oxidation rates by either photoinhibition of biota or photoreduction of oxides, or both. Therefore, we attempted to determine rates of photodissolution of preformed radioactive Mn oxides (see below).

Photoreduction of preformed Mn oxides.

In the first experiment radioactive oxides formed in surface samples from Buoy 127 were incubated in the dark or at ambient light intensity (full sunlight) and the rate of release of radioactive Mn was measured (Figure 6). Under the influence of light $^{54}Mn^{2+}$ was released as shown by the open symbols. In the dark (closed symbols) no $^{54}Mn^{2+}$ was released. When the light intensity decreased (in the beginning of the evening) the release of ^{54}Mn came to a standstill. The specific activity of the radioactive oxide was not determined, but at the end of the experiment all oxide was solubilized with hydroxylamine and the total soluble radioactivity was counted. The release of ^{54}Mn under influence of the light could then be calculated as a percentage of the total: it amounted to $2.2\% \cdot h^{-1}$.

In a second experiment 8 m samples from Buoy 127 were used. These contain more oxides, and their Mn^{-1} oxidation rates are higher, so that the amount of oxides accumulated on the filters prior to the photoreduction experiment was much higher (estimated to be a factor 10). Under the influence of the light, ^{54}Mn was released (Figure 7) whereas the

dark incubated sample did not release any ^{54}Mn. The rate of photoreduction amounted to $0.45\%\cdot h^{-1}$.

Discussion

These experiments clearly demonstrated that photoreduction may release Mn from Mn oxides formed in Oneida Lake. The first rate measured ($2.2\%\cdot h^{-1}$) is of the same order of magnitude as that reported by Sunda for oceanic waters ($4.3\%\cdot h^{-1}$, W.G. Sunda, In: S.A. Huntsman Solars X Cruise Report: Effect of sunlight on manganese redox cycling in oceanic and coastal seawater, submitted). When higher oxide concentrations were used, however, the rate of dissolution dropped dramatically, although the overall effect was very similar. We believe that the filter procedure used (as described by Sunda) can not be satisfactorily applied to waters containing high concentrations of particles. A large part of the oxide will be unavailable for the reduction reaction by the covering of other particles. Either small lake water volumes should be used and consequently labeled very high or, alternately, the oxides should be removed from the filters and be evenly suspended, e.g. by ultrasonication. Experiments of this type have to be performed before an estimation of the photoreduction rate in Oneida Lake can be made.

Determination of the manganese oxidation state of manganese oxides in lake water.

Two sets of experiments were performed to determine the average manganese oxidation state of manganese oxides in Oneida Lake.

Water samples were collected at Buoy 127 from the surface and the 8-m depth on July 23, 1987. Two portions of 150 ml from both the samples were filtered through glass fiber filters (Whatman GFA). Two other portions of 150 ml were filtered over nuclepore (1.2 um) filters. The average oxidation state was determined by measurement of the equivalent concentration of oxidized manganese on the filters with the iodometric titration method as described by Tebo (see Tebo methods) and the measurement of total manganese on the filters by atomic absorption spectrometry. The filters were incubated in the reaction mix (H_2SO_4, KI/KOH, dH_2O, see Tebo methods) for 15 minutes. One blank glass fiber and one blank nuclepore filter were incubated in the reaction/mix simultaneously to serve as controls.

After 15 minutes the filters were removed and starch solution was added to the incubation mixtures. The mixtures containing the blank filters did not contain any I_2 as determined with the starch solution. The samples were then titrated with umM $Na_2S_2O_3$ using a microburet. After titration they were filtered through 0.2 um nuclepore filters prior to measurement of atomic absorption. The calibration of the atomic absorption spectrometer is shown below:

Mn^{2+} conc. ppm	absorbance
0.1	0.007
0.5	0.033
1	0.066
2	0.130
3	0.189

Results

Titration of samples and determination of Mn^{2+} concentration with atomic absorption:

Table 2. Determination of Mn^{2+} concentration.

Sample	ul NaS_2O_3 titrated	absorbance AA	total volume(ml)	nmoles Mn^{2+}
Surface, glass fiber filt. 1	128.6	0.058	4.43	70.88
Surface, glass fiber filt. 2	138.6	0.059	4.44	72.15
Surface, nuclepore filt. 1	83.0	0.060	4.32	72.27
Surface, nuclepore filt. 2	106.0	0.052	4.41	63.06
8 m, glass fiber filt. 1	75.4	0.138	4.38	166.4
8 m, glass fiber filt. 2	80.6	0.135	4.48	166.7
8 m, nuclepore filt. 1	54.4	0.116	4.35	139.2
8 m, nuclepore filt. 2	54.4	0.119	4.35	142.7
blank glass fiber	--	0.001	4.30	--
blank nuclepore	--	0.002	4.30	--

Because the Fe concentration in the lake water was not determined, the average oxidation state of the oxides (x in MnO_x) was calculated using the formula:

$$x = \frac{(\text{vol. of } S_2O_3^{=})([S_2O_3^{=}])}{\text{moles of Mn in sample}} [1/2] + 1$$

Table 3. Oxidation state of Mn oxides in Oneida Lake samples.

Sample	x
surface, glass fiber filt. 1	1.91
surface, glass fiber filt. 2	1.96
surface, nuclepore filt. 1	1.57
surface, nuclepore filt. 2	1.84
8 m, glass fiber filt. 1	1.91
8 m, glass fiber filt. 2	1.97
8 m, nuclepore filt. 1	1.78
8 m, nuclepore filt. 2	1.76

No significant differences were found between the oxidation states of the oxides collected at the surface and those collected at 8 m depth.

The oxidation states of the oxides concentrated with nuclepore filters were consistently lower than those of the oxides concentrated with glass fiber filters. This may have been caused by underestimation of the amount of I_2 formed due to adsorption of the I_2 to the nuclepore filters, resulting in an underestimation of the oxidation state. Alternatively, the glass fiber filters may have adsorbed free Mn^{2+} ions, which would have resulted in an

overestimation of the oxidation state. To discriminate between these possibilities the following experiment was performed. Four 200 ml samples (8 m, Buoy 127, collected on July 28) were filtered over glass fiber filters, and four 200 ml samples were filtered over 0.2 um nuclepore filters. The filters were incubated in the H_2SO_4, KI/KOH, dH_2O reagent mix for 1 hour. Simultaneously one set of glass fiber filters and one set of nuclepore filters were incubated in scintillation vials containing the AA-Mn^{2+} standard solutions of 0.1, 0.5, 1, 2, and 3 ppm.

After 1 hour two of the glass fiber and two of the nuclepore filters were removed from the H_2SO_4, KI/KOH, dH_2O mix prior to the titration with $Na_2S_2O_3$. The other filters were removed after titration. The glass fiber and nuclepore filters were then also removed from the AA standard solutions, and all samples were filtered through 0.2 um nuclepore filters. Total manganese was then measured with atomic absorption.

Results

Table 4. Calibration of atomic absorption spectrometer.

Mn^{2+} conc. ppm.	absorbance	absorbance in filter incubated standards	
		glass fiber	nuclepore
0.1	0.007	0.007	0.007
0.5	0.029	0.031	0.030
1	0.058	0.063	0.058
2	0.123	0.124	0.125
3	0.182	0.183	0.176

Table 5. Removal of Mn^{2+} onto filters.

Sample	ul $Na_2S_2O_3$ titrated	absorbance AA***	total volume	nmoles of Mn	calculated x
glass fiber 1*	170.3	0.074	4.47	387	1.88
glass fiber 2*	163.2	0.076	4.46	412	1.79
glass fiber 3**	153.6	0.078	4.45	423	1.73
glass fiber 4**	152.4	0.077	4.45	418	1.73
nuclepore 1*	136.2	0.071	4.44	369	1.74
nuclepore 2*	130.6	0.070	4.43	367	1.71
nuclepore 2**	128.6	0.072	4.43	374	1.69
nuclepore 4**	127.5	0.073	4.43	379	1.67

* filters removed after titration
** filters removed prior to titration
*** absorbances minus absorbance of blank filters incubated in H_2SO_4/KI/KOH/dH_2O mix (glass fiber filter 0.003, nuclepore filter 0.005).

Conclusions

The data indicate that neither glass fiber filters nor nuclepore filters remove significant amounts of Mn^{2+} from solution. Except for sample glass fiber 1 the values of the average oxidation states do not differ greatly. This is ascribed to the longer incubation time of the filters in the H_2SO_4, KI/KOH, H_2O reaction mix as compared to the incubation time in the first experiment. The desorption of I_2 from the filters is presumably a relatively slow process. Consequently higher amounts of I_2 are found when filters are not removed from the reaction mixes prior to the titrations. The average of the oxidation states as determined in the oxides from the July 23 samples was 1.84, whereas the average determined on July 28 was 1.74.

David Bolgrien

"The Use of a Photosynthetron in Modeling the Primary Productivity in Oneida Lake"

Introduction

The use of remote sensing to assess the distribution and magnitude of primary production rates requires a clear relationship between productivity and surface chlorophyll concentrations. The extrapolation of this relationship to derive the rates of other processes further detached from chlorophyll (such as Mn cycling) is difficult (Figure 1).

remotely sensed data

chlorophyll concentrations

primary productivity

Mn reduction Mn oxidation

Figure 1. Schematic diagram of possible relationships.

The chlorophyll distribution of Oneida Lake, NY was successfully measured by remote sensing by Wrigley et al. (1987). The objectives of the present study were to determine if primary productivity could be coupled to chlorophyll concentration in a consistent manner and to assess variance of productivity based on three factors. The general experimental design was to collect from either many buoy surface waters (horizontal factors), many depths at few buoys (vertical factors), or few depths at a single buoy over time (temporal factor). Approximately 30 experiments were conducted in order to assess these factors. This includes a survey of surface water productivity which will be used to calibrate remote-sensing data by Wrigley and Richardson (see abstracts, this volume).

Methods

The rapid turnover of carbon in Oneida Lake required that primary productivity measurements be made using small volumes and short incubation times. These criteria were met by employing the methods of Lewis and Smith (1983). The exclusion of metazoan grazers, the reduction of photoinhibition in cells incubated for long periods at fixed light intensities, and the avoidance of particle size segregation through filtration lessened the systematic underestimation of daily production rates (cf. Harris 1980). Water samples were collected with a 2.5 L Van dorn and held in the dark until processed (typically within 2 h). An 80 mL subsample was inoculated with sufficient ^{14}C as $Na^{14}CO_3$ to achieve a specific activity of approximately 0.25-1.0 uCi mL^{-1}. The volume of the added isotope was assumed not to perturb the carbon content of the sample. Five mL aliquots were dispensed by repetitive pipetting (Eppendorf repeater pipette 4780) into 20 mL glass scintillation vials. Replicate 1.0 mL aliquots were taken to determine total activity. Various experiments were conducted using poisoned, filtered, and DCMU

inhibited controls, and time-zero samples in order to assess the efficiency of isotope uptake by abiotic process and stripping during post-incubation processing. Vials were illuminated from the bottom in a quantifiable light gradient in a temperature controlled photosynthetron. Irradiance received by each vial was measured by a LiCor Quantum light sensor after each experiment. Typically, irradiance ranges from 5 to 1500 uE/m^2/s.

At the end of the incubation (60-90 min), acid (0.1-0.5 mL 4N HCl) was added to each sample followed by agitation on a shaker table (approximately 200 rpm) for at least 60 min. After shaking, scintillation fluor (Opti-fluor, Packard or Aquasol, Beckman) was added directly to the scintillation vials. An approximate ratio of 5 mL sample to 15 mL fluor resulted in no separation of liquids. Samples were counted using a Packard 1500 Tri-Carb LSC. All sample preparation was done in a laboratory hood. Sample preparation (sample inoculation and dispensing) generally took less than 2 min per sample, post-incubation processing took approximately 1 min.

Additional samples (<1 L) were filtered through glass fiber filters (Whatman GFA) for chlorophyll a analysis (see methods of Riege, this volume). Filtered samples were homogenized and pigments extracted in 90% acetone. The extract supernate was measured spectrophotometrically. Chlorophyll concentrations obtained from the fluorometric calibration of Riege (this volume) and C. Aguilar (pers. comm.) were also used. Alkalinity was measured by titration with 0.02N H_2SO_4 to an endpoint of pH 4.2 according to standard methods.

Data Reduction

Production vs irradiance data were fit using the model of Fee (1984; pers. comm.). The rate of production at a given irradiance was calculated from an equation based on photosynthetic parameters (PBm and alpha). The parameter PBm is the rate of photosynthesis per unit of chlorophyll at optimal irradiance (mg C/(mg chl*h)). The parameter alpha is the slope of the light-limited portion of the photosynthesis vs irradiance curve per unit of chlorophyll (mg C/mg chl*E*m^{-2}). There is no parameter in this model which quantifies photoinhibition. The advantage of this approach is that estimates of primary production can be made in lakes for which only chlorophyll and transparency data are available. This study should be the initial step in the consistent collection of photosynthetic parameters from Oneida Lake.

Apparatus

A photosynthetron was engineered by the Instrument Shop of the Center for Great Lakes Studies modifying the design of Lewis and Smith (1983). It consists of a sheet metal box containing 4 projector lamps (GE model EYK; 300 W, 120 VAC). Pairs of lamps are controlled by dimmer switches. Two cooling fans are mounted on one side of the box (Figure 2). A glass filter envelope containing a $CuSO_4$ solution (20 g/L; pH 3.5) was placed on top of the box to filter infrared radiation. A diffusion plate (translucent glass) was placed between the filter and vials in order to achieve more uniform irradiance. Experimental light gradients were maintained by varying the number of plastic window screens, vial position in relation to the lamps, and the lamp intensity. Sixty-four holes, with a diameter slightly larger than the outer diameter of a scintillation vial, were machined into an aluminum block (Figure 3). Between the rows of vial holes, slots were cut to facilitate the flow of coolant water through the block (Figure 4). Flowing tap water was adequate to maintain the temperature of the sample in the vials to within 0.5°C of the

Table 1: Photosynthetic variables from Oneida Lake, NY.

Date	Buoy	z	t	Chl	P_{opt}	PB_m	A^B	n	SD	r^2	I_k
870728	B127	0	1330	8.74	13.00	1.49	2.45	3	2.03	.59	169
		1		9.97	10.00	1.48	1.63	4	0.36	.91	252
		2		9.97	11.00	1.10	2.00	5	0.60	.79	153
		3		10.27	10.42	1.01	1.32	3	0.23	.97	213
		4		9.97	11.78	1.18	1.89	3	0.43	.95	173
		5		9.66	29.52	3.06	9.45	4	1.60	.97	90
870731	B127	0	0600	9.36	23.58	2.52	8.35	2	NA	NA	84
		4		9.66	21.31	2.21	NA		NA	NA	
		10		5.09	12.04	2.37	4.97	2	NA	NA	132
		0	1200	9.36	65.22	7.01	16.38	5	4.61	.93	119
		4		12.10	88.27	7.30	12.29	5	2.74	.87	165
		10		4.78	35.86	7.50	16.34	3	1.84	.96	127
		0	1800	12.10	43.53	3.60	5.57	5	0.90	.93	180
		4		11.49	47.50	4.13	14.95	3	1.19	.99	77
		10		4.18	31.52	7.54	21.87	4	3.30	.95	96
870801	B127	0	0000	12.10	40.56	3.35	9.18	4	1.36	.96	101
		4		11.80	35.36	3.00	1.99	6	0.62	.72	419
		10		6.61	43.90	6.64	21.14	4	2.07	.99	87
		0	1200	8.44	51.36	6.08	10.53	3	0.64	.99	160
		4		9.97	54.25	5.44	12.57	3	0.38	.97	120
870804											
	B107	0	1030	10.05	18.82	1.87	2.91	5	0.32	.96	179
	B117	0	1045	5.18	12.83	2.48	5.17	4	0.71	.96	133
		4		8.83	10.63	1.20	2.33	5	0.13	.99	143
	B123	0	1100	3.35	10.99	3.28	5.27	5	1.36	.83	173
		4		6.40	7.18	1.12	2.05	4	0.01	.99	152
	B127	0	1115	3.96	9.81	2.48	4.67	5	0.21	.99	148
		2		10.66	12.95	1.21	1.82	5	0.22	.97	185
		4		7.61	7.36	0.97	2.40	4	0.32	.97	112
		8		7.00	7.17	1.02	2.28	5	0.40	.92	124

Table 1 (cont):

Date	(YYMMDD)
Buoy	(see lake map for location)
Z	(depth in meters)
t	(time of day sample taken (EDT))
Chl	(ug chlorophyll $\underline{a}(L^{-1})$)
P_{opt}	(assimilation number: mg $C(m^{-3}*h)^{-1}$)
P^{B}_{m}	(assimilation number: mg $C(mg\ chl*h)^{-1}$
A^{B}	(assimilation efficiency: mg $C(mg\ chl*Einstein*m^{-2})^{-1}$)
n	(number of observations used in linear regression to determine alpha)
SD	(standard deviation of $alpha^{B}$)
r	(correlation coefficient of linear regression to determine alpha)
I_k	(saturation irradiance: uE m^{-2} s^{-1})
NA	(insufficient light-limited production data to calculate alpha)

Fig 2: Photosynthetron front view (screen removed). All dimensions are in inches. Air flow is toward viewer.

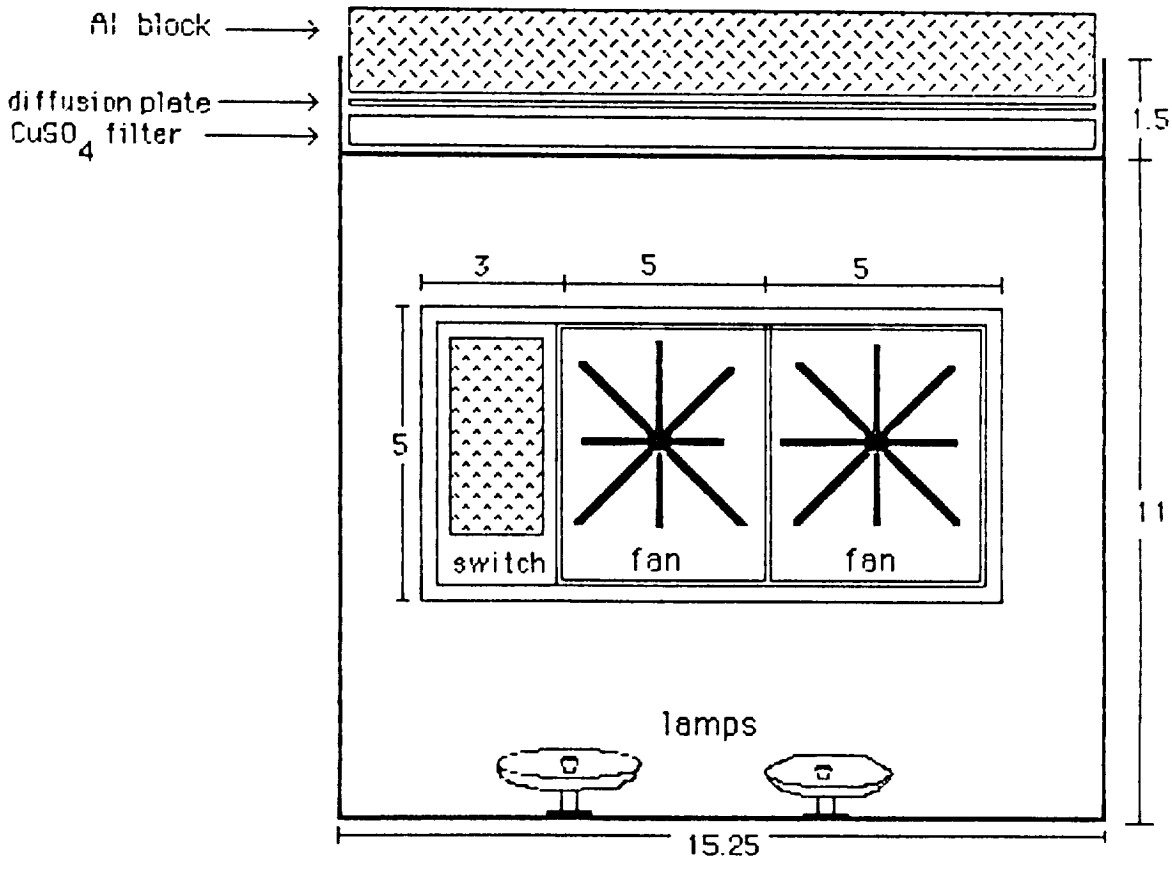

desired temperature. Temperatures in the lake ranged from 19-25°C over the course of the summer.

Results and Discussion

The horizontal distribution of productivity was assessed using samples from a lake transect from Buoy 109 to Buoy 127 on 04 Aug. At each buoy, temperature, dissolved oxygen, and fluorescence were measured in situ and surface water was collected for chlorophyll analysis and radioassay. This sampling coincided with the overflight of the MSS aboard a GOES satellite.

Surface chlorophyll a concentrations were high at Buoy 107 (10.05 ug/L), intermediate at Buoy 117 (5.18 ug/L), and uniformly low at Buoys 123 and 127 (3.35 and 3.96 ug/L, respectively) (Riege, this volume). Volumetric production (P_{opt}) followed this trend by steadily decreasing moving from east to west. A less definite trend was apparent when the data were normalized for biomass (Table 1). Assimilation capacity (PBm) and alpha were roughly uniform in the surface water, varying by less than a factor of 2. Buoy 123 showed slightly elevated values for both parameters. It is apparent that while surface chlorophyll concentrations varied over the area of the lake, photosynthetic parameters were generally homogeneous (Table 1). Production estimates of the entire lake could, therefore, be made via remote sensing methods if the photosynthetic parameters of a single site were known.

The vertical factors controlling productivity in the water column include light inhibition, density gradients, and mixing events. These factors induce physiological changes in phytoplankton through light history and nutrient availability considerations. The analysis of Riege (this volume) suggests that total chlorophyll maxima were typically subsurface (2-4 m) during the day and biomass was uniformly distributed throughout the water column during the night. Samples from Buoy 127 on 28 July show chlorophyll concentrations at 8.7 ug/L at the surface and increasing with depth to 10.3 ug/L at 3 m. Production data indicated maximum assimilation rates at 5 m (Table 1). Surface and 1 m samples had alpha values more similar to 5 m than the other depths. It can be postulated that nutrient concentrations may have been elevated in the top meter of water due to regeneration from the sediments. Cells in the middle of the water column appear to be nutrient limited relative to the surface and bottom water. Nutrient analyses will be completed at a later date.

The vertical distribution of production was more often seen to correlate with the ambient biomass abundance. At Buoy 127 on 04 August, peak productivity and peak biomass clearly coincided at 2 m. As with the surface samples, the photosynthetic parameters were uniform, although values were generally lower than at the surface. There is no evidence of stratification or nutrient regeneration on this date except for possible subsurface chlorophyll maxima at Buoys 123 and 127.

The temporal nature of production in Oneida Lake was assessed in a diel sampling on 31 July - 01 August. Samples were taken at 6-hour intervals (starting at 0600) from 3 depths (Table 1). Surface samples showed a typical diel cycle with low photosynthetic parameter values at dawn (alpha=9.53, PBm=2.52), a peak at noon (alpha=25.99, PBm=7.01), and an evening depression (alpha=11.70, PBm=3.60). This cycle was essentially repeated on 01 August. Phytoplankton became dark adapted during the night and had a lowered photosynthetic capacity at dawn. By noon, the production rates were higher as cells became more tolerant of irradiance. The 1800 h sample indicated possible photoinhibition above 4 m while maintaining noon levels at 10 m. The role of photoinhibition in

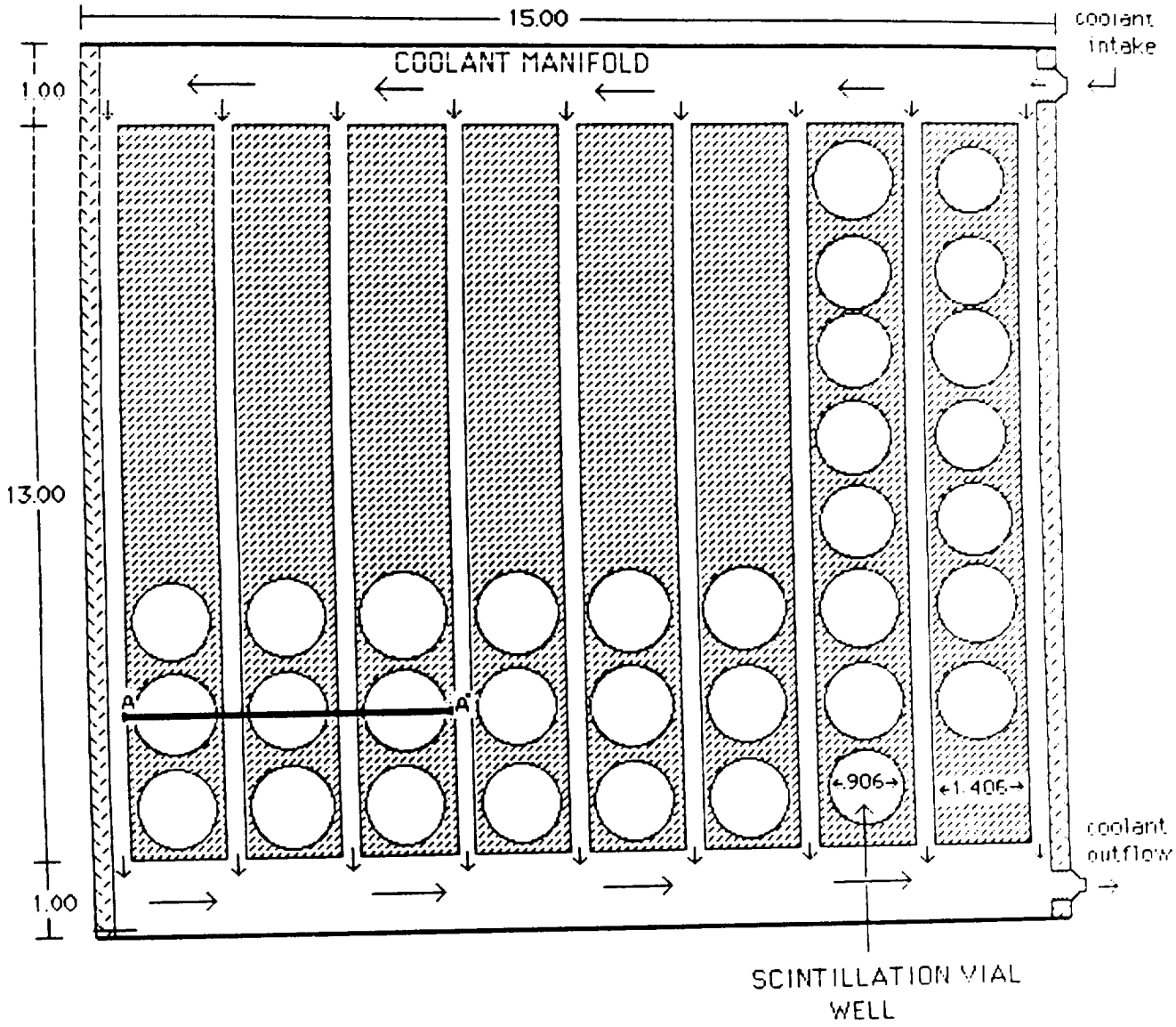

Fig 3: Bottom view of aluminum block with bottom plate removed. All dimensions are in inches.

Fig 4: Detailed cross section of photosynthetron aluminum block and filter. All dimensions are in inches.

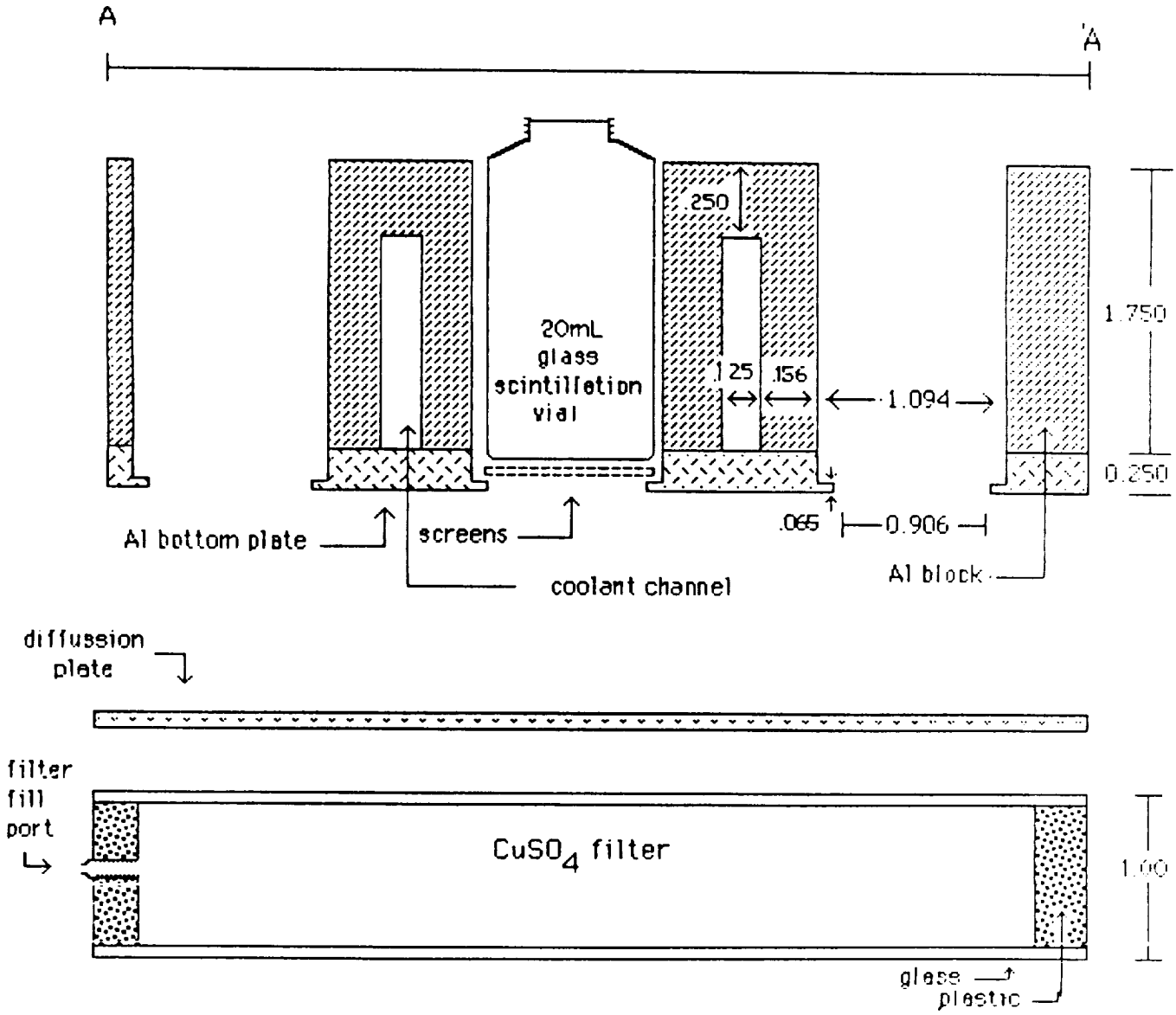

controlling the productivity in Oneida Lake may be underestimated by this study. A more complete array of in situ experiments, taking into consideration the natural mixing rates in the broad shallow basin, would be necessary.

Conclusion

This study has provided the first coordinated effort to measure primary production in Oneida Lake using the ^{14}C method. The results show that the lake is very productive throughout the middle of the summer. An obvious shortcoming here is that no seasonal trends are apparent. Changes in nutrient concentrations, predation pressure, and phytoplankton community composition all affect primary production but it is suggested here that chlorophyll concentration is the best representative of whole lake production.

References

Fee, E.J. (1984) Freshwater institute primary production model user's guide. Can. Tech. Rpt. of Fish and Aq. Sciences 1328.

Harris, G.P. (1980) Temporal and spatial scales in phytoplankton ecology. Mechanisms, methods, models and management. Can. J. Fish Aquat. Sci. 37:877-900.

Lewis, M.R. and J.C. Smith (1983) A small volume, short-incubation-time method for measurement of photosynthesis as a function of incident irradiance. Mar. Ecol. Prog. Series 13:99-102.

Wrigley, R. et al. Remotely sensed chlorophyll concentrations of Oneida Lake, NY (in press).

Hans de Vrind
Liesbeth de Vrind
Eleanora Robbins

"Isolation of a Leptothrix sp. from Bear Trap Creek (Syracuse, N.Y.)"

Introduction

Leptothrix discophora has been intensively studied for its manganese-oxidizing capability (van Veen, 1972; van Veen et al., 1978). Recently, an extracellular protein excreted by the sheathless Leptothrix discophora strain SS-1 has been identified as a factor that enters into the manganese-oxidizing capability of the bacteria (Adams and Ghiorse, 1987; Boogerd and de Vrind, 1987). The goals of our project were to isolate the species of Leptothrix in Bear Trap Creek and to investigate whether a similar Mn-oxidizing protein(s) could be extracted from both the sheathed cells and the spent culture medium.

Sample Collection

Bear Trap Creek is a small iron- and manganese-bearing creek near the Syracuse Airport, New York and the Taft Road offramp of Interstate 81N. Samples were collected immediately south of Taft Road in the extreme northwest corner of the Syracuse East 7 1/2 minute quadrangle. The bottom of this creek was covered with a thick reddish flocculent material in June and July of 1987; oil-like films on the water surface indicated the probable presence of Leptothrix species (W.C. Ghiorse, Cornell University, pers. commun.). The following samples were taken for the isolation of bacteria: 1) reddish flocculent material (floc), 2) water sample, and 3) detached deciduous leaves in the water.

Methods

The red floc appeared to consist of empty bacterial sheaths as revealed by light microscopy. The sheaths were encrusted with iron oxides and also contained manganese oxides as determined by reaction with Leucoberbelin blue (Krumbein and Altmann, 1973). The encrusting oxides were reduced with 0.5 M ascorbic acid at a pH of 5. The suspension was centrifuged into a pellet and washed twice with sterile deionized water and recentrifuged. The pellet was resuspended in sterile deionized water and plated onto M-100 plates. Water samples were plated directly onto M-100 plates. Scrapings from the leaves were suspended in sterile deionized water and plated onto M-100 plates.

L.D. medium, for growth of L. discophora was prepared as follows:

Combine in beaker:

0.4 g casomino acids (Difco)
0.4 g yeast extract (Difco)
0.1 g $(NH_4)_2SO_4$
0.2 ml trace element solution*
200 ml distilled water

Autoclave at 120°C for 20 min.

After cooling, add:

3.2 ml 1.25 M glucose (0.2 um filter sterilized)
2 ml 1M HEPES pH 7.5 (0.2 um filter sterilized)

* Trace element solution:

3.7 mM Fe(III) EDTA
420 mM $CaCl_2$
230 mM $MgCl_2$
0.1 mM $MnCl_2$
0.42 mM $CoCl_2$
0.75 mM $ZnSO_4$
0.26 mM Na_2MoO_4

M100 media, for Mn oxidation determinations, was prepared as follows:

75% seawater	1 L
$MnSO_4 \cdot 4H_2O$	0.2 g
$FeSO_4 \cdot 7H_2O$	0.001 g
Peptone	0.02 g
Yeast Extract	0.005 g
Agar	15 g

Mn oxides were assayed with Leucoberbelin blue (LBB). The purpose of the Leucoberbelin blue assay is to measure colorimetrically MnO_x concentrations in bacterial cell suspensions and spent culture media. Samples of 0.4 ml were added to 2 ml of 0.04 percent Leucoberbelin blue in 45 mM acetic acid, and the absorbance was read at 620 nm. Any cells present in the samples were removed by centrifugation prior to measurement of the absorbance.

For the determination of MnO_x concentrations in very dilute samples (creek water samples), the particulates were concentrated by filtration over 0.4-um or 1.2-um nuclepore filters (Krumbein and Altmann, 1973). The filters were incubated in 2 ml of 0.04 percent Leucoberbelin blue in 45 mM acetic acid for 15 min. The solution was then filtered again to remove non-dissolved particles, and absorbance was read at 620 nm.

When Gelman filters are used in this procedure, a blank filter should be incubated in a Leucoberbelin blue solution for the same period of time as the sample filters. Gelman filters contain substances that oxidize Leucoberbelin blue.

The Leucoberbelin blue assay follows Beer's law for absorbance values between 0 and 1.5 at 620 nm. Generally, if $KMnO_4$ (equivalent to 16.7 uM MnO_2) is present with an excess of the redox dye, the absorbance at 620 nm is 1.2 (Boogerd and de Vrind, 1987). In the present experiment, we calculated MnO_x concentrations by assuming it was all in the MnO_2 form.

Sodium dodecyl sulfate polyacrylamide gel electrophoresis (SDS-PAGE) was

performed as described below:

Prepare the following seven stock solutions

1. Acryl/bisacrylamide solution:

   29.1 g acrylamide
   0.9 g bisacrylamide
   100 ml distilled water

2. 10% sodium dodecyl sulfate (SDS) in distilled H_2O.

3. 1.875 M Tris in distilled H_2O, pH 8.8.

4. 1.25 M Tris in distilled H_2O, pH 6.8.

5. 10x concentrated electrode buffer:

   144.2 g glycine
   30.3 g Tris
   10 g SDS
   1 L distilled water

6. Sample buffer:

   2.5 ml 1.25 M Tris pH 6.8
   1.0 g SDS
   925 mg dithiothreitol
   5.8 ml 27% glycerol
   5 mg bromophenol blue
   50 ml distilled water

7. 10% ammonium persulfate (APS) in distilled H_2O (prepare fresh).

Prepare the separation gel:

Pipet into side-armed flask:

10% acrylamide gel, total volume 30 ml	7% acrylamide gel, total volume 30 ml
10 ml acryl/bisacryl solution	7 ml acryl/bisacryl solution
13.6 ml distilled H_2O	16.6 ml distilled H_2O
6 ml Tris pH 8.8	6 ml Tris pH 8.8

Evacuate, then add to each side:

300 ul 10% SDS
15 ul TEMED
100 ul 10% APS

Cover gel mix with thin layer of water-saturated isobutanol, and let gel polymerize for at least 1 hour.

Prepare the stacking gel:

Pipet into side-armed flask:

1.6 ml acryl/bisacryl solution
7.2 ml distilled H_2O
1.0 ml Tris pH 6.8

Evacuate, then add:

100 ul 10% SDS
10 ul TEMED
34 ul 10% APS

Remove isobutanol from separation gel, rinse with distilled H_2O and dry gel with Whatmann 3M filter paper. Pour stacking gel, insert comb, and allow gel to polymerize for 1 hour.

Remove comb, and apply samples (dissolved in sample buffer and centrifuged to remove insoluble material) to slots. Electrophorese at 100 V for 3-4 hours.

Protein staining: Stain gel in Coomassie solution for 15 minutes, destain in destaining solution.

Coomassie staining:

227 ml methanol
227 ml acetic acid
1.25 g Coomassie Brillant Blue
Fill to 500 ml with distilled H_2O

Destaining solution:

750 ml methanol
250 ml acetic acid
2.5 L distilled water

Mn staining: rinse gel in distilled H_2O for 1 hour, then incubate in 100 uM $MnCl_2$ in 10 mM HEPES at a pH of 7.5 until brown bands develop. Stop staining by incubating gel in distilled H_2O.

Results

No Mn-oxidizing colonies were detected on the M-100 plates that were inoculated with sheath material reduced by ascorbic acid. This result may indicate that the sheaths did not contain living cells or that living cells might have been killed by the ascorbic acid treatment.

Only a few Mn-oxidizing colonies were observed on the plates inoculated with water samples. Because these plates contained many non-oxidizing bacterial colonies and fungi as well, no further attempt was made to purify the Mn-oxidizing bacteria.

The plates inoculated with leaf scrapings contained many Mn-oxidizing colonies morphologically indistinguishable from Leptothrix discophora (W.C. Ghiorse, pers.

commun.). Several of these colonies were transferred to fresh M-100 plates. After two transfers, the plates contained colonies of only one type that was encrusted with Mn oxides. The colonies consisted of sheathed bacteria, tentatively identified as Leptothrix discophora. As far as could be judged by light microscopy, no other bacterial species were present. The isolated strain was called Leptothrix discophora N.C.1.

Preliminary Comparison of the Mn-Oxidizing Activities of Leptothrix Strain N.C.1. and of Leptothrix discophora Strain SS1

The bacteria were grown with continuous shaking in batch cultures (500 ml) in L.D. medium at room temperature. The culture of L. discophora SS1 consisted of a homogeneous cell suspension that could be enumerated by measuring the optical density at 660 nm (see Boogerd and de Vrind, 1987). The culture of Leptothrix N.C.1. consisted of flocs of sheathed cells that could not be enumerated by the optical density method. After two days, the culture of SS1 reached the stationary phase of growth (Optical Density at 660 nm of 1.0). Portions of both Leptothrix cultures were centrifuged to obtain the spent culture media. Subsequently, cultures and spent culture media were supplemented with $MnCl_2$ to a final concentration of 100 uM in order to measure the Mn-oxidation rate.

After 0, 15, 30, 60, and 120 minutes, the concentration of MnO_x was determined by means of the Leucoberbelin blue assay (Altmann, 1972). The results are presented in Figure 1. Most of the Mn-oxidizing activity appears to be associated with the cells in both strains of Leptothrix (Figure 1). The spent culture media of strain SS-1 and N.C.1 contained little or no activity. Leptothrix SS1 is generally known to release at least 50% of its compound that has Mn-oxidizing activity into the culture medium (Boogerd and de Vrind, 1987, Adams and Ghiorse, 1987). Sheathed Leptothrix strains also release a compound that has Mn-oxidizing activity into their media (W.C. Ghiorse, oral commun.). The Mn^{2+} in the trace-metal solution added to the culture media may explain the lack of Mn-oxidizing activity in the spent media. The Mn was probably oxidized to an oxide which in turn may have resulted in the removal of Mn-oxidizing proteins from the

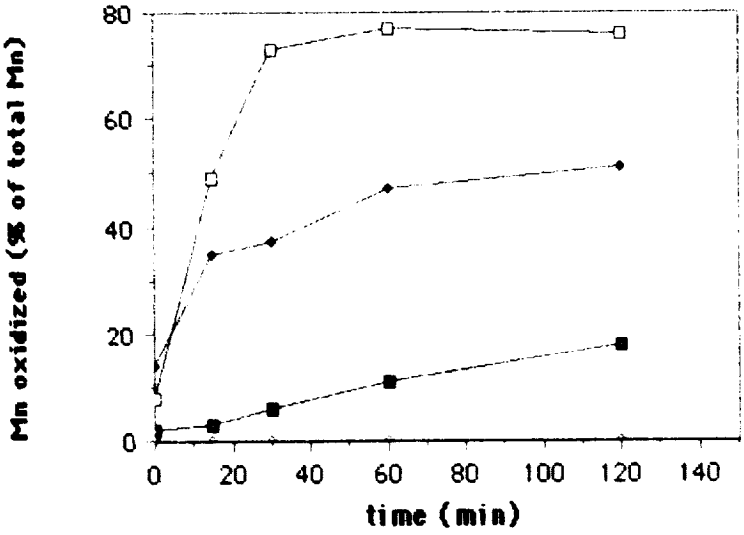

Figure 1. Mn oxidation by cell suspensions of Leptothrix discophora SS1 (open squares), Leptothrix N.C.1 (solid diamonds), spent culture media of L. discophora SS1 (solid squares) and Leptothrix N.C.1 (open diamonds).

solution as was seen previously in Boogerd and de Vrind (1987). This assumption is sustained by the presence of MnO_x in both the Leptothrix SS-1 and Leptothrix N.C.1 cultures at the onset of the Mn-oxidation experiment (Figure 1).

Polyacrylamide Gel Electrophoresis of Mn-Oxidizing Proteins

The Mn-oxidizing factor in the spent culture medium of Leptothrix discophora SS1 can be separated from other proteins by sodium dodecylsulfate polyacrylamide gel electrophoresis (SDS-PAGE). The factor can then be detected in the gel by rinsing the gel and incubating it in HEPES-buffered $MnCl_2$ solution. The main Mn-oxidizing factor released by L. discophora SS-1 is a protein having a molecular weight of 110,000, but Mn-oxidizing factors having lower molecular weights also can be detected in some strains (Adams and Ghiorse, 1987; Boogerd and de Vrind, 1987). In the present experiment, we investigated whether Mn-oxidizing proteins could also be detected in cultures of Leptothrix N.C.1. Because the Mn activity was mainly associated with the cells, both Leptothrix discophora SS-1 and Leptothrix N.C.1 cells were incubated in SDS and dithiothreitol-containing sample buffer for 30 minutes. The suspension was then centrifuged and the extract was submitted to SDS-PAGE at 100 V for 4 hours; the gel was then incubated in water for 35 minutes and subsequently stained in 100 uM $MnCl_2$ in 10 mM HEPES at a pH of 7.5. The extract of L. discophora SS-1 cells contained at least two Mn-oxidizing factors. Because no molecular weight markers were available, the molecular weights of the factors could not be determined. We assume that the most intensively stained (and thus most active band) in the Mn-oxidizing preparation of SS-1 represents the 110,000 D protein. This extract also contained a second factor having a lower molecular weight. The Leptothrix N.C.1 extract contained: 1) a Mn-oxidizing factor having a molecular weight similar to that of the second L. discophora SS-1 factor and 2) a factor having a still lower molecular weight which was represented by a faint band. It will be of interest to investigate whether the Mn-oxidizing factors from both Leptothrix strains are related with respect to composition and structure. A first step will be to react antibodies raised against the 110,000 D protein from L. discophora SS-1 with those of the Leptothrix N.C.1 extract.

Determination of Manganese Oxidation State of Manganese Oxides formed in Polyacrylamide Gels

The purpose of this experiment was to investigate whether the oxidation state of manganese oxides formed by individual Mn-oxidizing proteins from Leptothrix discophora N.C.1 could be determined. Cells were extracted with sample buffer, and the extract was submitted to gel electrophoresis to separate the Mn-oxidizing factors from other cellular proteins. In this experiment, only the 110,000 D Mn-oxidizing protein could be detected. The gel was incubated in $MnCl_2$ solution (100 uM in 10 mM HEPES, at a pH of 7.5) overnight to allow the protein to form a significant amount of oxide. Subsequently, two MnO_x-containing bands each having a surface area of about 25 mm^2 were cut from the gel and incubated in distilled water for 2 hours to remove non-oxidized Mn. Two bands having an area of 25 mm^2 but not containing oxides were incubated in distilled water simultaneously as blanks. The water was replaced every half hour. Then the equivalent concentration of oxidized manganese was determined with the micro-iodometric titration method as described by Murray et al. (1984). The gel parts were incubated in the reaction mix (dH_2O, KI/KOH, H_2SO_4) for at least 60 minutes to allow the I_2 formed by the oxidation of the I^- by the MnO_x to diffuse out of the gel bands. Then starch solution was added and the I_2 was titrated with 4 mM $Na_2S_2O_3$. In the incubation mix containing the blank gel bands, no I_2 had been formed, as determined with starch solution. The amount

of total soluble Mn^{2+} was then determined with atomic absorption spectrometry (Tables 1 and 2).

Table 1. Calibration of atomic absorption spectrometer.

Mn^{2+} concentration mM	Absorbance
0.1	0.007
0.5	0.035
1	0.067
2	0.129
3	0.193

Table 2. Titration of samples and total Mn^{2+} by atomic absorption.

Sample	$Na_2S_2O_3$ titrated (ul)	Absorbance (AA)	Total volume (ml)	Total Mn^{2+} (AA) (nmoles)
MnO_x1	100.9	0.173	4.401	209.6
MnO_x2	144.4	0.119	4.444	295.5
		(diluted 2x)		
blank 1	-----	0.003	4.300	3.0
blank 2	-----	0.003	4.300	3.0

Methods for determination of Mn oxidation are constantly evolving. Most of the analytical methods for measuring the oxidation state of Mn oxides involve measuring the total equivalent concentration of oxidized manganese which is equal to:

$$[O_x] - 2[Mn(IV)] + [Mn(III)]$$

and the stoichiometry of the oxides are represented as O/Mn ratios or MnO_x where:

$$x = 1 + \frac{1}{2}\left(\frac{2[Mn(IV)] + [Mn(III)]}{[Mn(Mn(IV)] + [Mn(III)] + [Mn(II)]}\right)$$

There are many methods for determining the oxidation state, however, Murray et al. (1984) have demonstrated that either the oxalate reduction method or the iodometric titration method are the most accurate and reproducible. Although Fe(III) interferes in the iodometric method and not in the oxalate method, the iodometric method was preferred because it involves less trial and error for choosing sample size than does the oxalate method (which is a method of differences). Corrections for Fe(III) can be easily applied simply by measuring total Fe (e.g. by the ferrozine colorimetric method or by atomic absorption spectroscopy). Of course in a laboratory situation, iron will seldom cause a measureable interference.

Iodometric method

The chemistry is similar to a Winkler O_2 titration. Mn(IV) is reduced by iodide (I^-) to produce iodine (I_2) which is then titrated with thiosulfate ($S_2O_3^=$). All reduced Mn(II) stays in solution. The number of equivalents consumed by thiosulfate is equal to twice the amount of I_2 produced.

$$MnO_2 + 4H^+ + 2I^- \rightarrow Mn^{2+} + I_2 + 2H_2O$$

$$MnOOH + 3H^+ + I^- \rightarrow Mn^{2+} + 1/2\ I_2 + 2H_2O$$

titration: $I_2 + 2S_2O_3^= \rightarrow 2I^- + S_4O_6^=$

I_2 forms a blue-colored complex with starch. When blue color disappears, titration is complete.

Reagents:

5 M H_2SO_4 (10 N)	=	28 ml conc. H_2SO_4/100 ml dH_2O
2 M KI/4 M KOH	=	33.2 g KI + 22.5 g KOH/100 ml dH_2O
starch solution	=	0.5 g/100 ml boiling dH_2O
0.5 to 1 mM $Na_2S_2O_3$	=	Concentration will depend on how much Mn oxide you are titrating - for small amounts use low concentrations.

Primary standard:

0.01 N KIO_3: 0.3567 g KIO_3/liter dH_2O. Potassium iodate should be oven dried at 105-110°C. (Weigh precisely known amount and calculate normality!!)

Procedure:

The procedure described is for a microanalysis of Mn oxidation state. Analytical precision, of course, will be greater for larger volumes and sample sizes. Volumes can be adjusted according to one's needs.

1) Standardize $S_2O_3^=$. Should be standardized every other day.

$$IO_3^- + 5I^- + 6H^+ \rightarrow 3I_2 + 3H_2O$$

$$I_2 + 2S_2O_3^= \rightarrow S_4O_6^= + 3H_2O$$

Add to small vial:
- 4 ml dH_2O
- 100 ul H_2SO_4 mix
- 100 ul KI/KOH dropwise, stirring
- 50-100 ul standard KIO_3, w/o vigorous stirring
- let react 1 minute

Titrate with thiosulfate until straw color
Add 100 ul starch solution (should turn blue)
Titrate until blue color disappears
Measure total volume of thiosulfate added

To determine reagent blank, add an additional aliquot of KIO_3 and titrate to endpoint again. Measure volume of thiosulfate added.

Repeat procedure 3-4 times at least. Average volumes of thiosulfate added independently for the primary and secondary KIO_3 additions. The difference between the two is the value of the reagent blank that should be subtracted from all sample titrations.

Calculate molarity of thiosulfate (be consistent with units and subtract reagent blank) =

$$(\text{vol. of } IO_3^-)([IO_3^-\text{standard}])\left(\frac{6 \text{ mol } S_2O_3^=}{1 \text{ mol } IO_3^-}\right)\left(\frac{1}{\text{vol. } S_2O_3^=}\right)$$

NOTE: You should do a standard curve with various KIO_3 additions to see how good you are at titrating to the same endpoint!! Practice will make your analyses more precise.

2) Analyze samples:

Prepare reaction mix (dH_2O, KI/KOH, H_2SO_4) as above.

Add sample (which can be in solution, on a filter or powdered). Let reaction proceed 5-10 minutes in the dark (to minimize photooxidation). If using filters, remove filter from solution. If visible particles remain, best results will be obtained by filtering reaction mixture (0.2 um) and measuring volume of recovered filtrate.

Titrate with standardized thiosulfate until straw colored, then add starch and titrate to endpoint.

Measure total volume of thiosulfate addded and calculate total volume in vial (don't forget to add in volume of starch solution). In order to calculate the moles of total Mn in your sample, you will need to know the total volume of the solution.

Measure Mn(II) by formaldoxime method or AA. Also, if present, measure iron content of sample.

3) Calculation (remember to subtract reagent blanks from volume of thiosulfate used in titration and be consistent with units):

$$x = \left(\frac{(\text{vol. } S_2O_3)([S_2O_3^=]) \text{ - moles Fe in sample}}{\text{moles of Mn in sample}}\right)\left(\frac{1}{2}\right) + 1$$

In these experiments the concentration of Fe in the samples was considered to be negligible because none was added to the gel, so the oxidation state of the Mn oxides formed by the 110,000 D protein from Leptothrix discophora was calculated as described above.

Using these methods the oxidation state thus calculated amounted to x = 1.96 for sample 1 and x = 1.98 for sample 2. These high oxidation states are in agreement with the oxidation state of the Mn oxide formed by spent culture medium of L. discophora SS-1 as determined by Boogerd and de Vrind (1987).

Conclusions

These experiments show that a new strain, tentatively identified as Leptothrix discophora N.C.1, has been isolated from the Fe- and Mn-bearing water of Bear Trap Creek, New York. The strain appears to have at least one Mn-oxidizing protein that was extracted from either sheaths or from sheathed cells and that could be detected by SDS polyacrylamide gel electrophoresis.

References

Adams, L.F. and W.C. Ghiorse (1987) Characterization of extracellular Mn(II)-oxidizing activity and isolation of an Mn(II)-oxidizing protein from Leptothrix discophora SS-1. J. Bacteriol. 169:1279.

Altmann, H.J. (1972) Bestimmung von in Wasser geloestem Sauerstoff mit Leukoberbelinblau I. Eine schnelle Winkler-Methode. Z. Anal. Chem. 262:97-99.

Boogerd, F.C. and J.P.M. de Vrind (1987) Manganese oxidation by Leptothrix discophora strain SS1. J. Bacteriol. 169:489.

Freeman, D.S. and W.G. Chapman (1971) An improved oxalate method for the determination of active oxygen in manganese dioxide. Analyst 96:865-869.

Kalhorn, S. and S. Emerson (1984) The oxidation state of manganese in surface sediments of the Pacific Ocean. Geochim. Cosmochim. Acta 48:897-902.

Krumbein, W.E. and H.J. Altmann (1973) A new method for the detection and enumeration of manganese oxidizing and reducing microorganisms. Helgol. Wiss. Meeresunters 25:347-356.

Murray, J.W., L.S. Balistieri and B. Paul (1984) The oxidation state of Mn in marine sediments and ferromanganese nodules. Geochim. Cosmochim. Acta 48:1237-1247.

van Veen, W.L. (1972) Factors affecting oxidation of manganese by Sphaerotilus discophorus. Antonia van Leeuwenhoek J. Microbial. Serol. 38:623-626.

van Veen, W.L., E.G. Mulder and M.H. Deinema (1972) The Sphaerotilus-Leptothrix group of bacteria. Microbiol. Rev. 42:329-356.

Michael Enzien

"Manganese Flux Chamber Experiments"

Introduction

The sources of reduced manganese [Mn(II)] in Lake Oneida are of considerable interest in understanding the manganese cycle in the lake and the formation of manganese nodules. Our working model suggests the main input of manganese into Lake Oneida is from rivers entering the lake in the south. These river waters are also the main source of nutrients entering the lake. The manganese comes from the weathering of manganese carbonates. These river waters contain a high carbonate content and act as the main buffering system of the lake. Once the manganese enters the lake it is kept at low concentrations in the lake waters by precipitation of manganese-oxides. The mechanism by which manganese [Mn(II)] is precipitated and its deposition is under study (see other reports, this volume). Presumably, phytoplankton and bacteria directly or indirectly oxidize the manganese which then settles.

The future of the settled manganese oxides then depends upon the area of deposition. The topology of the lake's bottom consists of two low points around 40-45 feet west and east of a central high point or shoal of around 25-30 feet. The high points are the areas where the manganese nodules are most abundant and completely cover the bottom surface in many areas. The low points of the lake contain very soft muddy bottoms which contain anoxic muds. The bottom waters in these basins tend to go anoxic during the summer months when there is little mixing. Our model suggests that many of the manganese oxides which end up in these basins can be reduced and then precipitated again at nodule sites.

The experiments described here were designed to determine the extent of this internal source of reduced manganese into the lake waters by monitoring flux chambers at the sediment water interface. In this way flux of reduced manganese from anoxic sediments can be empirically determined.

Materials and Methods

Flux chamber design and sampling:

Flux chambers were made from 18 L food grade plastic buckets obtained from the local Dunkin Donuts for a moderate fee. In two of the chambers (bucket #1 and #2) a 3-cm diameter hole was drilled in the center of the bottom. These buckets were then placed 15-20 cm in the anoxic sediments around Buoy 127 by scuba divers. After a 24-hour equilibration period the head space of the buckets was sampled using a 30 ml syringe and a well-fitting neoprene rubber stopper was carefully placed in the 3-cm hole in the top of the bucket (Figure 1).

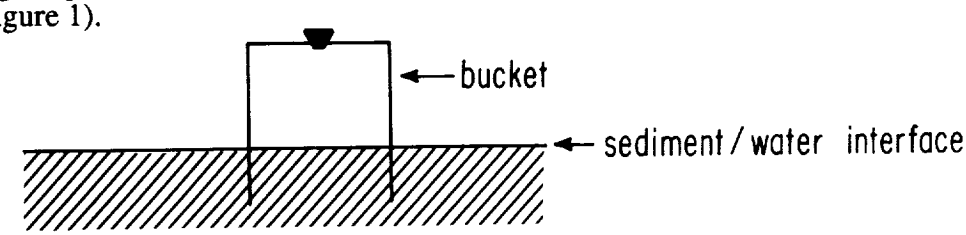

Figure 1. Schematic diagram of flux chambers constructed to measure manganese flux at the sediment water interface.

Subsequent sampling of the buckets was done via a syringe needle through the neoprene stopper. Whenever the buckets were sampled the syringe was pumped several times to mix the water in the headspace of the buckets. These two flux chambers were sampled every day, weather permitting.

Two more flux chambers were designed slightly differently. The bottom of the plastic buckets were completely cut out and a line 15 cm from the bottom of the bucket was drawn around the outside of the bucket. This line represented the depth the bucket was placed in the sediment so a more accurate volume of the headspace could be determined. The bucket was then placed in the sediments with the top off and allowed to equilibrate for 24 hours. These chambers allowed for better mixing and equilibration with bottom water because the tops were completely off instead of just a 3-cm hole. After equilibration the tops were placed on buckets and the first sample was taken. These tops also contained a neoprene stopper through which subsequent samples could be taken. Another very important addition to these flux chambers was that a string was tied to the handle of buckets and to a reference line at respective buoys, 123 and 127. This made sampling the buckets possible even when visibility was very low.

Chemical measurements:

Samples were fixed on the boat for Winkler determinations of O_2 concentration and soluble manganese. pH was determined within an hour after sampling using a pH minielectrode (Microelectrodes, Inc.).

MicroWinkler titrations for determination of O_2:

Reagents:

--Manganese sulfate solution - dissolve 480 g $MnSO_4 \cdot 4H_2O$ in distilled water, filter and dilute to 1 liter. Solution should not give a color with starch when added to an acidified solution of KI.

--Alkali-iodide-azide - dissolve 500 g NaOH and 135 g NaI (or 150 g KI) in distilled water and dilute to 1 L. Add 10 g sodium azide, NaN_3, dissolved in 40 ml dH_2O.

--concentrated H_3PO_4 (1.75 s.p.)

--Starch - 5 g of starch in 800 ml boiling dH_2O for a few minutes, dilute to 1 L and let settle overnight. Use supernate and preserve with 1.25 g/L salicylic acid.

--Sodium thiosulfate stock solution, 0.025 N - purchased from Fischer Scientific.

Procedure:

1. A sample is added to a 1.9 ml (absolute volume when completely filled) Eppendorf tube by placing the syringe at the bottom of a tube and allowing the sample to overflow. The tube is then tightly capped excluding all air bubbles, reopened, and 10 ul each of first manganese sulfate solution then alkali-iodide-azide is added below the surface, capped tightly and shaken. A brownish precipitate should form. Let the precipitate settle

completely. The sample is now fixed, but titration should still be completed as soon as possible.

2. Acidify the samples with 20 ul of H_3PO_4, cap and shake. The precipitate should dissolve completely within 10 seconds. Take a subsample from the Eppendorf tube with an accurately calibrated pippettman (two 700 ul subsamples were used in our titrations).

3. Samples were titrated in disposable plastic 1 cm cuvettes with a 'Flea' stirbar, and a 2 ml microburret (Gilson). The tip of the microburret was placed just below the air/water interface. Add 10 ul of starch, then begin titration with 0.025 N sodium thiosulfate. The endpoint is reached when the blue color of starch-iodine complex is completely gone.

Calculation:

V_T = volume (ml) titrant
V_S = volume (ml) sample titrated
V_C = volume (ml) sample contains with cap in place
R = volume (ml) of reagents, $MnSO_4$ and alkali-iodide-azide added

$$[O_2]\ mg/L = \frac{8\ (25\ mM)\ (V_T)}{V_S\ \frac{(V_C - R)}{V_C}}$$

$[O_2]$ mg/L ---> $[O_2]$ umol l^{-1}, divide by 32.

Soluble manganese determinations:

Samples were fixed on the boat with 0.5% v/v concentrated ultrapure nitric acid. Several samples were filtered through a 0.2 um membrane filter before fixing to see if particulate Mn-oxides were dissolving in unfiltered samples. Determination of soluble manganese was done using a Perkin-Elmer 305 Flame AAS under standard operating condition using a lean blue air-acetylene flame, and by colorometric methods.

Colorimetric determination of soluble manganese:

Reagents:

1. 0.001 M Bathopenanthroline - dissolve 0.0332 g batho in 50 ml 95% EtOH (isopropyl was used instead). Add 50 ml deionized distilled H_2O (ddH_2O).

2. 10% Hydroxylamine HCl, purified to remove iron contamination. Add 100 ml of 10% H-HCl (10 g/100 ml) to a 250 ml separatory funnel. Add 2 ml of batho, shake and let set a few minutes, then add 10 ml of butanol. Extract until organic layer is no longer pink. (Usually takes 3-4 extractions depending upon how clean your water and reagents are.)

3. Formaldehyde 37%.

4. Formaldoxime. Mix 200 ml of purified 10% H-HCl and 10 ml of formaldehyde and dilute to 500 ml with ddH_2O.

5. NH_4OH, dilute. Dilute ultrapure NH_4OH, 1:10.

6. Mixed Reagent, prepared daily. Mix formaldoxime and dilute NH_4OH in a proportion to obtain pH of 8.8-8.9 after addition of 5 ml to a 40 ml sample (about 2:1).

Standards:

1. Primary Standards, 2 mM, Dissolve 0.1688 g $MnSO_4 \cdot H_2O$ (FW=169.01) in 500 ml H_2O. $MnSO_4 \cdot H_2O$ is stable at 57-114°C, dry accordingly.

2. Make up standards for calibration curve in the range desired. We made standards of 1, 2, 4, 6, 8, 10, 15, 20, 40, 60, 80, 100 uM [Mn^{2+}].

Note: Standards should be made up daily from your primary standard.

Procedure:

The ratio of sample to mixed reagent is 7:1. When using small sample volume, as in porewater samples, 1.5 ml of sample requires 214 ul of mixed reagent. If samples have been acidified (0.5% v/v concentrated nitric acid) they will probably need additional 10% NH_4OH added to raise pH to 8.8-8.9. A 1.5 ml acidified sample needs an additional 200 ml of 10% NH_4OH. Sample and mixed reagent is conveniently mixed in plastic 5 ml scintillation vials. Absorbance of samples and standards are read in a 1 cm cuvette at 450 nm. If a large sample volume is possible a 10 cm cuvette will give a lower detection limit.

Results and Discussion

The results from the first two flux chambers, buckets #1 and #2, are illustrated in Figure 2. Bucket #1 was sampled when possible (weather permitting) over a 9-day period and bucket #2 over an 8-day period. In both buckets pH remained relatively stable and Mn^{2+} tended to increase. In bucket #1 initial Mn^{2+} values were very low, 1.0 uM, but after one day rose to 38 uM. This was the largest increase in any one-day period. It continued to increase to a value of 80 uM after 9 days. Likewise, bucket #2 increased from 34 uM - 83 uM in an 8-day period. Oxygen concentrations remained relatively constant for the first 7 days in bucket #1 then on the 9th day concentrations dropped very low. The oxygen values for bucket #2 are few and scattered. It is hard to discern whether the oxygen levels fluctuated or if there was just a sampling error. In both buckets there appears to be a correlation with final oxygen decrease and Mn^{2+} increase. There is, however, a noticeable increase in Mn^{2+} during a period of relatively stable oxygen values in bucket #1. This suggests that Mn^{2+} is fluxing out of the sediments into the water column and the increase is not just due to anaerobic conditions created by the isolated chamber. Variation in the initial Mn^{2+} values from both buckets could be due to how they were sampled. Two different divers sampled the two buckets and the amount of disturbance to the bucket may have varied enough to cause those differences in initial values.

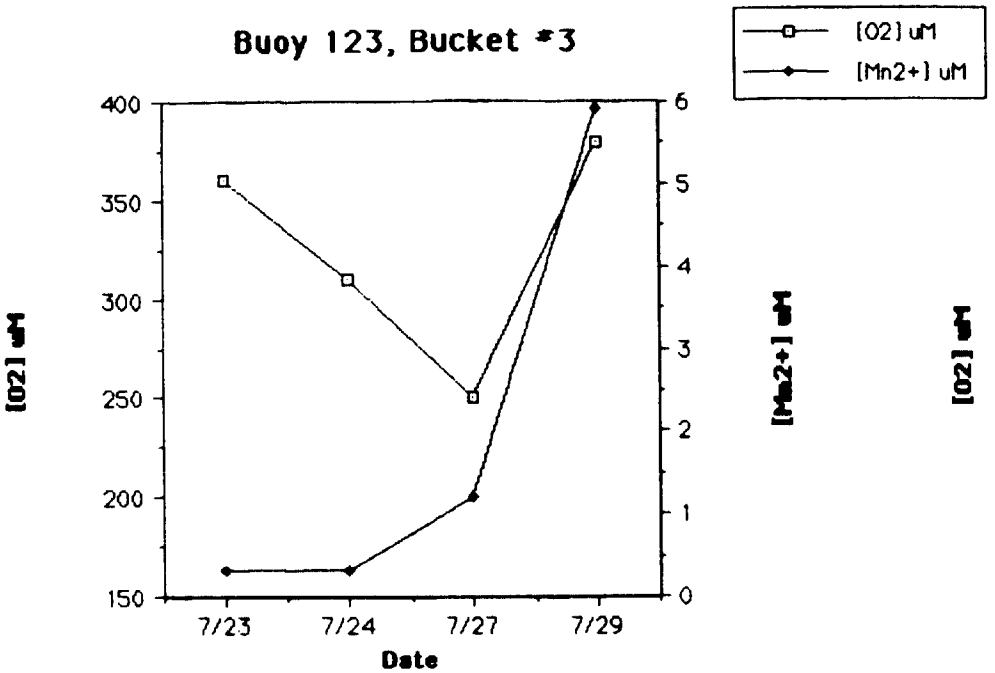
Buoy 123, Bucket #3
[O2] uM
[Mn2+] uM
[O2] uM
[Mn2+] uM
400
350
300
250
200
150
6
5
4
3
2
1
0
7/23
7/24
7/27
7/29
Date

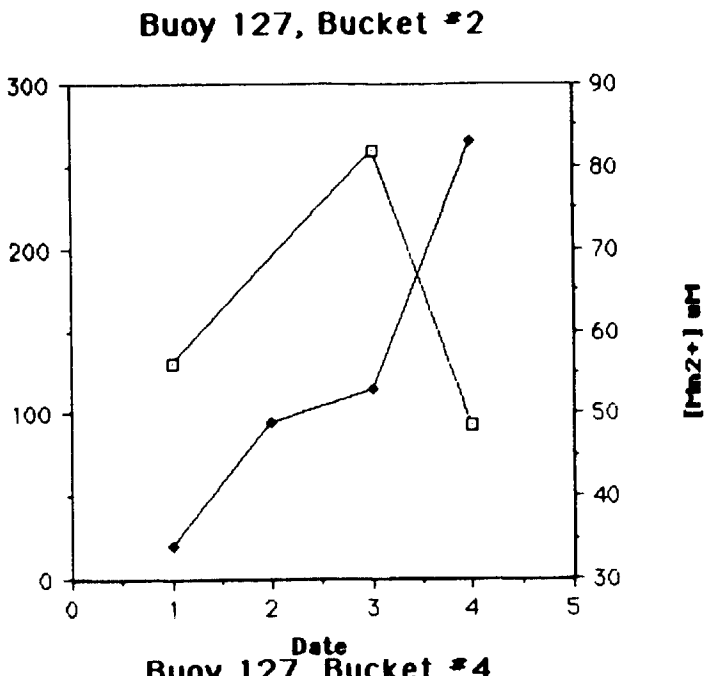
Buoy 127, Bucket #2
[O2] uM
[Mn2+] uM
300
200
100
0
90
80
70
60
50
40
30
0
1
2
3
4
5
Date

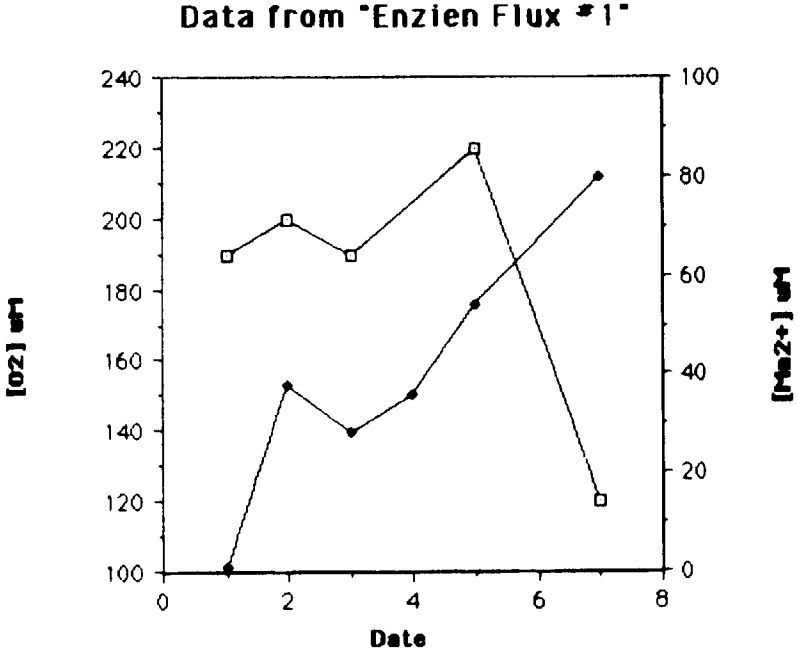
Data from "Enzien Flux #1"
[O2] uM
[Mn2+] uM
240
220
200
180
160
140
120
100
100
80
60
40
20
0
0
2
4
6
8
Date

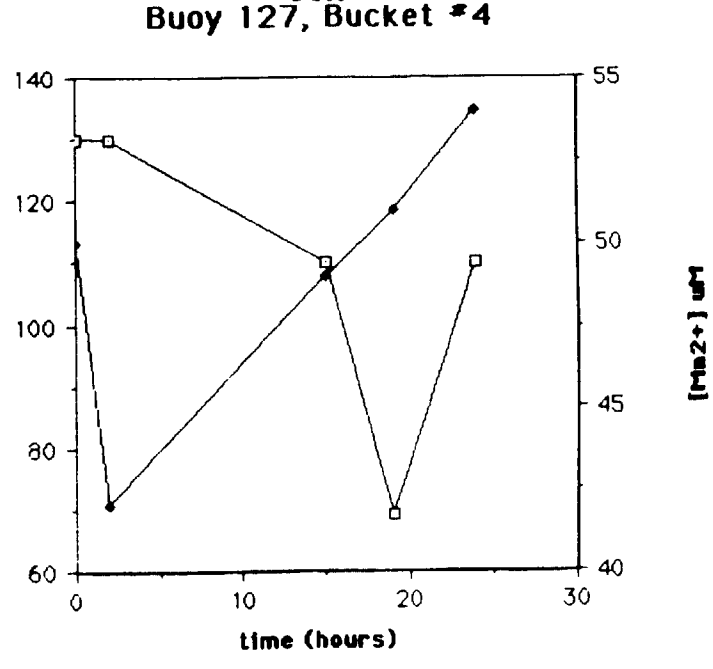
Buoy 127, Bucket #4
[O2] uM
[Mn2+] uM
140
120
100
80
60
55
50
45
40
0
10
20
30
time (hours)

Bucket #3 which was placed in a nodule area at Buoy 123 showed somewhat different results (Figure 2). This chamber was sampled over a 6-day period and showed very little change in Mn^{2+} from 0.3 - 5.9 uM. This increase was seen only after anaerobiosis was developed, (>5 days), and may in fact be falsely high. For the first five days pH remained relatively constant and oxygen levels remained fairly stable and much higher than buckets #1 and #2. The average oxygen value for bucket #1 was 180 uM while bucket #3 was 330 uM, consistent with the fact that bottom water oxygen levels are generally lower at Buoy 127 than at 123.

The 4th flux chamber was put down at Buoy 127 with design modifications to improve the results. This chamber was sampled five times in a 24-hour period (Figure 2). The short sampling intervals were designed to give a more accurate estimate of Mn^{2+} flux. Again pH remained stable and Mn^{2+} increased while oxygen decreased. The oxygen values from this chamber were very low, average around 100 uM. The starting values, however, were also very low, 130 uM. After 19 hours oxygen levels dropped to 69 uM and then went up again at 24 hours to 110 uM. This increase in oxygen may have been due to sampling errors and titrations because a different individual analyzed this sample from the rest. The oxygen values of the bottom waters at Buoy 127 were also very low at this time.

The high value of Mn^{2+} which drops with the next sampling and then steadily increases at a relatively constant rate suggests there might have been a sampling problem. The first sample was taken after the top of the bucket was snapped on and this process most likely disrupted the sediment. This could have caused porewater, which is very high in Mn^{2+}, to diffuse into the chamber. After subsequent settling of suspending sediments the Mn^{2+} levels stabilized. The lower second value might mean that the suspended material in the flux chamber adsorbed Mn^{2+} which had been forced (by advection or compression) upwards during chamber closure. The steady constant increase in the last four samples suggests there is a steady increase in Mn^{2+} which might or might not be due to oxygen decreases. More data are needed for both the short and long term flux chambers with careful monitoring of oxygen levels in these chambers. The microWinkler titration for oxygen concentrations is sensitive to sampling errors. A small sample contamination results in a large error. Possibly a larger collection vessel for Winkler titrations is needed to decrease sample contamination problems.

If we neglect the first Mn^{2+} value from bucket #4 we can calculate a Mn^{2+} flux from the sediments. Knowing the approximate volume of the head space to be about 12.5 L, the radius of the flux chambers to be 13 cm and the amount of Mn^{2+} increase in a 22-hour time period we arrive with 3.1 $mmol \cdot m^{-2} \cdot day^{-1}$. Assuming similar volumes for buckets #1 and #2, we also calculated fluxes for these chambers (using the difference from the ending and starting Mn^{2+} values and dividing by the number of days) to be: 2.1 $mmol \cdot m^{-2} \cdot day^{-1}$ and 1.4 $mmol \cdot m^{-2} \cdot day^{-1}$ for buckets #1 and #2, respectively. The flux chamber at the nodule area was not placed deeply into the sediment, but rested rather tightly upon the sediment

Figure 2. Opposite. Results obtained from flux chamber sampling (see text for details). Open squares are concentration of O_2 in uM; solid diamonds are concentration of Mn^{2+} in uM.

surface by placing a cinder block on top. Using an estimated volume of 18 liters the flux of bucket #3 is: 4.8 umol·m^{-2}·day^{-1}. From these numbers it is very clear that Mn^{2+} is fluxing from deep areas of the lake where thick anoxic muds are dominant as opposed to the nodule areas.

Table 1. Mn flux from sediments.

		Estimated Mn Flux
Aerobic sediments		
chamber #3, Buoy 123		4.8 umol/m^2/d
Anaerobic sediments		
chamber	Buoy	
1	127	2.1 mmol/m^2/d
2	127	1.4 "
4	127	3.1 "

Conclusions

Results from the flux chambers (Table 1) indicate that anaerobic sediments in the deep parts of Lake Oneida are acting as an internal source of Mn^{2+} to the lake waters. The low values of flux from the nodule area does not mean that it does not contribute as a source of Mn^{2+}, but it certainly is less significant, by an order of magnitude, than the anaerobic sediments. The oxygen values obtained from the flux chambers and Hydrolab profiles also indicated that the nodule areas are always more oxic than the deeper areas of the lake. This is consistent with our model as to how manganese is cycled within the lake and nodules formed. More work is required in order to obtain better numbers for Mn^{2+} flux; further modification for flux chambers is needed along with a more accurate way of measuring oxygen in the chambers.

Acknowledgements: I would like to thank all the scuba divers: Dave Bolgrien, Greg Hinkle, Ken Nealson, and Tom Schmidt, for their help in placing and sampling the flux chambers. Without their help this project would not have been possible. I also would like to thank Charlie Taylor of the Cornell Biological Field station for help in construction of the chambers.

Michael Enzien

"Enrichment for Manganese Reducing Bacteria Using an Anaerobic Chemostat"

A true manganese reducing bacterium, which would directly reduce MnO_x during anaerobic respiration, has not yet been isolated. An anaerobic chemostat was designed to enrich for such organisms. To do this, a medium with a very simple carbon source must be used to prevent reduction of MnO_x caused by organic acids (such as pyruvate) produced by fermentations. Succinate and acetate are two good choices for carbon sources which would not produce organic acids as an end product. If an organism is growing on one of these two carbon sources and Mn oxides are being reduced, there is good evidence for direct manganese reduction.

Design and Setup

Figure 1 illustrates the set-up for an anaerobic chemostat. It is very important to have stirbars in both reservoir vessels and chemostat, otherwise the MnO_x would settle. Very low concentrations of MnO_x were used because this was to be the limiting nutrient. It turns out if higher concentrations are used, turbidity due to growth cannot be detected because of the dark suspended MnO_x. The chemostat has an influent rate controlled with a peristaltic pump, and an effluent which is an overflow system.

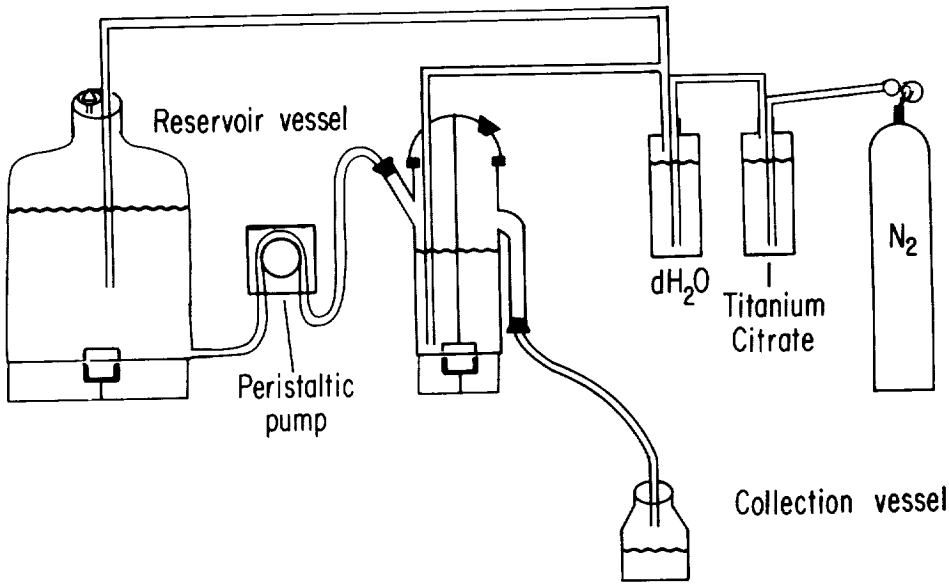

Figure 1. Diagram of an anaerobic chemostat designed to enrich for manganese reducing bacteria.

Nitrogen is used to keep the chemostat and reservoir vessel anaerobic. A reducing agent cannot be used in the medium because it could cause chemical reduction of MnO_x. A titanium citrate solution was used to scrub oxygen out of the nitrogen. The gas was then passed through dH_2O in case there were any volatiles from the titanium citrate solution. The chemostat was inoculated with sediment slurries from anaerobic cores or with enrichment cultures from manganese reducing enrichment vials (see Hinkle, this volume). The gas was continuously bubbled throughout the experiment in both chemostat and reservoir vessels. Every day a sterile pasteur pipet was used to sample the chemostat. An extra port in the chemostat vessel allowed for easy sampling without disassembly.

Media and Reagents

Manganese reducers media:
-- delta MnO_x, 0.005 g/L
-- Na-Acetate, 10 mM (1.3608 g/L)
-- yeast extract, 3 g/L
-- tryptone, 0.5 g/L
-- casein amino acids, 0.5 g/L
-- microelements solution, 10 ml/L
-- NaCl, 0.085% (.85 g/L)

Titanium citrate reducing solution:
-- 70 ml titanium trichloride (20%)
-- 54.70 g Na-Citrate
-- 930 ml ddH_2O

Add Na-Citrate to ddH_2O, then add titanium trichloride.

Results and Discussion

The anaerobic chemostat was successful in enriching for anaerobic microorganisms, but failing to select for manganese reducing bacteria. Several factors contributed to this failure. The medium used had too many nutrients upon which fermentative organisms could thrive, (e.g. casein amino acids, and tryptone). Both of these carbon sources should probably be eliminated from the media along with reducing the concentration of yeast extract. Failure of the peristaltic pump on several occasions also contributed to unfavorable culture conditions in the chemostat. Whenever using peristaltic pumps, it is most important to have the correct tubing made specifically for that pump. This was not available for the pumps we were using. Due to odorous gases from the effluent line caused by mixed anaerobic metabolism, the chemostat was shutdown by an overwhelming majority vote. The use of an anaerobic chemostat to enrich for true manganese reducing bacteria, however, is still a very clever way to try isolating these bacteria. Further design and media modifications may be needed for this technique to work.

Michael Enzien
Susan Rose
Kevin Mandernack

"Analysis of Core Samples from Oneida Lake"

Study site

We chose as our study site Buoy 127 in Oneida Lake. A sharp horizontal gradient exists at the lake's bottom which ranges from the nodule containing shoals, through more organic-rich transition zone where a manganese crust is buried at depth, to the deep organic-rich basin sediments. Therefore, our sample transect represented a full range of sedimentary environments encountered in this lake and over a relatively short distance of approximately 40 m. The sediment cores collected along this transect were designated 127A from the basin area, 127C when taken from the transition zone with the buried crust, and 127N from the nodule-containing area.

Materials and Methods

Sediment cores were taken by scuba divers. The inner diameter of the coring tubes was 6.5 cm and the length was 46 cm. Following calibration, the cores were taken back to the lab and immediately sampled. From the cores, analyses of the pore water and dried sediment fractions were made for each 1 cm section and unless indicated otherwise, all cores were sampled 1-2 cm into the underlying clay layer. These samples were weighed to obtain wet weight before centrifuging them to obtain pore water. After the pore water was collected and filtered through a 0.2 um membrane filter, the sediments were oven dried and the wet and dry weight of each 1 cm section was measured in order to obtain porosity values for the sediments. Porosity measurements were required for estimating sedimentation rates, as done by Dr. Willard Moore, Univ. of South Carolina, using the radioisotopes Pb-210 and Cs-137.

Pore water analysis

Measurements of pH were made from the filtered pore water using a combination pH mini-electrode. The initial measurements from the first few cores were inconsistent and erroneously low, presumably the result of insufficient rinsing of our acid washed containers. These measurements were not included with the pore water profiles of dissolved Mn contained in the results section. In addition, two pH profiles for cores taken on 7-25 and 7-28 were made with a standard pH electrode which gave consistent, although lower pH values. The average discrepancy was determined to be 0.4 pH units; therefore, the original pH profiles of these cores were corrected for.

Following pH measurements, the pore waters were acidified for soluble Mn^{2+} in 0.5% v/v concentrated ultrapure nitric acid. Soluble Mn^{2+} determinations of pore waters were made both on a Perkin-Elmer model 503 Flame Atomic Absorption Spectrophotometer operating with an air-acetylene lean blue flame, and by the flormaldoxime colorimetric method (see Enzien, this volume).

O_2 microelectrode calibration

The combination oxygen microelectrode (Diamond Electrotech., Inc.) was calibrated using a series of solutions from oxygen-saturated to oxygen-depleted samples of filtered lake water. Oxygen-saturated samples were those open to the atmosphere at room temperature. The next five series of vials were bubbled for increasing times with oxygen-scrubbed nitrogen up to 30 minutes. Measurements were made with the microelectrode using % mm Hg on the Diamond Microsensor picoammeter and immediately fixed for Winkler oxygen titrations afterwards. The values obtained from the microelectrode (mm Hg) were plotted against the oxygen concentrations (mg/L) obtained from Winkler titrations and a linear correlation of 0.985 was calculated. The y intercept corresponding to oxygen was 23.7 mm Hg. The strong linear correlation indicates that the microelectrode was working well in the range from oxygen-depleted to oxygen-saturated samples. This calibration line was used to calculate oxygen concentration values obtained using the microelectrode.

In order for an accurate interpretation of the Mn and pH profiles to be made, on our final day of sampling (8-3) in situ oxygen profiles within the cores were obtained through use of a combination oxygen microelectrode. Profiles were constructed from a representative core from each of the three sedimentary environments contained within our sampling area. Previously, this electrode was not available and attempts failed to measure dissolved oxygen from the collected pore waters by micro-Winkler techniques. The O_2 profiles were started several centimeters above the sediment water interface and lowered further using a micro-manipulator. Once the electrode tip was at the sediment water interface, it was carefully lowered at 1 mm intervals until zero oxygen values were obtained. The O_2 profiles are shown in Figure 1.

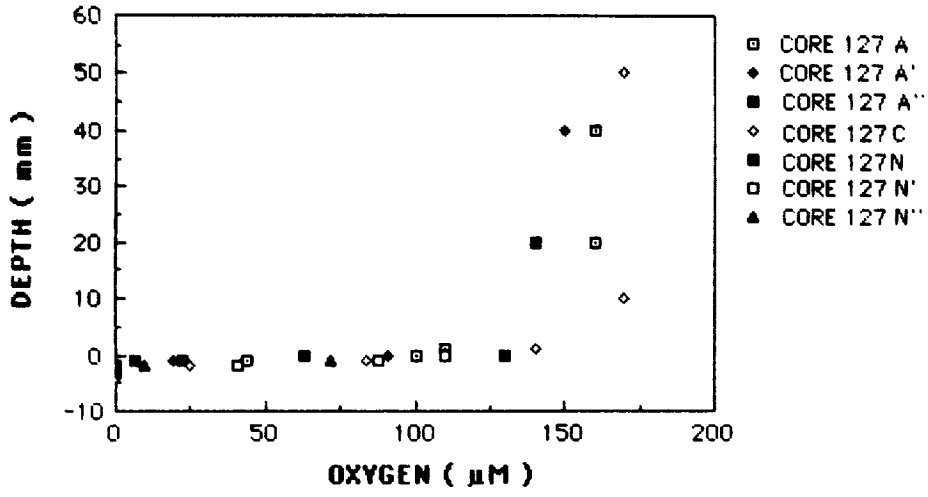

Figure 1. Combined O_2 profiles for water and sediments. Oxygen values are in umol/l (uM) for water and pore waters collected from seven cores at Buoy 127, August 3, 1987.

Sedimentation rates

Sediments from Buoy 127 were analyzed by both ^{210}Pb and ^{137}Cs to estimate rates of deposition (Figure 2). The results must be regarded as preliminary. The ^{137}Cs peak (indicating a 1962 timeline) is at about 8 cm, so 8 cm/25 yr yields a deposition rate of approximately 0.32 cm/yr. The ^{210}Pb data yield a rate of approximately 0.25 cm/yr, in good agreement with the ^{137}Cs estimates.

Results and Discussion

The oxygen, pH and dissolved manganese profiles of the pore waters yielded interesting trends along the transect of our sampling site. Oxygen measurements made on August 3 revealed that the sediments were anoxic by 3 mm depth at each of the three areas 127A, 127C, and 127N (Figure 1). Therefore, conditions for manganese reduction occur below this depth at each area. Values for pH were relatively constant, ranging between 7.0 and 8.2, with most centering around 7.8 (Figure 3). While there were no observable relationships between dissolved manganese and pH in most of the cores, at 127C subsurface peaks in dissolved manganese sometimes appeared to co-occur with a pH minimum, suggesting that levels of dissolved manganese may increase at depth as a result of increased acidity. In contrast, all profiles at 127A showed peak manganese levels within the top 2 cm of sediments, where pH levels normally remained high. From this it appears that the critical zone for manganese reduction at 127A is very close to the sediment water interface. Sedimentation rates for this area, as concluded from the radioisotope studies, were appoximately 2 mm/yr. From these sedimentation rates and the measured oxygen profiles and noticeable thick organic layer in these sediments, one can speculate that within the organic-rich basins there is a heavy influx of organic material and manganese oxides, both resulting from primary (and secondary) productivity in the water column. This results in rapid reduction of the manganese oxides at the sediment surface, which subsequently provides a flux of dissolved manganese to the lake water. From the final core taken at 127A on August 3, which contained the highest levels of dissolved Mn at its surface (258 uM), one might also assume that the flux of dissolved manganese to the lake water increases as summer progresses and sediments accumulate in the basins from continued productivity. As peak Mn levels are in the surface sediments at 127A, one can estimate what the flux of dissolved Mn^{2+} from the sediments to the overlying lake water might be if diffusion alone dominates the process. This is calculated simply from Ficks equation for diffusion, which is written as:

$$\frac{dc}{dt} = \text{phi } D \frac{dc}{dx}$$

where dc/dt is a measurement of the flux, phi = porosity = .90, and D = in situ diffusion coefficient = 3.3×10^{-6} cm^2/s, and dc/dx is the change in concentration of substance over a given distance x. Because manganese levels were determined for the lake water overlying the sediments in some of the cores, this diffusive flux can be approximated. For most cores, the overlying lakewater was collected 1-3 cm above the sediment water interface. Therefore, using 1 and 3 cm as values for dx, an approximate range for the diffusion flux can be made. For the 127A core collected on August 3, where the overlying lakewater had a concentration of 49 uM, the surface sediments contained 258 uM Mn, and using dx values of 1 and 3 cm, then solving for dc/dx we obtain a flux value of 2.67 $mmol/m^2/d$. This value approximates those values of 1 - 3 $mmol/m^2/d$ measured by Enzien's flux chamber experiments (see report by Enzien).

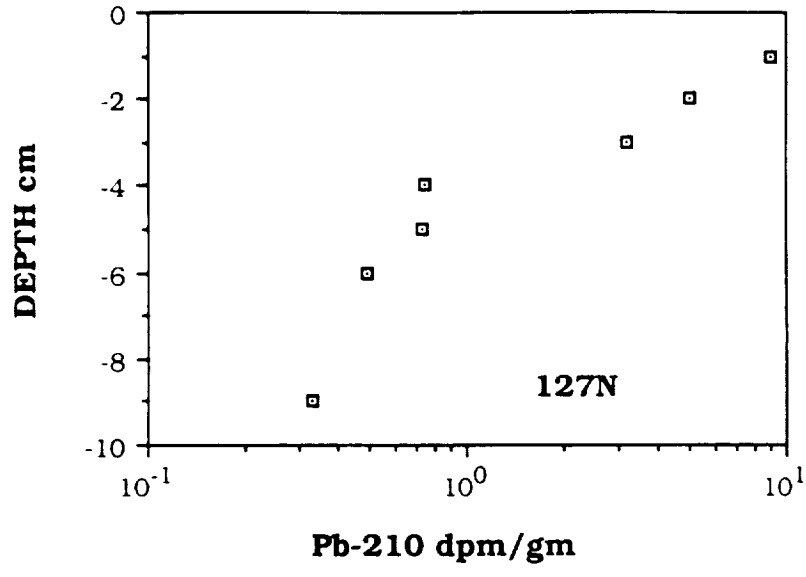
DEPTH cm
0
-2
-4
-6
-8
-10
10^{-1}
10^{0}
10^{1}
127N
Pb-210 dpm/gm

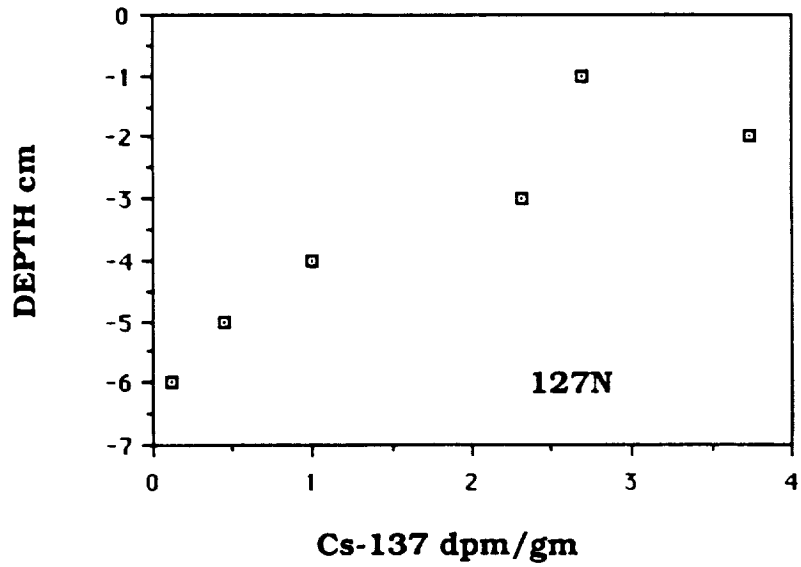
DEPTH cm
0
-1
-2
-3
-4
-5
-6
-7
0
1
2
3
4
127N
Cs-137 dpm/gm

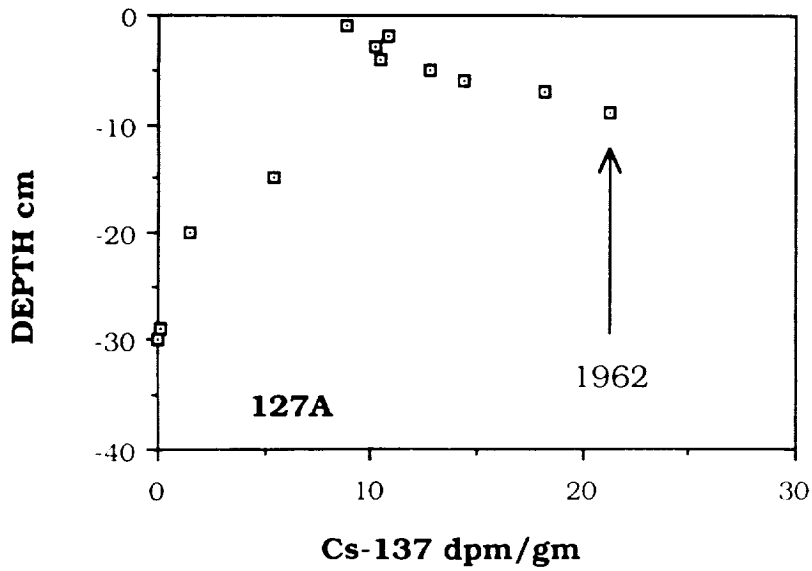
DEPTH cm
0
-10
-20
-30
-40
0
10
20
30
1962
127A
Cs-137 dpm/gm

Because high surface peaks of dissolved Mn within the sediments were characteristic of 127A, and were not present in the nodule area, it is apparent that the organic-rich basins provide the greatest flux of dissolved manganese to the lake water during summer months. This may be a primary source of dissolved manganese for nodule growth on the shoals.

Unlike the profiles of dissolved Mn observed for 127A, those in the nodule area normally contained a distinct subsurface peak illustrating manganese reduction at depth. Above this maximum zone, levels decreased towards the surface, but never declined to zero levels. Therefore, a flux of manganese to the surface sediments may also be occurring here during the summer, but less effectively than that at 127A. The low organic input to this area, although sufficient for consuming the oxygen, seems inadequate to produce a surface peak of dissolved Mn as at 127A. Profiles of particulate Mn will be important for this area, especially near the surface, for if particulate manganese is high here, it may indicate direct oxidation near the nodules and the lack of manganese flux.

Unlike other profiles at 127N, one such profile taken on 7-15 did not show a distinct subsurface peak. Instead, there was a steady decline from the surface downward. While this initially seemed inexplicable, a profile constructed from a core taken at the outer edge of the nodule area on 7-25 (127C/N), near the transition zone - 127C, gave a similar profile and provided an explanation. The steady decline in dissolved manganese with depth at 127C/N also appeared to have a minor peak transposed upon it at depth. This may represented the effects of both a subtle surface peak in dissolved manganese, as occurs at 127A, and subsurface peaks, as occurs at 127N. Therefore, the interplay of two such peaks, superimposed upon one another, could result in the steady decline with depth seen for core 127N of 7-15-87. In more central regions of the transition zone (cores 127C), these two distinct peaks in the manganese profile were very apparent (see 127 C^2 on 7-29), and seemingly portray the characteristic profiles of both its end members, 127A and 127N. However, the subsurface peak in this area may also be a consequence of reduction of the buried manganese crust. This seemed to explain the subsurface peak for core 127C taken 7-29, where it coincided with the depth of the crustal material. However, this did not explain the subsurface maxima noted for $127C^1$ taken on 7-29. Here the manganese crust was 5 cm beneath this peak, although a smaller peak was also noted in the crustal layer. In fact, another profile taken at 127C on 7-28 showed similar elevated levels at the surface, with a distinct maximal peak at a depth with an underlying minor peak near the crustal layer. Perhaps the presence of more than one peak represents pulses of increased manganese reduction at the crustal layer with subsequent diffusion upward.

From the results of this study, it is obvious that the primary flux of dissolved manganese to the lake water during summer months is from the organic-rich basins. It would be of importance to understand how this flux might change during winter months during which primary productivity is absent. Perhaps the well-oxygenated waters during winter months oxidizes any reduced manganese within the surface sediments of the organic-rich basins, thus shifting the manganese peak downward to where it mimics the profiles of 127N observed in this study.

Figure 2. Opposite. Profiles of ^{210}Pb and ^{137}Cs in three core samples from Buoy 127, Oneida Lake.

Figure 3. Following pages. Profiles of pH and soluble Mn in core samples.

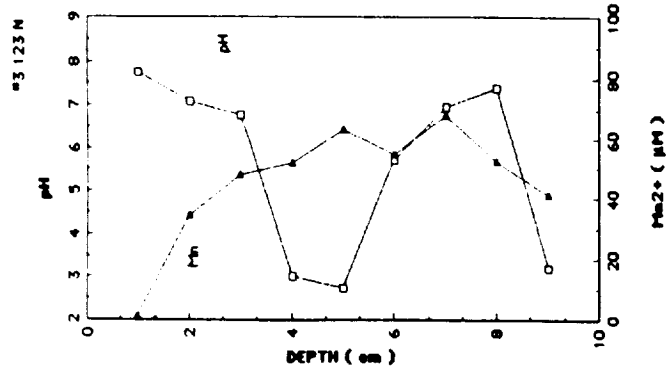

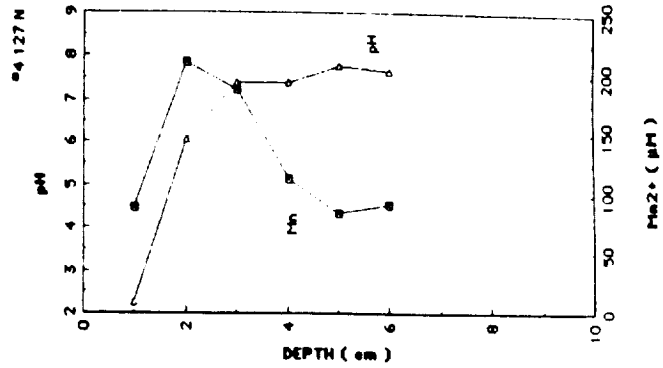

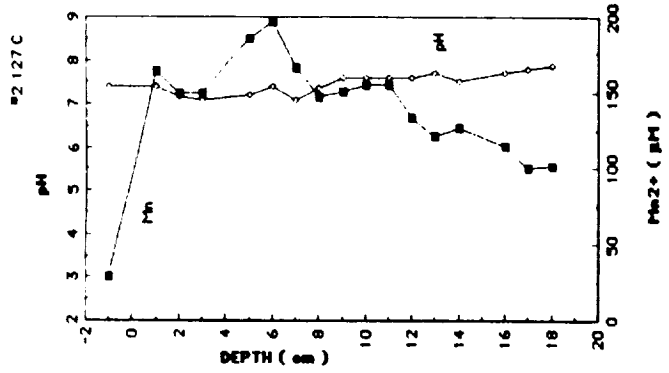

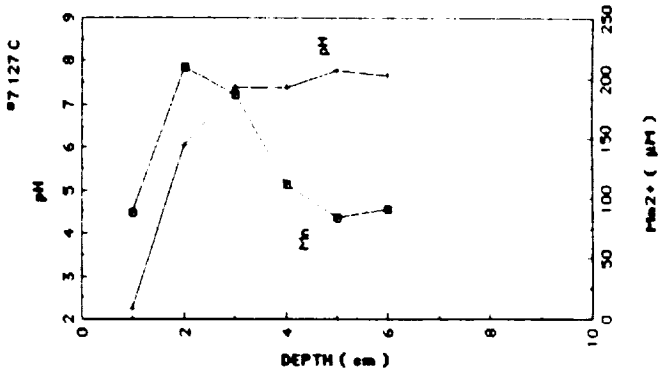

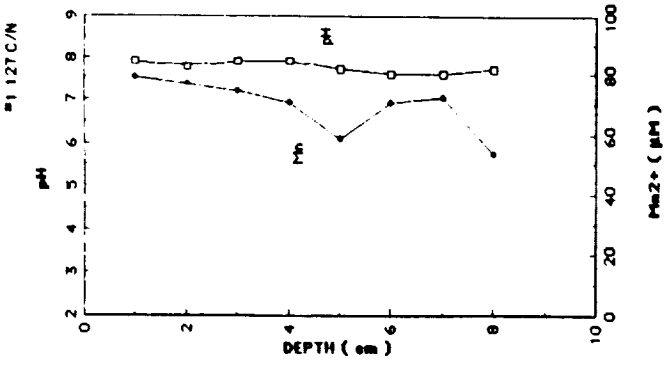

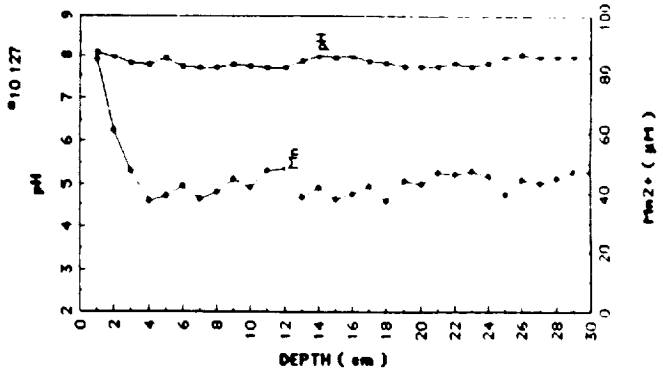

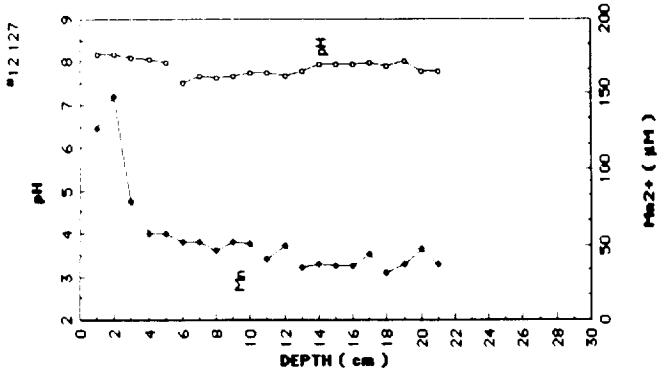

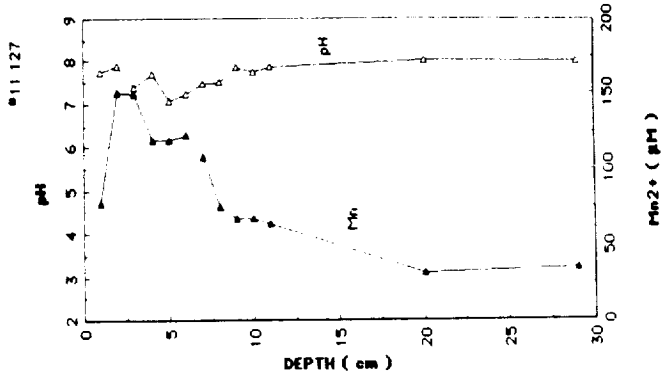

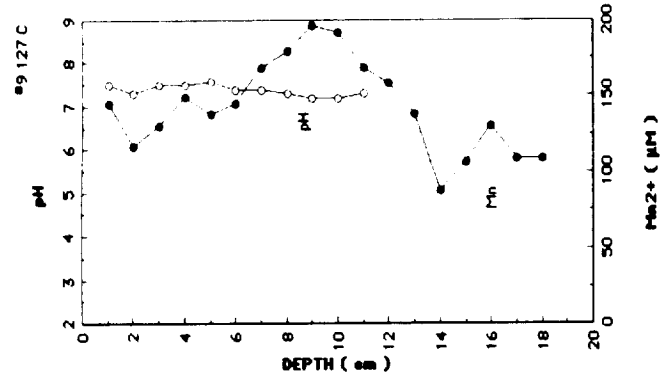

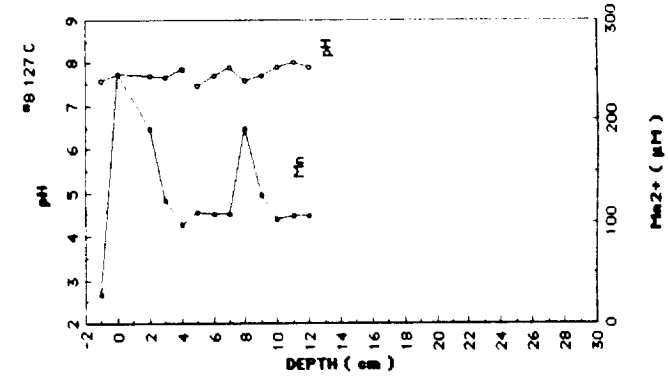

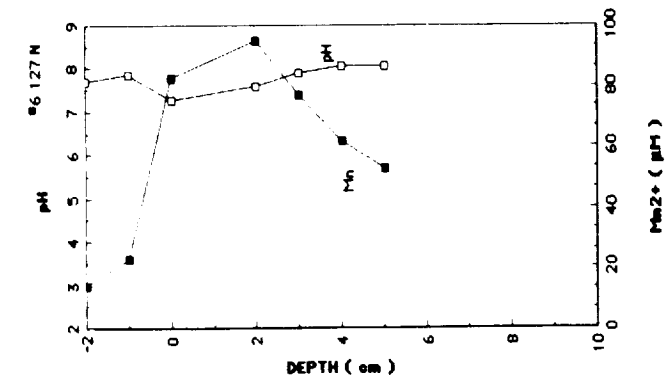

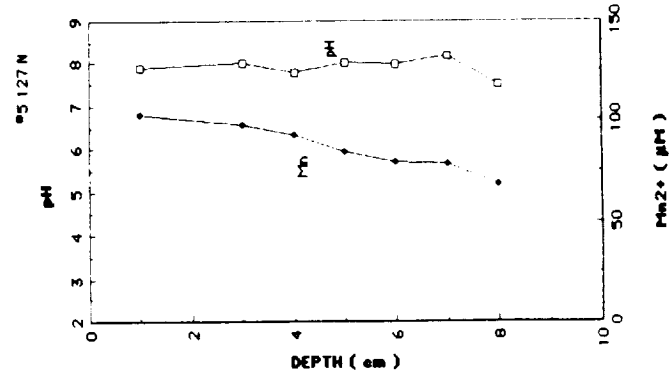

Greg Hinkle

"Secondary Productivity at the Sediment-Water Interface"

Secondary productivity due to heterotrophic bacteria at the sediment/water interface of a manganese nodule-rich area of Oneida Lake was measured using a technique developed by Farooq Azam which he demonstrated at the PBME course. The original methodology, designed for the open water, was modified to measure secondary activity in the soft (up to 30 cm) sediments overlying clay sediments at Buoy 127 on Oneida Lake. Secondary productivity in the sediments, under aerobic and anaerobic conditions, was compared with secondary productivity just above the sediment/water interface and with open water samples collected 1 m above the floc in an attempt to determine the significance of bacterial heterotrophy in a lacustrine system.

Materials and Methods

The following methodology for the measurement of bacterial secondary productivity through the use of tritiated thymidine was described by Farooq Azam at the PBME course and is detailed in: "Thymidine incorporation as a measure of heterotrophic bacterioplankton production in marine surface waters: evaluation and field results." J.A. Fuhrman and F. Azam (1982) Marine Biology 66:109-120.

Divers collected 250 ml samples of Oneida Lake water at Buoy 127 at three depths - 1 meter above the sediment water interface, a few centimeters above the sediment-water interface and right in the surface sediments. The samples were protected from light with aluminum foil and brought to the laboratory for analysis. Ten ml of each sample was assayed in duplicate in sterile, plastic 15 ml snap top tubes (the snap top tubes are easy to handle and keep the radioactivity in its place). The sediment samples were vigorously resuspended before being pipetted in the assay tubes. Killed controls for each sample were also run in duplicate with the addition of 0.37% formalin (final concentration). Sediment samples were assayed under anaerobic conditions by bubbling N_2 through the sample for 5 minutes before the incubation and then running the assay in a N_2-flushed Brewer jar. To each vial tritiated thymidine solution was added to achieve a final concentration in the vial of 10 nM thymidine and the vial capped and shaken. The amount of thymidine added will depend on the concentration of the stock solution. Farooq also suggested that since we were using a very dilute final concentration of thymidine to use tritiated thymidine with the highest specific activity available in order to get a statistically valid number of counts per vial. Each sample was assayed in the dark for 1 hour and then filtered thru a 0.2 um nuclepore membrane filter. After rinsing the sides of the apparatus with approximately 5 ml of 4°C distilled water and filtering again, 10 ml of 5% trichloroacetic acid (TCA) at 4°C was poured over each filter. After 3-5 minutes the TCA was drawn through the filter. (We kept the distilled water and 5% TCA in an ice bath next to the filtering apparatus.) The method calls for 0.45 um Millipore filters which are then dissolved in the scintillation vials with a small amount of ethyl acetate before adding the scintillation fluid. We modified the assay for use with nuclepore filters, which don't dissolve in ethyl acetate, by carefully placing the filters filtrate side up in the bottom of labelled scintillation vials and then adding 5.0 ml of Packard Opti-fluor scintillation fluid. The samples were then counted for 2 minutes each in a Packard 1500 scintillation counter. An internal control for each assay was also made by adding the 56 ul of tritiated thymidine and a filter to a scintillation vial and after the addition of fluor counting them for 2 minutes.

Based on Dr. Azam's estimate for DNA content per bacterium of 2.6×10^{-15} g/cell, one can calculate that for each mole of incorporated thymidine, 2×10^{18} cells will be produced. The number of moles of incorporated thymidine was determined in the assay from the following equation:

$$\text{moles of thymidine} = \text{dpm} \times (\text{Ci mol}^{-1})^{-1} \times 4.5 \times 10^{13}\ \text{Ci dpm}^{-1}$$

From the number of moles incorporated one can estimate the number of cells produced per unit time and volume:

$$\text{moles } {}^3\text{HThy} \times 2 \times 10^{18}\ \text{cells/mole/10 ml/hr}$$

Using the conditions described in the methods, this equation reduces to the simple formula of:

$$\text{cells/ml/hr} = \text{dpm} \times 1.475$$

The cell production rate of the formalin killed samples was subtracted from the experimental samples and was then plotted.

Results

Secondary productivity of the heterotrophic bacteria was consistently higher in the water column than in the sediments (roughly 2-3 times higher) under both aerobic and anaerobic conditions (Figure 1). Thymidine uptake 1 meter above the sediment water interface was approximately equal to the uptake just 10 cm above the bottom. Untreated sediment samples took up ^{3}H-thymidine approximately four to five times faster than the formalin-treated controls. Only two assays on sediment samples were run anaerobically, so the absolute uptake rate of thymidine under anaerobic conditions was not well established. However, the incorporation was substantially lower than that seen in the water column samples in both cases.

Discussion

The results presented here indicate that the production of cells per ml per hour was in general two to three times higher in the water column samples than in the sediments. This result may be due to an artifact of the technique, since much of the sediment in the reaction was not filtered and hence an undetermined number of counts were left behind in the vial. Furthermore, the build up of floc on the filter may have quenched the radioactivity. Both artifacts would lead to an underestimation of the cell production rate in the sediments. Since only two assays were run under anaerobic conditions one cannot estimate with any confidence the production rate in the sediments under aerobic versus anaerobic conditions. The anaerobic and aerobic rates on the 27th of July were similar while on July 29 the anaerobic rate was much higher. Since the sediments became anaerobic in the first few millimeters, one would expect anaerobic processes to predominate and hence may make questionable the data collected under aerobic conditions. The rates obtained in the water column samples are in agreement with those obtained by both Farooq Azam and Steve Wickham with Oneida Lake samples.

One can only speculate as to the basis of the difference in the secondary productivity rates. Perhaps elevated soluble manganese(II) levels in the anaerobic and reducing floc

poison the heterotrophic bacteria. It is equally likely that the uptake of thymidine by the bacteria in the sediments was not accurately measured using the methods heretofore described for water samples. Further refinements of the thymidine uptake technique will have to be developed in order to accurately measure secondary productivity in the sediments.

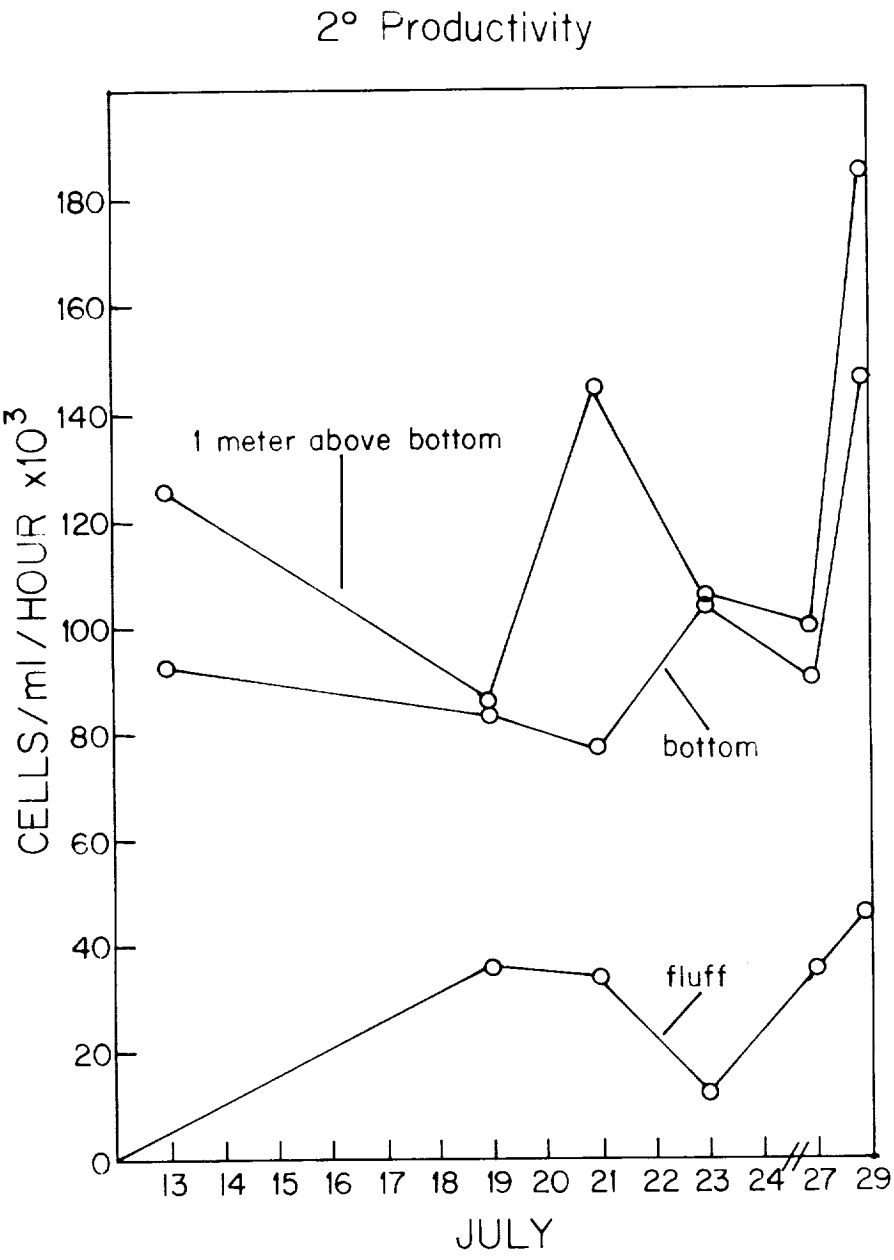

Figure 1. Secondary productivity of heterotrophic bacteria as measured by cells produced per ml per hour.

Greg Hinkle

"A Technique for the Detection of Manganese Oxide Reduction in Sediments"

The existence of bacteria capable of utilizing manganese oxides as an energy source has been previously hypothesized, though no direct evidence exists that manganese oxides can be used as a terminal electron acceptor (Nealson, 1987). Manganese oxide reduction in Oneida Lake sediments was determined using the following technique developed by Drs. T. Schmidt and K. Nealson to demonstrate the presence of manganese oxide-reducing bacteria. The procedure is as follows:

The three solutions below were prepared, autoclaved and cooled in a water bath to 50°C.

Solution A: 5 % MnO_x in distilled water

Preparation of delta-$Mn0_x$

This delta manganese oxide was prepared by the oxidation of Mn^{2+} by potassium permanganate in the presence of sodium ion according to the reaction:

$3Mn(II) + 2MnO_4^- + 2H_20$ ----> 5 delta $MnO_2 + 4H^+$

In 200 ml of distilled water, 8 gm of $KMn0_4$ were dissolved. The solution was continuously mixed and heated to just below boiling temperature. 10 ml of 5 N NaOH were then added to neutralize the acid produced by the above reaction, thereby keeping the reaction mixture alkaline and kinetically favoring the oxidation of Mn(II). In a separate flask, 15 gm of $MnCl_2 \cdot 4H_20$ were dissolved in 75 ml of distilled water. This solution was then slowly added to the basic permanganate solution and the resulting suspension heated and mixed for one hour to ensure complete reaction. After cooling, the manganate was washed several times by centrifugation and resuspension in distilled water. After the final resuspension, the solid was freeze-dried and stored as a fine dried powder in a dessicator.

Solution B: 0.05 % Sodium acetate
0.01 % Yeast extract
0.7 % Agar
5 ml/l Microelement mixture
0.085 % NaCl

Solution C: 1 % Agar in distilled water

In labelled, sterilized 20 ml borosilicate glass scintillation vials, 1 ml of Oneida Lake sediment (taken from sequential 2 cm sections of a 10-15 cm core from Buoys 121, 123 and 127) was mixed with 1.0 ml of the 1% agar in distilled water solution and placed in the refrigerator until the agar had set. Each 2-cm layer was assayed in triplicate. A slurry made from 1 ml of solution A and 12 ml of solution B was then poured into each vial over the solidified sediments. The vials were capped and allowed to cool at room temperature

after which about 5 ml of sterile distilled water was added to keep the agar from drying out. The enrichment vial is diagrammed below:

ENRICHMENT CULTURE FOR MnO_x - REDUCERS

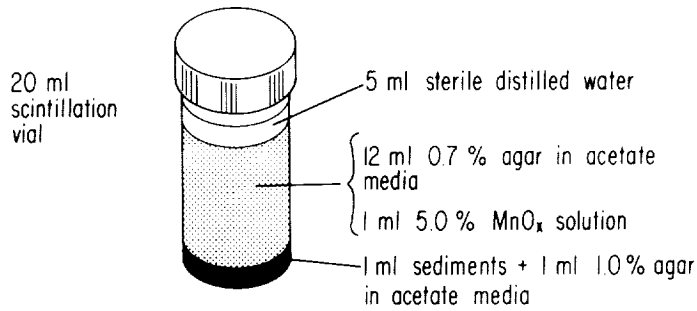

The occurrence of manganese oxide reduction was indicated by the formation of clear zones in the black, flecked MnO_x-containing layer of the vial, as insoluble manganese(IV) oxides were reduced to soluble manganese(II).

In the cores from each buoy, some of the sediment layers reduced manganese oxides though none of the individual layers in a single core were consistently positive for reduction. Often only one of a triplicate was positive and the reduction took from 24 hours to 3 weeks to become obvious. Vials containing surface sediments (from the first 2 cm) of a core were generally positive, while deeper sediments were less likely to develop clear zones. A few simple measurements of and alterations in the assay were conducted to help determine if the reduction was bacterially mediated and direct (i.e., the manganese oxide was being used as a terminal electron acceptor) or indirect (e.g., that the manganese oxides were being reduced simply by a drop in the pH). The pH of a number of vials that were completely clear was measured and all were found to be above 7.5. This would seem to indicate that the dissolution of the manganese oxides was not simply due to a drop in pH due to the release of organic acids. Dr. William Sunda suggested that the manganese oxides were being photo reduced, but vials that had begun to clear continued to clear even when wrapped in aluminum foil.

In many of the reduction positive vials a clear gas of unknown composition was produced. Since the media contained only acetate and was likely anaerobic, methanogens may have been present. But gas extracted with a syringe did not burn when exposed to an open flame and so it probably wasn't methane. No further attempts were made to determine the composition of the gas.

An attempt was made to isolate single colonies under anaerobic conditions with Brewer jars and oxygen-scrubbed nitrogen gas. Using petri plates instead of scintillation vials, bi-layer plates were made and inoculated with samples obtained from vials positive for manganese oxide reduction. No single clear zones were detected on any of the dozen samples assayed, during the time course of our experiments.

Many if not most of the nodules retrieved from the bottom of the lake have had a pock-marked appearance on the side buried in the sediments that suggests dissolution and

erosion. To see if the nodule material would break down in our enrichment vials, finely ground nodules were substituted in the assay for manganese oxides and the vials inoculated with surface sediments (ground-up nodules look surprisingly similar to lab-produced manganese oxides). After 4 weeks there was no sign that the nodule material was being dissolved.

None of these enrichments provided direct evidence that manganese oxides were being used as a terminal electron acceptor, and confirmation of the hypothesis that manganese oxides can serve as electron acceptors will have to await further tests. Yet in the absence of any detectable, gross chemical changes (such as a drop in pH) in the enrichment vials where reduction occurred, the presence of manganese oxide-reducing bacteria in Oneida Lake sediments is strongly suggested.

Heike Riege

"In situ Fluorometry of Phytoplankton and Chlorophyll Distribution in Oneida Lake"

Introduction

Oneida Lake is a eutrophic lake. Usually each year there are several blooms; in the spring the diatoms and during the summer, cyanobacteria. Some of the cyanobacteria Lyngbya, Anabaena and Microcystis oxidize manganese indirectly by producing an alkaline environment around their colonies. So, in order to understand the manganese cycle in this lake it is necessary to study the phytoplankton as well. By working with an in situ fluorometer, I tried to establish a fast and easy method to estimate the amount and distribution of phytoplankton in Oneida Lake.

Methods

Samples of lakewater (1 liter each) were filtered through glass fiber filters (Whatman GF-C or 934 AH, 4.25 or 5.5 cm diameter) by means of a vacuum pump. In the final phase of the filtration, 5 drops of a supersaturated $MgCO_3$ solution were added in order to prevent degradation of chlorophyll.

Afterwards the filters could be kept frozen or extracted immediately in 90% acetone in distilled water (w/v). For the extraction, the filters were put into tubes containing 7 ml of 90% acetone, vortexed, and extracted in the refrigerator (4°C) for approximately four hours. A filter through which nothing was filtered was treated like that as well to serve as a blank.

Disruption of the filters in a tissue grinder as recommended in "Standard Methods" was not necessary. Filters of the same sample gave the same results with and without disruption. (Table 1)

Table 1. Mean chlorophyll concentration for ground and unground filters (all from the same sample (= 8 liters surface water from Buoy 125)).
Volume of filtrate = 1 L each
Volume of extract = 10 ml each

Trichromatic reading

	ground	unground
chl a	6.83±.61	7.37±.37
b	1.75±.22	1.33±.21
c	1.15±.72	1.73±.82
a	6.61±1.07	7.14±.55
Phaeophytin	.780±1.54	.427±1.10
Total	7.39±.62	7.57±.72

After extraction the filters were removed from the tubes and the extract was centrifuged for a few minutes in a small lab centrifuge at maximum speed in order to remove fragments

of cells and filter. The absorbances of the supernatants were measured in a spectrometer (Bausch and Lomb Spec-20) at 630, 647, 664 and 750 nm (chlorophyll c, b, a and turbidity).

Then a drop of 15% HCl (w/v) was added to each cuvette in order to degrade chlorophyll a to phaeophytin, shaken, and after 30 seconds read again at 664 and 750 nm. The readings of the blank were subtracted from the readings of each sample for each wavelength. Afterwards these values were corrected for turbidity by subtraction of the values for 750 nm from the other values for each sample.

Trichromatic method:

The corrected absorbances at 630, 647 and 750 nm were used to calculate the concentrations of chlorophyll a, b, and c by insertion in the following equations:

$Ca = 11.64 \times A664 - 2.16 \times A647 + 0.10 \times A630$
$Cb = 20.97 \times A647 - 3.94 \times A664 - 3.66 \times A630$
$Cc = 54.22 \times A630 - 14.81 \times A647 - 5.53 \times A664$

for cuvettes with a 1-cm light path. This gives the concentration of pigment in the extract in mg/l. The concentration of chlorophyll in the sample is:

chlorophyll in ug/l = (Ca x volume of extract in ml)/(volume of sample in l).

Determination of phaeophytin: phaeophytin absorbs some light at 664 nm so that it can be calculated from the corrected absorbance at 664 nm before and after acidification (=A664b and A664a).

If there is only chlorophyll in a sample the ratio of A664b/A664a will be 1.7; if there is only phaeophytin in it the ratio is 1.0. For a sample that contains chlorophyll as well as phaeophytin there is:

A664b = x + y and A664a = (x/1.7) + y; where x = portion of absorbance of chlorophyll at 664 nm in the extract before acidification and y = portion of absorbance of phaeophytin at 664 nm, then:

$$\begin{aligned} y &= A664b - x \\ \rightarrow A664a &= (x/1.7) + A664b - x \\ \rightarrow x &= [1.7\,(A664b - A664a)]/.7 \\ &= 2.43\,(A664b - A664a) \\ \text{and } y &= A664b - [2.43\,(A664b - A664a)] \\ &= 1.43\,(1.7 \times A664a - A664b) \end{aligned}$$

As extinction coefficients E were used:

for Chl $EChla = 91.0\ (g/l)^{-1}\ cm^{-1}$
for phaeophytin $Eph = 53.5\ (g/l)^{-1}\ cm^{-1}$

so that the concentrations of chlorophyll and phaeophytin in the samples were:

Chl in ug/l = [26.7 (A664b - A664a) x volume of extraction ml]/volume of sample in l.

phaeophytin in ug/l = [26.7 (1.7 x A664a - A664b) x volume of extraction ml]/volume of sample in l.

Fluorescence

In order to measure the amount and distribution of phytoplankton in the lake, a fluorometer (SN 29, Sea Tech. Inc.) was used for in situ measurements in the water column. The excitation wavelength was 425 ± 200 nm, the emission wavelength was 685 ± 15 nm. This should be optimal for the detection of chlorophyll a (according to Sea Tech.). The instrument was connected to a battery and a multimeter and could then be lowered into the lake on a rope. Fluorescence was read in volts from the multimeter. The time constant was three seconds.

For vertical profiles the fluorescence was measured from approximately 15 cm below the surface of the water and in 1 m distances down to the bottom of the lake. The instrument was calibrated by measuring the fluorescence of 4 L of lakewater that was stirred in a bucket by a magnetic stirrer. Afterwards 1 L of the water was taken for chlorophyll measurement and substituted by tapwater. Again fluorescence and chlorophyll were measured and lakewater was further diluted with tapwater.

This was done several times with several water samples from the lake for medium sensitivity and two times for high sensitivity.

Results and Discussion

Calibration of the fluorometer SN 29:

For medium sensitivity of the fluorometer a calibration line for total chlorophyll (= chlorophyll a + phaeophytin) could be obtained so it was possible to convert the fluorescence data measured at this sensitivity into chlorophyll concentrations. These values (= chl_{fl}) were compared with the chlorophyll concentrations of water samples taken at the same time and site of the measurement of in situ fluorescence and extracted in acetone and read at 664 and 750 nm as recommended in the methods (=chl_{ac}).

In most cases chl_{ac} and chl_{fl} are different from one another (up to ± 4 ug chl/L). The differences are not so constant that a systematic error in chlorophyll measurement, sampling or the calibration of the fluorometer could be suggested.

In order to estimate the amount of these possible errors, it would be useful to measure the fluorescence of water samples before they are filtered for chlorophyll measurements. If the fluorescence were the same as that measured in the lake, but chl_{ac} were different from chl_{fl} then it is most likely an error in the chlorophyll measurement or in the calibration of the fluorometer (e.g. mixing of the sample). If the fluorescence differs in the sample from that in the lake, then the sampling technique could be the reason for this.

It is reported that fluorescence of living phytoplankton depends on the light intensity (e.g. Neale, P.J. and P.J. Richardson 1987). For Oneida Lake, no correlation between in situ fluorescence, chlorophyll concentration (chl_{ac}) and light intensity was seen. Further studies in the lake and with water samples in the lab under different light intensities would be useful. Another reason for the differences between chl_{fl} and chl_{ac}, especially in greater depths, could be light scattering by small particles in the water column.

Because of these differences between chl_{fl} and chl_{ac} and the lack of credible chlorophyll data no calibration line for high sensitivity could be obtained. But since the calibration line for medium sensitivity seems to be adequate, I assume that the in situ fluorescence data even at high sensitivity setting are comparable with one another.

Diurnal cycle

At Buoy 127 in situ fluorescence was measured and samples for chlorophyll measurement were taken at different times of day on 7/17/87 - 7/18/87 and 7/31/87 - 8/1/87 (Figure 1a-g). During the day under high light intensities there is usually a peak of maximum fluorescence between 2 and 5 m depth, whereas during the night and early in the morning (6 am) the fluorescence is nearly the same in the whole water column, except at greater depths where the fluorescence nearly always drops.

This phenomenon is generally explained by movement of the phytoplankton towards the site of optimal light intensity. During daytime the irradiance at the surface is too high, so the cyanobacteria and algae keep away from it as well as from greater depth where there is too little light for photosynthesis. During the night, in the absence of any optimal light conditions there is a random distribution of phytoplankton.

Since there was no thermocline in Oneida Lake during this time, it makes sense that the overall vertical distribution of phytoplankton is determined by light intensity rather than by temperature.

Horizontal distribution of phytoplankton in the lake

In situ fluorescence profiles were taken at several points of the lake (usually near the buoys). The profiles were slightly different from one buoy to the next. The data from three transects over the lake (7/20/87, 7/24/87 and 8/4/87) show that there is a higher density of phytoplankton near the eastern shore than in most other parts of the lake. Since the main wind-direction is from the west towards the east, it is possible that phytoplankton near the water surface is driven by surface currents caused by the wind in that direction. There seems to be a constant minimum in fluorescence near the bottom at Buoy 115 and 117. Except for this the horizontal distribution of phytoplankton changes at least within a few days (Figure 2).

Changes in fluorescence

Over a three-week period changes in fluorescence were measured at Buoy 127. Figure 3 shows the fluorescence at surface and in 4 and 8 m depths measured on different days always between 1:45 pm and 3:00 pm. These data show a slow increase in the amount of phytoplankton.

References

Golterman, H.L., R.S. Clymo, M.A.M. Ohnstad (1978) Methods for Physical and Chemical Analysis of Fresh Water, 2nd. ed. Blackwell Scientific Publications, Oxford, Edinburgh, London, Melbourne, pp.162-167.

Neale, P.J. and P.J. Richerson (1987) Photoinhibition and the diurnal variation of phytoplankton photosynthesis. I. Development of a photosynthesis-irradiance model from studies of in situ responses. J. Plankton Res. 9:167-193.

Standard Methods for the Examination of Water and Wastewater (1975) 14th ed. APHA-AWWA-WPCF, pp.1029-1033.

Figure 1a

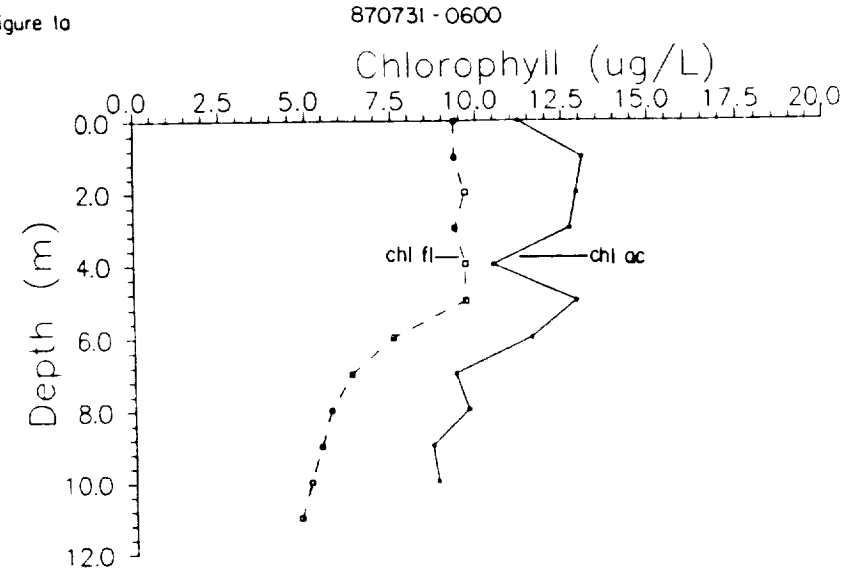

Figure 1b

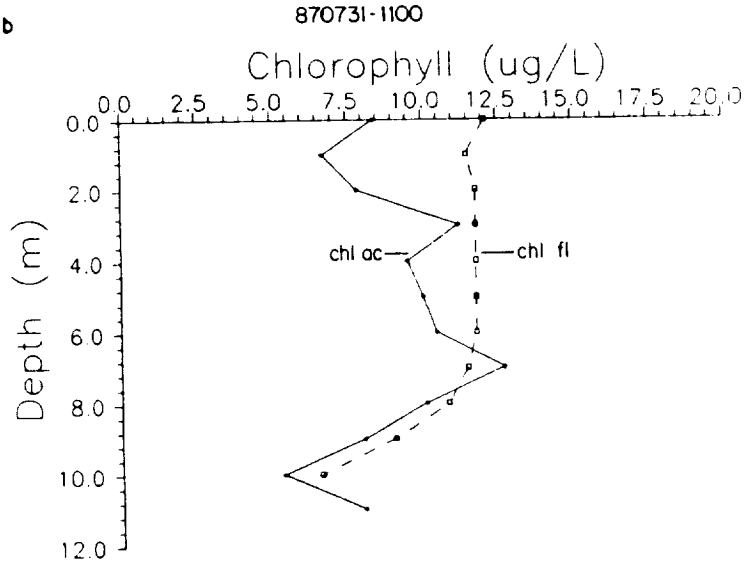

Figure 1c

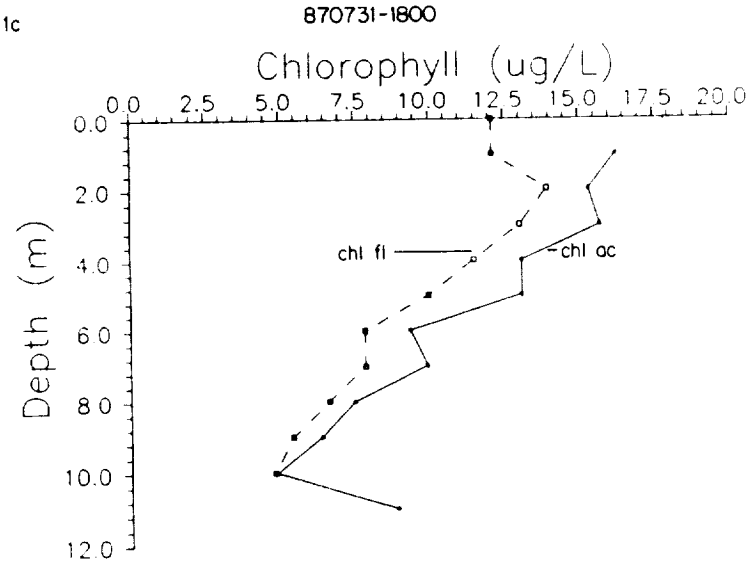

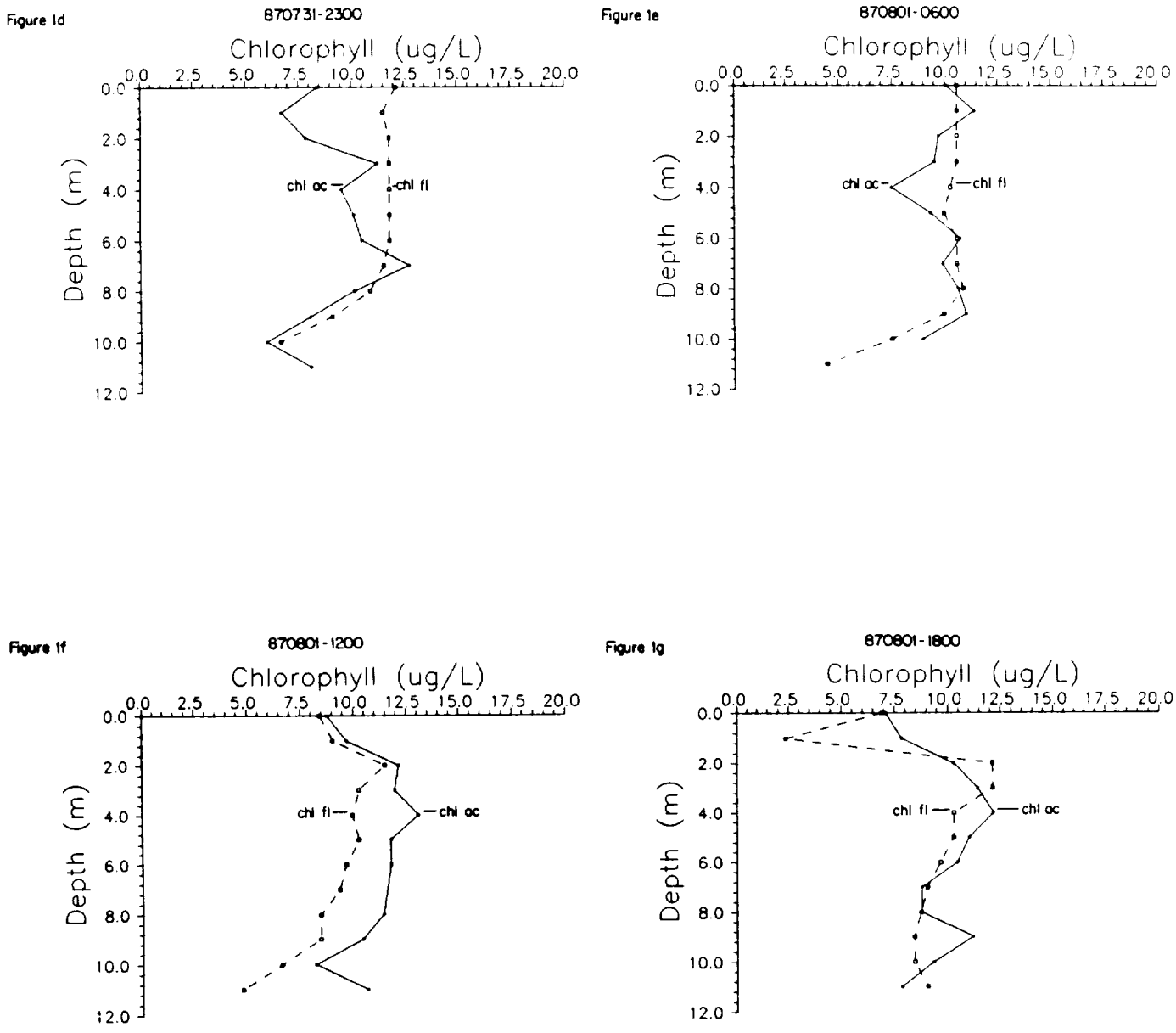

Figure 1. Changes in chlorophyll distribution in lakewater samples over a 36-hour period.

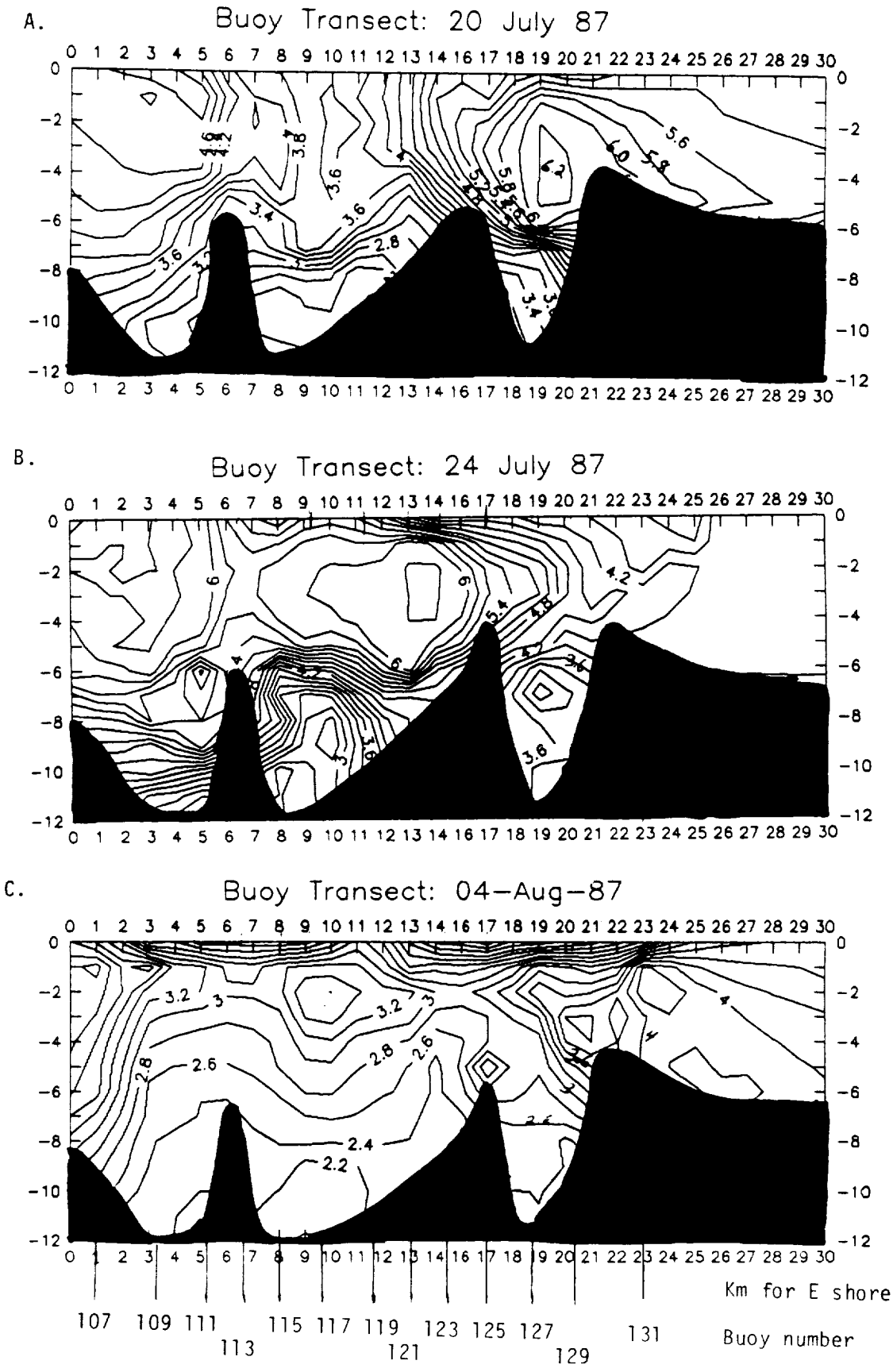

Figure 2: Relative fluorescence from buoy transect

fig. 3 in situ fluorescence at B127 (early pm)

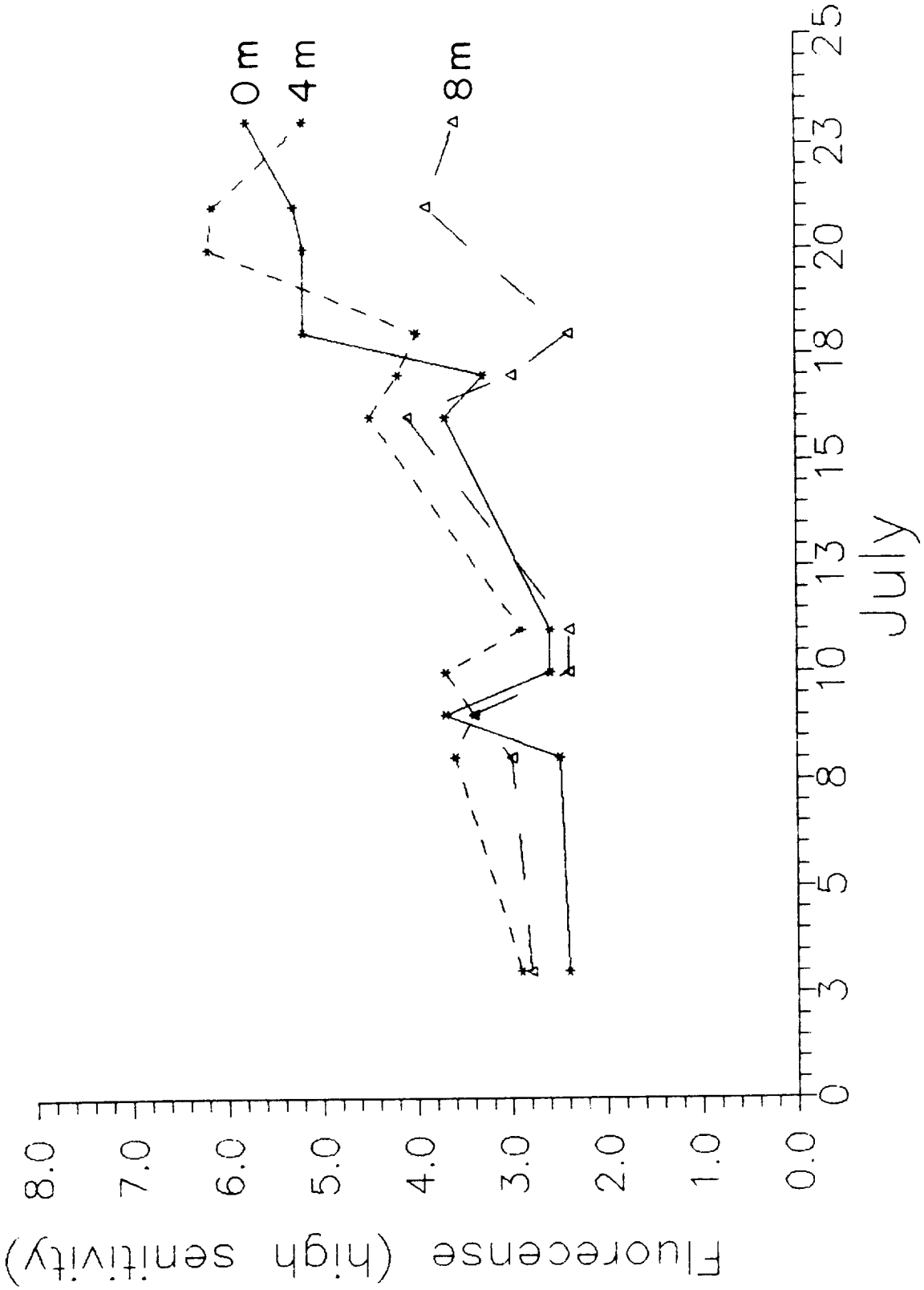

Eleanora Robbins
Alan Creamer
Dave Bolgrien

"Lithostratigraphy of Short Cores from Oneida Lake, New York"

Introduction

Lithostratigraphic changes observed in cores from Oneida lake, N.Y. have not been reported previously, but bottom sediments and chemical changes with depth have been the subject of several studies. Greeson (1972) mapped the bottom sediments of Oneida Lake (Figure 1A) and showed (1) cobble and rubble on high-standing ridges, (2) gravel along the northern margin, (3) sand at river junctions, particularly along the eastern margin, and (4) silt and clay across other areas of the lake bottom. Dean and Ghosh (1978) mapped the locations of manganese nodules found on the bottom of the lake. Dean and Ghosh (1978) and Dean et al. (1981) studied the water chemistry in short cores obtained from two of the locations sampled in the present study.

The geologic history of Oneida Lake can be inferred from cores taken in Lake Ontario because both lakes were part of glacial Lake Iroquois around 12,000 years B.P. Offshore cores, the longest of which was 18 m, from the eastern end of Lake Ontario showed a stratigraphic section that included from bottom to top, gravel of unknown thickness at the base, a 1-m-thick laminated silty clay, a 0.25-m-thick shell layer, and a 7.9-m-thick silty sandy clay with iron sulfide streaks at the top. Peat from a depth of 60 cm in a core from the southeastern shore of Lake Ontario yielded a radiocarbon date of 4,950 years B.P. (Anderson and Lewis, 1985).

Because neither deep drilling nor seismic profiling has been done in Oneida Lake, the total thickness of Pleistocene and Holocene sediments that overlay Silurian basement rocks is not known (Mills et al., 1978). Seismic work in the eastern basin of Lake Ontario indicated the presence of 30 to 35 m of glacial-lacustrine and post-glacial sediments (D.R. Hutchinson, USGS, oral commun., 1987). Seismic profiles in many of the Finger Lakes showed 100 to 200 m of unconsolidated sediment above an acoustic basement (H.T. Mullens, Syracuse University, oral commun., 1987). These data limit the maximum depth of sediments that might be expected in Oneida Lake.

Materials and Methods

Two-ft-deep cores were obtained by scuba divers. Clear-plastic core barrels, 2.5 inches in diameter, allowed the measurement of undeformed stratigraphic sections. The cores were extruded and allowed to dry at room temperature and are available for study at the Cornell University Biological Field Station on Oneida Lake. Several cores were obtained at each of seven localities in the vicinity of the permanent buoys that are maintained as part of the New York Barge Canal. Figure 1 shows the locations and stratigraphy of these archival cores.

Figure 1. Opposite. A. Map of sediments of Oneida Lake. Localization of the cores depicted in 1B are shown. B. Analysis of cores obtained from Oneida Lake.

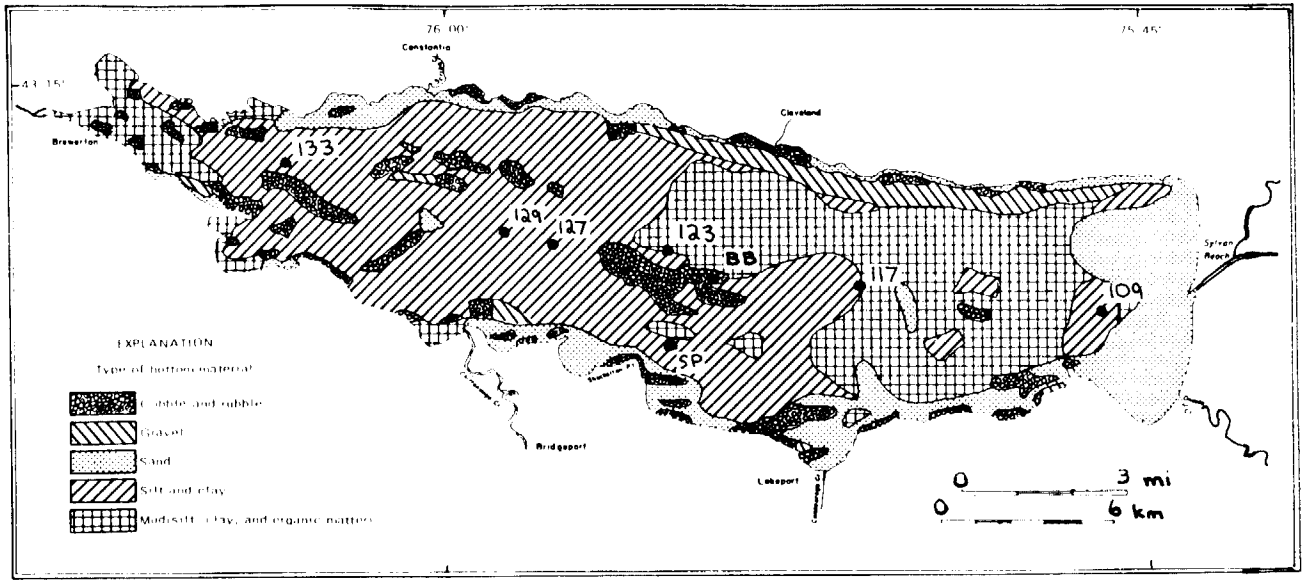

A

EXPLANATION OF SYMBOLS

- White snails
- Thioploca mats
- Manganese nodules
- Brown or black sand
- Brown silt
- Black and orange streaks
- Black silty clay
- Black "fingers"
- Gray clay
- Calcareous gray clay
- Laminated gray clay

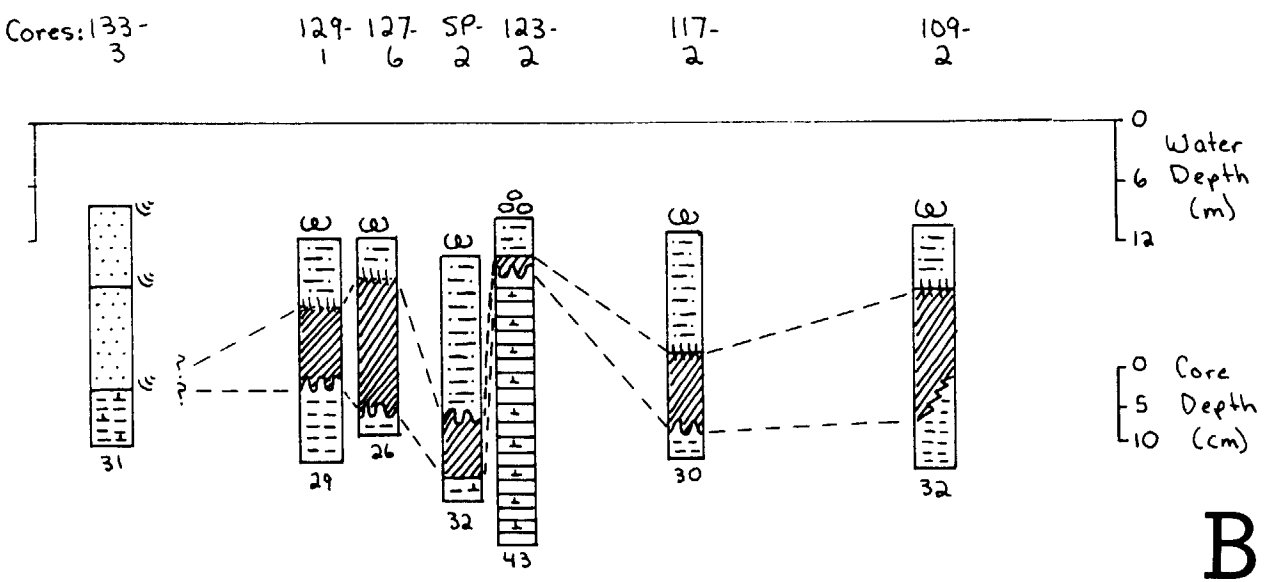

B

Results and Discussion

The general stratigraphic sequence in the cores includes, from bottom to top, a light to medium gray clay, and a brown silt. The basal gray clay is calcareous in cores SP (Shackelton Point), 123, and 133. The basal clay in core 123 is laminated, alternating gray and black. The brown silt, which coarsens upward, probably is the most bioturbated. Numerous worms, particularly Tubifex, are abundant where the bottom water is poorly oxygenated (Buoys 127 and SP). In contrast, most of the core at Buoy 133 is composed of sand.

Details at the sediment/water interface are shown in Figure 1B. In the anoxic or suboxic deep subbasins, mats of the sulfur-oxidizing bacteria Thioploca appear to hold together the loose silt surface, as seen in cores from Buoys 109, 117, 127 and 129 (see Robbins and Schmidt, this volume). The core at Buoy 123 on Shackelton Shoals, located in a highly oxygenated part of the water column, has abundant manganese nodules at the surface. In contrast, no nodules or Thioploca mats are seen around Buoy 133; instead, the surface is sandy. Furthermore, layers of white snails occur at distinct intervals, and whole mussels are apparent in other cores from 133. Most of the snails were around 1 cm in length and no mussel was longer than 6 cm.

In most cores, the contacts between units are not sharp. The transitions are marked by black and orange streaks or by black "fingers" that penetrate into the overlying or underlying units. Remnants of former black "fingers," seen distinctly in core 123, suggest that some of the black color of the sediment may be a transitory feature that may or may not remain after compaction of the clay to shale or mudrock. Sieving of samples from this unit (Robbins et al., this volume) liberated H_2S, and the sulfur odor was particularly intense in the black "fingers." The black "fingers," around 1 to 3 cm in length and 1/2 cm in width, may be caused by sulfate-reducing bacteria that form iron monosulfides and pyrite. Therefore, the black zone may extend up or down as the sulfate-reducing bacteria, which are anaerobes, migrate in reponse to the moving chemocline in the overlying oxygenated water. Hallberg et al. (1980) reported that such bacteria can migrate as much as 3 cm in one day.

The transitions that are marked by black and orange streaks are more subtle than the fingering. The archive cores were not cut in half, so the cause of streaking is unknown. In a core from another lake, the senior author noted that similar streaks were produced by coring through an overlying coarse-grained, Fe-oxide-cemented unit, and an underlying fine-grained, iron-sulfide-rich unit. The streaked layers in the Oneida Lake cores may represent times of shifting oxidation potential.

The presence of buried mussel layers and dark-colored sand at the western end of Oneida Lake is unusual. The sand was not mapped by Greeson (1972), possibly because its dark color makes it indistinguisable from the organic-rich brown silt. The mussel layers indicate the position of former lake bottoms that may have been buried catastrophically by the dark-colored sand. The presence of sand in this area is anomalous because this unit does not appear in cores from Lake Ontario nor in other cores from Oneida Lake. Furthermore, because sand is not a typical sediment near the outflow of a lake, the geologic history and sedimentology of the sandy unit remains as a future study.

References

Anderson, T.W. and C.F.M. Lewis (1985) Postglacial water-level history of the Lake Ontario basin. In: Quaternary Evolution of the Great Lakes, P.F. Karrow and P.E. Calkin (Eds.) Geol. Assoc. Canada Spec. Paper 30, pp.231-253.

Dean, W.E. and S.K. Ghosh (1978) Factors contributing to the formation of ferromanganese nodules in Oneida Lake, New York. U.S. Geological Survey J. Res. 6:231-240.

Dean, W.E., W.S. Moore and K.H. Nealson (1981) Manganese cycles and the origin of manganese nodules, Oneida Lake, New York, U.S.A. Chem. Geol. 34:53-64.

Greeson, P.E. (1972) Limnology of Oneida Lake with emphasis on factors contributing to algal blooms. U.S. Geological Survey Open-file Report 72-139.

Hallberg, R.O., B. Bubela and J. Ferguson (1980) Metal chelation in sedimentary systems. Geomicrob. J. 2:99-113.

Mills, E.L., J.L. Forney, M.D. Clady and W.P. Schaffner (1978) Oneida Lake. In: Lakes of New York State, Vol. 2, J.A. Bloomfield (Ed.) Academic Press, New York, pp.367-451.

Eleanora Robbins
Alan Creamer
Susan Rose

"Preliminary Analysis of Biostratigraphic Changes and Mineralogy of Short Cores from Oneida Lake, New York"

Introduction

Previous to this study, the sediments of Oneida Lake have not been systematically examined with regard to biostratigraphic changes. Cores were therefore collected from several localities in the lake near buoys (Figure 1). Three cores from Buoys 123 and SP (Shackelton Point) were chosen for detailed palynological, mineral, and microfossil analysis.

Oneida Lake is a remnant of the once larger Lake Iroquois that also included Lake Ontario during the Late Pleistocene (Mills et al., 1978). Cores 18 m in depth from Lake Ontario record both lithographic changes with time and biostratigraphic changes in pollen and spores, invertebrates and plant macrofossils. Major changes are shown in the abundance of herbaceous and arboreal tree pollen through the 12,000 years represented by those cores. Herbaceous tundra vegetation dominated by Artemisia gave way to spruce around 12,500 years ago (Anderson and Lewis, 1985). Then spruce gave way to pine domination about 10,000 years ago with the retreat of the northern glaciers. About 7,700 years ago, hemlock became the dominant species in pollen diagrams.

Sedimentation rates from varves have been calculated from cores extracted from other Finger Lakes in New York State. Annual varves in Fayetteville Green Lake showed that sedimentation rates have ranged from less than 1 mm/yr (wet thickness) in centuries old sediment to 1 to 3 mm/yr (wet thickness) in the 1970's. This indicated that sedimentation rates have accelerated from 392 gm/m^2/yr in the late 1800's to 581 gm/m^2/yr in the 1970's (Ludlam, 1981). A core 4 m in depth, taken from the deepest part of Seneca Lake, contained varved sediments that recorded a sedimentation rate of 2 mm/yr (O'Rourke, 1976). The data from the Seneca Lake core indicated that hemlock became prominent about 1300 AD. The core also recorded the distinct peak of Ambrosia pollen that is associated with European settlement (King et al., 1976). At the other extreme in sedimentation rate, Cayuga Lake accumulated sediment on the order of 2 cm/yr (wet thickness) from the early through the middle 1900's (Ludlam, 1967).

The cores from Oneida Lake used for our study are less than 50 cm in depth and, therefore, contain only sediments dating to the Late Holocene hemlock-dominated period. ^{210}Pb dating of another short core from Buoy 127 indicates a sedimentation rate of 2 to 3 mm/yr in the brown silt and black silty clay (W.S. Moore, Univ. of North Carolina, oral commun., 1987). If this sedimentation rate is applicable to other localities and to other lithologies in the lake, then the top 50 cm of sediment may represent the last 150-250 years of time. Events that might be recorded in these cores therefore are (1) climatic variations such as drought or long cold spells that affected the vegetation and occurred during the Little Ice Age (A.D. 1450-1850); (2) the beginning of European settlement, an event recorded by a decrease in tree species because of major land clearance and a consequent increase of Ambrosia pollen; (3) changes in fish populations such as the loss of Atlantic salmon and the invasion of predaceous perch and walleye; and (4) the connection of the

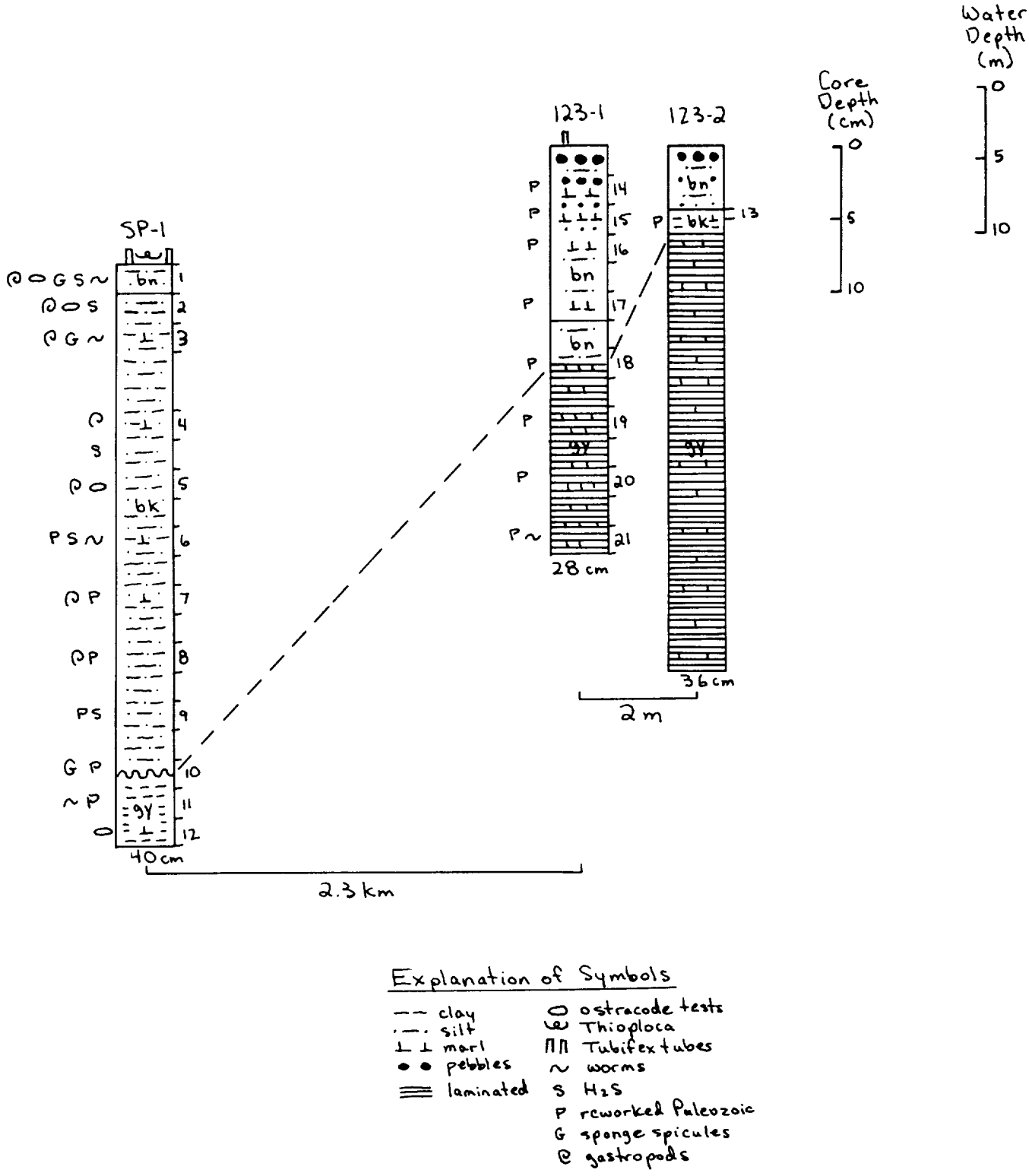

Figure 1. Analysis of three cores from Buoys SP and 123.

New York Barge Canal with Oneida Lake in 1916 which may have been accompanied by lower water levels and by an invasion of new plant and animal species.

Methods

The cores that were investigated in this study were collected from two localities in Oneida Lake. Core SP-1 is from a deep subbasin near the Shackelton Point Buoy. The water depth within this subbasin averages 12 m, and oxygen tensions often measure within the suboxic range. The surface sediment at Buoy SP is flocculent, and most of the subsurface sediment within the core is brown or black silt. Core 123-1 was collected from Buoy 123 on Shackelton Shoals. This shoal area is a basement high probably formed from a glacial ridge such as a recessional moraine. The water depth at Buoy 123 is 7 m. The bottom is oxygenated, swept by surface currents, and contains numerous manganese nodules. Sediments in the Buoy 123 cores typically contain a thin layer of brown nodules and silt overlying a thick section of dense gray clay. Generally, an intermediate black unit separates these two layers. Core 123-1 did not have this intermediate layer and so a sample of the black layer from 123-2 was included in this study.

The cores were extruded in 2-cm intervals, and each slice was divided into three fractions. Two of the fractions were subjected to acid and peroxide treatments and were taken from the center of each slice to avoid surface contamination. The third fraction was untreated.

Acidified fraction. The acidified fraction was used to study pollen and spores (Table 2), planktonic algae (Table 3), kerogen (Table 4), and residual materials (Table 5).

Sample processing with HCl and HF was conducted in an outdoor area because no fume hood was available. To account for contaminating pollen and spores that became incorporated during the outdoors processing, microscope slides were coated with glycerine and set out to collect the current modern pollen rain. The volume of sediment was kept constant for all samples by filling the plastic centrifuge tubes to 10 ml. The samples were treated with 10 percent HCl for 24 hours to remove carbonate minerals; HCl just covered the sediment which was stirred periodically. The HCl-treated samples that continued to react were decanted and then further treated with 30 percent HCl until all reaction ceased. The second treatment required an additional 24 hours. The samples were then transferred to plastic beakers, and after the sediment settled, HCl was removed by two decants with water. The prior removal of carbonate by the HCl treatment is important because a mixture of carbonate with HF can produce a violent exothermic reaction. To remove silicate minerals, 50 percent HF was added slowly to the moist sediment. The samples were then wet sieved, by using gravity settling, through 125-um and 25-um screens.

Oxidized fraction. This fraction was oxidized by using hydrogen peroxide and was studied for siliceous microfossils (Table 3). The oxidation produced two unexpected reactions. First, when 30 percent H_2O_2 was added to each sample, the reaction in the manganese oxide-rich samples from the top of core 123-1 gave off unmistakable chlorine gas. Second, the reaction of H_2O_2 with the carbonate in the carbonate-rich samples was violent; the white gas that formed indicated that the H_2O_2 was being disassociated into H_2 and O_2 (J.L. Haas, Jr., USGS, oral commun., 1987). This violent reaction was quenched with water, and, after decanting, a dilute concentration (7 percent) of H_2O_2 was added. After bubbling ceased, the H_2O_2 concentration was gradually increased to 15 percent as the sediment settled and the solute was decanted. The samples remained in the solution for 2 weeks and were frequently stirred; the solution in the samples was periodically freshened

Table 1. Mineralogy of cores.

	quartz	zircon	tourmaline	rutile	green amphibole	Fe-oxide coats	hematite crystals	pyrite	unidentified black minerals	Calcite?	other
Core SP-1											
1	?	rounded	-	-	+	+	-	-	spheres	-	-
2	+	+	-	+	-	+	-	-	subhedral, coats spheres	-	-
3	+	-	-	-	-	-	-	framboid?	subhedral, coats	+	-
4	+	?	-	-	-	+	-	framboid?	subhedral	+	-
5	-	?	-	-	-	+	-	-	-	-	-
6	-	?	-	-	-	-	-	framboid?	coats	+	-
7	vfg	+	-	-	-	+	-	framboids, enmeshed	-	+	-
8	vfg	?	-	-	-	+	-	framboids, enmeshed	-	-	-
9	vfg & ang	?	-	-	-	+	-	framboids, cubes	-	-	-
10	ang-round, vfg-fg rose	rounded	-	-	-	-	-	framboids	-	-	olivine?, quartzite, gypsum
11	ang-round, vfg-fg	euhedral	-	-	-	+	+	framboids	-	+	clear with low refrac., gypsum, quartzite
12	ang-round, vfg	subhedral	-	-	+	-	-	framboids, euhedral	coats	+	clear with low refrac.
Core 123-2											
13	ang, vfg-cg, & rose	-	-	-	-	+	-	framboids, enmeshed	-	?	quartzite, schist pebble
Core 123-1											
14	vfg-fg round	-	+	-	-	-	-	octahedral	-	++	clear high refrac., shale chips
15	vfg-mg, round	euhedral	-	-	-	+	hexagonal	enmeshed, framboids	-	+++	brown blades, clear high refrac., yellow, shale chips, quartzite
16	vfg	-	-	-	-	+	hexagonal	enmeshed, octahedral	coats	++	clear with low refrac.
17	+	euhedral	?	-	-	+	hexagonal	octahedral	-	++	yellow subhed. clear white balls
18	vfg, ang	subhedral	-	-	-	+	-	-	-	+++	-
19	vfg-fg ang	rounded	-	-	-	+	-	-	plates	+++	blue plates clear with low refrac.
20	-	+	blue	twins	+	+	-	octahedral	-	+++	round with low refrac.
21	-	-	-	-	-	-	-	enmeshed, octahedral	-	++	round with low refrac. blue coats

Abbreviations: +=present, -=absent, ?=uncertain, ang=angular, fg=fine graine, mg=medium grained, react=reactive, refract=refraction, round=rounded, vfg=very fine grained.

Table 2. Pollen and spores in cores.

Core Number	SP-1												123-2	123-1							
Sample Number	1	2	3	4	5	6	7	8	9	10	11	12	13	14	15	16	17	18	19	20	21
Tree pollen																					
Abies	-	-	1	1	-	-	-	-	3	26	69	53	12	-	-	2	2	-	4	2	3
Acer	-	1	-	-	1	-	-	-	-	2	-	-	8	-	-	-	-	-	-	-	-
Alnus	-	-	-	-	-	1	-	-	-	-	2	-	-	1	-	-	-	-	-	-	-
Betula	2	1	1	-	-	2	1	-	-	-	-	-	-	-	-	-	-	-	-	-	-
Carya	-	-	-	-	-	-	-	-	-	1	-	-	1	-	-	-	-	-	-	-	1
Juniperus	-	1	5	-	-	-	-	-	-	2	-	-	-	-	-	-	-	-	-	-	-
Picea	-	-	1?	-	-	-	-	-	2	-	-	-	3	-	-	-	-	-	-	-	-
Pinus	11	5	16	11	10	9	14	11	25	50	>200	>200	3	-	3	1	-	-	3	-	-
P. resinosa	1	-	-	-	-	-	-	-	-	-	-	-	-	-	-	-	-	-	-	-	-
Platanus	-	-	-	-	-	-	-	-	-	-	1	-	-	-	-	-	-	-	-	-	-
Prunus	-	-	-	-	-	-	-	-	-	-	1	1	-	-	-	-	-	-	-	-	-
Quercus	-	-	-	-	-	-	-	1	-	8	-	1	1	-	-	-	-	-	-	-	-
Salix	-	2	-	-	-	-	-	-	-	-	-	-	-	-	-	-	-	-	-	-	-
Tsuga	3	2	2	-	2	1	1	-	-	19	8	9	14	-	1	-	-	-	-	-	-
unknown bisaccate	-	-	-	-	-	1	-	-	-	-	-	-	2	-	-	-	-	-	-	-	-
unknown monosaccate	-	-	-	-	-	-	-	1	1	-	-	-	-	-	-	-	-	-	-	-	-
Herbaceous pollen																					
Ambrosia	2	2	6	2	2	2	1	-	-	2	-	-	-	-	-	-	-	-	-	-	-
Artemisia	1	-	-	-	-	-	-	-	-	-	-	-	-	-	-	-	-	-	-	-	-
Dianthus	-	-	-	-	-	-	1	-	2	1	-	-	-	-	-	-	-	-	-	-	-
Heliantum	?1	-	-	-	-	-	-	-	-	-	-	-	-	-	-	-	-	-	-	-	-
Liliaceae	-	-	-	-	-	1	-	-	-	-	-	-	-	-	-	-	-	-	-	-	-
Potomegeton	-	-	-	-	-	-	-	1	-	-	-	-	-	-	-	-	-	-	-	-	-
Prenanthes-type	-	-	1	-	-	1	-	-	-	-	-	-	-	-	-	-	-	-	-	-	-
Typha	-	1	-	-	-	?1	?1	-	-	-	-	-	-	-	-	-	-	-	-	-	-
Urtica-type	-	-	1	-	-	-	-	-	-	-	-	-	-	-	-	-	-	-	-	-	-
Utricularia	-	-	-	-	-	1	-	-	-	-	-	-	-	-	-	-	-	-	-	-	-
Viola	-	-	-	-	-	1	-	-	-	-	-	-	-	-	-	-	-	-	-	-	-
Cheno-Am	-	-	1	-	-	-	-	-	-	-	-	-	-	-	-	-	-	-	-	-	-
short-spine Compositae	-	3	-	-	-	1	-	-	-	-	-	2	1	-	-	-	-	-	-	-	-
long-spine Compositae	-	-	1	-	-	-	-	-	-	-	-	-	-	-	-	-	-	-	-	-	-
Cyperaceae	1	1	2	1	2	2	3	-	1	1	-	-	1	-	-	-	-	-	-	-	-
Tree or herbaceous pollen																					
unknown aletes	-	2	5	-	2	1	1	-	11	8	1	9	21	2	-	-	1	-	-	-	-
unknown monosulcates	2	1	3	1	3	1	1	1	-	-	-	-	1	-	-	-	1	-	-	-	-
unknown polyporates	-	-	-	2	2	-	2	2	1	-	-	1	-	-	-	-	-	-	-	-	-
unknown tricolpates	-	-	-	-	1	-	-	2	-	1	-	3	5	-	-	-	-	-	-	-	-
unknown triporates	2	-	2	-	-	3	-	-	3	1	-	-	2	-	-	-	-	-	-	-	-
unknown tricolporates	2	2	2	-	-	-	2	-	-	-	-	1	-	-	-	-	-	-	-	-	-
Lower plants																					
Alete spores																					
Diphyscium-type	1	1	-	2	1	-	1	-	1	-	-	-	-	-	-	-	-	-	1	-	-
mosses	2	1	1	2	1	-	-	-	1	5	2	1	2	1	-	-	-	-	1	1	1
Monolete spores																					
cicatricose spores	-	-	-	1	-	-	-	-	-	-	-	-	-	-	-	-	-	-	-	-	-
polypodes	1	1	-	-	-	-	-	-	1	-	-	1	3	-	-	-	-	-	-	-	-
unknown monoletes	-	-	-	-	-	-	-	-	1	-	-	8	1	-	-	-	-	-	-	-	-
Trilete spores																					
Botrychium	-	-	1	-	-	-	-	-	-	-	-	-	-	-	-	-	-	-	-	-	-
Lycopodium	1	-	-	-	-	-	-	-	-	-	-	-	-	-	-	-	-	-	-	-	-
Sphagnum	-	-	-	-	-	?1	?1	1	-	-	-	-	1	-	-	-	-	-	-	-	-
unknown triletes	-	1	2	-	1	-	-	-	-	-	-	-	1	-	-	-	-	-	-	-	-
Total counted:	33	29	53	23	28	30	30	20	53	126	>200	>200	84	4	4	3	4	0	9	3	5

or changed during that time. The samples were then wet sieved, by using gravity settling, through 125-um and 25-um screens.

Untreated fraction. The untreated fraction of the sample was used to study minerals (Table 1), Daphnia resting eggs (ephippia), and fish scales (Table 5). It was wet sieved into four subfractions by using screens of 1.4 mm, 150 um, and 25 um in size. Ephippia from D. pulex and D. galeata, two Daphnia species in Oneida Lake that produce resting eggs, were collected for reference. Modern fish scales of yellow perch, walleye, smallmouth bass, sunfish (pumpkinseed), Atlantic salmon, ciscoe, freshwater drum, white sucker and a number of smaller cyprinids were collected and pressed on plastic slides. Each sample was tested with a magnet for visible magnetite. Other minerals were identified by color and morphological characteristics.

Permanent slides of each subfraction smaller than 125 um were made. A drop of residue was mixed with two drops of glycerin jelly and heated on a hot plate at 50°C for 4 hours, and at 40°C for an additional 16 hours.

Results and Discussion

The difference between the overlying brown and black silt and the underlying gray clay (Figure 1) are distinct and probably represent a major change in sedimentary regime. Organic content, grain size, sediment color, chemical composition, sedimentary structures, and organic tissues color all change at this boundary. The underlying gray clay is dry, compact, and generally calcareous. In cores 123-1 and 123-2, the clay is laminated. This clay unit occurs in all cores examined from Oneida Lake. The overlying brown and black silt is an unconsolidated unit. These abrupt lithographic changes may indicate the presence of a stratigraphic hiatus.

The transition from the underlying gray clay to the overlying black and brown silt is irregular in the form of vertically oriented, interpenetrating black "fingers" (Figure 1). The irregularity made measuring the exact depth of the contact difficult.

The change from calcareous clay to generally noncalcareous silt could also represent a change in dominance of the rivers that fed into Oneida Lake. Today, the rivers that drain the Ordovician siliceous rocks to the north dominate the surface water budget of the lake (Greeson, 1972). In the past, rivers draining Silurian and Devonian calcareous rocks to the south could have dominated the surface water budget during the cooler period in the past, an interpretation that is supported also by increased pine pollen (Table 2).

Differences in palynomorph abundance in the cores (Table 2) also support the concept of a stratigraphic hiatus between the clay and the silt. Today, the dominant vegetation on the south side of the lake includes maple, ash and oak; on the north side of the lake, the dominant vegetation includes birch and pine. Spruce also is present and has been introduced into the modern watershed (E.L. Mills, Cornell Univ., oral commun., 1987). Pine dominates the underlying gray clay unit but is not dominant in the brown and black silt. Fir pollen is abundant in the basal clay samples but is rare in the overlying silt samples. This evidence suggests that there was a cooling event at the base of the silt, an event possibly associated with the Little Ice Age (A.D. 1450-1850) (Davis, 1983).

The change in pollen dominance from arboreal taxa in the basal clay unit to herbaceaous pollen in the upper silt unit (Table 2) is concurrent with the lithologic and color changes in vegetation because settlers cleared the land of trees for agricultural purposes (King et al.,

1976). The Oneida Lake watershed area was first settled between 1790 and 1810 (Mills and Ganon, 1983). Most interpretations of when settlement occurred add a lag time because the elimination of forests and the clearing of land occurred over a period of time (Davis et al., 1974). In core SP-1, the abundance of arboreal pollen over herbaceous pollen suggests that European settlers had begun to clear the land during the deposition of sediment in sample 10 and settlement was widespread by the deposition of sediment in sample 9. Charcoal, which is usually an indicator of forest clearing, is not present. Although Ambrosia is present, it never is abundant. However, in samples having low pollen sums, the mere presence of Ambrosia indicates its importance in the paleovegetation. These palynomorph data are only preliminary because time did not allow detailed counts.

While pollen of both Cyperaceae and Salix in the upper samples of cores (Table 2) shows the presence of bulrush-type plants and willow in the watershed, macroscopic plant remains in the cores can help locate ancient wetlands. As late as 1947, dense stands of bulrush (Scirpus) and water willow extended 100-300 m into areas that presently are offshore (Mills and Ganon, 1983). Today, submerged aquatic vegetation including Cladophora, Heteranthera, Myriophyllum, and Potomageton are present but not abundant. However, the sizes of samples below 6 cm in core SP-1 suggests that the plant sources may indeed have been closer to the site of deposition in the past.

The mineral components of the cores provide useful information on biological and chemical changes. The pyrite content of the cores increases with depth (Table 1). Pyrite is rare at the top of core SP-1 but becomes abundant in samples 7 to 21. H_2S, which marks the depth of active sulfide generation by the sulfate-reducing bacteria, was noted at several intervals (Figure 1). Iron is present as abundant iron-oxide coats in the cores (Table 1) and in the ferromanganese nodules precipitated in the lake (Dean and Ghosh, 1978). Gypsum platelets occur in samples 10 and 11 (Table 1). They may be detrital in origin, derived from gypsum in the southern watershed, or they may be authigenic and formed from the weathering of pyrite in the upper layers when water levels dropped. A distinctive spherical mineral (Table 1), having a very low index of refraction, may have been produced by the palynological processing. It may be a $CaSiO_2$ zeolite produced by the release of Ca by HCl and by the release of SiO_2 by HF.

The calcite in the calcereous layers was carefully examined for clues as to its formation. The calcite takes the form of rounded, clay-size platelets; no calcite-coated charophyte stems typical of nearby Fayetteville Green and Onondaga Lakes (Dean and Eggleston, 1984) were noted. Calcite rhombohedrons are present but rare. The calcite platelets are coated with a brownish or reddish dust that could not be resolved with a light or petrographic microscope. Therefore, the genesis of the calcite cannot be resolved by our methods. However, in Fayetteville Green Lake, temperature fluctuations in the epilimnion drive calcite precipitation and varve formation (Ludlam, 1981), although algae also may contribute to the precipitation of calcite (Busson et al., 1972). Oneida Lake, like Fayetteville Green Lake, is a hardwater lake and the same complex process may have operated there in the past.

Because magnetotactic bacteria are abundant in Oneida Lake sediments (J. Stolz, Boston University, oral commun., 1987, and pers. observation), magnetite should be present in untreated samples; no visible magnetite was noted. The lack of visible magnetite might indicate that bacterial magnetosomes are still intact in the sediments and that the nanometer-sized magnetite crystals produced internally by these bacteria have not yet dissolved and reprecipitated, or that these bacteria are not an important source of magnetite for this environment.

Both fossil and modern algae are present in the cores (Table 3). Acritarchs, which are extinct marine algae, are abundant in intervals throughout the cores (Figure 1), along with other reworked Paleozoic spores and chitinozoa. The acritarchs include Domasia elongata, Diexallophasis denticulata, Leiofusa sp., Tunisphaeridium cf., T. tentaculiferum, Multicisphaeridium arbusculiferum, Micrhystridium spp. and Verhachium spp. (E.R. Wicander, Central Michigan University, written commun., 1987). The presence of Domasia restricts the reworked assemblage to Silurian in age. The terrestrial spores are dark yellow to black and have characteristics consistent with a Paleozoic age. Fossil wood was found in sample 14.

The sediment in the above samples was examined in detail to discover the source of these reworked acritarchs. The sand- and pebble-sized fractions containing the fossils are composed of lithified green shale chips, probably derived from the Silurian Clinton Formation. The Clinton Formation completely underlies the lake (Broughton et al., 1961), and so the presence of clastics on Shackelton Shoals derived from the Clinton Formation is not unexpected.

The presence of acritarchs in green shale chips highlights a speculation that the water level of the lake may have been lower in the past. On the highest part of Shackelton Shoals under 1 m of water at Buoy BB, the green shale is cobble size. The cores on Shackelton Shoals in 7 m of water at Buoy 123, 1.6 km to the west, contain green shale chips. In addition, all the shale cobbles at Buoy BB have iron-rich weathering rinds which indicate a period of subaerial erosion. The presence of the cobbles at 1-m water depth and the tiny shale chips at 7-m water depth may indicate that the lake water level was lowered by 7 m at some time in the past. Chips could have formed if the now deeper part of the shoals was once in the swash zone. Although these data are not useful in dating such an event, the lowering of the water level may have been caused by the cutting through of the New York Barge Canal in 1916 (Mills and Gannon, 1983). Today, the lowering of water level is a normal occurrence in Oneida Lake. With dams at both ends, the water level is dropped about a meter every winter to protect shoreline property from ice damage (Mills et al., 1978).

The diatom populations in the lake and in the core sediments provide additional microfossil information (Table 3). In the lake, 20 genera of benthic and planktonic diatoms have been identified (Greeson, 1972), although none were found in the summer plankton tows. In the cores, 12 genera were identified. The diatom population of the sediment traps was dominated by Fragilaria; however Fragilaria was never observed in the cores. In core SP-1, Stephanodiscus/Cyclotella were dominant. Fragilaria in Oneida Lake probably undergo selective dissolution in the pore water (see Rose, this volume); in Fayetteville Green Lake, Fragilaria are subject to breakage into small fragments rather than to dissolution (S.D. Ludlam, University of Massachusetts, written commun., 1987). No evidence for the silt-sized diatoms exists within the underlying clay nor in the cores from Buoy 123.

Siliceous chrysophyte cysts and the remains of other algae were examined in the cores (Table 3). Few cysts were noted, although they may be abundant (D.P. Adam, USGS, oral commun., 1987). To observe cysts in the size range of 2 to 5 um, the clay fraction needs to be decanted numerous times to concentrate such small microfossils (Mahood and Adam, 1979).

The study of the HCl and HF acid-insoluble organic remains, or kerogen, revealed the possible presence of other hiatuses in the cores. Between samples 16 and 15 in core 123-1, transparent pollen grains change color from light brown to pale yellow, indicating a potential hiatus. In core SP-1, the color change is more gradational. The color changes

Table 3. Planktonic algae in cores.

Core Number	SP-1												123-2	123-1							
Sample Number	1	2	3	4	5	6	7	8	9	10	11	12	13	14	15	16	17	18	19	20	21
Sample Depth (cm)	0-2	2-4	4-6	10-12	14-16	18-20	22-24	26-28	30-32	34-36	36-38	38-40	4.5-5	2-4	4-6	6-8	10-12	14-16	18-20	22-26	26-28
Blue-greens																					
Aphanizomenon	-	-	+	-	-	-	-	-	-	-	-	-	-	-	-	-	-	-	-	-	-
Microcystis	+	+	+	-	-	-	-	-	-	-	-	-	-	-	-	-	-	-	-	-	-
Greens																					
Botryococcus?	-	-	-	-	-	-	-	-	-	-	-	-	+	-	-	-	-	-	-	-	-
Pediastrum	R	C	C	+	-	-	-	-	-	-	-	-	-	+	-	-	-	-	-	-	-
Pediastrum-like	+	-	-	-	-	-	-	-	-	-	-	-	-	-	-	-	-	-	-	-	-
Staurastrum	-	+	+	-	-	-	-	-	-	-	-	-	-	-	-	-	-	-	-	-	-
Green-1	+	+	+	+	-	-	-	-	-	-	+	-	-	+	-	-	-	-	-	-	-
Diatoms																					
Achnanthes	-	R	-	-	-	-	-	-	-	-	-	-	-	-	-	-	-	-	-	-	-
Attheya	-	R	-	-	-	-	-	-	-	-	-	-	-	-	-	-	-	-	-	-	-
Cymbella	R	R	R	-	-	-	-	-	-	-	-	-	-	-	-	-	-	-	-	-	-
Cymatopleura	-	R	-	-	-	-	-	-	-	-	-	-	-	-	-	-	-	-	-	-	-
Gomphoneis	R	R	-	-	-	-	-	-	-	-	-	-	-	-	-	-	-	-	-	-	-
Gyrosigma	R	C	R	-	-	-	-	-	-	-	-	-	-	-	-	-	-	-	-	-	-
Melosira	R	-	R	-	-	-	-	-	-	-	-	-	-	-	-	-	-	-	-	-	-
Navicula-like	R	R	R	-	-	-	-	-	-	-	-	-	-	-	-	-	-	-	-	-	-
Pinnularia	R	-	-	R	-	-	-	-	-	-	-	-	-	-	-	-	-	-	-	-	-
Stephanodiscus/ Cyclotella	A	A	A	A	C	C	R	R	R	R	-	-	-	-	-	-	-	-	-	-	-
Surirella?	R	R	R	R	-	-	-	-	-	-	-	-	-	-	-	-	-	-	-	-	-
Tabellaria	R	-	-	-	-	-	-	-	-	-	-	-	-	-	-	-	-	-	-	-	-
Chrysophytes	-	-	-	-	-	-	+	-	-	-	-	-	-	-	-	-	-	-	-	-	-
Dinoflagellates																					
Baculate-1	-	-	+	-	+	+	-	-	-	-	-	-	-	+	-	-	-	-	-	-	-
Spinate-1	-	-	+	-	+	-	+	-	-	-	-	-	-	-	-	-	-	-	-	-	-
"baggy" cysts	-	-	+	-	-	-	-	-	-	-	-	-	-	-	-	-	-	-	-	-	-
unknown	+	+	-	-	-	-	+	-	+	-	-	-	-	-	-	-	-	-	-	-	-
Unidentified clear round cysts	A	+	-	+	+	+	+	-	+	-	-	-	-	+	+	-	-	-	-	-	-
thick-walled Tasmanites-like	+	-	+	-	+	+	-	-	+	-	-	-	-	+	-	-	-	-	-	-	-
Diporate-1	+	+	+	-	+	-	+	-	-	-	-	-	-	-	-	-	-	-	-	-	-
Colonial-1	-	+	+	+	+	+	-	+	+	+	-	-	-	-	-	-	-	-	-	-	-
Green-Brown Bicells	-	-	-	-	-	-	-	-	-	-	-	-	-	-	-	+	-	-	-	-	-
Reworked Paleozoic spinate acritarchs	-	-	-	-	-	-	-	-	-	-	-	-	+	+	+	-	-	-	-	-	-

Abbreviations: A=abundant, C=common, R=rare, +=present, -=absent

were unexpected because this type of darkening of organic tissues is normally a function of higher temperatures with depth of burial and relative increase in carbon content with the loss of other components such as oxygen and nitrogen (Staplin, 1977). Although cyanobacteria such as Gleotrichia, Anabaena, Microcystis and Lyngbya were in bloom in the lake when this research was conducted, their remains were not obvious in the cores. Instead, most of the tissues were amorphous. The ball-shaped amorphous remains easily could have been degraded Gleotrichia.

A study of the different size fractions of kerogen reveals that silt is not present in the clay layers (Table 4). The clay unit therefore is not useful for observing changes in abundance of silt-sized pollen and spores, algae and invertebrates. Cores that penetrate below the clay layer may be more useful for interpreting past changes in the watershed and in water chemistry.

Many of the remains of organisms fall within the silt size range and their presence is useful to identify changes in chemistry of bottom waters (Table 5). Iron-coated filaments of a Sphaerotilus-type iron-oxidizing bacteria are abundant in certain intervals of core 123-1. Iron bacteria are usually common in oxygenated water which directly overlies anoxic water carrying ferrous iron. Iron bacteria may have been present at such interfaces when bottom anoxia was more widespread. The presence of laminations in the clay lends further support for more widespread anoxia; the benthic fauna that typically destroy laminations would have been excluded from such a lake bottom.

Fish scales (Table 5) collect on the coarsest sieve and are useful in identifying changes in fish populations. The present fish population bears little resemblance to the native population reported by settlers (Mills et al., 1978). Atlantic salmon was important as a commercial fish until the middle 1800's. The increase in logging and farming practices damaged the salmon's spawning streams and led to their decline. Ciscoes (whitefish) and American eels then became important. American eel declined throughout the latter part of the 1800's and early 1900's due to the development of the New York Barge Cannal. By the 1920's, walleye, northern pike, and pickerel had become the dominant species. The draining of wetlands for agricultural purposes brought about the decline of northern pike and pickerel. Since the 1940's, walleye and yellow perch have become important. The cores chosen for study did not provide any information on such changes in the fish populations. Only one scale was found in the cores. The scale may be that of a white perch and is darker in color than those from present day fish. Scales were more abundant in cores from the Buoy 127 subbasin which were not part of this study.

The presence of invertebrate remains (Table 5) is more useful for identifying changes in the populations of other animals. Nematodes first occur in sample 5 of core SP-1. Daphnia ephippia were found throughout core SP-1 but none were present in core 123-1. Resting eggs, rather than live young, are produced during periods of stress which may result from a number of circumstances. Such circumstances include overpopulation of Daphnia and subsequent accumulation of excretory products, a decrease in available food, a drop in water temperature to 14-17°, or the changing of light intensities (Pennak, 1978). Ephippia can withstand drying and freezing and may even remain viable after passing through the gut of a fish. Live young are produced when conditions are favorable, such as the summer of 1987. The rare ephippia in the plankton tows had one or two spines; the ones in the cores lacked spines. The fossil ephippia may be conspecific with the modern ones, and breakage may account for the loss of spines.

Table 4. Analysis of kerogen in acid-treated sediment from cores.

	Color of Pinus or Abies	Types of Amorphous Organic Tissues		Types of Structured Organic Tissues						Clay-Sized Organic Fraction		Volume of Acid-Insoluble Residue (ml)		
		"algal" balls	fecal pellets	p&s	algal	reworked older	char	plant tissues: cuticle	plant tissues: wood cells	amorphous fluff	broken larger tissues	<25um	25-125um	% organic tissues
Core SP-1														
1	trans. pale yw	++	++	++	++	-	-	+	+	+	+	0.8	3	99
2	do	++	++	++	++	-	+	+	+	+	+	0.6	2.2	99
3	do	++	++	++	++	-	+	+	+	+	+	1	5	99
4	do	++	++	++	+	-	+	+	+	+	+	2.2	5	99
5	trans. pale yw with bn tint	++	++	++	++	-	+	+	+	++	+	3.7	5.2	99
6	do	++	++	++	+	+	+	+	+	++	+	4.5	2.1	99
7	do	++	++	++	++	+	+	+	+	++	+	4	6	99
8	do	++	++	++	+	+	+	+	+	++	+	4	5	99
9	trans. lt bn	++	++	++	+	+	-	+	+	++	+	2.7	3.5	99
10	do	+	-	++	+	+	+	+	+	++	+	5.3	1.5	99
11	trans. lt yw bn	+	+	++	+	+	+	+	+	+	+	6.5	2.5	99
12	trans. lt bn	+	+	++	+	-	+	+	+	+	+	4.7	0.5	99
Core 123-2														
13	trans. lt bn	++	++	++	+	++	+	-	-	++	+	5	0.8	99
Core 123-1														
14	-	?	+	+	++	++	+	+	-	+	+	4.5	0.5	50
15	trans. lt yw	+	+	+	+	++	+	+	+	-	-	6	0.1	10
16	trans. lt bn	+	-	+	+	+	+	-	-	-	-	5	0.1	5
17	do	+	+	+	+	+	+	-	+	-	-	6.5	0.1	5
18	-	+	-	-	-	+	+	-	+	-	-	5.5	0.1	1
19	trans. lt bn	+	+	+	+	+	+	-	+	-	-	8	0.1	5
20	do	-	-	+	+	+	+	-	-	-	-	4.5	0.25	5
21	do	+	+	+	+	+	+	-	+	-	-	7	0.1	5

Explanation of symbols: ++=dominant, +=present, -=absent
Abbreviations: bn=brown, lt=light, p&s=pollen and spores, trans.=transparent, yw=yellow

Table 5. Other organisms in cores.

Core Number	SP-1												123-2	123-1							
Sample Number	1	2	3	4	5	6	7	8	9	10	11	12	13	14	15	16	17	18	19	20	21
Bacteria																					
Thioploca sheaths	+	+	+	+	+	+	+	+	+	+	+	+	+	-	-	-	-	-	-	-	?
Sulfate-reducers H2S	+	+	-	-	-	-	-	-	+	-	-	-	-	-	-	-	-	-	-	-	-
Fe-oxiding	-	-	-	-	-	-	-	-	-	-	-	-	-	-	-	-	+	+	-	+	+
Fungi																					
hyphae	+	+	+	+	+	+	-	+	+	+	+	+	+	-	+	-	-	-	+	+	-
spores	+	+	+	+	+	+	+	+	+	+	+	+	+	+	+	-	-	+	+	-	+
sclerotia	-	-	-	-	-	-	-	-	+	-	+	-	-	-	-	-	-	-	-	-	-
Invertebrates																					
testacate amoeba	+	-	-	-	+	-	-	-	-	-	-	-	-	-	-	-	-	-	-	-	-
living invertebrates	+	+	+	-	-	-	-	-	-	-	-	-	-	+	-	-	-	-	-	-	-
worms																					
Tubifex	+	-	-	-	-	-	-	-	-	-	-	-	-	-	-	-	-	-	-	-	-
T. tubes	+	-	-	-	-	-	-	?	-	-	-	-	+	-	-	-	-	-	+	-	-
nematodes	-	-	+	-	+	-	-	-	-	-	-	-	-	-	-	-	-	-	-	-	-
unidentified	-	+	+	+	-	+	+	+	+	-	+	+	+	-	+	-	-	-	+	-	-
insects																					
cuticle	-	-	-	-	-	-	-	-	-	-	-	+	+	-	-	-	-	-	-	-	-
legs	-	+	+	+	-	-	-	-	-	+	-	+	+	+	-	-	-	-	-	-	-
wing scales	+	-	-	-	-	-	-	-	-	-	-	-	-	-	-	-	-	-	-	-	-
microcrustaceans																					
exoskeletal parts	+	+	+	+	+	+	+	+	+	+	+	+	+	+	+	-	-	-	+	-	-
Daphnia ephippia	+	+	+	+	+	+	+	+	+	+	+	+	-	-	-	-	-	-	-	-	-
Daphnia abdominal claws	-	-	+	+	+	-	-	-	-	-	-	+	-	+	-	-	-	-	-	-	-
intact Daphnia	+	+	+	-	-	-	-	-	-	-	-	-	-	-	-	-	-	-	-	-	-
ostracodes	+	+	-	-	+	-	-	-	-	-	-	-	+	-	-	-	-	-	-	-	-
gastropods																					
shells	+	+	+	+	+	-	+	+	-	-	-	-	-	-	-	-	-	-	-	-	-
sponges																					
spicules	+	-	+	-	-	-	-	-	-	+	-	-	-	-	-	-	-	-	-	-	-
Vertebrates																					
fish																					
body parts	-	-	-	-	-	-	-	-	-	?	-	-	-	-	-	-	-	-	-	-	-
scales	-	-	-	-	-	-	-	-	-	-	-	-	-	-	-	-	-	-	+	-	-
birds																					
feather barbules	-	-	-	-	+	-	-	-	-	-	-	-	+	-	-	-	-	-	-	-	-

Explanation of symbols: +=present, -=absent, ?=questionable presence

Summary

All of these data suggest that Oneida Lake has had a varied history throughout the short period of time represented by the shallow cores. A compilation of the events that have stratigraphic importance in the cores is presented in Figure 2.

Possible hiatuses were noted in the cores. The difference in compaction between the clay and the overlying organic sediment suggests a hiatus. Another possible hiatus in the core from Buoy 123 is recorded by the color change of the pollen from brown in the basal samples to yellow in the overlying samples. The location of the core may be the reason for the upper hiatus; the presence of rocks, chips and Mn nodules and the absence of clay indicate that the shoal areas are swept clean by bottom currents. In retrospect, any core from Shackelton Shoals probably contains numerous stratigraphic breaks because of the currents.

A shift in climatic conditions following the Little Ice Age and European settlement may be the major events that affected sedimentation in the lake. The change in pollen abundance from fir and pine at the base to more herbaceous vegetation at the top suggests a change from cooler conditions to more equitable weather, but the evidence of European settlement and forest clearing cannot be separated in these data from the effects of climatic warming. Chips of Paleozoic rocks and weathered cobbles on the Shackelton Shoals ridge may indicate that the water level dropped far enough to expose these localities to subaerial erosion. The water-level drop may have resulted from the cutting through of the New York Barge Canal in 1916.

Chemical changes can be interpreted from changes in both the organic and inorganic components of the sediment. The transition from the lower mineral-rich gray clay to the upper organic-rich brown silt was accompanied by a change in lake chemistry. The clay, especially in cores from Buoy 123, is highly calcareous and nonfossiliferous, whereas the silt is calcareous only in layers having calcareous microfossils. Diatoms are absent in the gray clay and present in the brown silt. Amorphous organic tissues are in the shape of balls that could be the remains of cyanobacteria such as Gloeotrichia or perhaps a green algae such as Sphaerocystis that has been reported in the lake by Greeson (1972). All of these data combine to suggest that the brown silt may mark the onset of eutrophic conditions in Oneida Lake. A change in dominance of the inflowing rivers may have added nutrients that enhanced eutrophication.

The timing of these events is poorly constrained. More detailed radiometric dating could aid in placing accurate dates on the events outlined in Figure 2 and in supporting some of these preliminary interpretations. Biostratigraphic work in deeper cores undoubtedly would add other useful information on the history of sedimentation in Oneida Lake.

References

Anderson, T.W. and C.F.M. Lewis (1985) Postglacial water-level history of the Lake Ontario basin. In: Quaternary Evolution of the Great Lakes, P.F. Karrow and P.E. Calkin (Eds.) Geol. Assoc. Canada Spec. Paper 30, pp.230-53.

Broughton, J.G., D.W. Fisher, Y.W. Isachsen and L.V. Rickard (1961) Geologic map of New York State. New York State Geological Survey, Albany N.Y.

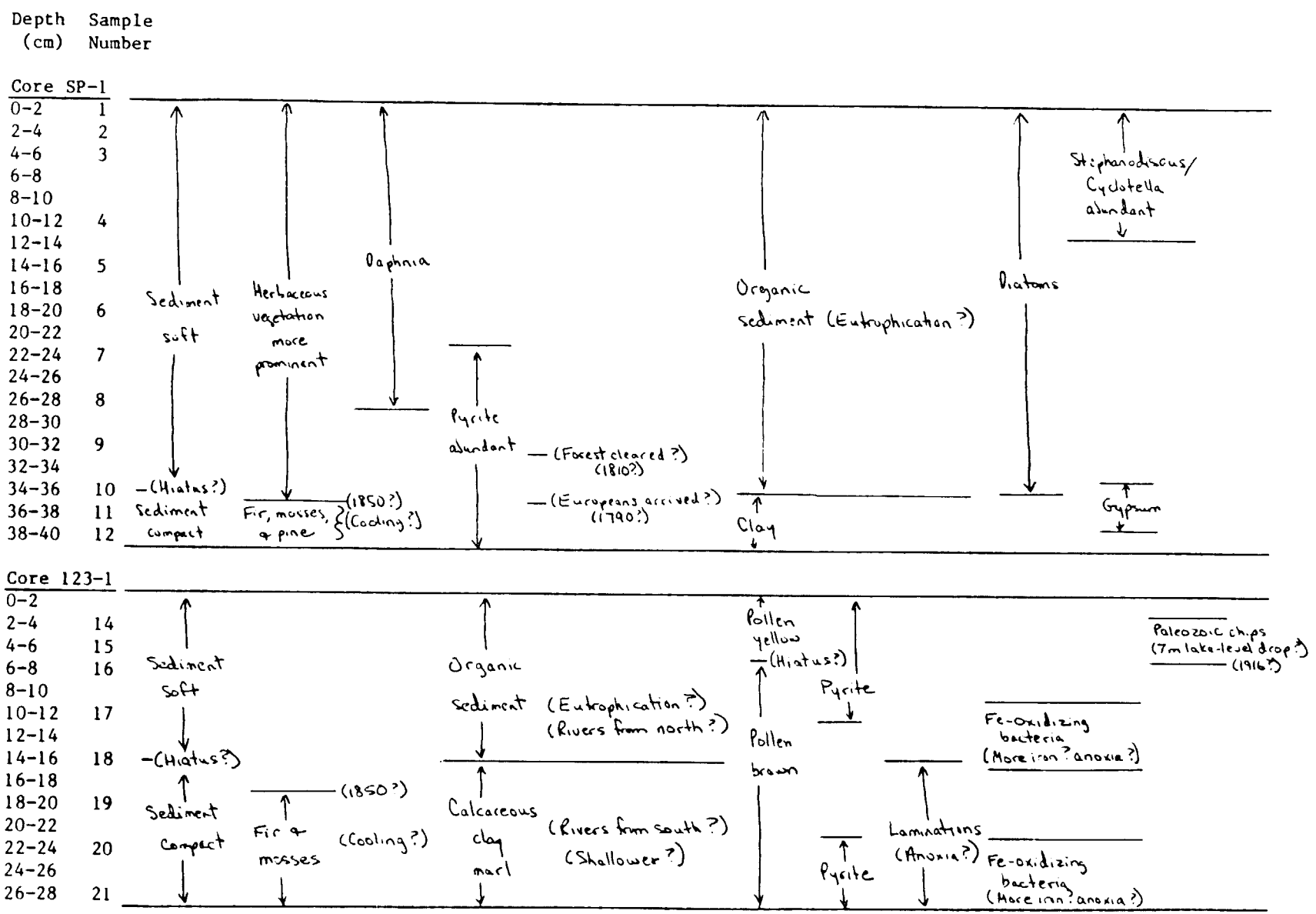

Figure 2. Compilation of possible events in Holocene history of Oneida Lake.

Busson, G., S.D. Ludlam and D. Noel (1972) L'importance des Diatomees dans les depots actuels varves (alternance de couches annuelles) de Green Lake (pres Fayetteville N.Y.) modele de sedimentation confinee. C.R. Acad. Sci. Paris 274:3044-3047.

Davis, M.B. (1983) Holocene vegetation history of the Eastern United States. In: Late-Quaternary Environments of the United States, H.E. Wright Jr. (Ed.) Univ. Minnesota Press, Vol. 2, pp.166-181.

Davis, M.B., L.B. Brubaker and T. Webb (1974) Calibration of absolute pollen influx. In: Quaternary Plant Ecology, H.J.G. Birke and R.G. West (Eds.) Wiley, New York, pp.9-27.

Dean, W.E. and J.R. Eggleston (1984) Freshwater oncolites created by industrial pollution, Onondaga Lake, New York. Sedimentary Geology 40:217-232.

Dean, W.E. and S.K. Ghosh (1978) Factors contributing to the formation of ferromanganese nodules in Oneida Lake, New York. U.S. Geological Survey Jour. Research 6:231-240.

Greeson, P.E. (1972) Limnology of Oneida Lake with emphasis on factors contributing to algal blooms. U.S. Geological Survey Open-file Report 72-139, 255 p.

King, J.E., J.A. Lineback, and D.L. Gross (1976) Palynology and sedimentology of Holocene deposits in southern Lake Michigan. Illinois State Geol. Survey Circ. 496, 24 p.

Ludlam, S.D. (1967) Sedimentation in Cayuga Lake, New York. Limnology and Oceanography 12:618-632.

Ludlam, S.D. (1981) Sedimentation rates in Fayetteville Green Lake, New York, U.S.A. Sedimentology 28:85-96.

Mahood, A.D. and D.P. Adam (1979) Techniques used for the cleaning, concentration and observation of chrysomonad cysts from sediments. U.S. Geological Survey Open-file Report 79-1431, 5 p.

Mills, E.L., J.L. Forney, M.D. Clady and W.R. Schaffner (1978) Oneida Lake. In: Lakes of New York State, Vol. 2, J.A. Bloomfield (Ed.) Academic Press, New York, pp.367-451.

Mills, E.L. and J. Gannon (1983) Oneida Lake profile. Oneida Lake Association, Syracuse, New York, 11 p.

O'Rourke, M.K. (1976) An absolute pollen chronology of Seneca Lake, New York. M.S. thesis, University of Arizona, Tucson, Arizona, 76 p.

Pennak, R.W. (1978) Fresh-water Invertebrates of the United States. Wiley, New York, 803 p.

Staplin. F.L. (1977) Interpretation of thermal history from color of particulate organic matter. Palynology 1:9-18.

Eleanora Robbins
Dave Bolgrien
Kevin Mandernack

"Possible Subsurface Discharge of Mn-rich Ground Water into Oneida Lake, N.Y."

Introduction

Many lakes receive nutrients by ground water seepage or spring discharge at depth. McBride and Pfannkuch (1975) showed that rather than being sealed systems, lakes can be part of the regional ground water flow; the greatest rates of seepage were measured at the lake's edge where ground water was found to seep into their test lake. Recent work on subsurface spring discharge into lakes had been performed by Winter (1984, 1986).

The relationship between Oneida Lake and its sources of ground water has not been studied. Instead, surface water input was the subject of a detailed study by Greeson (1972). In the subsurface, the direction of regional ground water flow probably is westward towards Lake Ontario (Kantrowitz, 1970). However, ground water seepage into Oneida Lake may depend upon local water-bearing units, but their presence has not been established.

The Mn content of both ground and surface water entering Oneida Lake could be anomalously high because the lake is wholly within the outcrop belt of the east-west-

Table 1. Chemical data for the Clinton aquifer. (Retrieved from WATSTORE by Paul Grim, USGS; nd, not determined)

	Station	
	308-536-1	308-536-2
Lat/Long	430807 / 0753658	430840 / 0753646
Date	11/04/64	01/16/52
Well depth (ft)	88	72
pH (lab)	7.6	7.3
alkalinity	187	119
bicarbonate	230	150
hardness	96	2,700
conductance	398	24,300
TDS (mg/L)	219	16,199
Ca (mg/L)	22	680
Mg (mg/L)	9.9	250
Na (mg/L)	50	5,300
K (mg/L)	4.7	
Cl (mg/L)	18	10,000
SO_4 (mg/L)	0.2	0.9
F (mg/L)	0.4	0.7
SiO_2 (mg/L)	9.5	9.2
Fe (mg/L)	430	30
Mn (mg/L)	20	nd
NO_3-N (mg/L)	1.3	79

striking Clinton Group (Broughton et al., 1961). The Mn content of the Clinton iron ore both in New York and elsewhere is anomalously high (Alling, 1947; Miller, 1947), although Mn has not been mined in New York (Guild, 1981). The one measurement available for the Clinton aquifer in upstate New York shows that the Mn content was within the potable limit of 0.05 mg/L (Hem, 1985) on the day of measurement (Table 1).

The temperature of ground water that feeds into Oneida Lake has not been measured. Ground water temperatures, particularly those from shallow flow systems, generally reflect mean annual air temperatures (Birman, 1969). Mean annual air temperature in the Syracuse area is 8.7°C (U.S. Department of Commerce, 1983). Ground water temperatures from deeper flow systems generally are warmer than mean annual air temperature (Birman, 1969), so temperatures of ground water in lakes should reflect such diverse sources.

If ground water discharges into Oneida Lake, it has numerous paths by which it can disperse. Water in Oneida Lake presently flows westward into the Oneida River, and ultimately, into Lake Ontario. During the Pleistocene, Oneida was part of the larger Lake Iroquois that had an outlet to the east down the Mohawk-Hudson drainage (Mills et al., 1978). Surface currents generally are driven eastward by the prevailing wind (Houde and Forney, 1970); a counter-current therefore is produced that drives deep bottom water westward. The submerged glacial ridges, Dakin, Grassy, Messanger, Pancake and Shackelton Shoals, are generally bathed by the eastward-moving surface current (J.L. Forney, Cornell Univ. Biological Field Station, pers. commun., 1987). There are major accumulations of Mn nodules on many of the ridges, and their presence may be related to the oxygenation of such high points in the lake, although other factors probably enter in as well to explain the localization of nodules (Dean and Ghosh, 1978).

The purpose of this research was to determine if ground water discharges Mn into the bottom of Oneida Lake, and in particular, to discover if any underwater springs feed Mn into Oneida Lake.

Methods

The primary method used to test for the presence of underwater springs was to query researchers on Oneida Lake about the presence of open water in the ice during the winter and about artesian flow into wells near the lake. Open water holes in the ice would be likely where 8.7°C ground water fed into a temperate-region lake that was equilibrated at 4°C during the winter (J.L. Haas, Jr., USGS, oral commun., 1987). The presence of artesian pressures in water wells would be caused by an upward pressure gradient into Oneida Lake at seepage localities and springs.

A piezometer, an instrument used on land to measure the height of the potentiometric surface, was constructed and deployed in the lake near Buoy 127 to test for the presence of underwater springs. When pressures are artesian, the potentiometric surface is above the height of the aquifer. The piezometer used consisted of a 2-ft-long PVC water pipe with an outside diameter of 3/4 in. The pipe was attached with epoxy onto a 1-ft-long PVC piezometer section with a pointed end and 15 basal slots.

Underwater piezometer arrays are generally sophisticated instruments monitored by manometers and encased in 50-gallon drums (T. Winter, USGS, oral commun., 1987). A simple balloon-type system was recommended for our studies. The water-collecting device used was an unlubricated condom (hereafter referred to as the balloon); this was used rather than a toy balloon because the diameter of a condom is wider than that of available

balloons. The device was affixed to the piezometer tube with rubber bands. A positive pressure response should be the filling and expansion of the balloon.

Scuba observations showed that the lake bottom at Buoy 127 was so unconsolidated that mud would clog the slots of the piezometer. In the spirit of the design, a pair of nylon stockings was sacrificed; the nylon netting was taped over the slots. The scuba divers noted during the initial dive of June 24 that the bottom could be characterized as having black unconsolidated sediments interspersed with lighter colored depressions. The piezometer was placed into the center of one of these depressions to the southeast of Buoy 127.

A nylon line marked off in 5-meter intervals was deployed from the bottom anchor of Buoy 127. The piezometer was tied off from the line at 44 m. It was deployed on July 13 into a 25-cm-wide depression. The flaccidness of the balloon was noted at each dive during the summer of 1987 whenever visibility on the bottom allowed observation. Temperature of the bottom was monitored by several methods. The scuba divers measured the water temperature of the lake bottom around Buoy 127 with two thermometers to determine if there were temperature differences in the vicinity of the depressions. At various times during the summer, a Hydrolab (DCP compatible Handor Data Sonde II produced by Hydrolab Environmental Systems) was deployed on the bottom at Buoys 123, 125, 127 and 129 to see if any temperature differences could be measured at random locations.

When the experiment was concluded, the balloon was tied off at the bottom. One ml of sample water was filtered on a 0.2-uM filter and the supernatant was acidified in 15 ml of ultrapure concentrated HNO_3. The sample was analyzed for Mn(II) in a Perkin-Elmer Model 503 flame atomic absorption (FAA) unit.

Results and Discussion

Holes called "gas holes" by local residents occur in the ice around Buoy 127 (E.L. Mills, Cornell Univ., oral commun., 1987). People also have referred to "gas holes" near the north shore in the proximity of Cleveland (P.E. Greeson, USGS, written commun., 1987). Bottom temperatures of the lake hover around 4°C in the winter (Mills et al., 1978).

The four wells at Shackelton Point flow in the spring (April and May) and sometimes in the fall (September, October and November); iron can be abundant and at levels high enough to be a nuisance at these times of artesian flow (E.L. Mills, oral commun., 1987). The wells were capped between 1930 and 1940, the deepest being about 50 ft (J.L. Forney, oral commun., 1987).

The bottom sediments at Buoy 127 are generally unconsolidated black mud that is easily disturbed. Interspersed with the mud are irregular depressions from 0.8 to 3 ft wide and 3 to 8 in long. The sediment within the depressions is lighter colored; tan, white and yellow were noted. It also appeared to be "quivering."

The balloon was flaccid through all observations; it was tied off on August 3 to preserve the collected water, and the experiment was concluded. The parts of the piezometer that were in the water, the balloon, PVC tubing, and orange flagging had a thin coating of brown Mn oxides; the coats tested the blue positive response with the addition of Leucoberbelin blue (LBB), a redox dye that turns blue in the presence of oxidized species of Mn. The parts of the piezometer that were in the deoxygenated bottom sediment, the

basal section of the PVC tubing and the nylon mesh, were LBB negative, as would be expected in anoxic sediment.

The fish distribution in Oneida Lake easily could support the idea of a thermal anomaly at Buoy 127. Ciscoes (whitefish), which are generally cold water fish, are abundant at that location, as are their lamprey predators (J.L. Forney, pers. commun., 1987). However, no temperature anomalies around 8.7°C were measured at Buoy 127 (Table 2). Instead, the hand-held thermometers that were placed in the depressions measured water temperatures of 17-18°C.

Table 2. Temperature data for selected locations on the bottom of Oneida Lake.

Location	Date	Depth	T(°C)
B-123	6/30/87	7.4	21.50
halfway between B-125 and B-127	"	7.98	21.53
north side of B-127	"	11.4	18.72
north side of B-128	"	7.6	21.3
north side of B-129	"	9.2	18.81
light colored depressions at B-127	7/01/87	11.1	17-18
B-127	7/08/87	11.4	22.05
0.1 mi SE of B-127	"	9.1	21.99
0.25 mi SE of B-127	"	8.2	21.99
B-127	8/01/87	10.4	23.63

The Mn(II) content of the water in the balloon was below the level of detection (0.1 ug/L) by FAA; the pH was 7.65. In contrast, the Mn(II) content at the water/sediment interface in Oneida Lake varied from less than limit of detection to 60 uM (3.3 mg/L) during the summer of 1987; pH values ranged between 7.7 and 8.2 (Mandernack et al., this volume). The highest Mn concentration in Oneida Lake pore water was 14 mg/L (see Mandernack et al., this volume); average values are around 0.15 mg/L (Dean and Ghosh, 1978).

Although the piezometer and temperature results were negative, the other data cited above suggest that winter, early spring, and fall may be the times of maximum spring discharge into the lake. Further work should include the deployment of a piezometer during these times to discover if underwater spring discharge of Mn takes place in Oneida Lake.

If there is spring discharge into Oneida Lake, then ground water could be a source of Mn. Ground water that issues from springs or wells is generally anoxic and Mn, when present, is in the reduced form (Hem, 1965). The Mn would be transferred away from the points of discharge, however, because pore water under Mn nodules is depleted of Mn in comparison to pore water in areas where Mn nodules are not present (Dean and Ghosh, 1978). The area with depressions around Buoy 127 had no nodules and was in a deep subbasin. Nodules are abundant and large on the Shackelton Shoals basement high, which is 100 m east of the subbasin. It is interesting to speculate that surface and subsurface circulation patterns of lake water currents and their eddy flows around the experiments might transport Mn from underwater springs to Shackelton Shoals. Some experiments that would test this idea would be: 1) to deploy a piezometer in the fall, winter or early spring; 2) to collect the water in the piezometer balloon and analyze for anomalous concentration of

Mn; 3) to deploy velocity meters between Buoy 127 and Shackelton Shoals to show upward and eastward movement of bottom water at the time of discharge; and 4) to use a conservative trace to estimate residence time in the lake. Deviations in residence time from the most simple model that includes river inflow into the lake, followed by internal mixing, and the flushing through the outlet to a more complex model might help to estimate whether groundwater input is an important component of the system.

References

Alling, H.L. (1947) Diagenesis of the Clinton hematite ores of New York. Geol. Soc. Amer. Bull. 58:991-1018.

Birman, J.H. (1969) Geothermal exploration for ground water. Geol. Soc. Amer. Bull. 80:617-630.

Broughton, J.G., D.W. Fisher, Y.W. Isachsen and L.V. Rickard (1961) Geologic map of New York State. New York State Geological Survey, Albany, New York.

Dean, W.E., and S.K. Ghosh (1978) Factors contributing to the formation of ferromanganese nodules in Oneida Lake, New York. U.S. Geological Survey J. Res. 6:231-240.

Greeson, P.E. (1972) Limnology of Oneida Lake with emphasis on factors contributing to algal blooms. U.S. Geological Survey, Open-file Report 72-139.

Guild, P.W. (1981) Preliminary metallogenic map of North America: a numerical listing of deposits. U.S. Geological Survey Circular 858-A.

Hem, J.D. (1985) Study and interpretation of the chemical characteristics of natural water. U.S. Geological Survey Water-Supply Paper 2245:84-89.

Houde, E.D. and J.L. Forney (1970) Effects of watercurrents on distribution of walleye larvae in Oneida Lake, New York. J. Fisheries Res. Board of Canada 27:445-456.

Kantrowitz, I.H. (1970) Ground-water resources in Eastern Oswego River basin, N.Y. New York Conservation Department Basin Planning Rept. ORB-2.

McBride, M.S. and H.O. Pfannkuch (1975) The distribution of seepage within lakebeds. U.S. Geological Survey J. Res. 3:505-512.

Miller, R.L. (1947) Manganese deposits of Aroostook County, Maine. Maine Geol. Survey Bull. 4.

Mills, E.L., J.L. Forney, M.D. Clady and W.R. Schaffner (1978) Oneida Lake. In: Lakes of New York State, Vol. 2, J.A. Bloomfield (Ed.) Academic Press, New York, pp.367-451.

U.S. Department of Commerce (1983) Annual summary for climatic data, Syracuse area. U.S. Department of Commerce.

Winter, T.C. (1984) Geologic setting of Mirror Lake, West Thornton, New Hampshire. U.S. Geol. Survey Water Resources Investigations 84-4266.

Winter, T.C. (1986) Effect of ground water recharge on configuration of the water table beneath sand dunes and on seepage in lakes in the Sandhills of Nebraska, U.S.A. J. Hydrol. 86:221-237.

Eleanora Robbins

"Manganese Cycling Through Fecal Pellets From Oneida Lake, New York"

Introduction

Fecal pellets may play an important role in the Mn cycle of Oneida Lake. Oneida Lake, which is a highly eutrophic lake in Upstate New York, is the site of deposition of Mn nodules in the more oxygenated parts of the lake (Dean and Ghosh, 1978). Bacteria and phytoplankton in the lake appear to be concentrating Mn (Dean and Greeson, 1979; Richardson et al., in press; Tebo, 1983). Animals that graze on Mn-rich organisms may further concentrate Mn in their fecal pellets, a process much like that suggested for the concentration of other elements, including Al, Ba, Ca, Cu, Mg, P, Si, Ti, and V (Honjo, 1976, 1978; Turner, 1977; Porter and Robbins, 1981).

The concentration process can even reach economic proportions. Porter and Robbins (1981) observed zooplankton-size fecal pellets in phosphorites and proposed a complex depositional cycle in which crustacean zooplankton processed such phosphate-rich compounds as algae, packaged phosphate into pellets protected by peritrophic membranes, and deposited numerous pellets in anoxic bottom water where they were protected from predation. High rates of production and reduced predation could result, therefore, in an economic phosphate deposit. Pellets from living animals, sediment traps, cores and a Mn nodule therefore were studied to learn about the possible role of fecal pellets in the Mn cycle of Oneida Lake. Invertebrates that have the shape of fecal pellets were included in the study because they could be mistaken for fecal pellets in the fossil record (Robbins et al., 1985).

Methods

From June to August 1987, a variety of organisms were assayed for the presence of oxidized species of Mn in their fecal pellets or coated on their tissues. Living microcrustaceans (ostracodes, copepods, cladocerans), worms and worm allies (Nais, Tubifex, planarian, Glossiphonia), and fish (yellow and white perch, gizzard shad, catfish, and sucker) were tested. Simple observations that have applicability to the fossil record form the body of this report. The presence of Mn(III) or Mn(IV) was noted with the application of a drop of Leucoberbelin blue (LBB), which is an acidic redox dye that turns blue in the presence of oxidized Mn.

Ostracodes

Methods Ostracodes were collected from the littoral area of Shackelton Point to compare their fecal pellets with those of Triassic age from North Carolina (Gore, 1986). The Oneida Lake ostracodes were collected from shallow water with a plankton tow net, and from degrading strands of the submerged aquatic plant, Myriophyllum. The genus of the ostracodes was not determined but the valves have distinct brown markings on top and along the sides. The ostracodes were separated from other plankton by using a medicine dropper and by viewing with a binocular microscope. Seven were placed in lake water filtered through a 0.2-um millipore filter in a petri dish with several strands of washed Myriophyllum for food. The largest ones appeared to have a coating of oxidized Mn. Within 10 h, numerous dark-brown fecal pellets were produced. Pellets and ostracodes

were picked up by using a medicine dropper and placed on another petri dish. Excess water was siphoned off with a kim-wipe wick. LBB was applied to 5 pellets and 2 ostracodes.

Results This unknown species of ostracode produces fecal pellets that are elongate and doubly terminated. The pellets have thick and distinct peritrophic membranes. All pellets tested positive for oxidized Mn after they were poked with a needle to get the LBB through the peritrophic membrane. Slides of pellets mounted in glycerin jelly were examined by P.J.W. Gore (Emory University), who measured a total of 27 pellets. Widths ranged between 90(110)180 um and lengths ranged between 140(220)330 um. (The number in parenthesis is the median value). Length to width values ranged between 1.3(1.9)3 um. The brown stains on the largest ostracodes also tested positive for oxidized Mn; the largest ostracodes probably were the oldest. The acid of the LBB solution caused the $CaCO_3$ of their valves to dissolve, as did an application of 10 percent HCl.

Copepods

Methods Copepods were collected from the littoral area of Shackelton Point bay. The experiment was run 4 times; in one experiment, approximately 10 Cyclops bicuspidatus and Diaptomus minutus were placed in a petri dish in filtered lake water (0.45-um millipore filter) along with washed Myriophyllum for food; in another fresh-capture experiment, 20 individuals were placed with washed Cladophora, Myriophyllum and sedge culms; the last two runs were done with no additional organic matter. Several of the copepods were preserved in glycerin jelly mounts.

Results Only amorphous disassociated globlike brown accumulations were observed in the 4 experiments. No discrete pellets were observed in the petri dishes or within the bodies of the copepods. Perhaps these genera do not make discrete pellets, the pellets are too small to study by using the methods tried, or the copepods were damaged by the eye dropper in transfer and did not behave normally.

Cladocerans

Methods The Cornell University Biological Field Station researchers make regular collections of organisms that are important in the fish food chain in Oneida Lake. The contents of a plankton tow from the middle of the lake had been separated into aquaria, and Daphnia pulex monocultures that had been fed their natural food over the course of a week were available for study. Numerous D. pulex were scooped into a 750-mL separatory funnel. Within 15 minutes, a layer of light-brown sedimented pellets were available for study and were withdrawn by opening the stopcock. The pellet layer was emptied into a petri dish and was examined for sample purity by using a binocular microscope.

Results D. pulex in Oneida Lake range in size from approximately 1 to 4 mm. Rather than producing fecal pellets, they make fecal masses. The masses are loose aggregates that appear to be held together by a mucoid substance rather than by a peritrophic membrane. This type of fecal mass is more sheetlike than discrete and would not be recognized in the fossil record as a pellet. Five individual fecal masses and two trapped Daphnia were separated and dried. Four of the five masses tested positive for oxidized Mn. The blue color of LBB slowly diffused from the masses and disappeared into the remaining solution. Daphnia surfaces did not respond to LBB; however, when the Daphnia were probed with a needle, the LBB diffused into the guts, and the guts and the embedded fecal material turned blue.

Nais

Methods A worm, tentatively identified as the oligochaete Nais, was inadvertently present in one of the copepod experiments. When the experiment was observed after 4 days, distinct pellets and a living Nais were present.

Results Numerous squared-off dark-brown pellets that looked like the pellets within the transparent Nais were dispersed in discrete paths along the bottoms of the petri dishes. The pellets held their shape, which suggests a peritrophic membrane was present. The pellets were not tested with LBB. However, similar squared-off pellets in the sediment trap experiment tested positive for oxidized Mn.

Tubifex

Methods As cores were being processed for other experiments, the presence of Tubifex, an oligochete, was noted because it is so distinctive. The top surfaces of cores from places where the bottom waters were suboxic had numerous Tubifex tubes. In the top of cores, Tubifex bodies were pale orange. Within the cores, the Tubifex are bright red from the presence of hemoglobin respiratory pigments (Pennak, 1978). Several experiments to collect fecal pellets were tried in petri dishes that were filled with some of their natural food, the sulfur-oxidizing bacteria, Thioploca (see Robbins and Schmidt, this volume).

Results In each experiment, the Tubifex worms died after a few hours and left no distinct pellets in the petri dishes. In retrospect, nitrogen should have been blown into the petri dishes to reduce the content of oxygen. Pellet aggregates, which were present within worm bodies, were not tested with LBB.

Because Tubifex is an important member of the infauna of Oneida Lake and because its pellets may be such an important silt-sized component of the sediment, several other observations that have applicability to the fossil record will be reported even though the role Tubifex plays in the Mn cycle of Oneida Lake is unknown. The pellets of Tubifex are produced at the sediment-water interface and within the sediment. The silt-sized fraction of the cores may be produced in situ by this worm. Two Tubifex specimens were measured from the lake and cores. The small bright-red one measured 1 by 11 mm, and the larger pale-orange one measured 2 by 20 mm. Tubifex was noted burrowing to a depth of 22 cm in core 129. It appears to have two feeding behaviors; the one used may depend on the oxygen content of the mud. At the sediment-water interface, Tubifex lives in tubes where its mouth is in the sediment and its tail is raised into the water column (Pennak, 1978). This behavior creates piles of fecal pellets surrounding the tubes at the sediment surface. Because Tubifex is present to a depth of 22 cm, it also may graze in the mud by moving through the organic tissues and excreting as it grazes. These activities serve to bioturbate the sediment, but only in a microscopic manner, eliminating the potential laminations in the mud, but not leaving macroscopic bioturbation as evidence of its former activities.

Planarians

Methods At the bottom of many Mn modules, the distinct black-stalked cocoons of planaria could be observed. Several were picked off a nodule from Buoy 123 and were placed in a petri dish that contained lake bottom water. The white planaria that hatched out

were elongate, much in the shape of fecal pellets. No attempt was made to identify the genus. LBB was applied to the dark-brown pigment spots on the ventral surface of the animal.

Results The general shape of the animal looks like an elongated fecal pellet, particularly when the animal is disturbed and becomes rigid. The end with the eyes is slightly more flattened than fecal pellets. The brown pigment spots did not test positive for Mn; instead, the acid of the solution caused the cells to lyse, although the brown-coated cells stayed intact.

Glossiphonia

Methods A very dark brown pellet-type particle was noted in the two-week-old contents of a sediment trap emplaced 1 m from the bottom at Buoy 127. It was tested with LBB.

Results The pellet-type particle was much darker in color than the fecal pellets in the sample. Although it looked like a fecal pellet, which is elongated and doubly terminated, one end seemed to bulge. A scan of several made it obvious that there was always a clear area like a bubble at the more bulging end, which served to identify the leech Glossiphonia. It tested positive for oxidized Mn.

Fish

Methods Fecal pellet pieces were squeezed or cut out by A.E. Creamer (Cornell Univ.) from fish that were trapped in gill nets. The pellets of predators (yellow and white perch), zooplankton eaters (gizzard shad), and detritus eaters (catfish, sucker) were dehydrated and then tested with LBB for oxidized Mn.

Results The pellets of gizzard shad, the planktovore, tested strongly positive. Those of the white sucker gave a very weak response to LBB. Pellets of the other fish gave negative responses.

Sediment Trap Data: Buoy 127

Methods A subsample of the contents of the sediment trap at Buoy 127 was tested with LBB. The sample was dispersed on a petri dish, particles were separated with a needle so that individual responses could be noted, and the particles were dried with a kim-wipe wick.

Results Table 1 shows the results of a test with LBB for oxidized species of Mn. Most of the tissues were amorphous, and, of the 14 types of particles examined, 7 were fecal pellets. Every fecal pellet in the sediment trap tested positive for Mn.

Table 1. Presence of oxidized Mn in a sediment trap from Buoy 127.

Type of Sediment Particle	Response to LBB[1]
Gleotrichia	-
amorphous algal ball	+
degraded algal ball	+
diatom	-
fecal ribbon	+
copepod-type pellet	+
copepod-type pellet	+
degraded copepod-type pellet	+
degraded squared-off pellet	+
degraded pellet	+
tiny pellet	+
squared-off pellet	+
Glossiphonia	+
zooplankton exoskeleton	-

[1] LBB - Leucoberbelin blue

Pellets in Cores: Core SP-4

Methods A 37-cm deep core was collected at the Shackelton Point Buoy; 1-cm slices were removed to a depth of 10 cm as the core was being extruded. The sediment was washed through 1.4-mm and 150-um screens. Fecal pellets were abundant in the +150-um to 1.4-mm fraction. The contents were tested with LBB.

Results Table 2 shows the results of testing the organic tissues in this fraction with LBB. Surprisingly, very few of the fecal pellets tested positive for Mn in the core sediment, including Tubifex-type pellets.

Table 2. LBB response of particles in the +150-um fraction from core SP-4.

Depth (cm)	Thioploca sheaths	Algal balls	Degraded Anabaena	Fecal pellets	Fecal ribbons	Black dots	Black mineral
0-1	some +	some +	-	-	-	o	+
1-2	o	some +	+	-	-	+	o
2-3	o	some +	+	-	-	+	+
3-4	o	some +	+	one +	+	+	o
4-5	o	some +	+	-	-	+	o
5-6	+	some +	o	-	o	+	+
6-7	+	some +	o	-	-	o	+
7-8	o	some +	o	one +	-	+	+
8-9	o	some +	+	-	-	+	o
9-10	o	some +	o	one +	-	+	o

Explanation of symbols: + = positive response, - = negative response, o = none present to test.

Pellets in Cores: Core SP-1

Methods A 38-cm deep core was collected at the same buoy as above; 2-cm slices were removed as the core was being extruded. Selected intervals were chosen for further study, and the sediment was sieved as above. Fecal pellets were the most abundant type of amorphous organic particles in the +150-um to 1.4-mm size sieve.

Results Table 3 shows that every sample in the core had fecal pellets. The core was composed of 3 cm of light-gray clay that was overlain by 33 cm of black silty clay. Above the black clay was 2 cm of brown silt. The top of the core had numerous Tubifex tubes, and the surface had a mat of Thioploca. Remains of invertebrates were found throughout the core. One particular type of fecal pellet with flattened termination dominated the amorphous organic matter. It has the appearance of being formed of small aggregates. The pellets may have either a weak peritrophic membrane or none because the pellet shapes varied but the size stayed uniform. A total of 10 pellets were measured. Widths ranged between 44(67)94 um and lengths ranged between 79(110)119 um. Length to width ratios varied between 1.3(1.8)1.9. This one distinct type of pellet may be that of Tubifex. Because of the important role of Tubifex in this lake, pellets need to be collected to compare with these data.

Table 3. Presence of organic tissues in the 150-um fraction from core SP-1.

Depth (cm)	0-2	4	6	12	16	20	24	28	32	36	38	40
										(much reduced in number)		
Thioploca sheaths	+	+	+	+	+	+	+	+	+	+	+	+
Algal balls	+	+	+	+	+	+	+	+	+	+	+	+
Algal filaments	+	-	-	-	-	-	-	+	-	+	-	+
Fecal pellets	+	+	+	+	+	+	+	+	+	+	+	+
Fecal ribbons	-	-	+	+	+	+	-	-	-	-	-	-
Exoskeletal body parts	+	+	+	+	+	+	+	+	+	+	+	+
Tubifex	2	-	-	-	-	1	-	-	-	-	1	-
Tubifex tubes	27	-	-	-	-	-	-	?	-	-	-	-
Nematodes	-	-	+	-	-	-	-	-	-	-	-	-

Explanation of symbols: + = present, - = absent, ? = presence uncertain

Mn Nodule

Methods A Mn nodule, probably from Buoy 127, was divided into three sections and processed for its content of organic tissues. Batch X-ray of nodules by Dean and Ghosh (1978) showed that the nodule-forming minerals are generally amorphous to X-rays, but weak peaks are present for todorokite, birnessite, and goethite. Typical of most nodules dredged from the lake, the test nodule was composed of a soft surficial layer of Mn oxide overlaying concentric Mn oxide rings. At the center of the nodule was an Fe-rich core. The nodule was divided into the following samples: 1) the soft blanketing layer of Mn oxide teased off with needles, 2) the outermost soft Mn oxide concentric ring broken off by hand and 3) the innermost hard iron core. The fractions were washed in tap water and then were crushed wet in a porcelain mortar and pestle. The three samples then were processed through 10 percent HCl and 50 percent HF in standard palynological treatment for kerogen (see Robbins et al. this volume). The acid residues were sieved through 25- and 125-um sieves and were mounted with glycerin jelly onto permanent microscope slides. The slides were scanned for their organic content. Slides also were made of crushed, but otherwise untreated, nodule fractions for a comparison.

Results The untreated fraction that comprised the outermost soft ring had black and red particles of various sizes and shapes; some of the black particles were elongate and doubly terminated much like fecal pellets. The treated surficial layer and Fe-rich center ring had very little residue left; the residues were clear in color and had very few tissues. These layers obviously were soluble in HCl-HF. The treated side ring had black-coated tissues as well as tissues that had been cleared of their mineral coats. Many of the tissues were in the shape of doubly terminated fecal pellets. The pellets, mostly from unknown animals, varied in size and shape — fecal ribbons (89 x 249 um), Tubifex-type (67 x 108 um), long skinny ones (26 x 70 um), squared off ones (53 x 89 um), and copepod-type pellets (61 x 103 um). Other tissues included pollen grains, algal balls, fungal hyphae, and sheaths of Fe-oxidizing bacteria. These results suggest that, at some time during formation, Mn nodules are subject to the same fecal pellet rain that fills the sediment traps.

Discussion and Speculation

The fecal pellets and pellet-shaped organisms in Oneida Lake are abundant and varied. In a eutrophic environment, such as Oneida Lake, biological mechanisms for concentrating Mn in bottom sediment are numerous; bacteria, cyanobacteria, algae, zooplankton and fish seem to have mechanisms for accumulating Mn. Fecal pellets may be very important in the Mn cycle primarily because much of the organic production of the lake appears to pass through the guts of zooplankton.

In Oneida Lake, many of the fecal pellets are rich in residual Mn. Fecal pellets are produced in large numbers, and the depth of Oneida Lake is so shallow (mean depth 6.8 m, maximum depth 16.8 m) (Mills et al., 1978) that pellets can represent a rapid transport of Mn from the water column to the sediments. Once pellets reach the bottom of the lake, their Mn content may be subjected to different fates depending on the chemistry and microbiology of the bottom water and sediments. In the Shackelton Point subbasin, where the bottom water is suboxic and the sediments are anoxic, very few of the pellets in the core sediment contained LBB-positive Mn. In the sediment trap at Buoy 127, where the water at 1-m below the bottom is oxygenated, all the pellets gave a positive response for oxidized species of Mn.

At oxygenated sediment-water interfaces, Mn-enhanced fecal pellets may play additional roles in the Mn cycle of Oneida Lake. The pellets may accrete Mn onto nodules, much like

the process observed in the marine environment by Lyle et al. (1984). Pellets may even enhance Mn-nodule formation by serving as nucleating microenvironments for Mn precipitation. One could speculate that heterotrophic bacteria growing within the fecal pellets could oxidize the remaining organic matter in the pellets, thereby creating local anoxic conditions that would cause the reduction and the dissolution of Mn. Fecal pellets that first were concentrated sources of oxidized Mn next would be sources of reduced Mn. The presence of reduced Mn could lead to the selection for Mn-oxidizing bacteria around the fecal pellet microenvironment. We envision that the aerobic outer surfaces of the pellets could serve as a suitable substrate for continuing oxidation of reduced Mn as it diffuses out of the fecal pellets. Aggregates of Mn-oxidizing bacteria growing around pellets could continue to oxidize the reduced Mn diffusing out of pellets and sediments. By such a mechanism, fecal pellet concentrations of Mn, therefore, may serve as one of many loci for Mn-nodule formation. Wherever some favorable substrate or catalyst is available, such as an iron pebble or a shell (Dean, 1970; Dean et al., 1981), accumulations of fecal pellets could serve as a pool of available Mn for the continued growth of nodules.

Whether or not fecal pellet bacteria enter into Mn-nodule formation, our experiments have shown that fecal pellet enhancement of Mn may be a general process in Oneida Lake. Microscopic and macroscopic pellets of zooplankton, invertebrates and vertebrates may contribute to the concentration of Mn at the sediment-water interface and to the cycling of Mn within Oneida Lake.

Acknowledgements

I would like to thank Allan Creamer, Dave Bolgrien, Ed Mills, Tom Schmidt, Susan Rose, Steve Wickham, and Pam Gore for their assistance in this work.

References

Dean, W.E. (1970) Fe-Mn oxidate crusts in Oneida Lake, New York. Proc. 13th Conf. Great Lakes Res. 1970, pp.217-226.

Dean, W.E. and S.K. Ghosh (1978) Factors contributing to the formation of ferromanganese nodules in Oneida Lake, New York. U.S.G.S.J.Res. 6:231-240.

Dean, W.E. and P.E. Greeson (1979) Influences of algae on the formation of freshwater ferromanganese nodules, Oneida Lake, New York. Arch. Hydrobiol. 86:181-192.

Dean, W.E., W.S. Moore and K.H. Nealson (1981) Manganese cycles and the origin of manganese nodules, Oneida Lake, New York, U.S.A. Chem. Geol. 34:53-64.

Gore, P.J.W. (1986) Fluvial and lacustrine deposits in the Triangle brick quarry. In: SEPM Field Guidebooks, D.A. Textoris (Ed.) Southeastern United States, Third Annual Mid-year Meeting, pp.103-107.

Honjo, S. (1976) Coccoliths: Production, transportation, and sedimentation. Marine Micropaleontology 1:65-79.

Honjo, S. (1978) Sedimentation of materials in the Sargasso Sea at a 5,327 m deep station. J. Mar. Res. 36:469-492.

Lyle, M., G.R. Heath and J.M. Robbins (1984) Transport and release of transition elements during early diagenesis: Sequential leaching of sediments from MANOP Sites M and H. Part I. pH 5 acetic acid leach. Geochim. Cosmochim. Acta 48:1705-1715.

Mills, E.L., J.L. Forney, M.D. Clady and W.R. Schaffner (1978) Oneida Lake. In: Lakes of New York State, Vol. 2, J.A. Bloomfield (Ed.) Academic Press, New York, pp.367-451.

Pennak, R.W. (1978) Fresh-water invertebrates of the United States. Wiley.

Porter, K.G. and E.I. Robbins (1981) Zooplankton fecal pellets link fossil fuel and phosphate deposits. Science 212:931-933.

Richardson, L.L., C. Aguilar and K.H. Nealson (in press) Manganese oxidation in pH and oxygen microenvironments produced by phytoplankton. Limnol. Oceanog.

Robbins, E.I., K.G. Porter and K.A. Haberyan (1985) Pellet microfossils: Possible evidence for metazoan life in Early Proterozoic time. Proc. Nat. Acad. Sci. 82:5809-5813.

Tebo, B.M. (1983) The ecology and ultrastructure of marine manganese-oxidizing bacteria. PhD dissertation, University of California, San Diego.

Turner, J.T. (1977) Sinking rates of fecal pellets from the marine copepod Pontella meadii. Mar. Biol. 40:249-259.

Eleanora Robbins

"Ecology and Distribution of the Sulfur-oxidizing Bacteria Thioploca in Oneida Lake, N.Y."

Introduction

This paper reports on the unexpected presence of Thioploca, a sulfur-oxidizing bacterium, discovered during the course of coring and sieving sediments from Oneida Lake, a highly productive eutrophic lake in Upstate New York. The ecology and distribution of Thioploca are discussed, and methods of collection and analysis are reported.

Although the presence of Thioploca was surprising, particularly because lakes generally contain only trace amounts of sulfur (Hutchinson, 1957), Thioploca has been collected before in lakes as well as in the ocean (Larkin and Strohl, 1983). During the 1950's and 1960's, polluted Lake Erie contained mats of Thioploca. It has also been collected in Lake Constance (Boden-See) in Germany. In the ocean Thioploca forms mats off the western margin of Peru and Chile, where high productivity in the water column supports high rates of sulfate reduction in the sediment. The fishermen of Peru refer to Thioploca as "estopa" or uncleaned wool, because of its appearance in clogged fishing nets.

Thioploca has not yet been isolated in pure culture, so details of its specific requirements have not yet been established. On the basis of knowledge of other sulfur-oxidizing bacteria and of studies in its environment, Thioploca is inferred to have metabolic pathways that allow it to take advantage of sulfur in the environment (Larkin and Strohl, 1983). Because Thioploca most likely requires both H_2S and O_2, it flourishes at redox interfaces where both compounds are present. It probably oxidizes the H_2S produced by nearby sulfate-reducing bacteria. Elemental sulfur inclusions are stored in the periplasm between the cell wall and the cell membrane. It appears that the elemental sulfur either can be oxidized to sulfate or reduced to H_2S depending on redox conditions in its environment.

Cyanobacteria were the dominant phytoplankton in the water column during the summer months when we did this research; diatoms were collected in sediment traps but were not present in plankton tows. Copepods, cladocerans and ostracodes were abundant. The populations of walleye and yellow perch make this eutrophic lake an excellent fishing locality (Mills et al., 1978; Mills and Gannon, 1983).

A likely source of the sulfur to Oneida Lake is a sulfur spring upstream from the southern end of the lake, 1.5 miles south of Chittenango, N.Y. Around 1800, a hotel was located at the spring, and people came by train to drink the "healing waters" (Janet Forney, Cornell Univ. Biological Field Station, Oneida Lake, N.Y., pers. commun., 1987). Abandoned brickworks mark the location of the old hotel. The bricks are coated with white, sulfur-filled Thiothrix species that flourish in fast-running water. Where they can attach in slack water, Beggiatoa probably is the taxon that forms a white film on the sediment surfaces. At depth below the white films, the sediments are black and smell of H_2S undoubtedly produced by sulfate-reducing bacteria. Gypsum of the Syracuse Formation (Fisher et al., 1978) in the watershed is probably the source of sulfur to the spring (Mills et al., 1978). Downstream from the white bricks, the white surface films and the black sediments, the spring water flows first into a bed of Chara and then into Chittenango Creek. Chittenango Creek is a major drainage into the southern end of Oneida Lake and it enters west of Shackelton Point.

Methods

Cores 40 cm long and 6.6 cm wide were taken at numbered barge canal buoys in Oneida Lake by scuba divers. Several cores were taken at each buoy and were identified by the buoy number, such as 127-1. A core extruder consisting of a water-driven pressure system allowed 1 centimeter of sediment at a time to rise above the core barrel; 1-cm slices were taken from the cores within 1 hour of their collection and the sediment was placed in closed centrifuge tubes. The tubes from one core were centrifuged in an oxygen atmosphere for 10 min at 3,000 rpm and the pore water was removed immediately. Concentrations of sulfide in the pore water were measured colorimetrically by using Kline's method (1969).

The most efficient method for enumerating the abundance of Thioploca from the soft brown silt was to sieve the sediment. Core slices were washed through a sieve stack that included a soft plastic screening material of 1.4 mm screen diameter on top, a 150-um sieve of 9-inch diameter in the middle, and a bucket to catch the -150 um fraction on the bottom.

The Thioploca strands generally occurred in clumps that were relatively easy to pick out of the 1.4-mm sieve with forceps. The strands were left in water in tubes until they could be weighed and examined. The clumps of strands were placed in weighed measuring trays and washed with tap water until the water ran clear and no obvious sediment was left in the trays. The strands were then patted dry and weighed (Table 1). Then the clumps were teased apart, mounted wet on microscope slides and examined by means of a light microscope using transmitted light and phase contrast for 1) the presence of living Thioploca, 2) the number of filled and empty sheaths, 3) the presence of single filaments and 4) the presence of other tissues and minerals that might add erroneous weight to the clumps. These results are enumerated in Table 2. Because a method to separate the strands from the entwined debris could not be devised, the weights in Table 1 carry an inherent error.

Table 1. Weight of Thioploca in cores 127-7 and SP-4.

Core 127-7		Core SP-4	
Depth (cm)	Weight (gm)	Depth (cm)	Weight (gm)
0-1	0.0462	0-1	0.0455
1-2	0.0408	1-2	0.0578
2-3	0.0293	2-3	0.0268
3-4	0.0211	3-4	0.0076
4-5	0.0364	4-5	0.0049
5-6	0.0075	5-6	0.0013
6-7	0.0209	6-7	0.0014
7-8	0	7-8	0

The distribution of Thioploca in cores around Oneida Lake in terms of absence and presence was noted. These data are shown in Table 3.

Table 2. Microscopic observations on clumps of Thioploca in cores 127-7 and SP-4.

Depth	Full sheaths (n)	Empty sheaths (n)	Individual living filaments	Individual dead filaments	Color of inclusions	Tissues entwined in sheaths: other bacteria	algae	fungi	plant parts	animal spoor
					Core 127-7					
0-1	>200	>200	+	+	gnish yw-ple	---	Oscillatoria green	---	---	Tubifex, zoo. exoskeleton, bird barbule
1-2	100+	>200	-	+	gnish yw	---	---	---	---	worm segment, nematode, zoo. exoskeleton, bird barbule
2-3	>200	>200	-	+	gnish yw	Sidero-cystis	Oscillatoria	hyphae	cuticle	nematodes
3-4	100+	>200	+	+	gnish yw-ple	---	---	---	---	nematode, zoo. exoskeleton, bivalve
4-5	150+	200+	?	+	gnish yw	---	segmented gn	---	tissue	zoo. exoskeleton
5-6	7	124+	?	+	gnish yw	---	diatom	---	---	zoo. exoskeleton, bird barbule
6-7	1	170+	?	+	yw	---	segmented gn	---	---	zoo. exoskeleton, bird barbule
					Core SP-4					
0-1	>200	>100	+	+	ple, yw gn	Micro-cystis	Oscillatoria, Fragillaria, Stephanodis-cus	---	---	Tubifex tube, zoo. exoskeleton
1-2	>200	>100	+	+	yw gn	---	Oscillatoria	---	cuticle, vasc. tissue	nematodes zoo. exoskeleton
2-3	>100	>200	+	+	ple, yw gn	---	---	---	cuticle, vasc.	nematode, zoo. exoskeleton
3-4	>200	>200	+	+	ple, ywish	---	---	---	tissue	Tubifex tube
4-5	>30	>50	-	+	ple, ywish	---	---	---	vasc. tissue, fibers	zoo. exoskeleton, zoo. fecal pellet
5-6	4	>50	+	+	ple, ywish	---	---	---	---	zoo. exoskeleton
6-7	>25	100+	?	+	ple, ywish	---	---	---	---	---

Abbreviations: +=present, -=absent, gnish=greenish, ple=purple, vasc.=vascular, ywish=yellowish, zoo.= crustacean zooplankton.

Table 3. Distribution of Thioploca in surface sediments of Oneida Lake.

Coring Locality (Buoys)	Number of Cores	Depth above Black Clay (cm)	Lake Water Depth (m)
Thioploca Present			
109	2	6,8	36
117	2	3,4	41
127	6	4,5,5.5,12,17.5,within black clay	33
129	2	4.5,9	28
SP	4	2,17,23,within black clay	40
Thioploca Absent			
123	2	---	13
133	2	---	22

One method of analyzing the ecology of an organism is to describe the organic and inorganic components in its environment. Table 4 shows the results of analyses in three cores from Buoy 127 and one core from the Shackelton Point station.

A new method was devised to try to isolate Thioploca. A gallon container was opened on the lake bottom and dragged below Buoy SP to collect the top 3 cm of sediment. Lake water was collected in another vessel. In the laboratory, N_2 gas was bubbled through the lake water to eliminate as much O_2 as possible. The mud was sieved through a 1.4-mm sieve and Thioploca sheaths clogged the filter. The filaments were washed with N_2-bubbled lake water, picked off with forceps and immediately inoculated into gradient agars in test tubes. Because Thioploca is considered to be a gradient organism, a gradient agar was devised so that filaments could migrate in the agar to find the gradient of oxygen and sulfide that was optimum. The air space above the test tube was the source of oxygen. The gradient was composed of an overlying soft agar layer (0.5% agar, 0.01% acetate in filtered and autoclaved lake water) and an underlying hard agar layer (2% agar, 10 mM sodium sulfide buffered to pH 8 in filtered and autoclaved lake water).

Oxygen measurements were taken at the bottom of Oneida Lake on some of the coring days. The data were collected by using the oxygen sensor on a Hydrolab (DCP compatible Handar Data Sonde II produced by Hydrolab Environmental Systems). These results are shown in Table 5.

Table 5. Oxygen measurements on the bottom of Oneida Lake at Buoy 127.

Date	Depth (m)	O_2 (mg/l)
6/30/87	11.4	4.02
7/8/87	11.4	8.11
8/1/87	10.4	6.44

Table 4. Organic constituents in sediments containing Thioploca.

	bacteria	algae	fungi	plant parts	worms	crustacean zooplankton	insects	molluscs	egg cases & resting cysts	other
Core 127-1										
0-2	Thioploca	amorph. Gleotr.	---	---	T. tubes, red Tubifex, Nais?	limpet, fecal pellets, exoskeletons, ostracodes	---	Pisidium?	---	---
2-4	Thioploca Fe-oxide flocs Lyngbya	Cladophora pennate diatoms, Melosira, amorph. Gleotr.	---	remains	T. tubes	fecal pellets, exoskeletons, ostracodes	---	Pisidium?	egg cases	---
4-6	Thioploca	amorph. Gleotr.	---	wood	T. tubes	exoskeletons, fecal pellets	---	Pisidium?	---	testacate amoeba
6-8	Thioploca	amorph. Gleotr.	---	---	---	fecal pellets, exoskeletons, ostrocodes	---	gastropod Pisidium?	---	---
8-10	Thioploca Fe-oxide flocs	amorph. Gleotr.	---	remains	---	exoskeletons, fecal pellets, ostracodes	---	---	---	---
10-12	Thioploca	---	---	remains, seed	---	exoskeletons, fecal pellets ostracodes	---	---	---	---
12-14	Thioploca Fe-oxide flocs	amorph. balls	---	remains	---	exoskeletons, fecal pellets	---	---	---	---
Core 127-2										
0-2	Thioploca, H2S	---	---	Myriophyllum	T. tubes, nonseg.	exoskeletons	---	shell	Planarian case	---
2-4	Thioploca, H2S	---	---	root?, Myriophyllum	T. tubes pale Tubifex	---	---	shell	---	---
4-6	Thioploca	---	---	---	arrow worm	fecal pellets, exoskeletons	---	Physa?	---	---
Core 127-3										
0-2	Thioploca	---	---	Myriophyllum	pale Tubifex T. tubes	exoskeletons	---	shells	---	---
2-4	Thioploca	---	---	---	T. tubes	exoskeletons	---	Physa?	statoblast	---
4-6	Thioploca				pale Tubifex T. tubes	exoskeletons		shells		
6-8	Thioploca	---	---	wood	T. tubes	exoskeletons, fecal pellets	---	shells	---	testacate amoeba
8-10	Thioploca, H2S	---	---	wood	pale Tubifex	fecal pellets, exoskeletons	---	shell	---	---
10-12	Thioploca, H2S, Fe-oxide flocs	---	---	leaf	---	fecal pellets, exoskeletons	---	---	---	---
12-14	Thioploca, H2S	---	---	Myriophyllum	Tubifex	fecal pellets, exoskeletons	---	---	---	fish scale
14-16	Thioploca, H2S	---	---	leaf	---	exoskeletons	---	shell	---	---
16-18	Thioploca	---	---	---	Tubifex	exoskeletons, fecal pellets	---	---	---	---

Table 4 continued.

	bacteria	algae	fungi	plant parts	worms	crustacean zooplankton	insects	molluscs	egg cases & resting cysts	other
Core SP-1										
0-2	Thioploca, nonpig. filaments H2S	amorph. balls, diatoms	hyphae, spores	p&s, cuticle, fibers	T. tubes Tubifex	exoskeletons, fecal pellets, ostracode	wing scale	---	egg case, resting cyst	testacate amoeba
2-4	Thioploca, H2S	amorph. balls, diatoms, dinocyst, Pediastrum	hyphae, spores	p&s, fibers, cuticle	---	exoskeletons, fecal pellets, ostracode, Daphnia ephip.	---	---	egg case, resting cyst	---
4-6	Thioploca	amorph. balls, diatoms, Pediastrum, dinocyst	hyphae, spores	vasc. tissue, twig, p&s,	nematode	exoskeletons, fecal pellets, fecal ribbons	---	---	egg case, resting cyst	---
10-12	Thioploca	amorph. balls, diatoms	hyphae, spores	vasc. tissue, cuticle, p&s	worm	exoskeletons, fecal pellets, fecal ribbons, abdominal claw	leg	---	egg case, resting cyst	---
14-16	Thioploca	diatoms, dinocyst, amorph. balls	hyphae, spores	vasc. tissue, p&s, cuticle	nematode	exoskeletons, ostracode, fecal pellets	---	---	egg case, resting cyst	testacate amoeba
18-20	Thioploca, H2S	amorph. balls, diatoms, dinocyst	hyphae, spores	vasc. tissue, cuticle, p&s	worm	fecal pellets, fecal ribbons, exoskeletons	---	---	egg case, resting cyst	---
22-24	Thioploca	amorph. balls, diatoms, dinocyst	spores	vasc. tissue, cuticle, p&s	worm	fecal pellets, exoskeletons Daphnia ephip.	---	---	egg case, resting cyst	---
26-28	Thioploca, filaments	amorph. balls, diatoms	hyphae, spores	twig, vasc. tissue, cuticle, p&s	T. tubes (?)	fecal pellets, exoskeletons	---	---	egg case, resting cyst	---
30-32	Thioploca	amorph. balls, diatoms	hyphae, spores, sclero.	wood, leaf, p&s	worm	fecal pellets, exoskeletons	---	---	egg case, resting cyst	---
34-36	Thioploca, filaments	amorph. balls	hyphae, spores	vasc. tissue, p&s, plant hair, cuticle	---	fecal pellets, exoskeletons	leg	---	resting cyst	---
36-38	Thioploca	amorph. balls	hyphae, spores, sclero.	wood, p&s, cuticle	worm	fecal pellets, exoskeletons	---	---	resting cyst	---
38-40	Thioploca, filaments	amorph. balls	hyphae, spores	p&s vasc. tissue, plant hair	---	fecal pellets, exoskeletons, abdominal claw	---	---	---	---

Abbreviations: a=angular, amorph.=amorphou, dinocyst=dinoflagellate cyst, Gleotr.=Gleotrichia, nonpig.=nonpigmented, p&s=pollen and spores, r=rounded, T=Tubifex.

Results and Discussion

Thioploca is a macroscopic, sheath-forming bacteria. As many as six individual filaments in one sheath could be seen in the species from Oneida Lake. Individual filaments could be observed gliding within the sheaths, and adjacent individuals glided in opposite directions. At the ends of sheaths, individual filaments could be seen moving in a waving motion. The number of sheaths and filaments were measured in two cores (Table 2). In the samples closer to the surface, the granules had a purplish cast. Deeper within the cores, the samples grade from greenish yellow to yellow in the deepest core slices.

Thioploca is present in Oneida Lake for a linear distance of 17 km between the eastern end of the lake at Buoy 109 and the western end of the lake at Buoy 129 (Table 3). It occurs predominantly in sediments from the deeper areas, probably because of the lowered oxygen content.

The mats are absent at Buoys 123 and 133. Buoy 123 is on the top of Shackelton Shoals, a glacial ridge. There the water is shallow, surface currents sweep the bottom of loose sediments, Mn nodules are abundant and the bottom is almost always fully oxygenated. The bottom of the lake at Buoy 133 is sandy, the sand is black and Mn nodules are not present. Large mussels, 3 to 4 in long, are abundant at the sediment-water interface.

The Thioploca mats could be observed through the clear-plastic core barrels. In most cores, the Thioploca mats were at the sediment-water interface. The surficial mats either occurred across the whole core barrel (Buoys 109, 127, 129, SP) or else they were in discrete small patches around 2 cm wide (Buoy 117). The thickest mat was 2.5 cm thick in core 127-6. Thioploca generally occurred in places where Tubifex worm tubes also were present. In core 127-1, the Thioploca mat was about 1 cm below the sediment surface rather than being at the sediment-water interface. In that core, the Tubifex tubes were especially abundant and bright red. Tubifex have hemoglobin-containing respiratory pigments and may control the distribution of Thioploca mats by bringing oxygen down from the surface via their food-seeking burrowing.

Thioploca was most abundant by weight in the top 2 cm (Table 1). Generally by 8 cm, no more intact sheaths were caught on the 1.4-mm sieve. However, fragmented sheaths have been observed down to the base of the cores (Table 4). Because the centimeter-thick samples averaged 35 mg in weight, Thioploca clearly accounted for only a very small (0.05 gm maximum) amount of the weight of the cores.

The clear-plastic core barrels allowed observations on apparant predation events in the Thioploca mats. The mat in core 127-1 was ragged, and holes could be observed by looking through the clear barrel. An individual ostracod, an amphipod and a copepod could be observed darting into the holes and appeared to graze in the mats. When filaments and Tubifex were put in the same petri dish, predation on the mats could be observed.

Living and dead organisms and inorganic minerals all form part of the habitat of Thioploca. Table 2 shows components that could not be washed from the filaments. The filaments entwine themselves around all types of debris—diatoms, Tubifex tubes and bodies, zooplankton exoskeletons, plants remains, fecal pellets, living algal filaments, bird feathers and so on.

Sieving of the mud allowed a study of organic and inorganic components associated with Thioploca. Organisms that were living in the same environment as Thioploca, such as

Pisidium, Tubifex and an unsegmented worm, were enumerated (Table 4). Fine-grained quartz also is present in the environment.

Although the colorimetric test for sulfide was negative, the presence of sulfide in the cores is obvious by its smell and black color. Table 3 shows the relationship between the depth of the black sulfide layer and the presence of the overlying Thioploca.

Thioploca was not successfully cultured during the time available, nor has it ever been. A white band was observed in one of the test tubes within 24 hours of inoculation, but the sulfur-oxidizing bacteria in the band was not Thioploca. The test tubes were taken to the University of Indiana for further observation. Therefore, isolation and chemical parameters remain to be done with the Thioploca from Oneida Lake. Hopefully, the bacteria can be isolated eventually, so that the metabolic capabilities of the organism can be better understood.

References

Fisher, D.W., et al. (1961) Geologic maps of New York. New York Geological Survey Map and Chart Series, No. 5, 1:250,000 scale.

Hutchinson, G.E. (1957) A Treatise on Limnology, Vol. 1. Wiley, New York, pp.753-787.

Kline, J.P. (1969) Spectrophotometric determination of sulfide in natural waters. Limnol. Oceanog. 14:454-458.

Larkin, J.M. and W.R. Strohl (1983) Beggiatoa, Thiothrix, and Thioploca. Annual Review of Microbiol. 37:341-367.

Mills, E.L., J.L. Forney, M.D. Clady and W.R. Schaffner (1978) Oneida Lake. In: Lakes of New York State, Vol. 2, J.A. Bloomfield (Ed.) Academic Press, New York, pp.367-451.

Mills, E.L. and J. Gannon (1983) Oneida Lake Profile. Oneida Lake Association, Syracuse, New York.

Susan Rose

"Dissolved Silicon and Diatoms in the Sediments"

Introduction

For several years in Oneida Lake, nutrient measurements (including silicon) have been done weekly on the water column. However, there are no data for silicon levels in the sediments. Considering the abundance of diatoms found in the sediment traps, it became interesting to know the silicon levels in the sediments. If the silicon levels were high in the sediments, then the sediments might be serving as a sink for silicon. If the levels were low, diatoms might be mineralized before they are buried.

Total silicon consists of both dissolved and particulate silica, with particulate usually being diatom silica. Dissolved silica, which is sometimes measured less accurately as soluble reactive silica, can be measured from the pore water of sediments, while particulate silica must be measured from the sediments or material trapped on filters.

These analyses included both the measurement of the dissolved silica in a sediment core and the examination of a core to see the depth to which diatoms occur. Particulate silica was to be analyzed at a later date.

Materials and Methods

Dissolved Silica

A core was taken at Buoy 123 by scuba divers, then extruded back in the lab by one-centimeter sections. The one-centimeter sections were centrifuged for 5 minutes and the pore water extracted and filtered through 0.2-um filters and saved in the refrigerator until analysis.

Since no commercial silicon standard was available, standards were made using Na_2SiF_6. 0.960 g of Na_2SiF_6 was dissolved in 1000 ml to make up the stock solution. For the first standard, 0.7 ml stock was added to 100 ml distilled water for a concentration of 983 $ug \cdot L^{-1}$ (5.23 uM). For the second standard, 2.0 ml of stock was added to 100 ml dH_2O for a concentration of 2808.6 $ug \cdot L^{-1}$ (14.9 uM).

Through previous trials, it was discovered that 0.5 ml of pore water needed to be diluted to a total volume of 3.0 ml in order to be read on our spectrophotometer (LKB model 405 U). The reagents were added to 3.0 ml of the pore waters and the standards in the following procedure: 0.24 ml sodium molybdate (29.25 g $Na_2MoO_4 \cdot 2H_2O$ in 500 ml 0.5 N H_2SO_4), wait 15 minutes, 0.6 ml 50% H_2SO_4, cool to room temperature, 0.4 ml $SnCl_2$ (stock-40 g $SnCl_2$ per 100 ml HCl conc.) working solution - 1 ml stock per 100 ml dH_2O and use immediately. Each sample must be read 10-15 minutes after the addition of the stannous chloride at 810 nm.

Core Analysis for Diatoms (Procedure by E. Robbins)

Two-centimeter sections of a core from Shackleton Point were sieved into three fractions: 1.4 mm, 150 um, and 20 um. Seven percent H_2O_2 was added and allowed to digest the sediment for 2 weeks. Samples were then washed with 4 water washes. A portion of the sediment went through the 20-um sieve, and a portion of the sediment that went through the 150-um sieve, but was retained on the 20-um sieve were mounted in glycerin jelly on glass slides.

Results and Discussion

Dissolved Silica

Analysis of dissolved pore waters can be seen in Figure 1. The point at depth zero is the water just above the sediment surface and the amount there is considerably lower than the amounts throughout the sediment core. The concentrations in the sediment core do not seem to show any general trends.

Diatom Distribution in Core Samples

Many genera were observed through the first six centimeters with Stephanodiscus/ Cyclotella being the most abundant (Table 1). Stephanodiscus was present, but it was unclear whether Cyclotella was also present. The centric diatoms steadily decreased throughout the depth of the core. By 34 cm, all the diatoms were gone. One interesting observation was that very few Melosira cells and no Fragillaria were in this core. In the sediment traps, however, Fragillaria and Melosira were the most abundant diatoms. The core and the trap were from different places in the lake, but it still seems unusual that the counts of Fragillaria were at least 1,000 cells·ml^{-1} and there were none in the core.

In conclusion, the dissolved silica levels in the sediments are higher than the water column which is generally about 2-3 uM. Without the particulate silicon levels, one cannot get the total amount of silicon in the sediments, and the number of diatoms in the core suggests that they would be contributing a substantial amount of silicon. Also, the number of diatoms in the core suggest that the sediments might be serving as a sink for silicon, because the diatoms are not being remineralized before they reach the sediments. Exceptions to this might be Melosira and Fragillaria, because their high numbers in the sediment trap are not represented in the core. Clearly the types of diatoms that bloom may have a major impact on the cycle of Si in Oneida Lake, both quantitatively and qualitatively.

Figure 1

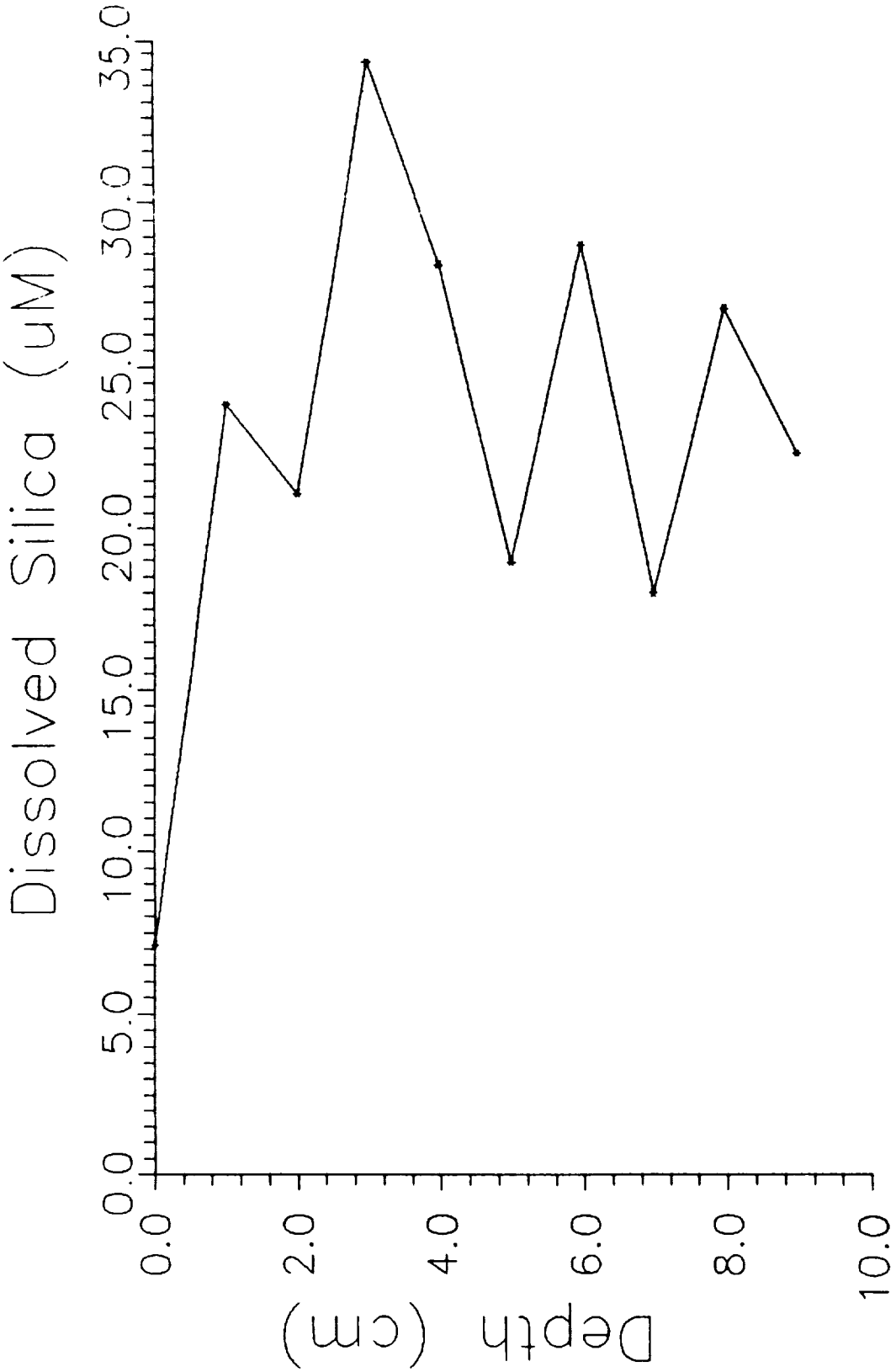
Dissolved Silica (uM)
0.0
5.0
10.0
15.0
20.0
25.0
30.0
35.0
Depth (cm)
0.0
2.0
4.0
6.0
8.0
10.0

Table 1. The results of the core analysis for diatoms.

	0-2	2-4	4-6	10-12	14-16	18-20	22-24	26-28	30-32	34-36
Stephanodiscus/ Cyclotella	A	A	A	A	B	B	C	C	C	
Gyrosigma	C	B	C							
Pinnularia	C			C						
Pediastrum (green)	C	B	B							
Tabellaria	C									
Surirella	C	C	C	C						
Navicula-like	C	C	C							
Gomphoneis	C	C								
Melosira	C		C							
Cymbella	C	C	C							
Achnanthes		C								
Attheya		C								
Cymatopleura		C								

A = abundant
B = common
C = rare

Figure 1. Opposite. Analysis for dissolved silica from pore water of a Buoy 123 core.

Susan Rose

"Flux into Sediment Traps in Oneida Lake"

Introduction

Sediment traps can be useful in ascertaining the amount of sediment being deposited as well as the type of material being deposited. One objective for this experiment was to obtain a sedimentation rate from the dry weight of the sediment collected and the second objective was simply to look at the material collected and see qualitatively what was being deposited.

Three sediment traps were used in this experiment. One was put down at Buoy 123 which is approximately 8 m deep with many manganese nodules on the sediment surface. The second was put down at Buoy 127 which is about 10 m deep with a layer of manganese oxide beneath the sediment surface (no surface nodules). During the last week of the experiment, a third trap with formaldehyde was put down at Buoy 123.

Methods and Materials

All three of the sediment traps used had the same dimensions. The column on each trap is 76 cm long, the inside diameter of the column is 15 cm and the outside diameter is 17.5 cm. Near the bottom column is a funnel, with the neck of the funnel occurring 7 cm from the bottom of the column. Surrounding the neck of the funnel is a cap to which the collection bottle can be attached. The traps were placed in the sediments so that the tops of the columns were approximately 1 m from the sediment water interface.

Collection bottles were changed on the first two sediment traps every 7 to 10 days by scuba divers. Generally, the bottles were processed on the same day as collection, but on three occasions (87/07/17, 87/07/22, 87/07/24) the bottles sat in the refrigerator for several days. Most of the water was siphoned from the collection bottle, then the sediment was allowed to settle out of the remaining water in a centrifuge tube for at least one hour. Remaining top water was removed, leaving wet sediment. 1.0 ml of this wet sediment was fixed with 1.0 ml buffered formaldehyde (100 ml of 37% formaldehyde with 5.0 g sodium borate) and 18.0 ml of distilled water. On two of the collections (87/07/22 and 87/07/24), 1.0 ml of the wet sediment was reduced with 0.1 ml of $1x10^{-3}$ M ascorbic acid to analyze for total manganese on the atomic absorption spectophotometer (Perkin-Elmer model 503 with air-acetylene flame). A drop of concentrated HCl was also added to this mixture to ensure that the pH remained low. This sediment was allowed to reduce overnight, then it was centrifuged and the liquid extracted. On all the collections, 0.1 ml of the wet sediment was added to 0.9 ml of distilled water and analyzed on an inverted microscope. The remaining wet sediment was dried, weighed and ground-up, with part of the sediment being saved for particulate metal analysis and part saved for C,H,N analysis.

After the last collection date, the formaldehyde-fixed samples from the first two traps were stained with DAPI (6-diamidino-2-phenylindole dihydrochloride) to count total bacteria. The working solution of DAPI was 0.1 $ug \cdot ml^{-1}$, and 120 ul of the working solution was added to 1.0 ml of the formaldehyde-fixed sample and stained for 5 minutes. This mixture was filtered through 0.2-um filters, and the filters were placed on glass slides.

The poison trap was put down from 87/07/24 - 87/08/01 (8 days). A mixture of formalin with sucrose and 37% formaldehyde was used as the poison. The sucrose formalin was added to ensure that the poison would be denser than the surrounding water. No material from the poison trap was stained with DAPI or reduced with ascorbic acid; the material was analyzed on the inverted microscope in the same manner as the other samples. The wet sediment was not dried and weighed.

Results

There were 7 collection dates from the first two sediment traps; 4 bottles were collected from Buoy 123 and 3 from Buoy 127. The dried sediment weights, the total dry weights, total number of days and the sedimentation rates can be seen in Table 1.

Table 1. Dried sediment weight, total dry weight, total number of days, and sedimentation rate for material collected from first two sediment traps.

Buoy 123

date	weight
870627-870706	0.791 g
870706-870713	0.240 g
870713-870722	0.140 g
870722-870729	0.318 g

Total dry weight = 1.489 g
Total # of days = 32 days
Sedimentation Rate = 2.63 g/m^2/day

Buoy 127

date	weight
870710-870717	0.370 g
870717-870724	0.050 g
870724-870731	1.028 g

Total dry weight = 1.448 g
Total # of days = 21 days
Sedimentation Rate = 3.9 g/m^2/day

DAPI staining of the 7 fixed samples showed presence of bacteria, but the bacterial cells were not distinct enough under the 40x objective to be counted. No oil immersion lens was present.

The two samples reduced with ascorbic acid (87/07/22 and 87/07/24) were analyzed on the atomic absorption spectrophotometer (AA). The water from each collection bottle for those two dates was also analyzed on the AA (no ascorbic acid added). The water from the sediment trap bottle from Buoy 127 had an undetectable reading, while the other 3 samples

had to be diluted. Five standards were run on the AA and a standard curve was generated (R^2 = .993). The results from the analysis are shown below in Table 2.

Table 2. Concentration of manganese in material collected from first two sediment traps, as determined by atomic absorption spectrophotometry.

Sample	Molarity of Mn	
Buoy 123: water from collection bottle	.0946 mM	
Buoy 123: reduced sediment extract	2.0960 mM	2.1 mM

Buoy 123 Total	2.1906 mM	
Buoy 127: water from collection bottle	0.000	
Buoy 127: reduced sediment extract	3.921 mM	
	---	3.9 mM
Buoy 127 Total	3.921 mM	

Analysis of the material from the sediment trap on the inverted microscope revealed diatoms (both live and dead), colonial greens, cyanobacteria and clumps of indistinguishable organic matter (including fecal pellets). No green algae or cyanobacteria were found in the bottles from Buoy 127. Several filaments of Anabaena were found in the trap at Buoy 123 (87/07/13) and colonies of Microcystis were occasionally observed in the trap at Buoy 123 (87/07/06 and 87/07/13) and also in the poison trap at Buoy 123. Diatom counts and green algae counts for the collection dates are shown in Table 3.

Table 3. Microscopic analysis of material from sediment traps.

Buoy	Collection Date	Diatoms (cells·ml^{-1})	Live Greens (cells·ml^{-1})
123	870627-870706	2016	857
123	870706-870713	1429	397
123	870713-870722	9429	349
123	870722-870729	29238	571
127	870710-870717	2889	0
127	870717-870724	1222	0
127	870724-870731	1206	0
123(p.t.)	870724-870801	61468	6429

Discussion

The sediment traps used worked effectively. The tops of the columns were high enough off the sediment surface to ensure that no extra sediment could be added by storms or divers stirring up the bottom.

Dry sediment weights were obtained in order to estimate the sedimentation rate in Oneida Lake. Since 1.1 ml of wet sediment was taken out of five collection bottles and 2.1 ml out of two bottles, the rate is an underestimate.

The AA analysis for total manganese indicated that the water in the collection bottle from Buoy 123 showed fairly high dissolved Mn levels as compared to the water from the collection bottle from Buoy 127 which was undetectable. One possible explanation for this difference is that the bottle from Buoy 123 was in the refrigerator for five days while the bottle from Buoy 127 was only kept in the refrigerator for three days. The bottle from Buoy 123 may have become anaerobic, allowing reducing conditions to form, thus changing particulate Mn to dissolved Mn.

Analysis of the assemblage of algal cells found in the two sediment traps was interesting. There were numerous diatom cells, with the most common genera being Asterionella, Stephanodiscus and Fragillaria. There were diatom blooms during the spring of this year, but no blooms during the summer. It is possible that the diatoms could have been deposited in the traps after being resuspended from the sediments, but as already stated, the traps were high enough off the sediment that this seems unlikely. Also, a majority of the diatoms were alive, which may indicate that they were still in the water column instead of being resuspended. Conversely, there were many cyanobacterial blooms during the summer, but very few cyanobacterial cells observed in the traps (zero at Buoy 127). Two possibilities exist: either the cells are decomposing in the traps or they are being grazed/decomposed before reaching the traps. To test for this, the poison trap was put down at Buoy 123. A few colonies of Microcystis were found in this trap, but no increase in cyanobacterial cells was seen compared to the collections from the regular trap at Buoy 123. Therefore, the cells seem to be eaten and/or decomposed before reaching the trap.

Use of the sediment traps has proved very useful in our study of Oneida Lake. The traps will be left down over the winter in order to see the assemblage after this period. One future experiment would be to see if this affects the number of diatoms or the overall algal numbers found in the traps.

Steve Wickham

"Bacterial Secondary Productivity"

Introduction

It has recently been demonstrated that bacteria make a significant contribution to the secondary production in marine ecosystems (Furhman and Azam, 1982). Furthermore, it has been proposed that there is a close relationship between marine algae and bacteria (Azam and Cho, 1987). Since bacterial production in lentic ecosystems has not been as well studied, an attempt was made to examine both the above hypotheses in Lake Oneida: that bacterial secondary productivity is significant; and that this productivity is tightly coupled to the phytoplankton.

Methods

The methods utilized were essentially those of Fuhrman and Azam (1982). ^{3}H-Thymidine incorporation was used as an estimate of bacterial secondary productivity. Whole water samples were taken using a Van Dorn bottle at approximately twice weekly intervals over the duration of the field course. Two liter samples were taken at 3 depths (usually 0, 4, and 8 m), at two buoys (initially Buoys 117 and 123, after 9 July, Buoys 123 and 127). The samples were stored in a cooler in order to maintain the ambient water temperature.

Ten ml samples were incubated in the dark at room temperature for 1 hour. ^{3}H-Thymidine was added at a concentration of 10 nM (specific activity: 61 Ci/mM). Five subsamples were incubated for each sample: 2 replicates of subsamples to be size fractionated into 2 groups, and a kill-control (0.1 ml sucrose-formalin added) to measure background radiation and nonbiotic adsorption of ^{3}H-Thymidine.

At the end of the 1-hour incubation, samples were put in ice water to stop ^{3}H-Thymidine incorporation. The samples were fractionated into 2 size classes, greater than 0.2 um and greater than 1.0 um, using 0.2-um Gelman GA-8 and 1.0-um nuclepore filters. The samples were then poured into the filter columns and filtered down into the appropriate filter. After washing with cold water, cold 5% trichloroacetic acid (TCA) was added to solubilize the bacterial cell walls. The TCA was filtered off after 3 minutes, filters were placed in 20 ml scintillation vials, and 5 ml of scintillation cocktail was added. Because DNA is not retained well by 1.0-um nuclepore filters (F. Azam, pers. comm.), a 0.2-um Gelman filter was placed under the 1.0-um filter before TCA was added. Since neither type of filter could be made to dissolve, internal standards of 6.1 uCi on the appropriate filters were used to correct for quenching. The samples were counted on a Packard LSC 1500 liquid scintillation counter, using a preprogrammed ^{3}H window.

Disintegrations per minute were converted to cells/ml/hr using the following two equations. The first is:

$$\text{Moles } ^{3}\text{H-Thymidine incorporated} = \frac{\text{dpm} \times 4.5 \times 10^{-13} \text{ Ci/dpm}}{\text{Ci/mol}}$$

where dpm are disintegrations per minute, Ci/mol is the specific activity of the ^{3}H-Thymidine solution and 4.5 x 10^{-13} is the number of curies per dpm.
The second equation:

$$\text{Cells produced} = \frac{\text{moles incorporated} \times 2 \times 10^{18}}{\text{vol}}$$

converts the moles ^{3}H-Thymidine incorporated to cells produced over the course of the incubation, per unit volume. Moles incorporated are the number of moles ^{3}H-Thymidine incorporated, calculated in the first equation; vol is the volume of sample incubated; 2 x 10^{18} is an estimate of number of cells produced per mole ^{3H}-Thymidine incorporated (Fuhrman and Azam, 1982).

Results

Figure 1 presents the bacterial secondary productivity estimates at Buoy 117. The production by particles retained on the 0.2-um filter was usually at least an order of magnitude greater than that retained on the 1.0-um filter. The data indicate that there is no consistent stratification of bacterial production in the water column. While at day 0 (26

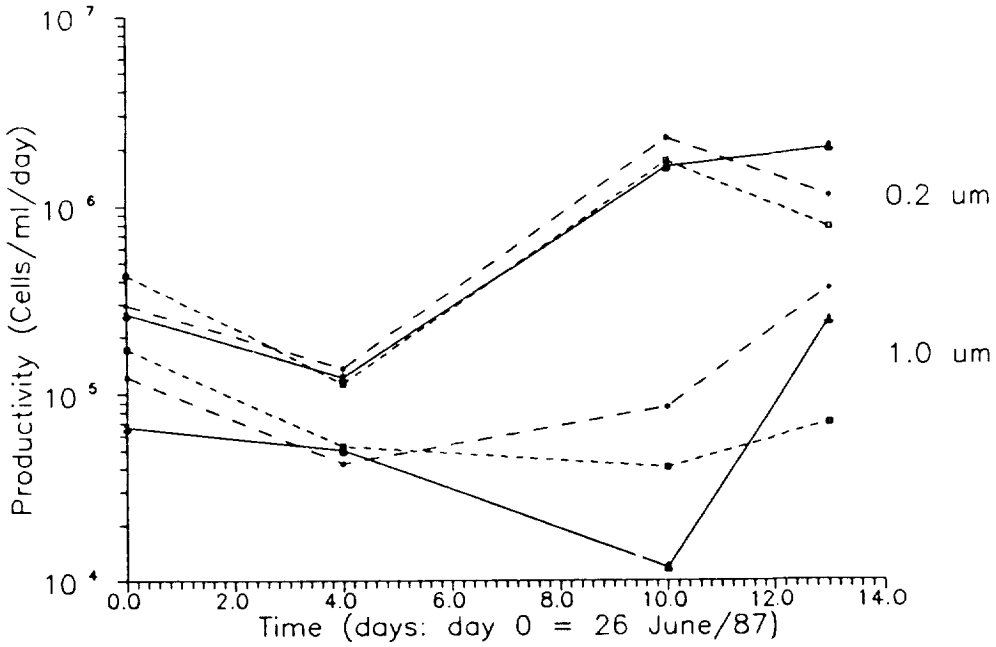

Figure 1. Bacterial secondary productivity versus time at Buoy 117. Abscissa: time measured in days, staring at 26 June. Mantissa: bacterial secondary productivity, in cells/ml/day. The wide dashed line with asterixes is the 0 m sample, the fine dashed line with open squares is the 4 m sample and the solid line with buoy symbols is the 8 m sample. The upper three lines are the greater than 0.2-um size fraction, the lower three lines are the greater than 1.0-um fraction.

June) there is a peak in production at 4 m, by day 4 (30 June) the three depths are indistinguishable by the bacterial production and on day 13 (9 July) the peak in production is at 8 m. There is also an increase in production, especially the greater than 0.2-um fraction, going from an average of 0.3 x 10^6 cells/ml/day to 2.0 x 10^6 cells/ml/day.

The bacterial productivity data for Buoy 123 are presented in Figure 2. Again there is no stratification of the water column evidenced by bacterial production. There is, however, a marked increase in bacterial production over the course of the experiment. Between day 4 (30 June) and day 17 (13 July) the bacterial production retained on the 0.2-um filter increased by approximately 100 times. Futhermore, this increase is log linear (slope = 0.145, $R^2 = 0.948$) when the logarithm of all four depths are regressed against time. The greater than 1.0-um size fraction does not show this increase. Instead, the production in this size fraction decreased such that after day 17 (13 July) dpm were no greater than the kill-controls.

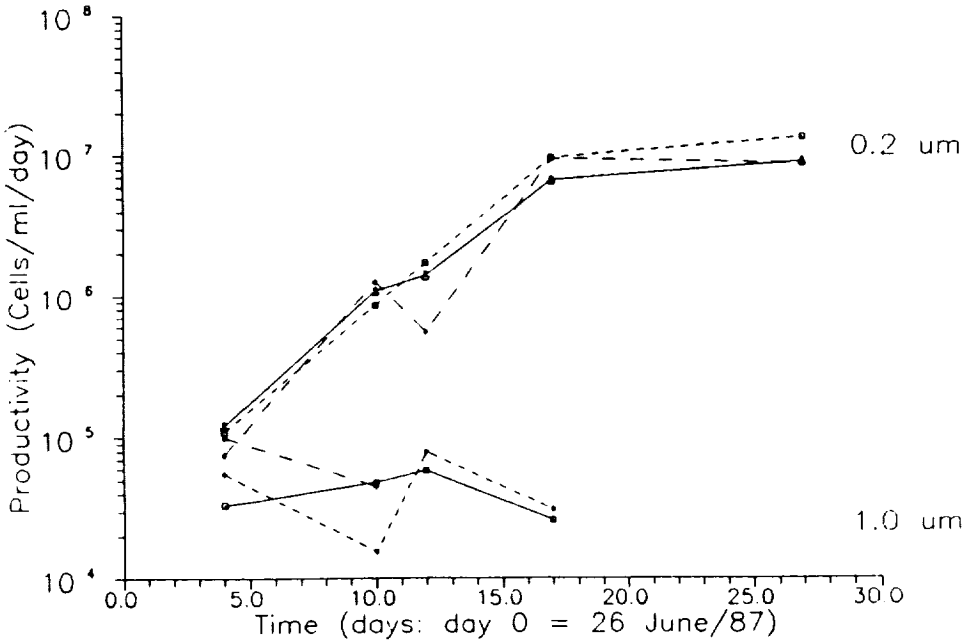

Figure 2. Bacterial secondary productivity versus time at Buoy 123. Axes and symbols are as for Figure 1.

Data for bacterial productivity at Buoy 127 are presented in Figure 3. Once again the greater than 1.0-um size fraction decreases to undetectable levels over the study period. As well, production at the three depths behave similarly. Between day 12 and day 17 (8-13 July) there is also a log-linear increase in bacterial production in the greater than 0.2-um size fraction (slope = 0.156; $R^2 = 0.835$). This is the same period where a log-linear increase in bacterial production can be seen at Buoy 123 (Figure 2). However, a similar log-linear increase (slope = 0.196; R^2 =0.992) was seen at Buoy 117 between day 4-day 10 (30 June-6 July).

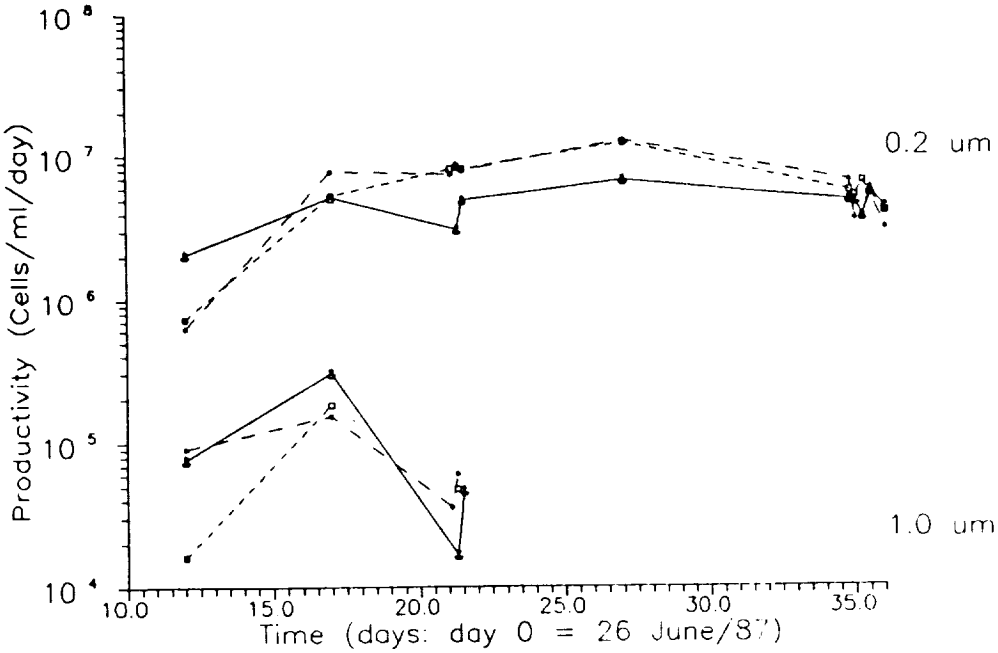

Figure 3. Bacterial secondary productivity versus time at Buoy 127. Axes and symbols are as for Figure 1.

Figure 4 is the bacterial secondary productivity at Buoy 127, measured over a 30-hour period (31 July-1 Aug). In this case, only the greater than 0.2-um size fraction was measured, and the depths from which the samples were obtained were 0, 3, and 10 m.

Discussion

There are some clear trends in the bacterial secondary productivity data. First, the greater than 1.0-um size fraction is always considerably less than the greater than 0.2-um size fraction, and as the summer progressed, this size fraction declined steadily. Presumably, the bacterial production associated with the greater than 1.0-um size fraction would be due to bacteria attached to particles, and the difference between the 0.2-um and 1.0-um size fractions would represent non-attached bacteria. Azam and Cho (1987) have postulated that in marine systems there is a tight coupling between primary and secondary production. One way this might be evidenced is if the larger size fraction formed an important part of the bacterial production. Especially later in the summer, this is not the case, indicating that if there is coupling between algae and bacteria, it is not so close such that the bacteria must be attached to the algae. This, however, is hardly a definitive test of the hypothesis. It is possible that tight coupling occurs only between bacteria and certain algal species. The relative importance of the larger size faction is high early in the summer (37% of total bacterial secondary productivity at Buoy 117 on 26 June) and this may reflect the presence of algal species with which the bacteria are closely associated. Moreover, the

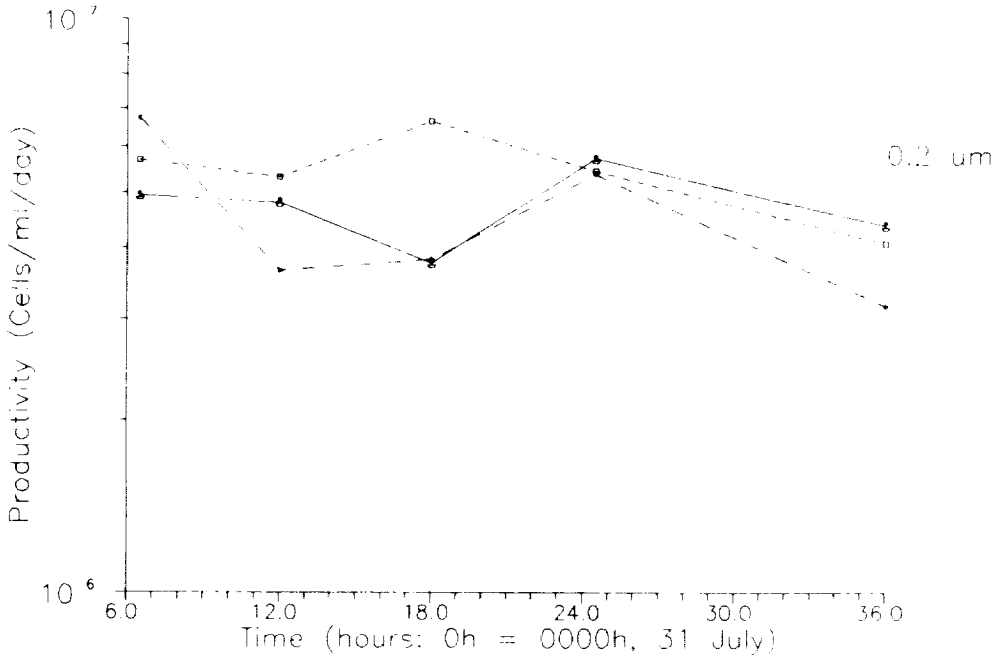

Figure 4. Bacterial secondary productivity versus time at Buoy 127 over a 30-h time course. Abscissa: time measured in hours, beginning at 0000 h, 31 July. Mantissa: bacterial secondary productivity, in cells/ml/day. The wide dashed line with asterixes is the 0-m sample, the fine dashed line with open squares is the 3-m sample, and the solid line with buoy symbols is the 10-m sample. All samples were filtered on a 0.2-um filter.

apparent decrease in the 1.0-um size fraction is due in part to an increase in the dpm recorded for the kill-controls. While the kill-control dpm was a minor proportion of the 0.2-um fraction (rarely more than 5% of total counts), it was nearly as great or greater than the 1.0-um fraction. The increase in counts in the kill-control is presumably due to an increase in adsorbed ^{3}H-Thymidine. To ensure that the sucrose-formalin addition was serving to stop metabolic activity, during one experiment (31 July, 1200 h) ten times the normal amount of fixative was added. No decrease in kill-control dpm was seen.

The second trend evident in the data is the increase in secondary productivity over the course of the summer. At the beginning of the experimental period, productivity values were in the order of 10^5 cells/ml/day. By 23 July values had increased to approximately 10^7 cells/ml/day (Figure 2). Between 30 June and 13 July this increase at Buoy 123 is log-linear. While data for the entire time period are not available for Buoys 117 and 127, the data that are available indicate similar increases over the same time period. After 13 July, however, the increase slowed considerably, and production values actually declined at Buoy 127.

The reasons for such a great increase in bacterial secondary productivity are not clear. If there is tight coupling between primary and bacterial secondary productivity it might be expected that secondary and primary productivity increase together. However, fluores-

cence values over the same period show only a small overall increase (H. Riege, this volume). There was an increase in water temperature over the study period, but the increase was far too small (2-3°C) to account for such a large increase in production. The samples were incubated at room temperature, which also increased over the study period. While this increase was greater (approximately 10°C) it is still implausible that this was sufficient to cause an increase of two orders of magnitude in bacterial secondary productivity.

The high levels of bacterial productivity lead to two obvious questions. Where is the production going, and what is the source of nutrients that allows such high production levels? Assuming an average 20fg C/cell (F. Azam, pers. comm.), 10^7 cells/ml/day is equivalent to 0.2 g C/m^3/day. If the water column is 10 m deep, this is equivalent to 2 g C/m^2/day. Sediment trap data (S. Rose, this volume) indicate that approximately 2-3 g dry weight/m^2/day was dropping out of the water column. Carbon would be some fraction of this. Unless an unusually high percentage of sediment trap material was bacterial in origin, it seems unlikely that sedimentation is a major loss of bacterial production.

Since sedimentation does not appear to explain what happens to bacterial production, predation or autolysis would be logical alternative explanations. However, these data were not collected, so this can only remain an area of speculation. Furthermore, bacterial densities were not successfully determined, making it impossible to find the relationship between bacterial production and biomass.

The obvious source of nutrients for the bacteria is from algae. Algal primary productivity values were in the order of 0.4-0.6 g C/m^3/day (D. Bolgrien, this volume). The maximal bacterial production estimated (0.2 g C/m^3/day) represents 30%-50% of primary productivity. The similarity in primary and bacterial secondary productivity implies a close relationship between the two parameters, but the lack of other evidence for this tight coupling leads to the suspicion that if there is an interaction, it is a complex one. Bacteria have traditionally been thought to be important in detrital pathways, and it is possible that the algal-bacterial interaction is indirect, through this pathway. Daphnia pulex, an efficient grazer of algae, reached high densities in Oneida Lake during the study period (E. Mills, pers. comm.). It may be that the coupling between algae and bacteria occurs through the fecal pellets of Daphnia.

Two diel studies were done in order to determine what, if any, variations occurred in bacterial production over a 24-h period. The results from the second, more complete diel study are shown in Figure 4. The surface sample shows some signs of photoinhibition of bacterial secondary production in the samples taken during the day (1145 h, 1750 h 31 July, 1200 h 1 Aug). However, the 10-m sample also shows a decrease during one daytime sample (1750 h, 31 July). Since the 10-m depth is beneath the 1% light level it is difficult to see how this might be due to photoinhibition, especially since a similar decrease is not seen in the 3-m sample. Further, no evidence for photo-inhibition was seen during the first diel study (17 July). Photoinhibition of bacterial secondary productivity may be taking place, but there is only equivocal evidence based on ^{3}H-Thymidine uptake. It seems clear that ^{3}H-Thymidine is a useful tool to determine the importance of water column bacteria. The results from this study indicate that these bacteria are very important, given the amount of carbon their production represents. However, almost all this production is in non-attached bacteria, and there was little evidence of tight coupling between algae and bacteria.

References

Azam, F. and B.C. Cho (1987) Bacterial utilization of organic matter in the sea. In: Biology of Microbial Communities, Fletcher (Ed.) Society of General Microbiology Symposium.

Fuhrman, J.A. and F. Azam (1982) Thymidine incorporation as a measure of heterotrophic bacterioplankton production in marine surface waters: evaluation and field results. Mar. Bio. 66:109-120.

Report Documentation Page

NASA National Aeronautics and Space Administration

1. Report No.	2. Government Accession No.	3. Recipient's Catalog No.
NASA CR-4295		

4. Title and Subtitle	5. Report Date
The Biogeochemistry of Metal Cycling	May 1990
	6. Performing Organization Code

7. Author(s)	8. Performing Organization Report No.
Kenneth H. Nealson,* Molly Nealson,* and F. Ronald Dutcher,** Editors	10. Work Unit No.

9. Performing Organization Name and Address	11. Contract or Grant No.
University of Wisconsin at Milwaukee, Milwaukee, Wisc. George Washington University, Washington, D.C.	NASW-4324
	13. Type of Report and Period Covered
	Contractor Report

12. Sponsoring Agency Name and Address	14. Sponsoring Agency Code
Office of Space Science and Applications National Aeronautics and Space Administration Washington, DC 20546-0001	EBR

15. Supplementary Notes

Previous documents in this series include NASA TM-86043 and NASA TM-87570.

*University of Wisconsin
**George Washington University

16. Abstract

This report summarizes the results of the Planetary Biology and Microbial Ecology's summer 1987 program, which was held at Oneida Lake, New York. The purpose of the interdisciplinary PBME program is to integrate, via lectures and laboratory work, the contributions of university and NASA scientists and student interns. The 1987 program examined various aspects of the biogeochemistry of metal cycling, and included such areas as limnology, metal chemistry, metal geochemistry, microbial ecology, and interactions with metals. A particular area of focus was the use of remoste sensing in the study of biogeochemistry. Abstracts and bibliographies of the lectures and reports of the laboratory projects are presented.

17. Key Words (Suggested by Author(s))		18. Distribution Statement
Biogeochemistry	Remote sensing	Unclassified - Unlimited
Microbial Ecology	Bacteria	Subject Category 55
Microbiology	Manganese	
Planetary Geology	Metals	

19. Security Classif. (of this report)	20. Security Classif. (of this page)	21. No. of pages	22. Price
Unclassified	Unclassified	228	A11